INRS-Institut Armand-Frappier

Étude des mécanismes de synthèse, de sécrétion et de dégradation des salmochélines et de l'entérobactine, et de leur implication pour la virulence de la souche *Escherichia coli* pathogène extra-intestinale aviaire χ7122

Par Mélissa Caza

Thèse présentée
pour l'obtention
du grade de Philosophiae doctor (Ph.D.)
en biologie

Jury d'évaluation

Président du jury et examinateur interne	Dr. Éric Déziel, INRS-Institut Armand-Frappier
Examinateurs externes	Dr. Michel Frenette, Faculté des sciences et de Génie Département de biochimie et microbiologie Université Laval
	Dr. Alain Stintzi Faculté de médecine Département de biochimie, microbiologie et immunologie Université d'Ottawa
Directeur de recherche	Dr. Charles M. Dozois, INRS-Institut Armand-Frappier
Codirecteur de recherche	Dr. François Lépine, INRS-Institut Armand-Frappier

Résumé

Les souches d'*Escherichia coli* pathogènes extra-intestinales (ExPEC) causent des infections urinaires, respiratoires et septicémiques chez l'homme et les animaux d'élevage. Les souches ExPEC utilisent des sidérophores pour séquestrer le fer pendant une infection, puisque le fer est peu disponible chez l'hôte et qu'il est un élément essentiel à la survie et la prolifération bactérienne. Les sidérophores catécholates, l'entérobactine et les salmochélines, et l'aérobactine, une molécule différente, sont des sidérophores produits par certaines souches ExPEC, dont la souche O78 χ7122, et d'autres entérobactéries pathogènes. Les salmochélines, encodées par les gènes *iroBCDEN*, sont des sidérophores dérivés de l'entérobactine, auquel la glucosyltransférase IroB ajoute des molécules de glucose. De plus, la dégradation de ces sidérophores par les estérases Fes, IroD et IroE génère treize molécules différentes dont neuf sont apparentées aux salmochélines et quatre à l'entérobactine.

Le rôle de chacun des gènes *iroBCDEN* a été testé pour la virulence et pour la production des salmochélines en introduisant des plasmides encodant différentes combinaisons de gènes dans une souche dérivée de la souche χ7122 ne produisant ni les salmochélines, ni l'aérobactine et qui est atténuée dans le modèle d'infection septicémique aviaire. La complémentation par les gènes *iroBCDEN* et les analyses en chromatographie liquide couplée à la spectrométrie de masse (LC-MS/MS) des surnageants de culture des différentes souches ont démontré que la glucosylation (IroB), le transport (IroC et IroN) et la dégradation (IroD et IroE) des salmochélines sont requis pour la virulence de la souche χ7122, bien qu'IroE semble jouer un rôle accessoire.

De plus, des mutants de synthèse (Δ*entD*, Δ*entD*Δ*iuc* et Δ*iroB*) et de sécrétion (Δ*entS*, Δ*iroC* et Δ*entS*Δ*iroC*) des sidérophores de la souche χ7122 testés dans le modèle d'infection septicémique aviaire ont démontré l'importance de la synthèse et la sécrétion des sidérophores catécholates pour la virulence de la souche. Des analyses en LC-MS/MS ont également démontré qu'EntS et IroC effectuent préférentiellement la sécrétion de certaines molécules de sidérophores catécholates. Ainsi, les résultats suggèrent que le

rôle de ces exportateurs pour la virulence des souches ExPEC est dépendant de la synthèse de l'entérobactine; synthèse qui n'est pas requise en présence de l'aérobactine.

Finalement, l'étude de la dégradation des sidérophores catécholates par les estérases Fes, IroD et IroE a démontré que Fes et IroD sont requis pour la virulence de la souche χ7122 dans le modèle d'infection septicémique aviaire et que ces deux enzymes sont également impliquées dans la biosynthèse des salmochélines.

En somme, l'étude des systèmes de sidérophores produits et utilisés par la souche ExPEC χ7122 a démontré l'importance de chacun des systèmes pour la virulence de la souche, ainsi que les interrelations des mécanismes moléculaires de la synthèse, de la sécrétion et de la dégradation des salmochélines et de l'entérobactine.

Étudiante

Directeur de recherche

Remerciements

Tout d'abord, je tiens à remercier mon directeur de recherche Charles Dozois pour les huit années passées dans son laboratoire à étudier sous sa direction. Je le remercie grandement de m'avoir accueillie dans son laboratoire et de m'avoir fait confiance. Au-delà de l'encadrement académique, il a su me transmettre sa passion et sa vision de la science et de la vie. Il a été un excellent mentor auquel je serais toujours reconnaissante. Merci de m'avoir fait découvrir les beaux côtés de la vie à travers la science. Merci pour tout!

Je tiens aussi à remercier mon co-directeur François Lépine pour l'enseignement de la spectrométrie de masse. Son encadrement et ses idées ont généré des découvertes scientifiques très bien reçues par la communauté scientifique. De plus, il a su me transmettre sa capacité à réaliser de façon simple des expériences complexes. Merci de m'avoir fait aimer les molécules chimiques!

De plus, je remercie également Sylvain Milot pour son aide technique à la spectrométrie de masse et à la résolution de divers problèmes reliés à la chimie analytique. Je remercie aussi Éric Déziel pour ses commentaires constructifs sur les comités d'évaluations et pour l'utilisation de ses divers appareils.

Sur le plan personnel, je tiens à remercier ma famille, ma petite sœur Marie-Michèle que j'aime tant et dont je suis tellement fière! Mon grand frère David avec qui j'aime tant discuter! Ma sœur Stéphanie et mon père Michel qui m'ont soutenu et motivé sans perdre confiance en moi. Je dois également remercier ma mère qui a su me transmettre en peu de temps une base solide sur laquelle j'ai grandi.

Finalement, je tiens à remercier mes amies Maria et Karel qui ont su me soutenir et m'encourager tout au long de cette étape importante et bien plus encore. Elles sont mes personnes références à qui je dois beaucoup. Je remercie aussi mes collègues et amies avec qui j'ai partagé mon quotidien pendant de nombreuses années et avec qui j'ai eu beaucoup de plaisir à travailler. Merci beaucoup!

Table des matières

RÉSUMÉ II

REMERCIEMENTS IV

TABLE DES MATIÈRES V

LISTE DES FIGURES ET TABLEAUX X

LISTE DES ABRÉVIATIONS XII

INTRODUCTION 1

REVUE DE LITTÉRATURE 4

1) *ESCHERICHIA COLI* 5

1.1 *Escherichia coli* pathogène intestinal 5

E. coli entérotoxinogène (ETEC) 5

E. coli entéropathogène (EPEC) 6

E. coli entérohémorragique (EHEC) 6

E. coli entéroaggrégative (EAEC) et d'adhérence diffuse (DAEC) 6

E. coli entéroinvasive (EIEC) 7

1.2 *Escherichia coli* pathogène extra-intestinal (ExPEC) 7

Pathogène humain 7

Pathogène animal 9

Réservoir animal et potentiel zoonotique des souches ExPEC 10

Résistance aux antibiotiques 11

Les facteurs de virulence des souches ExPEC 12

2) LE FER : ÉLÉMENT ESSENTIEL À LA VIE 14

2.1 Les protéines liant le fer chez les humains et les animaux 15

3) LES SYSTÈME D'ACQUISITION DU FER CHEZ LES BACTÉRIES 16

4) LES SIDÉROPHORES CHEZ LES BACTÉRIES PATHOGÈNES : FACTEUR DE VIRULENCE 18

5) L'HOMÉOSTASIE DU FER CHEZ *E. COLI* PAR FUR ET RYHB19

6) LE SIDÉROPHORE AÉROBACTINE 23

7) L'ENTÉROBACTINE 25

7.1 La sécrétion de l'entérobactine par EntS 28

7.2 Le transporteur de type ABC : FepA, FepB, FepD, FepG et FepC 29

7.3 La dégradation de l'entérobactine par l'estérase Fes 31

7.4 La régulation de l'entérobactine par Fur 33

8) LE LOCUS IROA OU LES GÈNES *IROBCDEN* 34

8.1 La synthèse des neuf molécules de salmochéline 35

8.2 La pompe à efflux des salmochélines IroC 37

8.3 Les estérases Fes, IroD et IroE 37

8.4 Le récepteur des salmochélines IroN 39

9) LES SIDÉROPHORES DES EXPEC : FACTEURS DE VIRULENCE ? 39

9.1 L'aérobactine est un facteur de virulence 39

Rôle physiologique de l'aérobactine 40

9.2 L'entérobactine peut être un facteur de virulence 41

Rôle physiologique de l'entérobactine 42

9.3 Les salmochelines représentent un facteur de virulence 44

Prévalence des gènes *iroBCDEN* 44

Implication des salmochélines dans la virulence des souches ExPEC 46

10) LE SIDÉROCALIN : NOUVELLE DÉFENSE ANTIBACTÉRIENNE DE L'HÔTE 47

PROBLÉMATIQUE DE LA RECHERCHE : 50

OBJECTIFS SPÉCIFIQUES : 50

ARTICLES 6

ARTICLE #1 52

ABSTRACT 55

INTRODUCTION 56

MATERIALS AND METHODS 59

RESULTS 66

DISCUSSION 73

ACKNOWLEDGEMENTS 79

REFERENCES 80

ARTICLE #2 95

Summary 98

Introduction 99

Results 101

Results 101

Experimental procedures 112

ACKNOWLEDGEMENTS 117

References 117

ARTICLE #3 140

ABSTRACT 143

INTRODUCTION 145

MATERIAL & METHODS 147

RESULTS 152

DISCUSSION 159

ACKNOWLEDGEMENTS 162

REFERENCES 163

RÉSULTATS SUPPLÉMENTAIRES 176

1) LE TAUX RELATIF DE GLUCOSYLATION DE L'ENTÉROBACTINE CHEZ LES ENTÉROBACTÉRIES. 177

2) TOLC EST IMPLIQUÉ DANS LA SÉCRÉTION DE SIDÉROPHORES CATÉCHOLATES 178

3) LE SYSTÈME DE TRANSPORT DE TYPE ABC DES SIDÉROPHORES CATÉCHOLATES 180

4) LA CROISSANCE DES BACTÉRIES MUTANTES POUR LES ESTÉRASES *FES*, *IROD* ET *IROE* EN PRÉSENCE DE CONALBUMINE. 183

5) LA QUANTIFICATION RELATIVES DES SIDÉROPHORES CATÉCHOLATES, AÉROBACTINE ET YERSINIABACTINE CHEZ LES ENTÉROBACTÉRIES PATHOGÈNES 184

DISCUSSION 177

1) LA CARACTÉRISATION DES GÈNES IROBCDEN 190

1.1 La synthèse des salmochélines 190

1.2 La sécrétion de l'entérobactine et des salmochélines 192

1.3 L'internalisation des sidérophores catécholates par IroN et FepDGC 194

1.4 La dégradation des sidérophores par Fes, IroD et IroE 195

1.5 Modèle proposé des mécanismes d'action des sidérophores catécholates chez χ7122 196

2) LA PRODUCTION DES SIDÉROPHORES CATÉCHOLATES, AÉROBACTINE ET YERSINIABACTINE CHEZ LES ENTÉROBACTÉRIES PATHOGÈNES. **198**

3) CONCLUSIONS **200**

PERSPECTIVES **191**

RÉFÉRENCES **204**

ANNEXE I **225**

ANNEXE II **237**

ANNEXE III **250**

ANNEXE IV **258**

Liste des figures et tableaux

Revue de littérature

Figure

Figure 1 : Structure et coordination avec le fer des sidérophores 17
Figure 2 : Mécanisme de la régulation négative par Fur 20
Figure 3 : Mécanisme de régulation de l'homéostasie du fer par Fur et RyhB chez *E. coli*. 21
Figure 4 : Schéma de la régulation du fer par Fur et RyhB chez *E. coli* 22
Figure 5 : Synthèse de l'aérobactine à partir de la L-lysine 24
Figure 6 : Région chromosomique de l'entérobactine d'E. coli K-12 MG1655 25
Figure 7: Biosynthèse du 2,3-DHB à partir du chorismate 26
Figure 8 : Activation des domaines T de EntB et EntF par EntD. 27
Figure 9 : Initiation de la synthèse de l'entérobactine. Transferts du 2,3-DHB au domaine T d'EntB par le domaine A d'EntE et de la sérine au domaine T d'EntF par son domaine A 27
Figure 10 : Élongation et terminaison de la biosynthèse de l'entérobactine par condensation et transfert des précurseurs 28
Figure 11 : Schéma de la dégradation de l'entérobactine par l'estérase Fes 32
Figure 12 : Schéma récapitulatif du système d'acquisition du fer par l'entérobactine chez *E. coli* 33
Figure 13 : Organisation génétique du locus IroA chez *E. coli* χ7122. 34
Figure 14 : Formation des salmochélines MGE, DGE et TGE par la glucosyltransférase IroB à partir de l'entérobactine 36
Figure 15 : Schéma de la synthèse par IroB et de la dégradation des salmochélines par Fes, IroD et IroE chez *E. coli* 38
Figure 16: Structure du sidérocalin liant l'entérobactine et l'encombrement stérique produit par l'ajout de glucoses à l'entérobactine 48

Tableau

Tableau 1: Facteurs de virulence des souches ExPEC 13

Résultats supplémentaires

Figure

Figure 1 : Concentrations moyennes des sidérophores catécholates des souches χ7122 et du mutant Δ*tolC* 179
Figure 2 : Concentrations moyennes des sidérophores catécholates des souches χ7122 et dérivées isogéniques 182
Figure 3 : Courbes de croissance des souches χ7122, des mutants de dégradation 184

Figure 4 : Concentration (µM) de sidérophores catécholates produits par la souche S. Typhi Ty2 en milieu M63-glycérol en présence et absence d'acides casaminés déférés (..... 187
Figure 5 : Quantification arbitraire et relative de l'entérobactine (Ent) / DHBS, des salmochélines (Sal) et de l'aérobactine (Aéro) de la souche χ7122 cultivée en milieu M63-glycérol et en M63-glycérol + 1mg/ml de conalbumine 188

Tableau

Tableau 1 : Taux relatif moyen (%) des molécules non-, mono- et di-glucosylées par rapport à la concentration totale des sidérophores catécholates sécrétées par la souche*..... 178

Discussion

Figure

Figure 1 : Modèle proposé des mécanismes d'actions des sidérophores catécholates...197

Liste des abréviations

Aéro :	aérobactine
Ap :	ampicilline
APEC :	*Escherichia coli* pathogène aviaire
Cm :	chloramphénicol
CFU:	unité formatrice de colonie
DAEC :	*Escherichia coli* d'adhérence diffuse
DGE :	entérobactine di-glucosylé
DHBS :	2,3-dihydroxybenzoyl sérine
EAEC :	*Escherichia coli* entéroaggrégative
ECOR :	Collection de références d'*Escherichia coli*
EHEC :	*Escherichia coli* entérohémorragique
EIEC :	*Escherichia coli* entéroinvasive
Ent :	entérobactine
Ent linéaire :	trimère de DHBS
EPEC :	*Escherichia coli* entéropathogène
ETEC :	*Escherichia coli* entérotoxinogénique
ExPEC :	*Escherichia coli* pathogène extra-intestinale
Fe^{2+} :	fer ferreux
Fe^{3+} :	fer ferrique
HPI :	îlot de haute pathogénicité
IroA :	*iroBCDEN*
LC-MS/MS :	chromatographie liquide couplée au spectromètre de masse
MRM :	« multiple reaction monitoring »
MGE :	entérobactine mono-glucosylé
Nal :	acide nalidixique
NE :	norépinéphrine
NGAL:	neutrophil gelatinase associated lipocalin
NMEC :	*Escherichia coli* causant la méningite néonatale
NRPS :	« non-ribosomal peptide synthetase »

PAIs :	îlots de pathogénicité
qRT-PCR :	réaction quantitative de polymérisation en chaîne de la réverse transciptase en temps réel
Sal :	salmochéline
SCOTS :	captures sélectives de séquences transcrites
Tc :	tétracycline
TGE :	entérobactine tri-glucosylé
UPEC :	*Escherichia coli* uropathogène
Ybt :	yersiniabactine

Introduction

Les souches d'*Escherichia coli* pathogènes causent une panoplie d'infections intestinales et extra-intestinales. Chez l'humain et les animaux d'élevage, les souches ExPEC (Extraintestinal Pathogenic *Escherichia coli*) causent des infections du tractus urinaire et respiratoire et des septicémies [1]. De plus, ces souches sont également le deuxième agent pathogène responsable de la méningite néonatale chez l'homme [2]. Bien qu'il existe une grande diversité génétique parmi les souches ExPEC, plusieurs facteurs de virulence sont reconnus comme participant au processus pathogénique de ces souches, dont les systèmes d'acquisition du fer [3].

D'ailleurs, l'acquisition du fer, qui est un élément essentiel à la survie et la prolifération bactérienne, est un domaine d'étude important de la pathogenèse bactérienne. Ceci débuta lorsque Schade et Caroline rapportèrent, en 1944, que la présence de protéines de haute affinité pour le fer dans le sang et dans les blancs d'œufs pouvait inhiber la croissance de plusieurs bactéries, dont *Escherichia coli* [4]. Ils ont déduit que ces protéines liaient trop fortement le fer pour le rendre disponible aux bactéries, inhibant ainsi leur croissance. Ces chercheurs ont aussi établi un premier lien entre la résistance naturelle de l'organisme hôte et la capacité de certaines bactéries pathogènes à faire fi de cette résistance. De plus, Bullen, Leigh et Rogers a démontré en 1968 que l'injection de fer chez des cobayes diminuait considérablement la dose létale de la souche *E. coli*, suggérant ainsi un rôle important du fer pour l'infection bactérienne [5]. Par la suite, Kochan proposa, en 1973, le concept d'immunité nutritionnelle afin de décrire ce phénomène de disponibilité limitée des nutriments essentiels, dont le fer, pour la survie microbienne chez l'hôte [6].

Cette disponibilité limitée du fer chez les humains et animaux s'explique par la séquestration du fer par des protéines de haute affinité. Cette séquestration est causée par l'extrême insolubilité et la toxicité du fer ferrique en présence d'oxygène et à pH neutre [7]. Il est donc primordial pour un organisme de séquestrer le fer de façon contrôlable à

l'aide de diverses protéines. La transferrine, la lactoferrine et l'ovotransferrine (aussi connu sous le nom de conalbumine) sont des protéines de séquestration du fer retrouvées dans le sang, le lait, la salive et les larmes, ainsi que dans le blanc des œufs [8]. En plus de posséder une constante d'affinité avec le fer de l'ordre de 10^{36} M^{-1}, ces protéines ne sont généralement qu'en partie saturées, ce qui rend la disponibilité du fer extrêmement faible chez les humains et les animaux [9]. En fait, l'équilibre entre le fer ferrique soluble disponible et le fer complexé aux diverses protéines se situe aux environs de 10^{-24}M [10, 11]. Or, les bactéries nécessitent une concentration interne de fer entre 10^{-7} M à 10^{-5} M et ce, afin de subvenir aux divers processus biologiques essentiels à leur prolifération [12, 13]. Ainsi, lors d'une infection par une bactérie pathogène, la quantité de fer libre disponible est nettement insuffisante pour permettre à cette dernière d'assurer sa survie et sa multiplication dans l'organisme hôte. Les bactéries ont donc développé des systèmes, tels que les sidérophores, afin de subvenir à leur besoin en fer. Les sidérophores sont des molécules de faible poids moléculaire ayant une forte affinité pour le fer ferrique [14]. Il existe plus de 500 différents sidérophores connus à ce jour [15]. L'entérobactine, les salmochélines et l'aérobactine sont trois sidérophores synthétisés et sécrétés par plusieurs entérobactéries pathogènes, dont la souche ExPEC aviaire χ7122.

Puisque l'obtention du fer est un processus important pour la prolifération bactérienne, plusieurs études sur l'importance des divers systèmes de sidérophores pour la virulence des souches bactériennes pathogènes ont été réalisées. En fait, l'aérobactine participe à l'établissement d'une infection bactérienne des souches ExPEC [16-19]. Cependant, l'importance de l'entérobactine pour la prolifération bactérienne *in vivo* varie selon les souches et les modèles animaux utilisés [19-23]. La découverte des salmochélines en 2003 par Hantke et ses collaborateurs généra quelques pistes de solutions au débat sur l'importance de l'entérobactine pour la virulence des entérobactéries pathogènes [24]. Les salmochélines, encodées par les gènes *iroBCDEN*, sont en fait des sidérophores modifiés de l'entérobactine, auquel la glucosyltransférase IroB ajoute des molécules de glucose. Cette modification de l'entérobactine empêche le NGAL, une protéine bactériostatique de l'hôte, de séquestrer les sidérophores modifiés, en plus d'éviter le déclenchement d'une réponse pro-inflammatoire par l'interleukine-8 [25-27].

Les divers objectifs de ce projet d'étude furent d'abord de déterminer le rôle de chacun des gènes *iroBCDEN* pour la virulence et la production des salmochélines chez la souche χ7122 dans le modèle d'infection septicémique aviaire. Par la suite, une étude portant sur l'importance de la sécrétion et la synthèse de l'entérobactine et les salmochélines pour la virulence de la souche χ7122 a été réalisée. Finalement, l'importance de la dégradation de l'entérobactine et des salmochélines pour la virulence et la synthèse des salmochélines chez la souche χ7122 a été démontrée.

Revue de littérature

1) *Escherichia coli*

La bactérie *Escherichia coli*, autrefois nommée *Bacterium coli* commune, a été isolée pour la première fois en 1885 des fèces d'un enfant par le pédiatre Theodore Escherich [1]. Cette bactérie à Gram négatif est membre de la famille des *Enterobacteriaceae* [28] et elle fait partie de la microflore intestinale humaine et animale. Elle est en fait très efficace pour s'établir et coloniser la couche de mucus du côlon des mammifères, et ce, dès les premières heures des nouveaux nés, et ainsi s'établit une relation de commensalisme avec l'hôte [29, 30]. Cependant, il existe plusieurs autres souches d'*E. coli* pathogènes qui causent des infections intestinales et extra-intestinales chez les humains et animaux [31]. Bien que ces micro-organismes soient génétiquement reliés entre eux, du matériel génétique supplémentaire et diversifié, localisé sur des plasmides ou sur des îlots de pathogénicité (large bloc d'ADN codant pour des gènes contribuant à la virulence insérés dans le chromosome bactérien), ainsi que des réarrangements de l'ADN chromosomique, provoqués par des délétions et des insertions de transposons et d'ADN de phages, sont responsables de la grande diversité phylogénique de la bactérie *E. coli* [29, 31-33]. Les différentes souches pathogènes d'*E. coli* ont été classées en deux catégories, soit les pathogènes intestinaux et les pathogènes extra-intestinaux [29].

1.1 *Escherichia coli* pathogène intestinal

E. coli entérotoxinogène (ETEC)

Puisqu'une grande variété de souches d'*E. coli* pathogènes existe, elles ont été classifiées selon leur pathotype, soit selon leur génotype et le type de maladie engendré [1, 29]. Il existe six catégories de souches *E. coli* pathogènes intestinaux. Tout d'abord, les *E. coli* entérotoxinogènes (ETEC) causent la diarrhée, parfois de la fièvre, des crampes abdominales et des vomissements [34]. Ces souches sont en fait l'agent pathogène responsable de la diarrhée des voyageurs, communément appelé « tourista » [34]. Elles peuvent également causer de la diarrhée chez les animaux d'élevage, soit les porcelets, les agneaux et les veaux [1, 31]. La principale caractéristique distinctive de ces souches est la sécrétion de deux types de toxines, soit la toxine thermolabile (LT) et les toxines thermostables (STa et STb). Ces toxines sont un mécanisme de virulence important pour les souches ETEC [1, 29, 34, 35].

E. coli entéropathogène (EPEC)

Les souches d'*E. coli* entéropathogènes (EPEC) causent de la diarrhée persistante, de la fièvre et des vomissements chez les enfants et les animaux. Ces souches possèdent un îlot de pathogénicité de 35 kb codant pour un locus d'effacement d'entérocytes (LEE) [31, 36]. Les souches EPEC ont la particularité de s'attacher aux cellules épithéliales de l'intestin et de causer un réarrangement du cytosquelette des cellules eucaryotes, incluant l'effacement des microvilli intestinaux et l'accumulation d'actine polymérisée en dessous de la bactérie par l'injection de protéines effectrices [37]. Ceci aura pour conséquence la formation d'une structure similaire à un piédestal et la formation de lésions A/E (attachement et effacement) [1, 29, 37]. Des homologues au LEE de EPEC sont retrouvés chez d'autres pathogènes humain et animal, tels que chez les souches d'*E. coli* entérohémorragique (EHEC) et les EPEC de lapin (REPEC) [36].

E. coli entérohémorragique (EHEC)

Les souches EHEC, bien qu'elles possèdent la capacité de produire des lésions A/E, se distinguent des EPEC grâce à la production et à la sécrétion de toxines de type Shiga [1, 29, 38]. Les souches EHEC causent *à priori* de la diarrhée qui peut progresser en fèces sanguinolentes et ulcération de l'intestin et occasionnellement dégénérer en syndrome d'urémie hémolytique (HUS), qui se résume en une anémie hémolytique, une thrombocytopénie et une ischémie rénale [1, 35]. Les souches EHEC sont des membres transitoires de la microflore intestinale des bœufs, chez qui aucun symptôme de maladie n'est apparent [35, 39]. Cependant, la contamination des viandes ou des aliments par des fèces de bœuf est la voie principale d'acquisition d'une infection par les souches EHEC [1, 29, 35, 39]. La souche O157:H7 est le représentant le plus connu et étudié des souches EHEC, bien que d'autres sérotypes tels que O26 et O111 causent une infection similaire [1, 35].

E. coli entéroaggrégative (EAEC) et d'adhérence diffuse (DAEC)

Certaines souches d'*E. coli* peuvent adhérer aux cellules HEp-2 en culture de façon comparable à un amoncellement de briques [1, 29, 35]. En fait, ces *E. coli*

entéroaggrégatives (EAEC) s'agrègent entre elles à l'aide d'un fimbriae d'adhérence agrégative nommé AAF [40]. Les souches EAEC expriment également la mucinase Pic [41], ainsi que trois entérotoxines Pet, ShET1 et EAST1 impliqués dans la pathogenèse des souches [42-45]. Les souches EAEC causent de la diarrhée persistante chez l'humain, ainsi qu'un endommagement de la muqueuse intestinale [46], mais n'engendrent ni de fièvre, ni de septicémie [34, 35]. Une deuxième catégorie de souches d'*E. coli* pouvant s'adhérer aux cellules HEp-2 en culture est celle dont les souches ont une adhérence diffuse (DAEC) [1, 35]. Cette adhésion est assurée par le fimbriae F1845 de la famille des adhésines Dr [47]. Tout comme les souches EAEC, les souches DAEC causent des diarrhées persistantes, surtout chez les nouveau-nés [1, 35].

***E. coli* entéroinvasive (EIEC)**

Les souches d'*E. coli* entéroinvasives (EIEC) ont la capacité de pénétrer les cellules de l'épithélium intestinal, d'échapper à la phagocytose en lysant les vésicules phagocytaires et ainsi se répliquer à l'intérieur de la cellule hôte [1, 29]. Les souches entéroinvasives sont intimement reliées à *Shigella* spp. tant au niveau biochimique et génétique qu'au niveau de la pathogénèse bactérienne [29]. D'ailleurs, il existe une impasse taxonomique entre les deux espèces. Les souches entéroinvasives causent principalement de la diarrhée aqueuse, avec ou sans présence de mucus et de sang, pouvant dégénérer en dysenterie et en colites inflammatoires, bien que *Shigella* spp. soit beaucoup plus fréquemment isolée de patients atteints de ces symptômes [29, 48]. La fièvre et des crampes abdominales peuvent également incommoder les personnes atteintes d'une infection aux souches EIEC et *Shigella* spp. [1, 34]. Les deux distinctions biochimiques entre *Shigella* et EIEC encore valide à ce jour sont la production de gaz à partir du glucose et la fermentation du xylose par les souches EIEC [1].

1.2 *Escherichia coli* pathogène extra-intestinal (ExPEC)

Pathogène humain

Une dernière catégorie d'*E. coli* pathogène, nommée ExPEC (extra-intestinal pathogenic *Escherichia coli*), est reconnue pour causer des infections extra-intestinales. Parmi ce groupe, on retrouve d'abord les souches uropathogènes d'*E. coli* (UPEC) qui, ayant la

capacité de coloniser le tractus urinaire humain, sont responsables de cystites (simples, compliquées et récurrentes), pyélonéphrites et urosepticémies [1, 29, 34]. De plus, les infections aux souches UPEC sont associés à la pose de cathéter chez les patients [49]. Les infections du tractus urinaire sont estimées entre 6 et 8 millions de cas aux États-Unis et entre 130 à 175 millions de cas à travers le monde chaque année [49]. *E. coli* uropathogène est à l'origine de ces infections dans plus de 80 % des cas [49, 50]. La contamination de la région urogénitale par la flore fécale et périnéale est à l'origine de la colonisation du tractus urinaire par les bactéries uropathogènes [3, 51]. La colonisation de la vessie, qui se fait par l'ascension bactérienne de l'urètre, est l'étape initiale de l'infection urinaire ascendante qui peut dégénérer en pyélonéphrite, si les bactéries atteignent les reins par les uretères. Les bactéries ayant atteint les reins peuvent ensuite traverser la barrière de cellules épithéliales tubulaires et se retrouver dans la circulation sanguine, causant ainsi une septicémie [29]. Les septicémies dues à *E. coli* causent en moyenne 40 000 morts chaque année aux États-Unis [49]. Les infections urinaires et septicémiques engendrent évidemment des frais de traitements et d'hospitalisation qui sont estimés à 175 millions de dollars par an [49].

Par ailleurs, les souches ExPEC sont également le deuxième agent pathogène responsable de la méningite néonatale, devancé par le streptocoque de groupe B (GBS) [2]. Ces souches, nommées NMEC pour « neonatal meningitis *E. coli* », engendrent la mort dans 15 à 40 % des nouveau-nés infectés et causent des lésions neurologiques sévères chez les survivants [1, 2, 29]. L'infection du nouveau-né débute par la colonisation du tractus intestinal de l'enfant suivant l'acquisition du pathogène du liquide amniotique ou de la flore vaginale de la mère [52]. Par la suite, il y a translocation bactérienne du lumen intestinal à la circulation sanguine, passage à travers la barrière hémato-encéphalique (BCB) et invasion de l'espace arachnoïdien [2]. De plus, les souches ExPEC peuvent également occasionner des pneumonies chez les patients hospitalisés et ceux nécessitant des soins de longue durée, en plus d'être une source majeure de bactériémie nosocomiale et de prostatites [49, 53]. Globalement, les frais médicaux engendrés directement par les infections à ExPEC sont estimés à plus de 2 milliards de dollars par an aux États-Unis [49].

Pathogène animal

Par ailleurs, il existe également des souches ExPEC associées à des infections chez les animaux. Par exemple, les souches d'*E. coli* pathogènes pour les espèces aviaires (APEC) causent de multiples infections et syndromes chez la volaille, telles que les infections de la membrane vitelline des œufs, le syndrome de la tête enflée, la salpingite, la péritonite, la cellulite aviaire et la colibacillose aviaire [31, 54, 55]. Cette dernière se détecte par différentes manifestations cliniques incluant l'aérosacculite, la péricardite, la périhépatite, la péritonite et la septicémie [56, 57]. L'aérosacculite, communément appelée la maladie du sac aérien, est causée par une infection du tractus respiratoire par les souches APEC. Généralement, l'infection des voies respiratoires a lieu suite à une infection préalable du tractus par des agents pathogènes tels que le virus de la maladie de Newcastle (NDV), le virus de la bronchite infectieuse (IBV) ou par *Mycoplasma gallisepticum*. De plus, l'infection du tractus respiratoire peut se transformer en une septicémie et une infection systémique. À ce stade, plusieurs lésions sont observables au niveau du péricarde, du foie et de la membrane péritonéale et l'animal souffre de colibacillose [54, 55]. Les causes de la contraction des infections causées par les souches APEC sont la promiscuité des lieux d'élevage et la contamination par la nourriture et l'eau. Toutefois, la principale route d'infection est l'inhalation de la poussière contaminée par les fèces des animaux [54].

Le modèle d'infection septicémique aviaire utilisé au laboratoire consiste à recréer d'abord une infection respiratoire en inoculant les bactéries dans le sac aérien des poulets. Par la suite, les bactéries coloniseront les poumons et le sang des animaux, pour finalement se multiplier dans les organes viscéraux, telles que le foie et la rate. Cette colonisation engendre des lésions visibles aux niveaux des sacs aériens, du péricarde et du foie. Ce modèle expérimentale de la colibacillose aviaire est un modèle efficace et hautement reproductible dans lequel la totalité des animaux traités sont infectés [58].

Par ailleurs, ces différentes infections sont responsables de mortalité et de morbidité chez les animaux atteints [54, 55]. En 2008, le réseau d'alerte et d'information zoosanitaire (RAIZO) du ministère de l'Agriculture, des Pêcheries et de l'Alimentation du Québec

(MAPAQ) a publié dans son bilan annuel que la colibacillose est le diagnostic le plus fréquent chez les poulets à chair, les poules pondeuses, les reproducteurs à chair de remplacement et les dindes [59]. Chez le porc, le bœuf et le mouton, c'est la septicémie et la colibacillose qui guettent les nouveau-nés dès la première semaine de vie [60-62]. Plusieurs manifestations cliniques sont observables chez un animal infecté dont la mort survient généralement dans les 48 h suivant les premiers signes d'infection [60-62]. Chez les femelles adultes, c'est l'infection des mamelles par *E. coli*, nommé mastite, qui cause des problèmes de septicémie et d'allaitement des nouveau-nés dans les troupeaux d'élevage [60-63]. Les infections du tractus urinaire chez le porc adulte causé par *E. coli* sont aussi une cause importante de mortalité chez ces animaux d'élevage [64]. En somme, ces diverses infections à *E. coli* engendrent évidemment de pertes économiques importantes pour l'industrie animale principalement causées par la condamnation ou déclassement des carcasses et une perte de productivité [54, 55].

Réservoir animal et potentiel zoonotique des souches ExPEC

Les souches ExPEC, incluant les souches UPEC, NMEC et APEC, ont la caractéristique commune d'établir des infections dans des niches extra-intestinales de leur hôte respectif. Bien que ces souches causent des infections spécifiques à leur hôte et appartiennent à des groupes phylogéniques distincts, certaines souches UPEC, NMEC et APEC partagent des facteurs de virulence, une phylogénie rapprochée et des similarités des manifestations cliniques de l'infection suggèrent une relation génétique entre ces souches ainsi qu'un risque potentiel zoonotique provenant des souches APEC [65-68]. Une étude sur 1074 souches ExPEC, dont 452 APEC, 91 NMEC et 531 UPEC, a révélé que la majorité des souches appartenant à un groupe a des caractéristiques différentes et font partie de regroupements de souches génétiquement distinctes. Cependant, un petit nombre de souches ExPEC, 108 isolats d'origines variées, ont été identifiés comme étant génétiquement reliées puisqu'elles possédaient un chevauchement substantiel de facteurs de virulence. Plus de 90 % de ces souches UPEC, NMEC et APEC font partie du groupe phylogénétique B2 de la collection ECOR (*Escherichia coli* Reference Collection; qui comprend 72 souches d'*E. coli* isolées d'une variété d'hôtes et de localisations géographiques différentes) et sont de sérogroupe O1, O2 et O78 [68, 69]. Ces mêmes

sérogroupes sont d'ailleurs les plus souvent incriminés lorsqu'un poulet est atteint de colibacillose [54, 70]. D'autres études, de plus petite envergure, ont démontré également une relation génétique entre certaines souches ExPEC d'origine humaine et animale suggérant un risque zoonotique potentiel par les souches APEC [65, 67, 71-74]. En d'autres mots, le poulet est soupçonné d'être un réservoir important de souche ExPEC causant des infections chez l'humain.

Or, il faut savoir que c'est le tractus intestinal des humains qui est le réservoir immédiat des souches ExPEC. Ces souches sont retrouvées dans la flore intestinale normale de l'homme, et ce, sans causer de symptômes indésirables [3]. Tel que mentionné ci-haut, c'est la contamination fécale-urogénitale qui est responsable de l'établissement d'une infection urinaire chez l'homme [51] et c'est la contamination de la flore vaginale de la mère qui est soupçonnée d'engendrer des méningites chez les nouveau-nés [52]. Toutefois, quelques études ont démontré que les viandes de consommation, principalement le poulet, mais aussi le porc et le bœuf, peuvent être contaminées par des souches ExPEC, et que certaines de ces souches sont identiques à celles causant des infections extra-intestinales chez l'homme [66, 75-77]. Ceci suggère que les viandes de consommation seraient une source potentielle d'acquisition des souches ExPEC par l'homme.

Résistance aux antibiotiques

Une conséquence importante de cette hypothèse est l'augmentation de la résistance aux antibiotiques par les souches ExPEC et/ou *E. coli* pathogène. L'utilisation d'antibiotiques comme facteur de croissance est une pratique courante chez les éleveurs, puisqu'elle permet une meilleure absorption des nutriments et une prévention des infections bactériennes, ce qui en résulte par une baisse de morbidité et de mortalité chez les troupeaux d'élevage [78]. Par ailleurs, cette pratique crée une pression de sélection constante sur les bactéries de la flore intestinale des animaux et engendre inévitablement des résistances aux antibiotiques [79]. À cause de cette utilisation massive d'antibiotique lors de l'élevage, les viandes de consommation peuvent être fréquemment contaminées par des souches bactériennes résistantes, dont *E. coli* [79, 80]. Ces souches résistantes

peuvent ensuite coloniser le tractus gastro-intestinal de l'homme et ainsi créer des infections gastro- et extra-intestinales. L'utilisation d'antibiotiques, telles que les β-lactames, pour contrer ces infections devient alors problématique [80]. Toutefois, la proportion de souches ExPEC résistantes aux antibiotiques est plutôt faible en comparaison avec les souches commensales des animaux, bien que cette résistance soit de plus en plus rapportée [76, 81, 82]. À ce jour, seulement quelques corrélations ont été établies entre la résistance aux antibiotiques des souches ExPEC et le réservoir animal [83-85]. Cependant, l'acquisition de gènes de résistance aux antibiotiques par transfert horizontal par les souches ExPEC en provenance des souches commensales des animaux est un élément important à considérer et à surveiller.

Les facteurs de virulence des souches ExPEC

Plusieurs facteurs de virulence sont reconnus pour leur importance dans l'établissement d'une infection extra-intestinale par les souches ExPEC. Bien qu'il existe une grande diversité génétique entre elles, plusieurs facteurs de virulence connus sont majoritairement présents chez bon nombre de souches ExPEC et participent à leur virulence (Tableau 1). De plus, ces facteurs de virulence sont fréquemment retrouvés en association avec d'autres gènes de virulence, et ce, à l'intérieur des îlots de pathogénicité (PAI) ou sur des plasmides. En effet, les souches ExPEC possèdent généralement plusieurs îlots de pathogénicités et/ou plasmides codant pour une grande diversité de facteurs de virulence, ce qui résulte en une mosaïque génomique où plus d'une copie d'un gène de virulence s'y retrouve [3, 33, 86]. Cette variabilité génétique explique la grande diversité pathogénique des souches ExPEC.

Tableau 1: Facteurs de virulence des souches ExPEC adapté et modifié de [3]

Catégorie fonctionnelle	Gène ou opéron	Fonction	Expérimentation *in vivo*
Adhésine	*Pap*	Fimbriae P	UPEC [87]
	sfa / foc	Fimbriae S et F1C	UPEC [88]
	Fim	Fimbriae type 1	UPEC [89]
	Iha	Adhésine et récepteur de sidérophore	UPEC [90, 91]
	csgA	Curli	APEC [92]
Toxine	*Hly*	α-hémolysine	ExPEC [93]
	cnf1	Facteur de nécrose cytotoxique 1	UPEC & NMEC [94, 95]
	Sat	Autotransporteur	UPEC [96]
Nutrition	*irp, fyuA*	Yersiniabactin et récepteur	UPEC [97]
	iucABCD, iutA	Aérobactine et récepteur	UPEC [19] APEC [16]
	iroBCDEN	Salmochéline et récepteur	APEC [16, 98]
	ireA	Récepteur de catécholate	UPEC [99]
	chuA	Récepteur de l'hème	UPEC [19]
	tonB	Énergie de transport sidérophore	UPEC [19]
	sitABCD	Transporteur ABC du fer ferreux et manganèse	APEC [100]
	znuACB	Transporteur ABC du zinc	UPEC [101]
	pstSCAB	Transport du phosphate	APEC [102]
	fbpABCD	Transport du fer (putatif)	UPEC [103]
Protectine	*kpsMT* II	Capsule polysaccharide groupe II	NMEC [104]
	Ksl (k) ABCDE	Capsule polysaccharide groupe II	UPEC [105]
	kps (k1)	Capsule polysaccharide groupe I	APEC [106]
	Rfc	Synthèse LPS O4	UPEC [107]
	proP	Osmoprotection	UPEC [108]
Divers	*ompA*	Invasion cellulaire de la barrière hémato-encéphalique (BBB)	NMEC [109]
	traJ	Invasion cellulaire de la BBB	NMEC [110]
	ibe A-C	Invasion cellulaire de la BBB	NMEC [111]
	aslA	Invasion cellulaire de la BBB	NMEC [112]
	malX	Marqueur de PAI	APEC [113]
	yjjQ	Régulateur de fer (putatif)	APEC [114]
	hofQ / yheF	Sécrétine du système de sécrétion type II (T2SS) et pili type 4 homologue (T4P)	UPEC [115]
	sisAB	Suppresseur de l'inflammation, homologue à ShiA	UPEC [103]
	upaH	Autotransporteur	UPEC [116]
	picU	Autotransporteur	UPEC [103]
	tosA	Exoproteine de la famille RTX	UPEC [103]
	c3405-10	Système de transport phosphotransferase (putatif) chez CFT073	UPEC [103]
	TcpC	Homologue au récepteur Toll/interleukine-1, inhibiteur de la réponse immunitaire par MyD88	UPEC [117]

2) Le fer : élément essentiel à la vie

Le fer est élément essentiel à la vie pour une très grande majorité d'organismes [7]. Il fait partie, en tant que cofacteur, de plusieurs processus biologiques connus. Par exemple, chez les mammifères et les bactéries, il participe au métabolisme du peroxyde et du superoxyde (catalase et peroxydase) ainsi qu'à plusieurs processus biologiques, notamment le cycle du citrate, le transfert d'électrons par la phosphorylation oxydative, ainsi que la régulation et la biosynthèse de l'ADN [7, 14, 118]. Le fer existe sous deux formes, soit sous la forme réduite Fe^{2+} ou fer ferreux, soit sous sa forme oxydée Fe^{3+} ou fer ferrique [7]. Cependant, sous des conditions physiologiques, en présence d'oxygène et à pH 7.0, le fer ferrique (Fe^{3+}) libre est toxique et tend à s'oxyder, s'hydrolyser et polymériser, ce qui génère des polymères insolubles d'oxyhydroxyde et d'hydroxyde ferrique [118]. Or, le fer est pratiquement toujours incorporé à des protéines ou en complexe avec des centres fer-soufre ou à l'hème, ce qui permet sa solubilité et une protection contre sa toxicité [7, 118].

La toxicité du fer s'explique par une suite de réactions chimiques. Tout débute lorsque des molécules d'oxygène acceptent un électron et forment le radical superoxyde $O_2^{\cdot-}$. En ajoutant un deuxième électron à ce superoxyde, un ion peroxyde O_2^{2-} est produit. Cet ion n'est pas un radical et n'est pas toxique. Cependant à pH physiologique, il y a protonation spontanée de l'ion peroxyde, ce qui résulte en la production de peroxyde d'hydrogène H_2O_2 et d'oxygène O_2. La réaction s'écrit comme suit :

$$2O_2^{\cdot-} + 2H^+ \longrightarrow H_2O_2 + O_2$$

Cette réaction se complique lorsque le peroxyde d'hydrogène rencontre le fer ferreux Fe^{2+}. Le mélange de ces deux réactifs produit spontanément un radical OH• et l'oxydation de Fe^{2+} en Fe^{3+}. Cette réaction, mieux connue sous le nom de réaction de Fenton, s'écrit comme suit :

$$Fe^{2+} + H_2O_2 \longrightarrow OH\bullet + Fe^{3+} + OH^-$$

Une autre réaction peut avoir lieu s'il y a rencontre du radical superoxyde O_2^- et le peroxyde d'hydrogène H_2O_2 [7, 119]. C'est la réaction de Haber – Weiss qui mènera à la formation du radical hydroxyle OH•:

$$O_2^- + H_2O_2 \xrightarrow{\text{catalysé par Fe}} OH\bullet + OH^- + O_2$$

Le radical hydroxyle OH• est de loin le plus toxique. En fait, il réagit fortement avec plusieurs molécules organiques cellulaires, telles que les membranes cellulaires et l'ADN et cause leur destruction [118]. Il est donc essentiel pour un organisme de séquestrer le fer de façon contrôlée, et ce, afin d'éviter la formation du radical hydroxyle OH• et d'obtenir efficacement le fer nécessaire à sa prolifération.

2.1 Les protéines liant le fer chez les humains et les animaux

Chez les humains et les animaux, le fer se retrouve complexé à des protéines de haute affinité principalement la transferrine, la lactoferrine et l'ovotransferrine. La transferrine se retrouve dans le sérum, tandis que la lactoferrine est incluse dans les granules des neutrophiles, le lait, la salive et les larmes [8]. Par ailleurs, ces protéines ont une constante d'affinité avec le fer d'environ 10^{36} M^{-1}, en plus de n'être saturées qu'à 30 à 40 %, ce qui est crucial pour assurer une séquestration constante du fer pouvant se retrouver momentanément libre dans l'organisme [118, 120]. De plus, il existe d'autres protéines de séquestration du fer, dont l'hème et l'hémoglobine, qui ont besoin du fer pour accomplir leurs fonctions biologiques [8]. La ferritine, que l'on retrouve à travers le règne animal, végétal et bactérien est une protéine d'entreposage intracellulaire du fer [9, 121]. Cette protéine est composée de 24 sous-unités formant une sphère pouvant lier jusqu'à 4500 atomes de Fe^{3+} [7, 9, 121]. Chez les bactéries, il existe une variante de la ferritine, la bactérioferritine, qui possède un hème, mais qui a une fonction similaire à la ferritine [9] .

Ces protéines de haute affinité pour le fer ont pour fonction de séquestrer le fer soluble et toxique et font en sorte que la disponibilité du fer chez les humains et animaux est

extrêmement faible. La concentration du fer ferrique soluble et disponible se situe aux environs de 10^{-24} M [10, 11, 13]. Cependant, les cellules bactériennes ont besoin de 10^5 à 10^6 ions ferriques par génération pour maintenir une concentration interne entre 10^{-7} M à 10^{-5} M [7, 12, 13]. La quantité de fer libre totale disponible aux bactéries pathogènes est donc nettement insuffisante pour permettre à cette dernière d'assurer sa survie et sa prolifération dans l'organisme hôte. Les bactéries ont donc développé diverses stratégies pour acquérir cet élément essentiel.

3) Les système d'acquisition du fer chez les bactéries

Parmi le règne bactérien, on distingue quatre grandes stratégies pour acquérir le fer nécessaire à la prolifération [7]. Il y a d'abord les sidérophores (dérivé du grec signifiant *porteur de fer*) qui sont des molécules de faible poids moléculaire ayant une forte affinité pour le fer ferrique [14]. Cette approche est utilisée par une grande variété de bactéries, mais aussi par les levures, moisissures et plantes. C'est la mycobactine qui fut le premier sidérophore à être découvert en 1949 par Snow et ses collaborateurs [122]. À ce jour, on compte plus de 500 sidérophores connus et la plupart d'entre eux se classent parmi cinq groupes selon leur structure chimique et groupement de liaison au fer (Figure 1) [15, 123, 124]. Il y a d'abord les sidérophores de type catécholate, dont le plus connu et étudié est l'entérobactine [14, 125]. L'entérobactine, aussi nommé entérochelin, est un triester cyclique de 2,3-dihydroxy-*N*-benzoyl-L-serine [126, 127]. Les sidérophores de type catécholate lient le fer ferrique avec ses groupements hydroxyles des catéchols de la molécule. La présence de trois catéchols et leur hydroxyle procure une liaison hexadentate avec le fer ferrique et fait de l'entérobactine un ligand extrêmement puissant (constante de formation 10^{52} M^{-1}) [123, 128].

Les sidérophores de type phénolate s'apparentent aux catéchols, avec un hydroxyle en moins sur l'anneau de benzène. La yersiniabactine de *Yersinia pestis* et la pyocheline de *Pseudomonas aeruginosa* sont des sidérophores de type phénolate [15].

Les sidérophores de type hydroxamate constituent la troisième catégorie dont fait partie une molécule bien connue, soit le ferrichrome qui est synthétisé par le basidiomycète

Ustilago maydis [129]. Ce dernier forme également une liaison hexadentate avec le fer ferrique grâce à ses atomes d'oxygène. La staphyloferrine A de *Staphylococcus* et l'achromobactine de *Erwinia chrysanthemi* font partie de la catégorie des carboxylates, puisque leurs structures contiennent des groupements carboxyles [15]. La dernière catégorie représente les sidérophores de structures mixtes. L'aérobactine, qui est un dérivé de l'acide 6-(*N*-acetyl-*N*-hydroxyamino)-2-aminohexanoïque et de l'acide citrique, fait partie de cette catégorie. Une liaison hexadentate avec le fer ferrique a également lieu [129, 130].

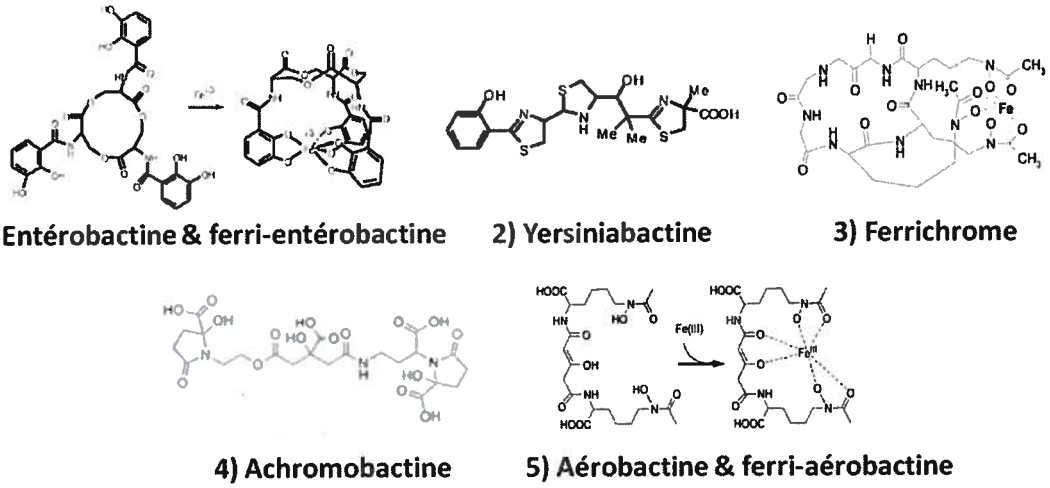

Figure 1 : Structure et coordination avec le fer des sidérophores 1) catécholate 2) phénolate et 3) hydroxamate 4) carboxylate et 5) mixte. Adapté de [7, 15, 123, 131]

Une deuxième stratégie grandement utilisée par les bactéries pathogènes est l'incorporation des protéines de l'hôte, soit la transferrine, la lactoferrine et l'hémoglobine, à l'aide de récepteurs spécifiques de la membrane externe énergisés par le complexe TonB-ExbB-ExbD [14, 132]. *Neisseria meningitidis*, *Neisseria gonorrhoeae* et *Haemophilus influenzae* possèdent des récepteurs spécifiques, TbpAB et LbpAB, qui captent et internalisent les complexes Fe^{3+}-transferrine et Fe^{3+}-lactoferrine, respectivement [14, 132]. L'hémoglobine et le complexe hémoglobine-haptoglobine peuvent aussi être canalisés par les récepteurs HpuAB et HmbR de *N. gonorrhoeae* et *H. influenzae*, respectivement [14, 133]. De plus, de nombreuses bactéries pathogènes prélèvent directement l'hème du milieu extracellulaire [132]. Par exemple, on retrouve le

récepteur ChuA chez *E. coli* uropathogène CFT073 et son homologue ShuA chez *Shigella dysenteriae* [19, 133]. Il existe également des hémophores (HasA, HasAp et HxuA) sécrétés par certaines bactéries dont *Serracia marcescens, P. aeruginosa* et *H. influenzae*, qui lient l'hème de la myoglobine et de l'hémopexine et qui sont ensuite saisi par le récepteur HasR, de façon similaire aux sidérophores [133, 134].

La troisième stratégie d'obtention du fer est la réduction du fer ferrique en fer ferreux et le transport du fer ferreux. On retrouve chez *E. coli* le système de transport du fer ferreux FeoAB qui est induit principalement en condition anaérobique et qui transporte et réduit le fer ferrique en fer ferreux [135].

Finalement, la dernière stratégie d'acquisition du fer se fait par les transporteurs de métaux de type ABC. Plusieurs transporteurs d'ions métalliques divalents, dont Fe^{2+}, sont connus tels que les systèmes SfuABC, SitABCD, YfeABC, FbpABC et FutABC que l'on retrouve chez plusieurs bactéries, soit *S. marcescens*, *Salmonella typhimurium*, *Y. pestis*, *N.gonorrhoeae* et *Synechocystis* PCC 6803, respectivement [136-140]. Le rôle du système SitABCD pour la virulence de la souche APEC χ7122 a d'ailleurs été démontré par notre groupe de recherche (Annexe II) [100].

4) Les sidérophores chez les bactéries pathogènes : facteur de virulence

Chez les humains et les animaux, le fer est complexé à diverses protéines, le rendant ainsi très peu disponible pour les bactéries. La capacité des bactéries à obtenir le fer nécessaire à leur croissance et leur prolifération dans un organisme est considérée comme un déterminant de virulence important [141]. Afin de contrer cette immunité nutritionnelle, plusieurs systèmes de sidérophores sont nécessaires pour la virulence des diverses bactéries pathogènes. D'abord, la synthèse et l'internalisation de la yersiniabactine produit par la bactérie *Y. pestis*, agent pathogène de la peste, est requis pour la virulence de la souche puisque des mutants de synthèse (Δ*irp2*) et du récepteur et (Δ*pns*) sont atténués dans le modèle d'infection sous-cutanée murin [142]. Chez *Burkholderia cenocepacia*, pathogène respiratoire opportuniste chez les patients atteints de fibrose kystique, la synthèse et l'internalisation du sidérophore ornibactine par le récepteur OrbA

sont requises pour la virulence de la souche dans un modèle d'infection respiratoire chronique de rat [143, 144]. La synthèse de la vibriobactine par *Vibrio cholerae*, agent pathogène responsable du cholera, est un facteur important de la virulence de la souche, puisqu'un mutant *vib*- colonise moins bien les intestins que la souche sauvage et ne causent pas de diarrhée chez le modèle d'infection de souris néonatale [145].

La redondance des systèmes d'acquisition du fer peut parfois masquer l'importance individuelle de chaque système pour la virulence de la souche. C'est d'ailleurs le cas pour le pathogène respiratoire opportuniste *P. aeruginosa* qui possède deux systèmes de sidérophores, soit la pyochelin et la pyoverdine. Dans le modèle d'infection intramusculaire de souris immuno-supprimées, seul un double mutant pyochelin et pyoverdine négatif a démontré une atténuation de la virulence. Cependant, dans un modèle d'infection intranasale, un mutant de synthèse de la pyoverdine et le double mutant pyochelin et pyoverdine négatif ont été retrouvés en moins grand nombre dans les poumons et le sang des animaux infectées en comparaison avec la souche sauvage. Ceci suggère un rôle combiné des systèmes de sidérophore pour la virulence de la souche [146].

Chez la souche APEC χ7122, on retrouve trois systèmes d'acquisition du fer par les sidérophores, soit l'entérobactine, les salmochélines et l'aérobactine, Le rôle des ces sidérophores pour la virulence des entérobactéries et de la souche APEC χ7122 sera discuté et démontré dans les sections sous-jacentes.

5) L'homéostasie du fer chez *E. coli* par Fur et RyhB

Fur est une protéine régulatrice de 17 kDa qui se dimérise en solution en présence de zinc et forme un complexe avec le fer ferreux (Fe^{2+}) [147, 148]. Ce complexe reconnait une séquence consensus de trois ou quatre hexamères adjacents et imparfaits de 5'-GATAAT-3', nommée boîte Fur, qui sont généralement situées entre les sites -35 et -10 des promoteurs [149]. Lorsque la concentration intracellulaire en fer est suffisante, le complexe Fur-Fe^{2+} s'apparie à l'ADN de la boîte Fur des promoteurs et empêche ainsi la transcription du gène en aval (Figure 2) [7].

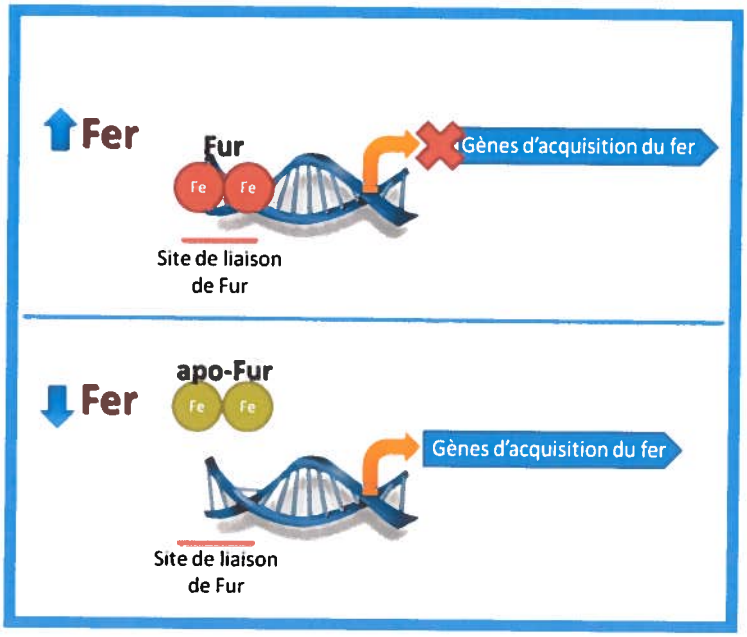

Figure 2 : Mécanisme de la régulation négative par Fur. Adapté et modifié de [7]

Par ailleurs, un profil transcriptionnel du modulon Fur a été effectué chez *E. coli* MC4100 et son dérivé *fur* ⁻ [150]. Il a été trouvé que 101 gènes sont différentiellement exprimés en présence d'un chélateur de fer et chez le mutant Δ*fur*, dont 53 sont sous le contrôle négatif du régulateur [150]. Ces gènes se regroupent en trois catégories fonctionnelles, soit la réponse à une carence en fer, le métabolisme énergétique et des gènes de fonctions inconnues ou diversifiées. Parmi ces gènes, 48 sont induits par le complexe Fur-Fe^{2+}, et ce, toute catégorie confondue. Fur ne joue donc pas seulement le rôle de répresseur de système d'obtention du fer, il est en fait un régulateur global [150]. D'ailleurs, Fur module l'expression des gènes de transport et d'immunité de la colicine V, *cvaA* et *cvi* chez *E. coli* [151]. Le gène *sodB* codant pour une superoxyde dismutase d' *E. coli* est également sous le contrôle positif de Fur [152]. Chez *S.* Typhimurium, c'est le système de sécrétion type III de l'îlot de pathogénicité 1 (SPI1) qui est régulé notamment par Fur [153]. Il a été proposé que la régulation positive par Fur agirait sur des gènes impliqués dans la virulence de souches pathogènes, puisque, lors d'une infection chez l'humain et les mammifères, elles se retrouvent en milieu où le fer n'est pas disponible [154]. Toutefois, les mécanismes sous-jacents la régulation positive par Fur restent encore à élucider.

Or, la découverte d'un petit ARN régulateur, RyhB, a permis de fournir une partie de la réponse. En effet, un deuxième niveau de régulation de l'homéostasie du fer s'ajoute à celui établi par Fur et c'est celui de la répression post-transcriptionnelle générée par l'ARN non codant RyhB [155]. Cet ARN de 90 nucléotides, également régulé négativement par Fur, stimule la dégradation des ARNm cibles et de lui-même en recrutant le dégradosome d'ARN, un complexe formé de l'ARNaseE, du polynucléotide phosphorylase, de l'enolase et de l'hélicase d'ARN [156]. De plus, RyhB nécessite la chaperonne Hfq pour sa stabilité et pour l'appariement antisens avec les ARNm cibles [155, 156]. Ainsi, lors d'une carence en fer, RyhB sera transcrit et ira s'apparier aux ARNm cibles, soit les transcrits codants pour les protéines ferriques non essentielles et les protéines d'entreposage du fer, et recrutera la machinerie de dégradation des ARNm cellulaires afin d'initier la dégradation du complexe (Figure 3) [156]. Ce mécanisme de sélection permettra une augmentation prompte du fer intracellulaire, une utilisation du fer libre par des protéines essentielles et une levée rapide de la régulation orchestrée par RyhB [157].

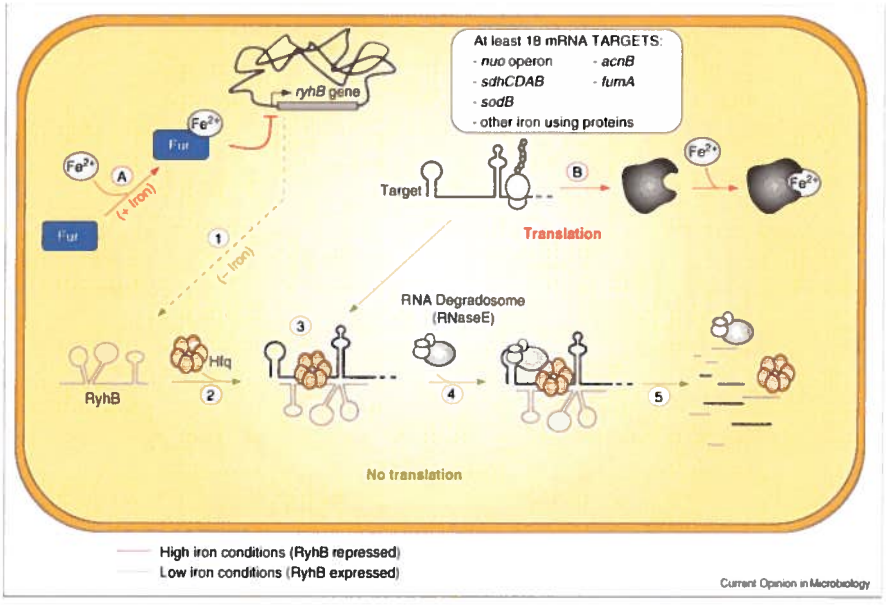

Figure 3 : Mécanisme de régulation de l'homéostasie du fer par Fur et RyhB chez *E. coli*. Tiré de [158]

De plus, une étude sur la surexpression de RyhB démontra que ce dernier semble moduler l'expression d'au moins 18 opérons chez *E. coli* K12 reliés de près ou de loin à l'utilisation du fer [159]. RyhB régule notamment l'expression des gènes codant pour des enzymes ferriques du cycle TCA, soit *sdhCDAB*, *fumA* et *acnA*, le gène de la superoxyde dismutase, *sodB*, les gènes codant pour les protéines ayant un centre Fe-S, *iscRSUA* et *sfuABCDSE*, ainsi que deux gènes codant pour les ferritines et bactérioferritines, qui sont des protéines d'entreposage du fer, soit *ftnA* et *bfr* [159]. Fait à noter, ces gènes ont également été classés sous le contrôle positif du régulateur Fur et seule l'activation directe de *ftnA* par Fur a été clairement démontrée à ce jour [155, 160]. En fait, il faut comprendre que pour certains gènes, la répression de RyhB par Fur en milieu riche en fer permet l'expression de ces gènes dits positivement régulés par Fur. À ce jour, le mécanisme exhaustif de la dégradation des ARNm par RyhB a été démontré seulement pour les ARNm de *sodB* et *iscRSUA* [156, 161]. De plus, RyhB régule également la synthèse de Fur, puisqu'une séquence en amont du codon d'initiation est reconnue par RyhB dont l'appariement en antisens réprime l'expression de Fur [162]. En somme, la régulation du fer par Fur et RyhB chez *E. coli* est un mécanisme complexe, dont le principe est résumé simplement par le schéma ci-dessous (Figure 4).

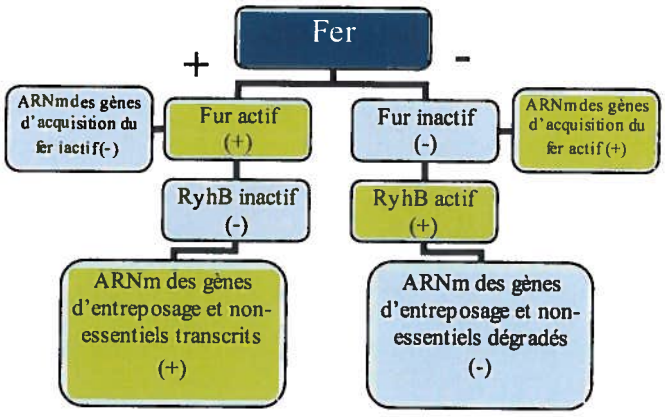

Figure 4 : Schéma de la régulation du fer par Fur et RyhB chez *E. coli*. Tiré de [155, 162]

Par ailleurs, un deuxième mécanisme d'action de RyhB, outre la dégradation des ARNm, a été découvert chez *E. coli*. RyhB permet la destruction d'une structure inhibitrice

intrinsèque de l'ARNm de *shiA*, qui code pour un récepteur de l'acide shikimique, et qui séquestre le site de liaison du ribosome, soit la séquence Shine-Dalgarno, empêchant ainsi sa traduction [163]. RyhB, dont la séquence est complémentaire à la séquence inhibitrice, s'apparie à la structure répressive dégageant ainsi la séquence Shine-Dalgarno, ce qui permet alors la traduction de *shiA* [163]. C'est d'ailleurs le premier exemple d'une activation directe par RyhB de la traduction d'un gène.

Puisque ShiA est un récepteur de l'acide shikimique et que ce dernier est un précurseur du chorismate, qui lui-même entre dans la composition de l'entérobactine, il est raisonnable de penser que l'absence de RyhB aura une incidence sur la synthèse de l'entérobactine. Ce fut d'ailleurs l'hypothèse de départ qui mena à une collaboration entre le groupe de recherche du Dr. Massé de l'Université de Sherbrooke et celui du Dr. Dozois/Dr. Lépine de l'Institut Armand-Frappier. Or, il a été trouvé que RyhB affectait bel et bien la synthèse de l'entérobactine, mais par un autre mécanisme impliquant la sérine acetyltransférase CysE (Annexe III).

6) Le sidérophore aérobactine

L'aérobactine a d'abord été isolée et caractérisée en 1969 à partir de cultures d'*Aerobacter aerogenes* cultivées dans un milieu pauvre en fer [164]. Ce système a d'abord été identifié sur le plasmide de virulence ColV retrouvé chez des souches d'*E. coli* septicémiques, sans toutefois isoler spécifiquement les gènes responsables de ce nouveau système d'acquisition du fer [17, 18, 165]. Les gènes responsables de la synthèse de l'aérobactine, *iucABCD* (iron uptake chelate) et son récepteur, *iutA* (iron uptake transport), ont finalement été identifiés et caractérisés [166, 167]. Ces gènes sont d'ailleurs sous le contrôle négatif du régulateur Fur et c'est l'étude de cet opéron qui est à l'origine de la découverte de la séquence consensus de reconnaissance par Fur [168]. Tout d'abord, *iucD* code pour une L-lysine 6-monooxygénase dépendante du NADPH et qui catalyse l'hydroxylation du groupe ε-amino de la L-lysine et forme ainsi du N^6-hydroxy-L-lysine [169]. Ensuite, IucB, qui est une N^6-hydroxylysine *O*-acetyltransferase, catalyse l'acétylation du groupement hydroxylamine résultant en une molécule de N^6-acetyl-N^6-hydroxy-L-lysine [170]. Cette réaction nécessite l'apport de l'acétyl-CoA.

Ensuite, IucA catalyse l'acylation du groupe α-amino du N^6-acetyl-N^6-hydroxy-L-lysine avec un groupement carboxyle de l'acide citrique pour former le précurseur N^6-acetyl-N^2-citryl-N^6-hydroxy-L-lysine. Finalement, IucC condensera le produit catalysé par IucA avec une molécule de N^6-acetyl-N^6-hydroxy-L-lysine et ainsi il y aura formation de l'aérobactine (Figure 5) [130, 171].

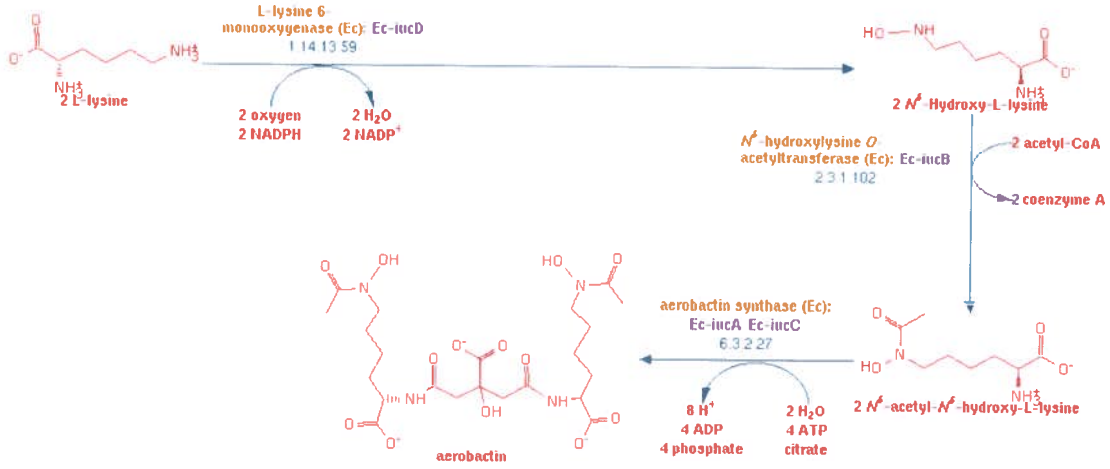

Figure 5 : Synthèse de l'aérobactine à partir de la L-lysine. Tiré de [172]

L'aérobactine est ensuite capté par un transporteur de type ABC, soit tout d'abord par le récepteur IutA [167]. Le complexe fer-aérobactine est en fait internalisé au niveau du périplasme et sera pris en charge par la protéine périplasmique FhuD [173]. FhuD acheminera ensuite le complexe au transporteur de la membrane interne composé de la perméase FhuB et de l'ATPase FhuC [174-176]. Les gènes codant pour le transporteur de la membrane interne font partie de l'opéron *fhuABCD*, dont le gène *fhuA* code pour le récepteur du ferrichrome, mais la machinerie de transport interne est partagée avec l'aérobactine [173]. De plus, cet opéron est sous la régulation de Fur [177].

7) L'entérobactine

L'entérobactine est produit par plusieurs entérobactéries, dont *E. coli, Salmonella* spp. et *Klebsiella* spp. [123]. La découverte de l'entérobactine a été faite en 1970 simultanément par deux groupes de chercheurs. Tout d'abord, O'Brien et Gibson [126] ont isolé une molécule chez *Escherichia coli* qu'ils ont nommé entérocheline et ensuite Pollack et Neilands ont baptisé entérobactine la même molécule retrouvée chez *S.* Typhimurium [127]. C'est O'Brien et Gibson qui soumirent l'article en premier, mais ce fut le papier de Pollack et Neilands qui fut d'abord publié, aboutissant en une utilisation courante des deux noms pour le même sidérophore.

La biosynthèse et le transport de l'entérobactine sont codés par 15 gènes, soit les gènes *entABCDEFHS, fepABCDEG* et *fes,* présents sur le chromosome bactérien totalisant une grande région de 22 kb (Figure 6) [123].

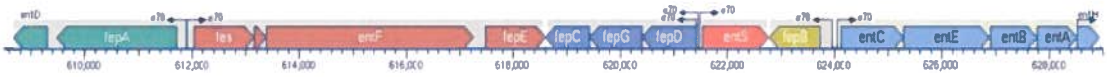

Figure 6 : Région chromosomique de l'entérobactine d'E. coli K-12 MG1655 [172].

La biosynthèse de l'entérobactine se fait en deux parties et nécessite l'apport de six gènes [178]. La première étape de la synthèse de l'entérobactine débute à partir du chorismate qui est isomérisé en isochorismate par EntC, qui est une isochorismate synthétase [178, 179]. Le groupement enolpyruvyl de l'isochorismate est retiré par EntB, qui est isochorismatase, et il y a production de 2,3-dihydro-2,3-dihydroxybenzoate (2,3-diDHB) [180, 181]. Ce dernier est oxydé par l'action de EntA, qui est une 2,3-dihydro-2,3-dihydroxybenzoate déshydrogénase, produisant ainsi du 2,3-dihydrozybenzoate (2,3-DHB) à l'aide du NAD+ (Figure 7) [181, 182].

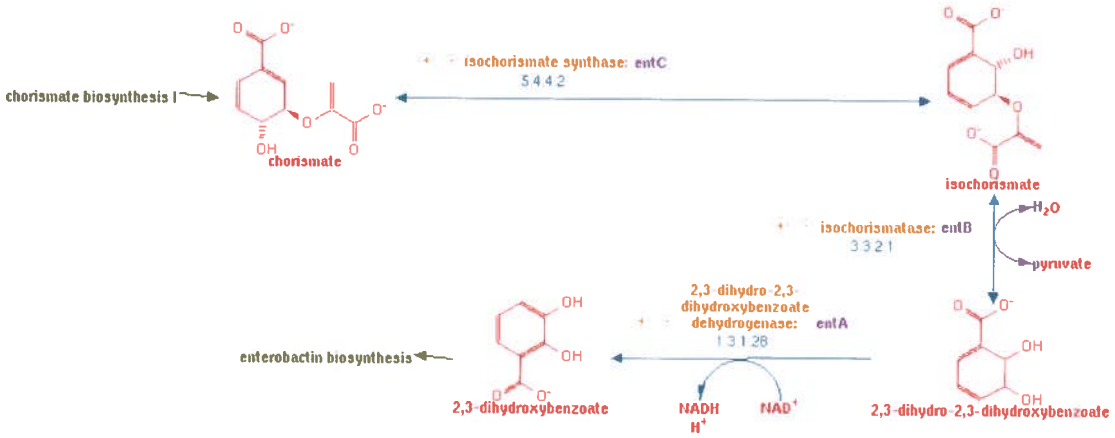

Figure 7: Biosynthèse du 2,3-DHB à partir du chorismate [172].

Par la suite, il y aura formation de l'entérobactine à partir du 2,3-DHB grâce à l'enzyme EntD et à trois enzymes du complexe « non-ribosomal peptide synthetase » (NRPS), soit EntB, EntE et EntF [123]. Les NRPS sont composés d'enzymes à plusieurs domaines enzymatiques de fonctions spécifiques qui produisent des peptides sans une matrice ARN [123, 183-185]. Les domaines nécessaires au fonctionnement du système sont la condensation (C), l'adénylation (A), la protéine « peptidyl carrier » (PCP) et le domaine thioestérase (TE). Dans ce cas-ci, EntE possède un domaine d'adénylation (A) et EntB, outre son domaine isochorismate lyase, dispose d'un domaine PCP, aussi nommé ArCP (aryl carrier protein) ou domaine de thiolation (T) [186-190]. De plus, EntF, qui est une protéine de 142 kDa, possède les quatre domaines mentionnés ci-haut, soit les domaines A, C, T et TE [187, 188]. Ainsi, ces trois enzymes constituent à elles seules le système NRPS.

En premier lieu, il y a activation des domaines T de EntB et EntF par la phosphopantetheinyl transférase (PPTase) EntD, qui catalyse une réaction de transfert de la partie phosphopantetheine (4'-PP) du coenzyme A au domaine T (Figure 8) [186, 190]

.

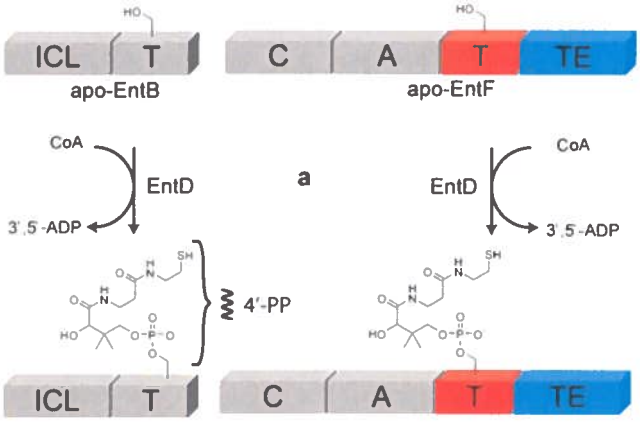

Figure 8 : Activation des domaines T de EntB et EntF par EntD. Tiré de [190]

Ensuite, c'est l'étape de l'initiation. Le domaine T activé d'EntB accueillera la molécule de 2,3-DHB, transfert effectué à l'aide d'EntE et de son domaine d'adénylation. Ceci formera l'intermédiaire 2,3-DHB-*S*-EntB [191]. Il y aura également ajout d'une sérine à la 4'-phosphopantetheine du domaine T d'EntF grâce à l'activité de son domaine A (Figure 9) [187, 191].

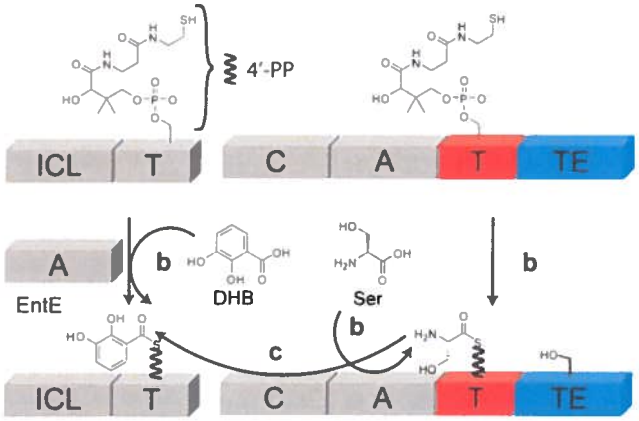

Figure 9 : Initiation de la synthèse de l'entérobactine. Transferts du 2,3-DHB au domaine T d'EntB par le domaine A d'EntE et de la sérine au domaine T d'EntF par son domaine A. Tiré de [190].

Vient ensuite l'étape de l'élongation. Le domaine de condensation d'EntF transférera la molécule de 2,3-DHB du domaine T de EntB à la sérine liée à la partie phosphopantetheinyl du domaine T de EntF, libérant la chaîne 4'-PP du domaine T de EntB [187, 188]. À cette étape, le DHB-Ser présent sur le domaine T sera transféré au

domaine TE adjacent, afin de transférer le 4'-PP qui accueillera à nouveau une molécule de sérine. La condensation du DHB et de la sérine aura lieu deux autres fois, afin d'accumuler assez de précurseurs pour former le triester de DHBS [187, 188]. Finalement, il y aura cyclisation intramoléculaire de la molécule linéaire par le domaine TE et relâche de l'entérobactine cyclique (Figure 10) [190].

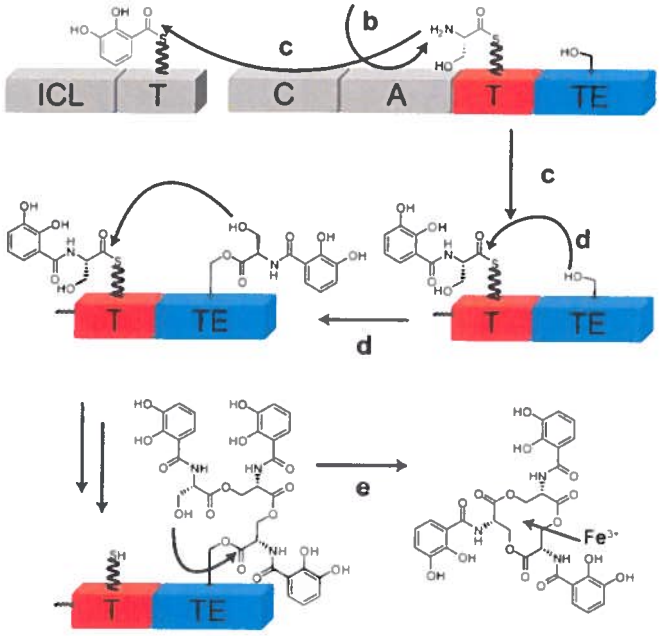

Figure 10 : Élongation et terminaison de la biosynthèse de l'entérobactine par condensation et transfert des précurseurs. Tiré de [190]

La formation de l'entérobactine par le complexe NRPS est un processus complexe et laborieux. Plusieurs précurseurs de l'entérobactine (monomère et dimère de DHBS) sont d'ailleurs relâchés prématurément lors de la synthèse de ce dernier en conditions physiologiques. En fait, une agglomération trop importante de ces précurseurs intracellulaires serait à l'origine de cette relâche précoce [192].

7.1 La sécrétion de l'entérobactine par EntS

Le sidérophore entérobactine est synthétisé dans le cytoplasme de la bactérie pour être ensuite exporté par la protéine transmembranaire EntS de 43 kDa, autrefois nommé P43

[193]. Cette protéine est le produit du gène *entS*, antérieurement nommé *ybdA*, qui se situe en antisens entre les gènes *fepB* et *fepD* (figure 6) [194]. Une mutation dans le gène *entS* ne permet plus la détection de l'entérobactine cyclique dans le surnageant de culture bactérien, alors que les molécules dégradées, soit le monomère, dimère et trimère de DHBS, sont toujours présentes [193]. Ceci suggère que le sidérophore cyclique ne s'accumule pas dans le cytoplasme de la bactérie, mais qu'il est dégradé par l'estérase Fes même si la molécule n'a jamais été sécrétée [195]. Les molécules de DHBS dégradées sécrétées sont de faibles sidérophores, mais assez efficaces pour nourrir la bactérie en fer [196]. Lorsque la molécule d'entérobactine est sécrétée à l'extérieur de la bactérie, cette dernière séquestrera le fer ferrique de l'environnement et ainsi il s'y formera le complexe ferri-entérobactine (Fe^{3+}-Ent) [128].

De plus, la protéine de la membrane externe TolC est également impliquée dans la sécrétion de l'entérobactine chez la bactérie *E. coli* K-12 W3110, puisqu'une délétion de ce gène cause une déficience de croissance en milieu pauvre en fer et un arrêt de la sécrétion de l'entérobactine, bien que l'expression du gène ne soit pas régulée par la présence ou l'absence de fer [197]. TolC est une protéine tunnel de la membrane externe également impliquée dans les systèmes de résistance aux antibiotiques multiples et macrolides, dont AcrAB-TolC, EmrAB-TolC et MacAB-TolC qui pompent les molécules hors du cytoplasme bactérien [198, 199]. De plus, TolC facilite l'importation de la colicine E1, interagit avec HlyBD pour la sécrétion de l'hémolysine, en plus d'être impliqué dans la sécrétion d'entérotoxines [200-202]. TolC n'est donc pas un transporteur spécifique de l'entérobactine.

7.2 Le transporteur de type ABC : FepA, FepB, FepD, FepG et FepC

Le transport du complexe ferri-entérobactine du milieu extracellulaire jusqu'au cytoplasme bactérien nécessite l'apport d'un transporteur de type ABC qui est encodé par les gènes *fepABCDG* [194]. Il y a d'abord le gène *fepA* qui code pour le principal récepteur de l'entérobactine localisé dans la membrane externe [203, 204]. FepA est une protéine de 81 kDa constituée de deux domaines. Le premier domaine transmembranaire est formé de 22 feuillets bêta antiparallèles organisés spatialement en forme de baril [205,

206]. Le deuxième domaine est constitué d'un mélange de quatre feuillets bêta, de courtes hélices alpha et de boucles formant le « plug domain » du récepteur [205]. Ce domaine a la propriété de lier le complexe ferri-sidérophore qui ainsi subi un changement de conformation permettant la translocation du complexe [207]. Une mutation chez *E. coli* K-12 dans le gène *fepA* abolit le transport du complexe ferri-entérobactine vers le périplasme bactérien [203, 208]. De plus, le récepteur FepA peut lier d'autres substrats de type catécholate, tels que le DHBS et les analogues synthétiques de l'entérobactine TRENCAM et MECAM, ainsi que les colicines B et D [196, 206, 209-211]. De plus, d'autres récepteurs de DHBS ont été identifiés. Les récepteurs Cir, Fiu et Iha sont des protéines de la membrane externe qui internalisent le DHBS préférentiellement à l'entérobactine [91, 196, 212]. Les récepteurs Cir et Fiu sont retrouvés chez la très grande majorité des *E. coli*, tandis qu'Iha est plutôt associé aux souches UPEC [91]. D'ailleurs, une étude effectuée dans le laboratoire du Dr. Dozois a démontré le rôle d'Iha pour la virulence de la souche UPEC UCB3, ainsi que sa fonction double de récepteur de sidérophore et d'adhésine (Annexe I).

Par ailleurs, les récepteurs de sidérophores, dont FepA, translocalisent le complexe ferri-sidérophores au périplasme grâce à la force protomotrice générée par le complexe protéique TonB-ExbB-ExbD, déclenchant ainsi un changement de conformation de ce dernier menant à l'internalisation du complexe [213, 214]. Ce système de transduction d'énergie est composé d'une protéine TonB, deux protéines ExbD et sept protéines ExbB [215]. De plus, ce complexe transmembranaire de la membrane interne est constitué de domaines logés de part et d'autre de la membrane cytoplasmique. En fait, ExbD possède un domaine logé du côté périplasmique, tandis qu'un domaine de ExbB se situe du côté cytoplasmique [216]. Tout d'abord, le complexe ExbB-ExbD utilise la force protomotrice de la membrane cytoplasmique et transmet l'énergie à TonB [216]. Ensuite, TonB, qui se situe au niveau du périplasme, fait la navette entre le complexe ExbB-ExbD et FepA, à qui il transmet son énergie [217]. C'est d'ailleurs la présence du complexe ferri-sidérophore qui recrute TonB à la membrane externe [217]. TonB a la propriété d'interagir avec d'autres protéines de la membrane externe, dont FhuA, BtuB et FecA [216, 218].

Lorsque la translocalisation du complexe ferri-entérobactine au niveau du périplasme a eu lieu, ce dernier va se lier à la protéine périplasmique FepB [203, 208, 219]. FepB sert de navette entre le récepteur FepA et les protéines transmembranaires FepCDG afin de livrer le complexe ferri-entérobactine au transporteur spécifique de la membrane interne [220]. L'étape finale de translocalisation du complexe ferri-entérobactine du périplasme au cytoplasme nécessite l'apport des protéines transmembranaires FepCDG localisées dans la membrane interne de la bactérie [220, 221]. Tout d'abord, FepC est une protéine cytoplasmique possédant un site de liaison de l'ATP, tandis que FepD et FepG sont deux protéines hydrophobes membres de la famille des perméases [220-222]. FepD et FepG forment en fait un hétérodimère transmembranaire, dont la translocation du complexe ferri-entérobactine est facilitée par deux protéines FepC qui transmettent l'énergie nécessaire au transport [220, 222]. Une mutation dans l'une de ces trois protéines abolit le transport du complexe ferri-entérobactine [221], ainsi que le transport de la salmochéline S4 ou DGE, qui est un sidérophore modifié de l'entérobactine [223]. Toutefois, aucune accumulation périplasmique du complexe ferri-entérobactine n'a lieu en absence de FepB, bien que FepA soit actif. En fait, il semblerait que le complexe soit évacué du périplasme vers l'extérieur par TolC [224].

7.3 La dégradation de l'entérobactine par l'estérase Fes

L'estérase Fes a la propriété d'hydrolyser les liaisons ester de l'entérobactine afin de libérer le fer complexé à la molécule [225, 226]. Cette hydrolyse est nécessaire pour le relâchement du fer ferrique dans le cytoplasme bactérien qui ainsi boucle le cycle d'acquisition du fer par l'entérobactine [226]. La protéine responsable de la dégradation de l'entérobactine a été d'abord isolée en 1971 par chromatographie sur colonne de Sephadex avec une protéine de ~140 000 Da, nommée composante A et une protéine de ~ 22 000 Da, appelée composante B. L'activité enzymatique de chacune de ces composantes sur l'entérobactine purifié était alors de l'ordre de 10 % et grimpa à 120 % en combinant les deux composantes [195]. Par la suite, on testa biologiquement la dégradation de la entérobactine par des extractions cellulaires de mutants Δ*fesB*; et seul le composant B possédait l'activité enzymatique recherchée [226]. On nomma ainsi *fes* le

gène localisé à la 14^{e} minute sur le chromosome d'*E. coli* et oublia la composante A [195, 227]. Des études plus récentes démontrèrent que Fes est une protéine de 43 kDa qui est difficile à purifier, puisqu'elle est fortement associée à deux autres protéines [228, 229]. Neanmoins, l'enzyme Fes purifiée reconnaît les trois liens esters de la molécule d'entérobactine liée ou pas au fer ferrique [228, 229]. Ainsi, il existe trois formes de produits de dégradation de l'entérobactine, soit le monomère, le dimère et le trimère de DHBS (ou entérobactine linéaire) (Figure 11) [195, 230]. Il a été noté très tôt que l'hydrolyse de l'entérobactine est un processus irréversible, bien que le monomère de DHBS soit biologiquement actif, mais de moindre efficacité [196, 231].

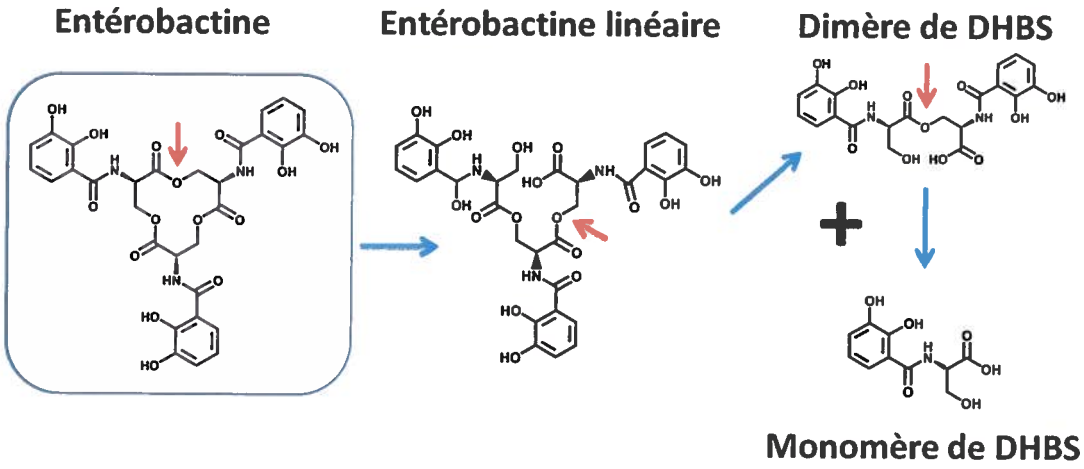

Figure 11 : Schéma de la dégradation de l'entérobactine par l'estérase Fes aux liaisons ester (flèches rouges) et production des molécules linéaires et dégradées (flèches bleues).

En somme, le système de l'entérobactine est constitué des protéines de synthèse (EntABCDEF), de sécrétion (EntS, TolC), de transport (FepABCDG) et de dégradation (Fes) (Figure 12).

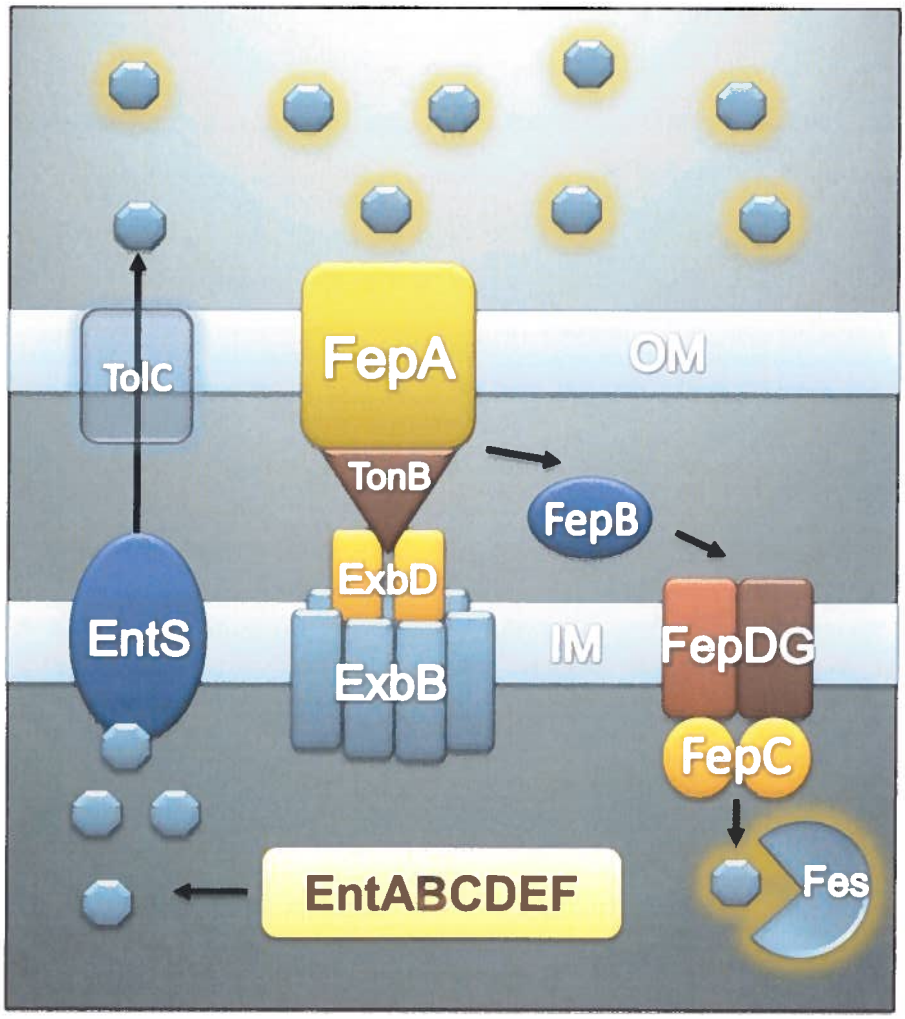

Figure 12 : Schéma récapitulatif du système d'acquisition du fer par l'entérobactine chez *E. coli*.

7.4 La régulation de l'entérobactine par Fur

La régulation de la synthèse de l'entérobactine se fait par la protéine Fur (Ferric-uptake regulator) dont la découverte eut lieu en 1978 chez des mutants de la bactérie *S.* Typhimurium qui exprimaient constitutivement les systèmes de transport de l'entérobactine et ferrichrome [232]. C'est en 1981 que l'on identifia le régulateur Fur responsable de l'expression des récepteurs de sidérophores, dont FepA, FhuA et Cir, chez *E. coli* [177]. On nota alors que Fur réprimait l'expression de gènes responsable de l'acquisition du fer, et ce, en présence de fer et que sa délétion supprimait cette répression [177, 232]. La grande région chromosomique codant pour le système de l'entérobactine

possède trois régions régulées par Fur tel que décrit à la figure 6 [233-235]. Fur joue donc le rôle de répresseur du système d'obtention du fer par l'entremise de l'entérobactine en milieu riche en fer.

8) Le locus IroA ou les gènes *iroBCDEN*

Le locus IroA, constitué des gènes *iroBCDEN*, a d'abord été trouvé chez *S. enterica* sérovar Typhimurium à la suite d'une étude portant sur l'effet d'une mutation du gène codant pour le régulateur Fur sur la synthèse des protéines régulées par le complexe fer-Fur [236]. Cependant, ce ne fut que quelques années plus tard que l'on identifia pour la première fois les gènes *iroBC* comme étant des gènes régulés par le régulateur Fur [237]. L'organisation génétique complète du locus IroA fut mise à jour deux années plus tard par le même groupe de recherche, qui, par le fait même, caractérisa partiellement le récepteur de la membrane externe IroN chez *S. enterica* [238]. Le locus IroA consiste donc en deux régions convergentes, soit un opéron *iroBCDE* possédant un promoteur en amont du gène *iroB* et le gène *iroN* dont le promoteur est indépendant des autres gènes *iro* (Figure 13) [238]. Les auteurs ont aussi noté la présence d'un site de liaison à l'ADN par le régulateur Fur dans la région en amont du codon d'initiation de la transcription du gène *iroN*. Ce site de liaison putatif est homologue à la séquence consensus de liaison de Fur, suggérant ainsi une régulation de l'expression du gène par Fur [238]. Depuis, le locus IroA a été retrouvé chez plusieurs *Enterobacteriaceae* notamment *S.enterica, E. coli, K. pneumoniae* et même chez une souche de *Shigella dysenteriae* [25, 238-242].

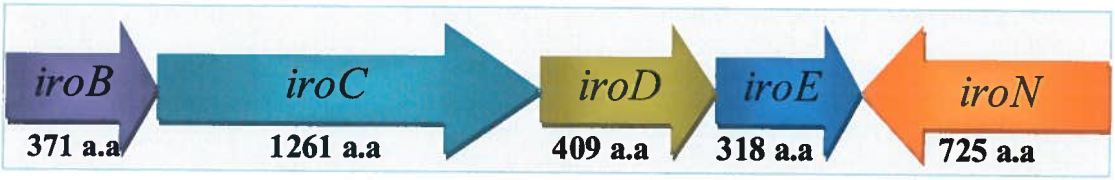

Figure 13 : Organisation génétique du locus IroA chez *E. coli* χ7122.

8.1 La synthèse des neuf molécules de salmochéline

Les salmochélines ont d'abord été découvertes en 2003 par Hantke et ses collaborateurs [24]. Les auteurs ont partiellement caractérisé ces molécules chez *S. enterica* sérovar Typhimurium et chez *E. coli* CA46. Bien qu'ils n'aient pas élucidé la structure exacte des salmochélines dans cette publication, les auteurs ont réussi à purifier partiellement certaines salmochélines et ont démontré l'incorporation du complexe salmochéline S2-^{55}Fe par le récepteur IroN présent chez *S.enterica* sérovar Stanleyville [24]. Il fallut attendre deux années de plus pour obtenir les premières structures de ces molécules. En effet, Bister et ses collaborateurs ont élucidé la structure de la salmochéline S4 ou DGE, ainsi que quatre autres salmochélines, SX, S1, S2 et S5, à partir de la souche *S. enterica* sérotype Paratyphi B IHS1319 [243]. Les quatre autres salmochélines ont été identifiées à partir d'enzymes et de substrats purifiés et non pas à partir d'une culture bactérienne [244].

Les salmochélines sont en fait des sidérophores modifiés de l'entérobactine par la glucosyltransférase IroB et dont la synthèse dépend de celle de l'entérobactine. Cette glucosyltransférase, encodée par le gène *iroB*, transfère les groupes glucosyl de l'uridine-5'-diphosphoglucose en C5 des résidus 2,3-dihydroxybenzoyl de l'entérobactine [244]. Cette enzyme peut donc ajouter un, deux ou trois glucoses à l'entérobactine, générant ainsi les trois salmochélines cycliques nommées monoglucosyl-*C*-entérobactine (MGE), diglucosyl-*C*-entérobactine (DGE) et triglucosyl-*C*-entérobactine (TGE) (Figure 14). De plus, il a été démontré de façon *in vitro* qu'IroB est la seule enzyme nécessaire pour convertir l'entérobactine en salmochélines [244]; la délétion de ce gène inhibe la synthèse des salmochélines [243].

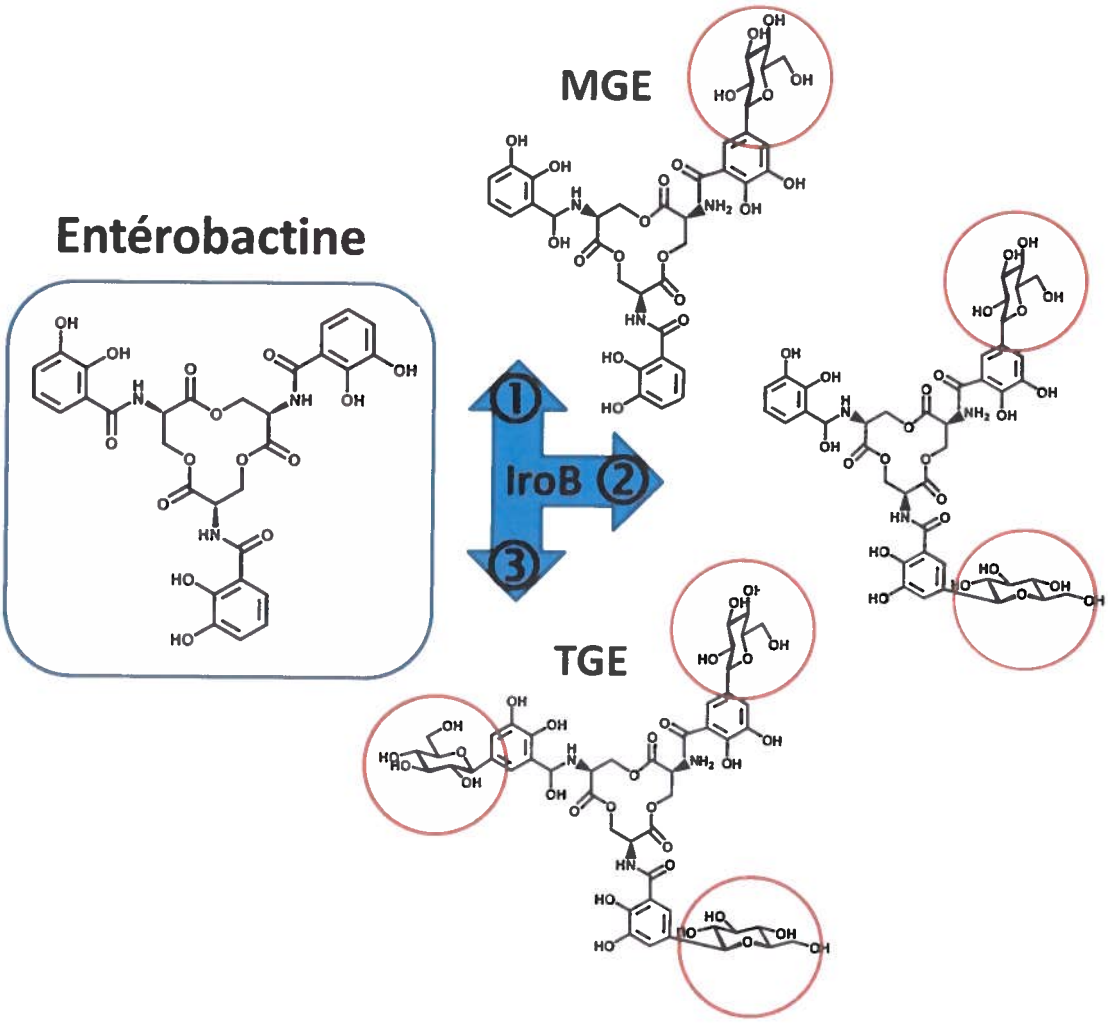

Figure 14 : Formation des salmochélines MGE, DGE et TGE par la glucosyltransférase IroB à partir de l'entérobactine.

Les six autres salmochélines sont générées à la suite de l'hydrolyse des liens ester des salmochélines cycliques. C'est d'ailleurs une étude biochimique sur les estérases IroD, IroE et Fes qui dévoila les multiples formes de salmochélines possibles. En effet, Lin et ses collaborateurs démontrèrent la production des salmochélines linéaires et dégradées à partir de salmochélines cycliques et des estérases IroD, IroE et Fes purifiées [229]. Il y a d'abord les salmochélines linéaires, soit les salmochélines MGE linéaire, DGE linéaire ou S2 et TGE linéaire, qui ayant subi une première hydrolyse, possèdent encore deux liaisons ester susceptibles à l'hydrolyse. Ainsi, les salmochélines linéaires peuvent être dégradées subséquemment en salmochélines S1 et S5 selon le niveau de glucolysation de

la molécule de départ. La salmochéline S1 est en fait un dimère de DHBS couplé à un glucose et provient de l'hydrolyse des salmochélines MGE et DGE; tandis que le dimère de DHBS possédant deux glucoses forme la salmochéline S5 et provient de la dégradation de la salmochéline TGE, seulement due à une activité régiospécifique de IroD [229]. Finalement, une hydrolyse complète des molécules S1 et S5 engendre la salmochéline SX, qui est la plus petite unité possible de salmochéline, puisqu'elle est composée d'une unité de DHBS lié à un glucose [243]. La structure de SX est aussi identique à l'acide pacifarique identifié en 1975 par Wawszkiewicz et ses collaborateurs; cet acide est d'ailleurs nommé facteur de résistance à la bactérie *Salmonella* (SRF) [245]. La figure 15 dresse un portrait de la formation des salmochélines linéaires et dégradées en fonction de leur niveau de glucolysation initial.

8.2 La pompe à efflux des salmochélines IroC

Par ailleurs, le gène *iroC* possède une forte homologie avec les pompes impliquées dans la résistance aux antibiotiques multiples (multidrugs resistance pumps) [16, 223]. En fait, IroC est responsable de la sécrétion des salmochélines S4 ou DGE, S1 et SX, en plus de sécréter en partie l'entérobactine avec EntS chez *S.* Typhimurium 140285s [223]. Or, la sécrétion des autres salmochélines (MGE, MGE linéaire, DGE linéaire, TGE, TGE linéaire et S5) par IroC et/ou EntS n'a pas été étudiée.

8.3 Les estérases Fes, IroD et IroE

Les gènes *iroD* et *iroE* codent pour des estérases de salmochélines et de l'entérobactine [229, 246]. IroD est une estérase cytoplasmique qui peut hydrolyser tous les liens ester de l'entérobactine et des salmochélines, générant ainsi les neuf molécules de salmochélines possibles [229, 246]. Fes, qui est l'estérase endogène de l'entérobactine, peut également hydrolyser certaines salmochélines dont S1, MGE, DGE et leurs formes linéaires [229]. Une étude biochimique a démontré qu'IroD, ainsi que Fes, catalysent plus efficacement l'hydrolyse des sidérophores couplés à une molécule de fer que les sidérophores non chargés. Cependant, IroE, qui est une hydrolase périplasmique, préfère seulement linéariser les formes apo des salmochélines et entérobactine (Figure 15) [229]. La linéarisation des sidérophores s'avère être un moyen efficace pour diminuer l'affinité des

membranes lipidiques et ainsi augmenter l'acquisition de fer par ces molécules. La glucosylation de l'entérobactine par IroB diminue la séquestration du sidérophore par les membranes, suggérant que IroB et IroE augmentent la capacité des pathogènes dépendants de l'entérobactine à obtenir le fer lorsque ces dernières se retrouvent dans un environnement riche en membranes lipidiques [247].

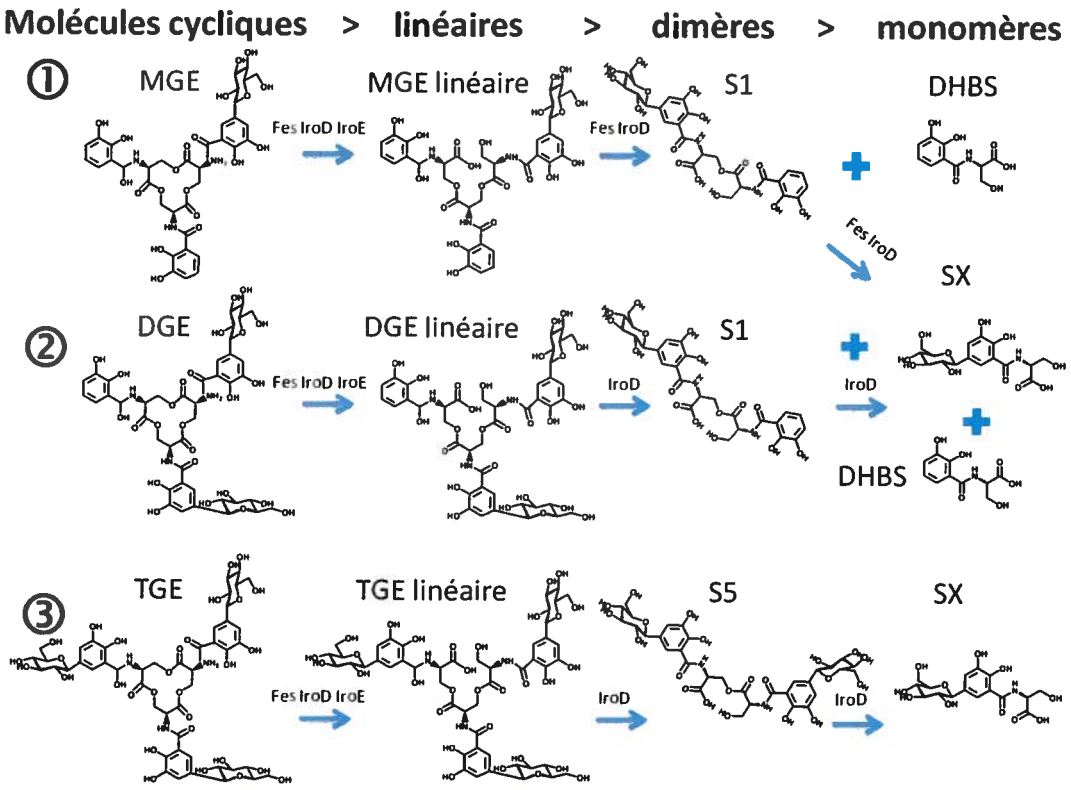

Figure 15 : Schéma de la synthèse par IroB et de la dégradation des salmochélines par Fes, IroD et IroE chez *E. coli*.

Par ailleurs, des études sur les microcines bactériennes E492, H47, M et I47 ont révélé la présence de gènes homologues à *iroB* et *iroD* dans les opérons codant pour la maturation de ces peptides antibactériens [248-251]. En fait, ces microcines subissent une modification post-traductionnelle par l'ajout de la salmochéline MGE linéaire ou S1 ou SX à l'extrémité carboxyle de la microcine [251-255]. Cet ajout permet à la microcine un spectre d'activité plus large et une plus grande puissance antibactérienne, bien qu'elle soit dépendante de la synthèse de l'entérobactine [252, 256]. De plus, l'internalisation de

ces microcines par les bactéries se fait par les récepteurs de sidérophores FhuA, FepA, Cir, Fiu et IroN et est également dépendante du complexe TonB-ExbB-ExbD [249, 251, 252, 257]. Finalement, TolC est aussi impliqué dans leur sécrétion [248, 258].

8.4 Le récepteur des salmochélines IroN

Finalement, le gène *iroN* a suscité beaucoup d'intérêt lors de sa découverte, puisque sa séquence protéique indiquait une forte homologie avec les récepteurs de l'entérobactine dépendante de TonB de plusieurs bactéries [238, 259]. IroN est en fait le récepteur des salmochélines et peut également internaliser l'entérobactine, le DHBS, la myxocheline A, la corynebactine et les microcines M, H47 et E492 [24, 243, 249, 260]. L'internalisation de ces molécules par IroN est d'ailleurs dépendante du complexe TonB-ExbB-ExbD [261]. En outre, d'autres bactéries pathogènes dont *Bordetella pertussis* et *Bordetella bronchiseptica* captent et internalisent la salmochéline S4 ou DGE par le récepteur BfeA dépendant de TonB [262].

9) Les sidérophores des ExPEC : facteurs de virulence ?

9.1 L'aérobactine est un facteur de virulence

Tout d'abord, un nouveau système d'obtention du fer encodé sur les plasmides de type ColV a été identifié comme un composant spécifique impliqué dans la virulence des souches septicémiques d'*E. coli*, et ce, de façon indépendante à l'entérobactine [18, 165]. Des expériences d'infection chez de jeunes souris adultes ont démontré que l'acquisition du fer est un élément clé dans la virulence des souches possédant le plasmide ColV [18]. De plus, ce nouveau système d'acquisition du fer confère aux souches pathogènes la capacité d'acquérir le fer de la transferrine [18]. Peu après, ce système fut identifié comme étant responsable de la production du sidérophore aérobactine et associé spécifiquement aux plasmides ColV [17]. Par la suite, on identifia les gènes codant pour l'aérobactine et l'on s'aperçut que ces gènes pouvaient se retrouver sur le chromosome bactérien de souches d'*E. coli* responsables de méningites néonatales [166, 167, 263, 264]. L'association obligatoire entre l'aérobactine et les plasmides ColV fut alors invalidée [265]. Subséquemment, on trouva préférentiellement ce système chez les souches ExPEC (UPEC et APEC) plutôt que dans les souches d'origines fécales, ce qui

associa l'aérobactine à la virulence de ces souches pathogènes [266-274]. De plus, on identifia une relation entre la présence de l'aérobactine et la haute virulence des souches APEC, déterminée par LD_{50} sur des poussins d'un jour [267, 271]. Finalement, on démontra que la souche APEC χ7122 Δ*iucABCD*Δ*iutA*, qui est incapable de produire et d'acquérir l'aérobactine, est diminuée dans sa capacité à établir une infection chez les poulets âgés de trois semaines [16]. Ainsi, ces résultats démontrèrent que le sidérophore aérobactine participe à la virulence des souches ExPEC.

Rôle physiologique de l'aérobactine

Bien que l'aérobactine participe à la virulence des souches pathogènes, il n'en reste pas moins que le sidérophore possède une constante d'affinité pour le fer 29 fois inférieure à celle de l'entérobactine (10^{23} M^{-1}) [132]. Ainsi, la redondance des systèmes d'obtention du fer suscita un questionnement quant à l'utilité de chacun et de nombreuses explications ont été proposées. Tout d'abord, la concentration d'aérobactine requise pour stimuler efficacement la croissance bactérienne en présence de streptonigrine, un agent bactéricide dépendant du fer, est 500 fois plus basse que celle de l'entérobactine [275]. Une explication plausible à cette observation est que l'aérobactine est une molécule réutilisable contrairement à l'entérobactine, ce qui expliquerait cette faible concentration nécessaire à la croissance bactérienne [275]. De plus, l'activité de l'entérobactine est diminuée significativement en présence de sérum humain et d'albumine, ce qui n'est pas le cas pour l'aérobactine [275, 276]. En fait, l'acquisition du fer par l'aérobactine à partir de la transferrine, présente dans le sérum humain, est supérieure à celle de l'entérobactine, bien que ce dernier possède une plus grande affinité pour le fer libre [277]. En outre, la rapidité de sécrétion des sidérophores semble aussi différencier les deux systèmes. Une étude a démontré qu'en condition de stress ferrique, l'aérobactine est rapidement sécrétée, tandis que l'entérobactine semble s'accumuler au niveau du périplasme pour ensuite être relâché dans le milieu externe [278]. Les conditions environnementales affectent également la production de l'aérobactine, dont la synthèse est optimale lorsque le pH est de 5.6, la température à 37°C et que le glycérol soit la source de carbone prédominante. De plus, la production d'aérobactine n'a pas lieu en milieu minimal si la température est de 42°C. Toutefois, à cette température c'est la

synthèse de l'entérobactine qui est favorisée, bien que le système de transport de ce dernier soit réprimé sous ces conditions [279, 280]. En somme, ces différences expliquent l'utilité de la redondance de ces systèmes d'acquisition du fer pour la pathogenèse des bactéries, ainsi que le rôle physiologique de l'aérobactine.

9.2 L'entérobactine peut être un facteur de virulence

La participation de l'entérobactine pour la pathogénèse bactérienne est encore un propos controversé. En fait, il a été rapporté à quelques reprises que l'entérobactine participe à l'obtention du fer lors d'une infection par des entérobactéries pathogènes, bien que cela semble être spécifique à certaines souches dans certaines conditions.

Tout d'abord, des infections intra-péritonéales de souris par des souches d'*E. coli* non-virulentes ont démontré que l'injection de fer et/ou d'entérobactine dans les animaux provoquait une augmentation significative du taux de mortalité [141, 281]. Aussi, la croissance d'*E. coli* virulents et non-virulents est inhibée dans le sérum bovin et humain, dans le lait et dans les blancs d'œufs à cause du manque de fer dans ces milieux, et que cette inhibition est levée par l'ajout de fer et/ou d'entérobactine exogène [141, 282]. L'entérobactine peut d'ailleurs prendre le fer couplé de la transferrine et de la lactoferrine [282, 283]. Aussi, l'entérobactine et ses dérivés ont été isolés de la cavité péritonéale de cobayes infectés par *E. coli*, démontrant ainsi la synthèse *in vivo* de ces molécules [284]. De plus, des études transcriptomiques ont démontré que plusieurs gènes de synthèse et de transport de l'entérobactine sont surexprimés chez la souche UPEC CFT073 cultivée dans l'urine humaine par rapport au milieu LB, ainsi que dans les communautés bactériennes intracellulaires (IBC) causées par la souche UPEC UTI89 lors d'une infection du tractus urinaire murin [285, 286].

De façon similaire, on démontra que l'ajout de fer lors d'une infection par *S.* Typhimurium virulente ou non-virulente chez la souris augmentait la létalité des souches, mais qu'un ajout d'entérobactine était profitable seulement pour les souches virulentes [287]. Finalement, un mutant incapable de synthétiser l'entérobactine chez *S.*Typhimurium exhiba un regain de virulence à l'ajout de l'entérobactine, ce qui diminua

la dose létale nécessaire pour tuer 50 % des souris infectées [288]. De plus, chez *Salmonella* Typhi, l'administration intrapéritonéale de fer confère une susceptibilité à l'infection bactérienne chez les souris, suggérant ainsi une déficience dans l'acquisition du fer par la bactérie *in vivo* [289]. Bien avant la découverte des salmochélines, il a été démontré que *S.* Typhi synthétise seulement l'entérobactine et que le récepteur FepA génère une réponse immunologique, par la présence d'anticorps anti-FepA dans le sérum, chez les patients atteints de fièvre typhoïde [290]. Ainsi, un mutant déficient dans le transport ou la synthèse de l'entérobactine présente une virulence moindre, tel qu'observé chez les souris infectées, de même qu'une croissance moindre en présence des cellules Hela et Mono Mac 6 en culture et dans le sérum humain [21, 291]. Ainsi, ces expériences suggèrent fortement que l'entérobactine participe à la pathogenèse de ces bactéries.

Or, quelques groupes de recherches ont obtenu des résultats contraires. Tout d'abord, Benjamin et ses collaborateurs ont trouvé que, bien qu'elle soit nécessaire pour la croissance dans le sérum murin, l'entérobactine n'est pas important pour la virulence des souches de *S.* Typhimurium chez les souris [22]. D'ailleurs, les gènes codant pour la synthèse de l'entérobactine sont réprimés lorsque cette bactérie se retrouve dans les macrophages murins en culture [292]. Torres et ses collaborateurs ont également constaté qu'un mutant Δ*entF*, codant pour la synthèse de l'entérobactine, chez la souche UPEC CFT073 n'est pas affecté dans sa capacité à coloniser le tractus urinaire murin [19]. De façon indirecte, un mutant de la souche APEC χ7122, possédant seulement l'entérobactine comme système fonctionnel d'obtention du fer, ne peut établir une infection systémique chez le poulet [16]. Ces publications jetèrent un doute sur l'importance de l'entérobactine pour la pathogenèse de ces bactéries.

Rôle physiologique de l'entérobactine

Plusieurs recherches ont mené à l'élucidation de diverses fonctions physiologique de l'entérobactine. D'abord, une étude sur les différents récepteurs de sidérophores de type catécholate, soit FepA, Cir et IroN révéla que seule une triple mutation des récepteurs diminue la virulence de la souche *S.* Typhimurium dans un modèle d'infection intra-gastrique murin [23]. En fait, les mutants Δ*fepA* Δ*iroN* et Δ*fepA*Δ*iroN*Δ*iroBC* ne sont pas

atténués dans ce modèle d'infection, suggérant que ni l'entérobactine, ni les salmochélines ne sont impliqués dans la pathogenèse de la bactérie, mais que le récepteur Cir et le DHBS sont des composants importants pour la virulence de la souche. Il est à noter que le DHBS est aussi un sidérophore et il provient de la dégradation de l'entérobactine et des salmochélines [196, 229]. Cependant, cette atténuation n'est pas conservée à travers les modèles d'infections, puisque la capacité infectieuse des mutants Δ*fepA*Δ*iroN*Δ*cir* et Δ*fepC* n'est pas affectée lors d'une infection par *S.* Typhimurium dans un modèle de colonisation du tractus gastro-intestinal des cobayes [293]. Par ailleurs, une mutation dans les gènes de dégradation de l'entérobactine, soit Δ*fes* et Δ*iroD*, affecte grandement la capacité infectieuse de *S.* Typhimurium chez les souris, ce qui appuie l'importance des produits de dégradation de l'entérobactine lors d'une infection systémique par le pathogène [261]. Or, ces études démontrèrent également que la norépinephrine est requise pour l'acquisition du fer de la transferrine et que l'administration de la norépinephrine chez les souris augmentait la capacité infectieuse de la souche sauvage sans affecter celle des mutants [261, 294].

Le rôle de la norépinephrine lors d'infection bactérienne a d'ailleurs été l'objet de plusieurs études. Une étude de Freestone et ses collaborateurs a démontré que la croissance d'*E. coli* dans un milieu minimum avec 30 % de sérum (SAPI+sérum) est stimulée lors de l'ajout de norépinéphrine (NE), une hormone neuroendocrine des mammifères [295]. En fait, la présence de la NE aide la séquestration du fer à partir de la transferrine et de la lactoferrine, ce qui permet à l'entérobactine de capter le fer de la catécholamine et ainsi de fournir les quantités de fer nécessaires pour la croissance des bactéries dans ce milieu [296-298]. En revanche, cette stimulation de croissance en réponse à la NE est abolie s'il y a une mutation dans la synthèse (Δ*entA*), le transport (Δ*fepA*Δ*iroN*Δ*cir*, Δ*tonB* et Δ*fepDGC*) ou la dégradation (Δ*fes* et Δ*iroD*) de l'entérobactine [293, 296, 297]. Ces données suggèrent fortement que plusieurs composantes du système de l'entérobactine sont requises afin de bénéficier de la stimulation de croissance par la NE, et ainsi valide l'importance du système pour la pathogenèse de certaines bactéries. En effet, il a été proposé que la hausse de la NE chez l'hôte pendant un stress physiologique puisse moduler l'expression de certains gènes des bactéries pathogènes et servirait de senseur physiologique [297, 299]. Cependant, chez *S.*

Typhimurium, l'expression de plusieurs gènes régulés par Fur est réprimée en présence de la NE, dont les gènes *entE, fes, ryhB, fepA, iroN, fepC, iroC, sitB* et *iroB* [293, 299]. Les auteurs expliquent ces résultats par la présence d'une grande quantité de NE qui a pour effet d'augmenter rapidement la quantité de fer intracellulaire, ce qui a pour conséquence la répression des systèmes d'acquisition du fer [293]. Par ailleurs, il a été démontré que la présence de catécholamines, dont la NE, induit la croissance d'*E. coli* commensales et pathogènes, suggérant un rôle possible dans l'induction des septicémies suite à un traumatisme [300]. En somme, la stimulation de la croissance bactérienne par la NE est reliée à l'exploitation du système de l'entérobactine, ce qui suggère un rôle physiologique important à ce sidérophore.

9.3 Les salmochelines représentent un facteur de virulence

Prévalence des gènes *iroBCDEN*

Puisque le locus IroA a été d'abord découvert chez *S. enterica*, la prévalence du gène *iroB* a été examinée chez les deux espèces de *Salmonella*. On détecte d'ailleurs *iroB* chez les six sous-espèces de *S. enterica* : *enterica* (I), *salamae* (II), *diarizonae* (IIIb), *houtenae* (IV), *arizonae* (IIIa) et *indica* (VI), mais pas chez l'espèce *S. bongori* [301]. Par la suite, un criblage moins exhaustif des gènes *iroCDEN* valida la présence du locus IroA chez les différentes sous-espèces de *S. enterica* [238]. Bien que le locus IroA ait été criblé sans succès chez quelques souches d'*E. coli*, le gène *iroN* fut identifié pour la première fois chez la souche d'*E. coli* uropathogène CP9 lors d'une étude visant à identifier les gènes bactériens surexprimés dans l'urine humaine [241]. Ceci mena à une évaluation de la présence du gène *iroN* chez d'autres souches UPEC. On retrouva d'ailleurs le gène *iroN* chez 39 % des 67 isolats cliniques [242]. Par la suite, on découvrit le locus IroA chez plusieurs autres souches pathogènes d'*E. coli*, notamment chez les souches uropathogènes archétypes *E. coli* 536 [86], CFT073 [302] et UTI89 [303]. Une étude comparative sur 508 souches associées aux infections urinaires et 416 souches d'*E. coli* fécales, vaginales et périurétrales démontra que le gène *iroN* est retrouvé entre 2.1 à 3.6 fois plus souvent chez les souches uropathogènes que les autres souches, indiquant une prévalence du gène et possiblement du locus IroA chez les souches UPEC [304]. Une étude similaire révéla la présence du gène *iroN* dans 54% des isolats sanguins d'*E. coli* de

patients atteints de bactériémie de source diverse (tractus urinaire et pulmonaire), suggérant ainsi une corrélation entre le gène *iroN* et les souches ExPEC [305].

Par ailleurs, il est intéressant de noter que la localisation du locus IroA sur le chromosome bactérien varie entre les souches ExPEC. En effet, les gènes *iroBCDEN* ont d'abord été localisés à l'intérieur de l'ilot de pathogénicité de l'ARN de transfert *thrW* de la souche *E. coli* 536, soit l'ilot PAI III_{536} [86]; tandis qu'ils se retrouvent dans l'ilot de pathogénicité de l'ARN de transfert *serX* chez *E. coli* CFT073 [302]. De plus, un criblage par PCR chez 65 souches d'*E. coli* (fécale, pathogène intestinale et extra-intestinale) démontra que le locus IroA se retrouve adjacent à un locus codant pour des fimbriae appartenant à la famille Sfa, soit F1C, SfaI, SfaII, Sfr et Fac. Les auteurs ont ainsi suggéré une corrélation entre les deux opérons en tant que membres d'un ilot de pathogénicité conservé chez plusieurs *E. coli* pathogènes ou faisant partie d'un élément génétique transférable conservé [86], tandis que cette association entre les gènes *iro* et les opérons fimbriaires n'est pas toujours conservée chez les souches d'*E. coli*. En fait, les gènes *iro* peuvent également être trouvés sur différents ilots de pathogénicités et sur des plasmides de virulence en présence et absence des gènes codant pour les fimbriaes S [86, 306-310].

L'évolution rapide des méthodes de séquençage et de criblage génétique a permis le décryptage et l'analyse de plusieurs génomes de souches bactériennes. Ceci a mené d'ailleurs à l'identification des gènes *iroBCDEN* chez les souches d'*E. coli* causant la méningite néonatale (NMEC) [2, 311, 312], chez les souches pathogènes aviaires (APEC) [16, 65, 74, 309, 313-315] et ainsi que celles causant des septicémies chez l'homme (SEPEC) [316]. Bien que les gènes *iro* aient été identifiés chez de nombreuses souches d'*E. coli* pathogènes extra-intestinaux (UPEC, APEC et NMEC), le locus IroA a également été retrouvé chez des souches d'*E. coli* probiotique Nissle 1917, asymptomatique ABU83972 et commensale A0 34/86 [307, 317, 318]. Les gènes *iro* sont donc fortement associés aux souches ExPEC, bien qu'il existe un plus faible pourcentage de souches fécales qui possèdent le locus IroA.

Implication des salmochélines dans la virulence des souches ExPEC

Tout d'abord, le récepteur IroN est important pour la virulence de la souche uropathogène CP9. En effet, la souche CP9 mutante dans le gène *iroN* est atténuée dans sa virulence lors d'une infection en compétition avec la souche sauvage dans le modèle d'infection ascendante du tractus urinaire murin [259]. De plus, l'importance du récepteur IroN pour l'infection d'une souche NMEC a été rapportée. Cette souche possède en fait plusieurs systèmes d'acquisition du fer, mais seul le récepteur de la salmochéline IroN semble important pour permettre à la bactérie d'établir une infection chez le modèle de méningite néonatale du rat [312, 319]. Par ailleurs, l'invasion des cellules uroépithéliales HCV29 est favorisée par la présence du récepteur IroN lorsqu'il est surexprimé ou natif chez des souches ExPEC (CFT073, TH2 et Do768) [320]. Ainsi, le récepteur jouerait un double rôle dans l'établissement des infections du tractus urinaire, soit au niveau de l'acquisition du fer ainsi qu'en tant que facteur d'internalisation intracellulaire [320]. L'expression du gène *iroN* est d'ailleurs augmentée de 234 fois dans les IBC (intracellular bacterial communities) présents dans les vessies de souris infectées avec la souche UPEC UTI89 par rapport à l'expression du gène dans les caecums de souris gnotobiotiques [286].

L'importance du récepteur IroN pour la virulence des souches uropathogènes fait de ce récepteur une excellente cible pour le développement d'un vaccin. Ainsi, des expériences d'immunisations sous-cutanées avec le récepteur dénaturé ont conféré une protection significative contre une infection au niveau des reins, mais se sont avérées inefficaces au niveau de la vessie, chez le modèle d'infection ascendante du tractus urinaire de la souris [321]. De plus, plusieurs récepteurs de sidéropho es, dont IroN, IutA et IreA, sont des protéines de surface exprimées par les souches UPEC cultivées dans l'urine humaine, ce qui en fait d'eux d'excellents candidats vaccinaux [322, 323]. Cependant, seuls IutA et IreA ont conféré une protection contre la souche sauvage lors d'une infection du tractus urinaire murin par la souche UPEC CFT073 [323].

Le gène *iroC* a été repêché par la technique de capture sélective de séquences transcrites (SCOTS) lors d'une infection systémique par la souche *E. coli* χ7122 chez des poulets. L'identification du gène a mené à la découverte de la région *iroBCDEN* et à sa mutation

sur le plasmide de virulence pAPEC-1 de cette souche [16]. La délétion du locus IroA résulta en une baisse significative de la persistance et de la capacité à établir une infection dans les poumons et la rate. De plus, l'élimination des séquences codant pour les gènes de synthèse et de transport de l'aérobactine et des salmochélines empêcha l'établissement d'une infection systémique chez les poulets, un phénotype qui peut être renversé à l'ajout d'un plasmide codant pour le système IroA [16]. De plus, l'introduction du locus IroA chez une souche d'*E. coli* non-pathogène procure à cette dernière la capacité d'infecter les souris intrapéritonéalement ainsi que de croitre en présence de sérum murin d'infection aiguë [26]. Chez *S.* Typhimurium, la sécrétion des sidérophores, ainsi que leurs synthèses font partie du processus infectieux chez le modèle d'infection murin, puisque les mutations individuelles Δ*entC,* Δ*entB*, Δ*iroB*, Δ*iroC* et Δ*entS*Δ*iroC* augmentent significativement la survie des animaux [223]. Ces expériences confirment le rôle important des salmochélines chez certaines souches pathogènes.

10) Le sidérocalin : nouvelle défense antibactérienne de l'hôte

La transformation de l'entérobactine en salmochéline suscite un questionnement sur la pertinence d'une telle activité par les bactéries pathogènes. Bien que les salmochélines soient des sidérophores plus efficaces que l'entérobactine en présence d'albumine [243], une autre explication de la nécessité pour les bactéries d'effectuer ce type de transformation réside en l'importante découverte en 1993 par le groupe de Borregaard qui identifia pour la première fois la protéine NGAL, soit la «neutrophile gelatinase-associated lipocalin» [324] et qui depuis porte plusieurs noms, dont lipocalin 2 (LCN2), neutrophile lipocalin humain (HNL), 24p3 ou utérocalin chez la souris et *neu*-related lipocalin chez le rat ou sidérocalin [325-327]. Cette protéine a été d'abord identifiée dans les granules spécifiques des neutrophiles et elle peut être relâchée sous diverses formes, soit comme monomère de 25 kDa, comme homodimère de 46 kDa lié par une liaison disulfure ou comme hétérodimère de 125 kDa lié à la gélatinase B (ou la matrice métalloprotéinase 9) par une liaison disulfure [324, 328, 329]. Toutefois, la synthèse du sidérocalin ne se fait pas dans les neutrophiles matures, mais bien dans ses précurseurs, soit les myélocytes et les métamyélocytes de la moelle osseuse [330]. Les protéines

synthétisées étant entreposées dans des granules spécifiques, il n'y a pas d'ARNm du sidérocalin dans les neutrophiles matures du sang [327, 330].

En 2002, le groupe de recherche de Strong a démontré, à la suite de la cristallisation de la protéine, que le sidérocalin séquestre fortement l'entérobactine, ainsi que ses produits de dégradation et précurseurs, soit le 2,3-DHBS et le 2,3-DHBA [326]. Flo et ses collaborateurs ont d'ailleurs démontré l'effet bactériostatique du sidérocalin lorsqu'une souche d'*E. coli* exprimant seulement l'entérobactine se retrouve dans le sérum des souris exprimant la protéine. Cet effet bactériostatique est attribuable à la présence du sidérocalin dans le sérum, puisque l'inhibition de croissance est levée dans le sérum de souris mutantes pour le sidérocalin [331]. De plus, ils démontrèrent que la souche non-pathogène peut établir une infection chez les souris déficientes pour le sidérocalin et que cette incapacité à établir une infection dans les souris exprimant le sidérocalin est abolie suite à l'administration de ferrichrome aux animaux, démontrant ainsi la spécificité du sidérocalin à capter l'entérobactine [331]. Une étude complémentaire a démontré que l'ajout du locus IroA à la souche *E. coli* non-pathogène contrecarrait l'effet bactériostatique du sidérocalin et conférait à la souche la capacité d'établir une infection chez les souris exprimant ou pas la protéine [26]. L'ajout d'un glucose à l'entérobactine est suffisant pour créer un encombrement stérique et ainsi empêcher la séquestration du sidérophore par le sidérocalin (Figure 17) [26].

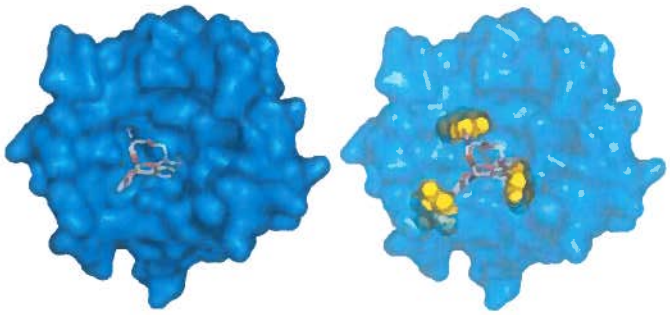

Figure 16: Structure du sidérocalin liant l'entérobactine et l'encombrement stérique produit par l'ajout de glucoses à l'entérobactine. Tiré de [26]

De plus, l'ajout d'apo-entérobactine purifiée à des cellules épithéliales du tractus respiratoire humain en culture (A549) induit la sécrétion de l'interleukine 8, qui est une importante chimiokine pro-inflammatoire aidant au recrutement des neutrophiles humains. Cette sécrétion est par ailleurs potentialisée à l'ajout du sidérocalin purifié, suggérant ainsi que l'entérobactine peut servir de signal pro-inflammatoire, permettant la détection de bactérie, et que ce signal est amplifié par la captation du sidérophore par le sidérocalin [27]. Ce phénomène a été démontré également par une souche de *Klebsiella pneumoniae* exprimant l'entérobactine, les salmochélines et la yersiniabactine. L'activation de la sécrétion de l'interleukine 8 et le recrutement des neutrophiles sont d'ailleurs augmentés chez les souris infectées par un mutant Δ*iroA*, et ce, de façon dépendante au sidérocalin [25]. Ces données corroborent celles suggérant que l'entérobactine servirait de signal de détection de présence bactérienne par le sidérocalin.

Tel que discuté plus haut, la présence de la norépinephrine aide les bactéries à obtenir le fer nécessaire à leur croissance via l'entérobactine. Il n'est donc pas surprenant de constater que le sidérocalin séquestre également cette catécholamine couplée au fer, et ce, afin d'éviter l'acquisition du fer par les bactéries [332]. Finalement, un sidérophore mammalien a été identifié tout récemment comme étant le substrat original du sidérocalin [333]. En fait, la molécule d'acide 2,5-dihydroxybenzoique (2,5-DHBA), qui est similaire au précurseur de l'entérobactine, soit le 2,3-DHBA, est produite par l'enzyme murine BDH2, un homologue à EntA. Une répression de cette enzyme par interférence d'ARN résulte en une répression de la synthèse du 2,5-DHBA, une accumulation anormale du fer dans le cytoplasme et une carence en fer pour les mitochondries. Ces données révèlent en fait de nouveaux aspects de l'homéostasie du fer qui peuvent avoir été conservés à travers les espèces [333].

Problématique de la recherche :

Les souches d'*Escherichia coli* pathogène extra-intestinal (ExPEC) aviaires causent des infections respiratoires morbides et mortelles chez la volaille engendrant des pertes économiques importantes pour l'industrie aviaire. L'augmentation alarmante des souches bactériennes résistantes aux antibiotiques nécessite l'exploration d'autres avenues thérapeutiques et prophylactiques. L'étude des systèmes de virulence des bactéries pathogènes est essentielle à l'identification de cibles vaccinales et/ou thérapeutiques. Les gènes *iroBCDEN* encodent pour un système de modification du sidérophore entérobactine, les salmochélines, et sont nécessaires à la virulence de la souche ExPEC aviaire χ7122. Cette souche pathogène possède un troisième système de sidérophore, soit l'aérobactine, qui participe également à la virulence de la souche. L'étude des interrelations moléculaires entre les divers systèmes de sidérophores et de leur implication pour la virulence de la souche χ7122 permettra de mettre en lumière les mécanismes de virulence requis pour l'établissement d'une infection et d'identifier de nouvelles cibles vaccinales.

Objectifs spécifiques :

1) La détermination du rôle de chacun des gènes *iroBCDEN* pour la virulence de la souche χ7122 et pour la production des salmochélines

2) La détermination de l'importance de la synthèse et la sécrétion des sidérophores catécholates pour la virulence de la souche χ7122.

3) La détermination du rôle des estérases Fes, IroD et IroE pour la dégradation et la biosynthèse des salmochélines, ainsi que de leur implication dans la virulence de la souche χ7122.

Articles

Article #1

Specific Roles of the *iroBCDEN* Genes in Virulence of an Avian Pathogenic *Escherichia coli* O78 Strain and in Production of Salmochelins.

Mélissa Caza, François Lépine, Sylvain Milot and Charles M. Dozois **(2008)** ***Infection and Immunity* 76:3539-49**

A) Contribution de l'étudiante

1- L'étude présentée dans l'article publié dans Infection and Immunity, avait comme objectif la détermination du rôle de chacun des gènes *iroBCDEN* pour la virulence de la souche χ7122 et pour la production des salmochélines. En utilisant une souche atténuée ne produisant que l'entérobactine, la complémentation plasmidiques de différentes combinaisons des gènes *iro* a permis de mettre en évidence le rôle auxiliaire de l'hydrolase périplasmique IroE, ainsi que les rôles essentiels des gènes *iroBCDN* dans la virulence de la souche APEC chez un modèle d'infection septicémique aviaire. De plus, la distribution relative des sidérophores produits par la souche χ7122 lors d'une infection chez le poulet a été déterminée.

2- L'étude a été réalisée en utilisant une approche multidisciplinaire regroupant des techniques de génétique bactérienne, un modèle d'infection septicémique aviaire, ainsi que de la chromatographie liquide couplée au spectromètre de masse.

3- L'étudiante a réalisé, avec l'aide de ses directeurs de recherches, toutes les étapes de conceptions et réalisations des expériences, ainsi que l'écriture du manuscrit.

B) Résumé de l'article :

Les souches d'*Escherichia coli* pathogènes pour les espèces aviaires (APEC) font partie du groupe des souches d'*E. coli* pathogènes extra-intestinaux (ExPEC); et sont associées aux infections respiratoires et septicémiques chez la volaille. Les gènes *iroBCDEN* codent pour les salmochélines, un système de sidérophore présent chez *S. enterica* et certaines souches ExPEC. Le rôle des gènes *iro* pour la virulence et pour la production

des salmochélines a été étudié en introduisant des plasmides codant différentes combinaisons des gènes *iro* dans une souche dérivée de la souche O78 χ7122 qui ne produit plus les salmochélines ni l'aérobactine, en plus d'être atténuée chez le modèle d'infection septicémique aviaire. La complémentation par les gènes *iroBCDEN* a résulté en un regain de la virulence, tandis que l'absence des gènes *iroC, iroDE* ou *iroN* empêche cette restauration. Le gène *iroE* n'est pas requis pour la virulence, puisque l'introduction des gènes *iroBCDN* redonne la capacité à la bactérie de coloniser et de causer des lésions dans les tissus extra-intestinaux des poulets. Une étude de prévalence a indiqué que les séquences *iro* sont associées à la virulence des souches APEC. Des analyses en chromatographie liquide couplée à la spectrométrie de masse des surnageants de culture des souches χ7122 et mutants complémentés ont indiqués que I) les salmochélines composent 14 à 27 % des sidérophores présents dans un milieu pauvre en fer ou dans des tissus infectés par χ7122; II) la complémentation du mutant Δ*iroBCDEN* Δ*iucABCD*Δ*iutA* avec le locus *iroA* augmente les niveaux de dimères glucosylés (S1 et S5) et monomères (SX) glucosylés en comparaison avec la souche APEC χ7122; III) les gènes *iroDE* sont important pour la génération de S1, S5 et SX; IV) *iroC* est requis pour l'exportation des trimères et dimères de salmochélines et V) *iroB* est requis pour la génération de salmochélines. En somme, la glucosylation (IroB), le transport (IroC et IroN) et la dégradation (IroD et IroE) des salmochélines sont requis pour la virulence des souches APEC, bien qu'IroE semble jouer un rôle auxiliaire.

Specific roles of the *iroBCDEN* genes for the virulence of an avian pathogenic *Escherichia coli* (APEC) O78 strain and for the production of salmochelins

Running title: Roles of *iro* genes for APEC virulence and salmochelin production

Mélissa Caza, François Lépine, Sylvain Milot, and Charles M. Dozois*

INRS-Institut Armand-Frappier, Laval, Québec, CANADA

*Corresponding Author:

Charles M. Dozois

Canada Research Chair on Infectious Bacterial Diseases

INRS-Institut Armand-Frappier

531 boul. des Prairies

Laval, Québec, CANADA H7V 1B7

Phone : 450-687-5010 ext. 4221 Fax : 450-686-5501

E-Mail : charles.dozois@iaf.inrs.ca

ABSTRACT

Avian pathogenic *Escherichia coli* (APEC) are a subset of extra-intestinal pathogenic *E. coli* (ExPEC) associated with respiratory infections and septicemia in poultry. The *iroBCDEN* genes encode the salmochelin siderophore system present in Salmonella enterica and some ExPEC. Roles of the *iro* genes for virulence in chickens and production of salmochelins were assessed by introducing plasmids encoding different combinations of *iro* genes to an attenuated salmochelin- and aerobactin-negative mutant of O78 strain χ7122. Complementation with the *iroBCDEN* genes resulted in a regain in virulence, whereas the absence of *iroC, iroDE,* or *iroN* abrogated restoration of virulence. The *iroE* gene was not required for virulence, since introduction of *iroBCDN* restored the capacity to cause lesions and colonize extra-intestinal tissues. Prevalence studies indicated that *iro* sequences were associated with virulent APEC strains. Liquid chromatography-mass spectrometry analysis of supernatants of APEC χ7122 and the complemented mutants indicated that: 1) For χ7122, salmochelins comprised 14-27% of the siderophores present in iron-limited medium or infected tissues; 2) Complementation of the mutant with the iro locus increased levels of glucosylated dimers (S1 and S5) and monomer (SX) compared to APEC strain χ7122; 3) The *iroDE* genes were important for generation of S1, S5, and SX; 4) *iroC* was required for export of salmochelin trimers and dimers; and 5) *iroB* was required for generation of salmochelins. Overall, efficient glucosylation (IroB), transport (IroC and IroN), and processing (IroD and IroE) of salmochelins are required for APEC virulence, although IroE appears to serve an ancillary role.

INTRODUCTION

Escherichia coli is a commensal resident of the intestine as well as a pathogen that can cause both enteric and systemic diseases of humans and animals (11, 31, 52). Certain commensal intestinal *E. coli* isolates can cause disease at extra-intestinal sites, and these strains have been collectively termed extra-intestinal pathogenic *E. coli* (ExPEC) (53). Among ExPEC strains, uropathogenic *E. coli* (UPEC) is the most common cause of human urinary tract infections (UTIs) (37, 52). Avian pathogenic *E. coli* (APEC) strains share some virulence traits with ExPEC from human infections, and are responsible for extra-intestinal infections of economic importance to the poultry industry (11, 15, 49, 50). One of the most common forms of disease associated with APEC is avian colibacillosis, which starts as a respiratory infection (airsacculitis) that is frequently followed by generalized infections such as perihepatitis, pericarditis, and septicemia (11, 25).

One attribute associated with APEC and other ExPEC is the presence of multiple iron uptake systems, including siderophores, which play an important role in extra-intestinal virulence (13, 55, 57). Siderophores are high-affinity iron-chelating molecules that can contribute to bacterial survival during infection by sequestering iron, which is an essential trace element for most bacteria (24, 42, 46). Most *E. coli* strains, including non-pathogenic *E. coli* K-12, and other enterobacteria such as *Salmonella enterica* and *Klebsiella spp.* produce the catecholate siderophore enterobactin, which is a cyclic trimer of 2,3-dihydroxybenzoyl serine (DHBS) (24, 42). Enterobactin is very efficient at sequestering iron in vitro, however, it is less able to compete for iron during infection, as it is inhibited by serum albumin (32) and specifically binds to the host innate defense

protein NGAL (neutrophil gelatinase-associated lipocalin) (also called lipocalin 2 or siderocalin) (22, 39). By contrast, aerobactin and salmochelins, which are siderophores associated with APEC and UPEC strains (15, 42, 49, 57), can effectively acquire iron in the presence of serum albumin or NGAL (3, 19, 32). Aerobactin is a hydroxamate siderophore produced by most APEC (11), certain pathogenic *E. coli, Klebsiella pneumoniae,* and *Shigella* strains (9, 23, 42). Aerobactin is synthesized by the *iucABCD* encoded gene products, and aerobactin uptake occurs via the *iutA* encoded receptor protein (23, 42). Salmochelins are C-glucosylated derivatives of enterobactin and DHBS molecules (glucosylated linear trimers, dimers and monomers of DHBS) that were initially described by Hantke *et al.* (27). Salmochelins are produced by *Salmonella enterica*, and certain ExPEC strains (3, 18, 27, 36, 62). In *E. coli* and *Salmonella enterica,* the salmochelin encoding system comprises two divergently transcribed sets of genes, *iroBCDE* and *iroN,* which constitute the *iro* gene cluster (13, 17, 42, 56) (Fig. 1). The *iroB* gene encodes a glucosyltransferase that glucosylates enterobactin, *iroC* encodes an ABC transporter required for transport of salmochelins , and *iroD, iroE,* and *iroN* encode respectively for a cytoplasmic esterase, a periplasmic hydrolase and an outer membrane siderophore receptor (10, 18, 27, 36, 62).

APEC strain χ7122 (O78 : K80 : H9) has been used as a model strain to study molecular mechanisms of APEC pathogenicity (4, 13). Strain χ7122 possesses the chromosome-encoded enterobactin siderophore system and also produces the aerobactin and salmochelin siderophores, which are encoded by genes present on a large virulence plasmid pAPEC-1 (13). The salmochelin and aerobactin systems are required for full

virulence of the strain in a chicken infection model (13). The loss of either of these systems reduced the capacity of the APEC strain to colonize extra-intestinal tissues. Moreover, loss of both the aerobactin and salmochelin encoding gene clusters resulted in an avirulent strain that was unable to colonize extra-intestinal sites, such as the lungs and liver, compared to the wild-type parent strain. Complementation of the salmochelin- and aerobactin-negative APEC strain with a plasmid encoding the *iro* gene cluster, resulted in a regain of virulence comparable to that of the wild-type parent strain, despite the lack of the aerobactin gene cluster (13). However, the specific roles of *iro* genes for complementation of the attenuated strain have thus far not been established. Further, to our knowledge, the quantities of enterobactin, DHBS molecules and the salmochelins produced by APEC or other pathogenic *E. coli* have not been assessed.

In this report, we introduced plasmids containing different combinations of *iro* genes to an attenuated APEC salmochelin- and aerobactin-deficient strain, in order to determine which *iro* genes were required to complement virulence of this strain in a chicken experimental infection model. By using this approach, we were able to specifically investigate the contribution of *iro*-encoded gene products for APEC virulence without the influence of the other virulence-associated siderophore aerobactin. Further, we used LC/MS/MS to determine the relative levels of siderophores produced by strain χ7122 from the tissues of infected chickens and quantitate siderophores produced directly from culture supernatants of strain χ7122 and complemented mutants.

MATERIALS AND METHODS

Bacterial strains, plasmids, media and growth conditions. Bacterial strains and plasmids used in this study are listed in Table 1. APEC strain χ7122 is an O78:K80:H9 strain and produces enterobactin, salmochelins, and aerobactin. In addition, APEC and *E. coli* fecal isolates from healthy poultry were used to screen for the presence of *iro* genes. The 298 APEC isolates were previously described elsewhere (14). Thirty-two *E. coli* fecal isolates from healthy poultry were kindly provided by J. M. Fairbrother (University of Montreal, Canada). APEC strains and commensal fecal poultry isolates were previously classified for virulence based on lethality for 1-day-old chicks following subcutaneous inoculation, where LC1 corresponds to the high-lethality class, LC2 to the low-lethality class, and LC3 to the non-lethal class (14).

Luria-Bertani (LB) broth and Tryptic Soy Agar (Difco Laboratories, Detroit, MI) were routinely used for growing *E. coli* strains and clones. *E. coli* strain DH5α was used for plasmid cloning and recovery. For infection studies, strain χ7122 and derivatives were grown in brain heart infusion (BHI) broth (Difco). For production and detection of catecholate siderophores, bacteria were grown at 37°C for 17 h in iron-poor M63-glycerol minimal medium containing per liter: 5.3 g KH_2PO_4, 13.9 g $K_2HPO_4 \cdot 3H_2O$ and 2.0 g $(NH_4)_2SO_4$. The pH was adjusted to 7.5 with KOH and medium was supplemented with 1 mM $MgSO_4$, 1 mM $CaCl_2$, 1 mM thiamine and 0.6 % w/v glycerol before inoculation. The minimal medium was inoculated with 0.6 % of a 5 h culture grown in TY medium (containing per liter: 5 g yeast extract, 5 g sodium chloride and 8 g tryptone) according to previous reports (27, 58, 59, 62). Iron-poor medium was prepared in plastic

bottles to reduce trace contamination of iron. Antibiotics were added as required at the following concentrations: kanamycin (30 μg ml^{-1}), chloramphenicol (30 μg ml^{-1}), nalidixic acid (30 μg ml^{-1}). All of the strains tested demonstrated similar growth curves to APEC wild-type APEC strain χ7122 following growth in either LB or iron-poor medium (data not shown).

Construction of plasmids. Enzymes used for generation of constructs were purchased from New England Biolabs (NEB). For PCR generated fragments, Elongase® DNA polymerase (Invitrogen) was used at an annealing temperature of 52 °C. Plasmid constructs were derived from pYA3661, and are all illustrated in Fig. 1. pYA3661 (13) encodes the full *iro* gene cluster (*iroBCDEN*) of APEC strain χ7122 on a 11.5 kb *Hin*d III fragment cloned into vector pACYC184 (6) (Fig. 1). Plasmid pIJ34 (*iroBCDE*) was produced by digesting pYA3661 with *Hin*d III and *Ssp* I, and cloning the appropriate fragment into the *Hin*d III and *Eco*R V sites of pACYC184. Plasmid pIJ37 (*iroBDEN*) was produced by digesting pYA3661 with *Kpn* I, which results in a 2861 bp in-frame deletion of the 3' end of *iroC*. Plasmid pIJ53 was generated by digesting pYA3661 with *Hin*d III and *Pvu* II, and cloning the fragment encoding *iroB* into the *Hin*d III and *Eco*RV sites of pACYC184. Plasmid pIJ121 (*iroBC*) was generated by digesting pYA3661 with *Hin*d III and *Acl* I and cloning the *iroBC*-containing fragment into the *Hin*d III and *Nar* I sites of pACYC184. Plasmids pIJ135 (*iroBCN*) and pIJ136 (*iroBCEN*) were produced by amplifying two PCR fragments from pYA3661, ligating them with *Xho*I linkers within the primers and cloning them into the *Hin*d III site of pACYC184. For pIJ135 the *iroBC* genes were amplified using primers CMD81 (5'-TCAGAGCAAGAGATTACGCGCAG-

AC-3') and CMD91 (5'-TTCTCGAGACCGCCGCTTCTGACTGTGT-3') and the *iroN* gene was amplified using primers CMD277 (5'-CGCCCTCGAGACTACGATCAGAA-TGATGCGGT-3') and CMD87 (5'-CAGTACCGGCATAACCAAGCCTAT-3'). Primers CMD91 and CMD277 each contain a *Xho* I site (underlined). Primers CMD81 and CMD87 correspond to pACYC184 vector sequences flanking either side of the cloned *iro* locus in pYA3661, and generate fragments containing *Hin*d III sites. The pIJ136 construct encoding *iroBCEN* was similarly obtained using primers CMD81 and CMD91 for amplification and generation of the X*ho* I-*Hin*d III fragment encoding *iroBC* and primers CMD90 (5'-ACCTCGAGGAAACGGTACAGACTTCCTG-3') (*Xho*I site underlined) and CMD87 for amplification and generation of the X*ho* I-*Hin*d III fragment encoding *iroEN*. Plasmid pIJ137 (*iroBCDN*), was generated by three cloning steps. First the *iroN* gene was obtained from pYA3661 following digestion with S*ph* I and cloned into the S*ph* I site of pACYC184, resulting in plasmid pIJ33. The *iroBCD* encoding fragment was amplified by PCR with primers CMD81 and CMD278 (5'-AAAGTCTCGAGGGGTCAACTCAACCC-3') (X*ho* I site underlined) and cloned in vector pBC SK (-) at the *Hind* III and *Xho* I sites. This intermediate vector was then digested with *Ssp* I and *Eag* I, and the appropriate fragment was then cloned at the *Nru* I and *Eag* I sites of pIJ33, generating plasmid pIJ137. The specific deletions in the *iro* cluster for each of the plasmids generated were confirmed by PCR in the cloned strains and in χ7304 complemented derivatives.

Prevalence of the *iro* genes in APEC and fecal commensal strains. 298 APEC and 32 commensal fecal isolates were screened by PCR for the presence of the *iroB* and *iroN*

genes. Crude bacterial lysates were obtained as described elsewhere (47). The primers used to generate a 663 pb fragment corresponding to *iroB* were IROBKO1 (5'-AGGCGCGCCTCTCTATGGGC-3'), and IROBKO2 (5'-CTCTAGATCAAGGCC-GTCAACC-3'). The primers used to specifically amplify a 549 pb fragment of the *iroN* gene were IRON1 (5'-TATTCGTGGTATGGGGCCGGA-3') and IRON2 (5'-GCCCGC-ATAGATATTCCCCTG-3'). The PCR reactions were achieved using *Taq* DNA polymerase (NEB), at an annealing temperature of 58°C and an extension time of 1 minute at 72°C for 25 cycles.

Sequencing of the regions adjacent to the *iro* locus of pAPEC-1.The *iro* gene cluster from strain χ7122 was previously characterized and sequenced. The flanking DNA regions of the *iroBCDEN* cluster were sequenced from APEC strain χ7122 by using custom primers. The sequencing was done at the Genome Québec facility (Montreal, QC, Canada). Sequences were analysed with ORF finder and Blast programs available on-line at http://www.ncbi.nlm.nih.gov. The updated nucleotide sequence is available as GenBank accession number AF449498.

Experimental infections of chickens via the air sacs. For infection studies, eight groups of 3-week-old White Leghorn specific-pathogen-free chickens (Canadian Food Inspection Agency, Ottawa, Canada) were inoculated in the right thoracic air sac with 0.1 ml (10^7 CFU) of a bacterial inoculum grown overnight in BHI broth. Experimental infections and the lesion scoring were carried out as previously described (33). Chickens were euthanized at 48 h post-infection and the spleen, liver and lung were removed,

weighed, suspended in buffered saline with gelatin (BSG) (for 1 L: 8.5 g NaCl, 0.3 g KH_2PO_4, 0.6g Na_2HPO_4, 0.1 g gelatine), and homogenized with an Omnimixer homogenizer. Samples were diluted 1:3, 1:30 and 1:300 in (BSG). Bacterial counts were performed by plating 100 µl of each diluted sample on MacConkey agar plates supplemented with the appropriate antibiotics.

Analysis of siderophores from culture supernatants and tissues of infected chickens. Supernatants of 17 h cultures were obtained following centrifugation of bacterial cells at 3200 X *g* for 15 minutes and addition of 5 mM $FeCl_3$ to each supernatant. The precipitate was removed by centrifugation and the supernatants were filtered on 0.2 µm membranes. Aliquots of 1 ml of supernatant were then prepared in 5 % vol/vol formic acid and 0.12 ng / ml of 5,6,7,8-tetradeutero-3,4-dihydroxy-2-heptylquinoline was added as an internal control (34). Each strain was cultured in triplicate and a sample of each culture supernatant was analyzed by liquid chromatography coupled to a mass spectrometer (LC/MS/MS).

For detection of siderophores during infection, two groups of 20 chickens were infected as described above with a 0.1 ml inoculum containing either 10^7 or 10^8 CFU of strain χ7122. 24 h post-infection, pericardia, air sacs, livers, and blood were removed from surviving chickens, pooled, weighed, suspended in a solution of methanol and formic acid (19:1) and homogenized with an Omnimixer. Homogenates were centrifuged at 3200 X *g* for 15 minutes. The supernatants were retained, and the insoluble pellets were then extracted three times with methanol: formic acid (19:1). The supernatants from each of

the extractions were then combined and concentrated by evaporation. 500 µl aliquots were then prepared with 5,6,7,8-tetradeutero-3,4-dihydroxy-2-heptylquinoline as an internal control. Samples were analyzed three times by LC/MS/MS.

Liquid chromatography / Mass spectrometry analyses. Multiple reaction monitoring (MRM) analyses were performed using an Agilent HP 1100 HPLC (Agilent Canada, Mississauga, ON) coupled to a Micromass QuattroII spectrometer (Micromass Canada). Samples were injected onto a Zorbax Eclipse XDB-C8 4.6 mm X 150 mm column at a flow rate of 400 µl / min and a linear gradient of water / acetonitrile with 1% acetic acid. The HPLC effluent was directed to the mass spectrometer through a Valco T splitter. The analyses were performed in positive electrospray ionization mode with a cone voltage of 30 V. Monitoring of daughter ions from specific pseudomolecular ions was performed by collision induced dissociation (CID) with argon at different collision energies for each molecule ranking from 15 eV to 55 eV. Information concerning the different salmochelin and enterobactin related molecules detected by MRM mass spectrometer analyses is presented in Figure 2. The specific transitions ions monitored from pseudomolecular ions to daughter ions of salmochelins SX, S1, linear DGE (S2), DGE (S4), S5, MGE, linear MGE, TGE and linear TGE were 404>299, 627>224, 1012>224, 994>224, 789>386, 832>224, 850>224, 1156>266 and 1174>266 m/z, respectively. The transitions ions monitored for enterobactin and its linear trimer ($(DHBS)_3$), dimer ($(DHBS)_2$) and monomer (DHBS) derivatives were 670>224, 688>224, 465>224 and 242>137 m/z, respectively. The transition ion monitored for the internal standard and aerobactin was 244>159 and 565>205 m/z, respectively. Quantification for each compound, with the

exception of aerobactin, was determined from the response factor of enterobactin and corrected with the intensity of the signal of the internal standard.

Purification of enterobactin. Enterobactin was purified as described by Léveillé *et al.* (35) with additional purification by thin layer chromatography (TLC) on a 1 mm glass silica gel 60 Å plate (Whatman). A calibration curve was established from purified enterobactin, and this curve was used to estimate the quantities of all catecholate siderophores, on the basis that salmochelins and enterobactin-related molecules have a response factor similar to cyclic enterobactin.

Statistical analyses. Statistical analyses were performed using the Prism 4.0b software package (GraphPad Software, San Diego, CA, USA).

RESULTS

Comparison of the *iro* encoding region of pAPEC-1 with other *iro* encoding regions. A 21 019 bp region of pAPEC-1 encoding the *iro* gene cluster and spanning from the *iss* gene to the *cvaB* gene was sequenced (accession number AF449498). This region, or specific segments of it, are highly homologous to other sequences encoded on plasmids or genomic islands of other *E. coli* strains (5, 8, 28, 29, 56, 60). The regions immediately adjacent to the *iro* cluster on plasmid pAPEC-1 are also conserved in the pathogenicity island (PAI)-encoded *iro* cluster from CFT073 (Fig. 1), although an additional 24.5 kb (spanning ORFs *c1249* to *c1221*) upstream of the *iroN* gene encodes for F1C fimbriae and microcin H47 (Fig. 1). The regions flanking the *iro* genes in PAIs from UPEC 536 (PAI III_{536}) (5, 12), UTI89 (8), and probiotic strain Nissle 1917 (Genomic Island I-Nissle 1917) (26) are organized similarly to those in strain CFT073. An *iro* gene cluster is also present on virulence plasmid pLVKP from *Klebsiella pneumoniae* CG43 (9) (Fig. 1). The pLVKP-encoded *iro* genes exhibit from 85-90% nucleotide identity (82-92% identity at the amino acid level) to those of APEC χ7122. However, in the *iro* cluster from *K. pneumoniae* CG43 the orientation of the *iroN* gene is inverted and the *iroE* gene is absent (Fig. 1). In addition, a DNA region which flanks *iroB* in pAPEC-1, corresponding to orfs 3 and 4, exhibits 76% nucleotide identity to a putative integrase encoding gene LV233 upstream of the *iro* genes of pLVKP (Fig. 1). These comparative sequence analyses are in support of a lateral transfer of salmochelin encoding *iro* gene clusters among PAIs and different plasmids in *E. coli* and *K. pneumoniae*.

The *iro* genes are associated with clinical isolates and virulence among avian *E. coli*. The presence of *iro* genes was investigated in avian *E. coli* isolates from clinical cases (APEC) and isolates from the feces of healthy poultry (environmental isolates). 298 APEC strains and 32 environmental isolates were previously classified into three lethality classes according to results from virulence assays in one-day-old chicks. APEC strains classified as LC1 are highly virulent, LC2 are moderately virulent, and LC3 are of low virulence. PCR amplifications with primers specific to *iroB* and *iroN* genes determined the presence or absence of the *iro* cluster among strains. There was a 100 % correlation between results obtained using primers specific to either the *iroB* or *iroN* genes. *iro* sequences were present in 244 of the 298 (82 %) APEC and were significantly associated ($P<0.0001$) with APEC compared to environmental isolates, for which only 10 of 32 (31%) isolates contained *iro* sequences. Among APEC isolates, *iro* sequences were also significantly associated with the lethality of the strains, with 91% of the highly virulent (LC1) strains containing *iro* sequences compared to only 45% of the low virulence (LC3) strains (Table 2). Taken together, results demonstrate an association of *iro* genes with both clinical origin and increased virulence of avian *E. coli*.

Role of *iro* genes for APEC virulence. To characterize the importance of specific *iro* genes for APEC virulence, we determined the capacity of different mutants to infect chickens. Groups of three week-old birds were inoculated in the right caudal thoracic air sac with χ7122 or its isogenic mutant derivatives. From the inoculation site, virulent strains are typically able to invade and infect deeper tissues, generate gross lesions and

cause a systemic infection (43). However, in this model, attenuated strains are impaired in their capacity to colonize deeper tissues (4, 13, 33).

Bacterial counts from internal organs at 48 h post-infection (Fig. 3) demonstrated a systemic infection in chickens infected with virulent strains. Wild-type APEC χ7122 colonized the lung, liver, and spleen, whereas the Δ*iro*Δ*iucABC*Δ*iutA* mutant χ7304 was not isolated from the lungs or livers, and was present in very low numbers from the spleens of infected chickens (Fig. 3). Complementation of χ7304 with the complete *iro* gene cluster (pYA3661) restored the capacity to colonize organs, although bacterial numbers in the lungs were significantly reduced (P=0.003) compared to the wild-type parent strain χ7122 (Fig. 3). The introduction of plasmids lacking either *iroN* (pIJ34-*iroBCDE*), *iroC* (pIJ37-*iroBDEN*) or *iroDE* (pIJ135-*iroBCN*) was not effective at complementing strain χ7304, and very few bacteria were isolated from the tissues of chickens infected with these strains (Fig. 3). Compared to complementation with the complete *iro* cluster (pYA3661), the absence of *iroD* (pIJ136) conferred a significantly reduced capacity to colonize the liver (P=0.007), spleen (P=0.03), and lungs (P=0.003), although levels were markedly higher than those observed in the absence of *iroN*, *iroC*, or both *iroDE* (Fig. 3). By contrast, when χ7304 was complemented with pIJ137 (*iroBCDN*), which lacks *iroE*, complementation was as effective as complementation with the complete *iro* gene cluster. In fact, χ7304 (pIJ137) demonstrated no significant difference in colonization of tissues compared to χ7304 (pYA3661). In addition, χ7304 (pIJ137) demonstrated no significant difference in colonization of the lungs or liver compared to wild-type APEC strain χ7122.

Gross lesions of colibacillosis present in the air sacs, livers, and pericardia of infected chickens were also in accordance with the bacterial levels observed in different tissues (Table 3). Gross lesions were present in the air sacs, livers, and hearts of chickens infected with APEC strain χ7122 or χ7304 complemented with the complete *iro* gene cluster (pYA3661) (Table 3). By contrast, lesions were minimal or absent in chickens infected with strain χ7304 or χ7304 complemented with plasmids lacking either *iroN* (pIJ34), *iroC* (pIJ37) or *iroDE* (pIJ135). Strain χ7304 (pIJ136), which lacks *iroD*, generated lesions of airsacculitis that were somewhat less than those induced by χ7304 (pYA3661), although this reduction was not significant (P=0.07). However, χ7304 (pIJ136) generated lesions of pericarditis/perihepatitis that were significantly decreased compared to strain χ7304 (pYA3661) (P=0.003). By contrast, strain χ7304 complemented with pIJ137, which lacks *iroE*, demonstrated no significant difference in generation of lesions of airsacculitis or pericarditis/perihepatitis compared to χ7304 (pYA3661).

Detection of siderophores produced by APEC χ7122 in vitro and in vivo. Relative levels of siderophores were initially determined from culture supernatants and from tissues of chickens infected with APEC strain χ7122 by LC/MS/MS using a multiple reaction monitoring approach. Relative quantities of specific siderophores detected from samples are detailed in figure 4. Siderophores were detected from the air sacs and pericardia of chickens infected with 10^8 CFU. Attempts to detect siderophores from blood or liver or at an infective dose of 10^7 CFU were not successful. Culture supernatants following overnight growth in iron-poor M63 medium comprised a mean of 77.1 ± 3.3 %

of non-glucosylated enterobactin derivatives, 21.1 ± 2.6 % of salmochelins, and only 1.9 ± 0.65 % of aerobactin (Fig. 4). By contrast, in extracts from air sac tissues, aerobactin comprised 58.9 ± 3.4 % of the siderophores, enterobactin-derivatives 27.1 ± 1.5 %, and salmochelins 14.0 ± 4.9 %. In extracts from pericardial tissues aerobactin, salmochelins, and enterobactin derivatives respectively comprised 48.0 ± 4.5 %, 27.1 ± 5.1 %, and 24.9 ± 0.59 % of the siderophores detected. Overall, there was a major shift in the relative quantities of aerobactin and enterobactin and DHBS molecules produced in vitro compared to in vivo, whereas salmochelin levels were similar from either culture supernatants or from tissues of infected chickens.

Quantification of siderophores from APEC χ7122 and mutant derivatives. As iron-poor M63 medium was suitable for production of salmochelins from supernatants of strain χ7122, salmochelins, enterobactin, and linear DHBS molecules were quantified directly from the supernatants of strain χ7122, χ7304 and complemented strains grown in this medium. As expected, deletion of the *iro* gene cluster eliminated production of salmochelins in isogenic strain χ7304 (Fig. 5, Table 4). Loss of the *iro* gene cluster in strain χ7304 also resulted in a mean overall 2.9-fold increase in enterobactin and DHBS molecules compared to wild-type strain χ7122 (Fig. 5).

Complementation of strain χ7304 with plasmid pYA3661 (*iroBCDEN*) increased salmochelin levels by a mean of 2.3-fold overall compared to APEC χ7122, and reduced the overall level of enterobactin related molecules by 2.1-fold (Fig. 5). Specifically, introduction of the complete *iro* gene cluster conferred an increase in glucosylation of

enterobactin derivatives and an increased hydrolysis of these products into linear DGE (S2), S1, S5 and SX compared to levels produced by wild-type strain χ7122 (Tables 4 and 5). Complementation of χ7304 with plasmid pIJ34 (*iroBCDE*), which lacks the *iroN* gene encoding the salmochelin receptor, resulted in catecholate siderophore levels that were similar to those observed with pYA3661 (*iroBCDEN*) (Fig. 5). However, the lack of *iroN* resulted in an increase in linear DGE (S2) and a reduction in MGE, linear MGE, enterobactin, and $(DHBS)_3$ compared to pYA3661 (Tables 4 and 5).

Complementation of χ7304 with pIJ137 (*iroBCDN*), which lacks the *iroE* gene encoding a periplasmic hydrolase, did not alter the overall production of enterobactin or salmochelin molecules, compared to χ7304 (pYA3661) (Fig. 5), although profiles for specific catecholate molecules differed (Tables 4 and 5). By contrast, complementation with pIJ136 (*iroBCEN*), which lacks the *iroD* gene encoding a cytoplasmic esterase, resulted in a global 1.4-fold and 1.6-fold decrease in salmochelins and enterobactin derivatives respectively compared to χ7304 (pYA3661) (Fig. 5).

Complementation of mutant χ7304 with a plasmid encoding only *iroB* (pIJ53) resulted in a marked overall decrease of enterobactin related molecules and salmochelins (Fig. 5). Traces of S1 were detected in the supernatants of this strain (Table 5), and although enterobactin levels in χ7304 (pIJ53) supernatants were similar to those from χ7304 (pYA3661), all linear DHBS products were greatly reduced (Table 4). Complementation of strain χ7304 with either pIJ121 (*iroBC*) or pIJ135 (*iroBCN*) restored production and secretion of salmochelins to some extent, although overall salmochelin levels were 4.0-

fold lower than those in supernatants of χ7304 (pYA3661) (Fig. 5). Despite the overall decrease in salmochelins, introduction of either pIJ121 (*iroBC*) or pIJ135 (*iroBCN*) to χ7304 resulted in high levels of DGE (S4) and TGE and reduced levels of SX, S1 and S5 (Table 4). χ7304 (pIJ121) and χ7304 (pIJ135) also generated higher levels of enterobactin and $(DHBS)_3$, whereas levels of DHBS were greatly reduced compared to χ7304 (pYA3661) (Table 5). Taken together, these results suggest that enterobactin molecules underwent increased glucosylation in the presence of the IroB glucosyltransferase, but that the tricyclic salmochelins could not be efficiently secreted in the absence of the IroC transporter and were poorly processed in the absence of the IroD and IroE hydrolases.

Complementation of χ7304 with plasmid pIJ37 (*iroBDEN*), which lacks the *iroC* gene, further demonstrated the importance of this gene for secretion of salmochelins, as only the monomeric SX salmochelin was present at appreciable levels in the supernatant of χ7304 (pIJ37) (Table 4). However, the overall level of enterobactin and DHBS molecules detected was similar to χ7304 (pYA3661) (Fig. 5), and in fact levels of enterobactin, $(DHBS)_3$, and $(DHBS)_2$ were increased when compared to χ7304 (pYA3661) (Table 5). Hence, overall *iroC* was important for secretion of salmochelins in the supernatant, but was not important for secretion of enterobactin.

DISCUSSION

The *iro* genes encoding the salmochelin siderophore system were initially identified as an iron- and pH-regulated locus (named the *iroA* locus) in *Salmonella enterica* serovar Typhimurium (20, 21). Further studies determined that the *iroA* locus comprised two divergently transcribed sets of genes (*iroBCDE* and *iroN*) (2). The *iro* sequences which are present in all phylogenetic lineages of *S. enterica* (2), are associated with the Fels-2 prophage region inserted at the TmRNA *(ssrA)* site (61), and were likely acquired through horizontal gene transfer. *iro* gene clusters were also identified within pathogenicity islands located at different tRNA sites on the chromosomes of several ExPEC strains (12, 51, 60). In addition, some *E. coli* and *Klebsiella pneumoniae* strains contain *iro* sequences localized to plasmids (9, 13, 28, 29, 56). The presence of common sequences bordering *iro* genes in different strains suggests a possible common ancestry of these horizontally acquired genes (Fig. 1).

Among *E. coli*, *iro* sequences were shown to be associated with ExPEC isolated from neonatal meningitis (38), urinary tract infections, and prostatitis in humans (1, 30, 51) as well as APEC (15, 48). In accordance with these reports, in our study *iro* sequences were highly associated with the virulence of APEC strains in 1-day-old chicks, and *iro* sequences were also significantly associated with APEC compared to fecal commensal *E. coli* isolates from poultry (Table 2). The increased association of *iro* sequences among ExPEC and APEC also correlates with the importance of *iro* genes for the virulence of *E. coli* in different infection models (13, 19, 38, 54). However, prior to our current study,

aside from the IroN salmochelin receptor, the individual roles of *iro*-encoded genes for *E. coli* virulence had not been investigated.

To our knowledge this is the first study to compare relative levels of catecholate siderophores (salmochelins, enterobactin, and derivatives) and aerobactin produced by *E. coli* during infection of host tissues as well as following growth in iron-poor culture medium. The proportion of salmochelins produced in tissues and in vitro was quite similar. By contrast, clearly there were major differences between the relative amounts of aerobactin and enterobactin siderophores present in vivo and in vitro, and there was a marked increase in aerobactin and a decrease in enterobactin observed from host extra-intestinal tissues (Fig. 4). The production of different siderophores by ExPEC is likely required to provide an adaptive advantage, as different siderophores may exhibit optimal activity under varying conditions including pH, carbon availability, and growth temperature. From this standpoint, the increased level of aerobactin detected in vivo may be due to the fact that aerobactin acts as an effective siderophore under the physiological conditions present in these tissues, and therefore its expression may be upregulated in vivo. In vitro, aerobactin was better produced under slightly acid conditions, whereas the catecholate siderophores were more abundant at neutral or slightly alkaline pH by strain Nissle 1917 (59). These findings suggest that important regulatory mechanisms, in addition to iron availability itself, can alter production of siderophores in vitro as well as in vivo, and further emphasize the role aerobactin may contribute to *E. coli* extra-intestinal virulence. In addition to regulatory changes that may occur in vivo, it is also

possible that for enterobactin the decreased detection from tissues may in part be due to association of this siderophore with host proteins such as albumin or NGAL orthologs.

As the presence of multiple iron-uptake systems may hinder the analysis of the roles of specific iron transport systems or their individual components in extra- intestinal *E. coli* infections (13, 54, 57), we used plasmid complementation of an attenuated salmochelin- and aerobactin-negative APEC strain to assess the specific importance of individual *iro* genes for APEC virulence and for the production of different types of salmochelin molecules. Complementation of the attenuated mutant with the complete *iro* gene cluster on a medium-copy plasmid restored lesion scores to levels similar to the wild-type parent strain χ7122 (Table 3), and considerably increased colonization of systemic organs even in the absence of aerobactin (Fig. 3). Compensation for the lack of aerobactin and the regain in virulence is likely due to an increased capacity to produce and process salmochelins. Introduction of the *iro* genes on pYA3661 resulted in over twice the production of salmochelins and a greater level of glucosylated dimers and monomers when compared to the wild-type parent (Table 5, Fig. 4).

Complementation of attenuated strain χ7304 with plasmids containing different combinations of *iro* genes demonstrated that in particular, the *iroN* and *iroC* genes, as well as the combination of *iroD* and *iroE* genes were critical for virulence. The IroN salmochelin receptor encoding gene did not affect salmochelin production, although it was required for virulence. These results are in line with the attenuation of ExPEC *iroN* mutants (38, 54). Recently, IroN has also been shown to demonstrate a cell invasion

phenotype, which could further contribute to its importance for ExPEC virulence (16). In contrast to ExPEC, loss of IroN, together with FepA, in *Salmonella enterica* serovar Typhimurium and *S. enterica* serovar Enteritidis had little effect on systemic spread in mouse and chicken models respectively, indicating that salmochelin and enterobactin uptake are not critical for Salmonella virulence (45). However, since the combined loss of IroN, FepA, and Cir resulted in attenuation, uptake of DHBS and enterobactin breakdown products appear to contribute to Salmonella virulence (45). Thus, although ExPEC possess numerous catecholate siderophore receptors including FepA, Fiu, Cir, Iha, and other uncharacterized putative siderophore receptors, it is likely that only IroN functions as the salmochelin receptor, and that the uptake of salmochelins is a prerequisite for full virulence.

χ7304 pIJ37 (*iroBDEN*), which lacks only *iroC*, secreted no detectable cyclic glucosylated salmochelins, very little glucosylated linear trimers and dimers, and a substantial level of SX monomer (Table 4). However, in the absence of *iroC*, enterobactin, $(DHBS)_3$ and $(DHBS)_2$ were abundant. These results support a role for the *iroC* gene product in the export of salmochelins, with the exception of the SX monomer which may possibly be exported by another pathway. Further, the attenuation of this mutant indicates that enterobactin and its breakdown products could not serve as efficient siderophores *in vivo*. Recently, Crouch *et al.* (10) also demonstrated the role of *iroC* for secretion of DGE (S4) and linear DGE (S2) as well as the importance of this gene for virulence of *Salmonella enterica* serovar Typhimurium in the mouse.

χ7304 pIJ135 (*iroBCN*) which lacks both the *iroD* and *iroE* genes encoding salmochelin hydrolases (62) secreted low amounts of SX monomer and S1 and S5 dimers, and some of the highest amounts of TGE and DGE (S4) detected in supernatants. Hence, the lack of virulence of this strain is likely due to a reduced processing of cyclic salmochelins for efficient iron acquisition during an infection. The IroD hydrolase appeared to play a predominant role for virulence compared to the IroE hydrolase (Fig. 3, Table 4). These results are in accordance with the enzymatic activities of these hydrolases (36). Purified IroE demonstrated higher selectivity for apo-siderophores and mostly only cleaved cyclic compounds into linear trimers (36), suggesting IroE may be more important for export or processing prior to release of siderophores for iron scavenging. By contrast, IroD demonstrated higher affinity for Fe+3-loaded siderophores and efficiently processed cyclic salmochelins and enterobactin into trimers, dimers, and monomers, favoring its role in cytoplasmic release of iron (36). The lack of IroE in the *iro* gene cluster of *K. pneumoniae* strain CG3, a bacteremia isolate that is highly virulent in mice (7), further supports that *iroE* may be of minimal importance for a fully functional salmochelin system. Although the importance of salmochelins for virulence of *K. pneumoniae* remains to be established, *iroE* may have been lost by attrition, at least in this *K. pneumoniae* strain, if it provided no selective advantage. However, since *iro* gene clusters have been shown to be present in multiple copies in certain *E. coli* strains, the possibility that additional copies of *iro* genes, including an *iroE* ortholog, within certain *K. pneumoniae* strains cannot be excluded.

The importance of salmochelins as newly discovered siderophores that are able to evade the mammalian innate immune response protein NGAL (lipocalin 2, siderocalin) have been revelatory for furthering our understanding of the role of the enterobactin pathway as a precursor required for the generation of these glucosylated virulence factors (18, 27), and the importance of NGAL as a host response protein that plays a critical role in host protection from certain bacterial infections and possibly detection of enterobactin (19, 22, 40). In the avian host, it is clear from our study that the enterobactin system alone is insufficient for APEC virulence, and it is thus probable that an avian host defense protein akin to NGAL plays a similar role in protection against enterobactin-mediated iron acquisition. A number of different chicken lipocalins which have been shown to be upregulated during inflammation or in response to bacterial signaling molecules have been identified (41), and one of these may have a protective role against enterobactin-mediated bacterial iron acquisition. However, as demonstrated in the current work, the salmochelin-siderophore system, comprised of functional synthesis, export, import, and processing components encoded on the *iro* gene cluster, is efficient at circumventing any avian innate host defenses that may respond to or sequester enterobactin.

ACKNOWLEDGEMENTS

M.C. was funded by a Fondation Armand-Frappier scholarship. Funding for this project was provided by the Natural Sciences and Engineering Research Council of Canada (NSERC), the Canadian Foundation for Innovation, and the Canada Research Chairs programs.

REFERENCES

1. **Bauer, R. J., L. Zhang, B. Foxman, A. Siitonen, M. E. Jantunen, H. Saxen, and C. F. Marrs.** 2002. Molecular epidemiology of 3 putative virulence genes for *Escherichia coli* urinary tract infection-*usp*, *iha*, and *iroN*(*E. coli*). J Infect Dis **185:**1521-4.
2. **Baumler, A. J., T. L. Norris, T. Lasco, W. Voight, R. Reissbrodt, W. Rabsch, and F. Heffron.** 1998. IroN, a novel outer membrane siderophore receptor characteristic of *Salmonella enterica*. J Bacteriol **180:**1446-53.
3. **Bister, B., D. Bischoff, G. J. Nicholson, M. Valdebenito, K. Schneider, G. Winkelmann, K. Hantke, and R. D. Sussmuth.** 2004. The structure of salmochelins: C-glucosylated enterobactins of *Salmonella enterica*. Biometals **17:**471-81.
4. **Brown, P. K., and R. Curtiss, 3rd.** 1996. Unique chromosomal regions associated with virulence of an avian pathogenic *Escherichia coli* strain. Proc Natl Acad Sci U S A **93:**11149-54.
5. **Brzuszkiewicz, E., H. Bruggemann, H. Liesegang, M. Emmerth, T. Olschlager, G. Nagy, K. Albermann, C. Wagner, C. Buchrieser, L. Emody, G. Gottschalk, J. Hacker, and U. Dobrindt.** 2006. How to become a uropathogen: comparative genomic analysis of extraintestinal pathogenic *Escherichia coli* strains. Proc Natl Acad Sci U S A **103:**12879-84.
6. **Chang, A. C., and S. N. Cohen.** 1978. Construction and characterization of amplifiable multicopy DNA cloning vehicles derived from the P15A cryptic miniplasmid. J Bacteriol **134:**1141-56.
7. **Chang, H. Y., J. H. Lee, W. L. Deng, T. F. Fu, and H. L. Peng.** 1996. Virulence and outer membrane properties of a *galU* mutant of *Klebsiella pneumoniae* CG43. Microb Pathog **20:**255-61.
8. **Chen, S. L., C. S. Hung, J. Xu, C. S. Reigstad, V. Magrini, A. Sabo, D. Blasiar, T. Bieri, R. R. Meyer, P. Ozersky, J. R. Armstrong, R. S. Fulton, J. P. Latreille, J. Spieth, T. M. Hooton, E. R. Mardis, S. J. Hultgren, and J. I. Gordon.** 2006. Identification of genes subject to positive selection in uropathogenic strains of *Escherichia coli*: a comparative genomics approach. Proc Natl Acad Sci U S A **103:**5977-82.
9. **Chen, Y. T., H. Y. Chang, Y. C. Lai, C. C. Pan, S. F. Tsai, and H. L. Peng.** 2004. Sequencing and analysis of the large virulence plasmid pLVPK of *Klebsiella pneumoniae* CG43. Gene **337:**189-98.
10. **Crouch, M. L., M. Castor, J. E. Karlinsey, T. Kalhorn, and F. C. Fang.** 2008. Biosynthesis and IroC-dependent export of the siderophore salmochelin are essential for virulence of *Salmonella enterica* serovar Typhimurium. Mol Microbiol. **67:** 971-83.
11. **Dho-Moulin, M., and J. M. Fairbrother.** 1999. Avian pathogenic *Escherichia coli* (APEC). Vet Res **30:**299-316.
12. **Dobrindt, U., G. Blum-Oehler, G. Nagy, G. Schneider, A. Johann, G. Gottschalk, and J. Hacker.** 2002. Genetic structure and distribution of four pathogenicity islands (PAI I(536) to PAI IV(536)) of uropathogenic *Escherichia coli* strain 536. Infect Immun **70:**6365-72.

13. **Dozois, C. M., F. Daigle, and R. Curtiss, 3rd.** 2003. Identification of pathogen-specific and conserved genes expressed in vivo by an avian pathogenic *Escherichia coli* strain. Proc Natl Acad Sci U S A **100:**247-52.
14. **Dozois, C. M., M. Dho-Moulin, A. Bree, J. M. Fairbrother, C. Desautels, and R. Curtiss, 3rd.** 2000. Relationship between the Tsh autotransporter and pathogenicity of avian *Escherichia coli* and localization and analysis of the Tsh genetic region. Infect Immun **68:**4145-54.
15. **Ewers, C., G. Li, H. Wilking, S. Kiessling, K. Alt, E. M. Antao, C. Laturnus, I. Diehl, S. Glodde, T. Homeier, U. Bohnke, H. Steinruck, H. C. Philipp, and L. H. Wieler.** 2007. Avian pathogenic, uropathogenic, and newborn meningitis-causing *Escherichia coli*: how closely related are they? Int J Med Microbiol **297:**163-76.
16. **Feldmann, F., L. J. Sorsa, K. Hildinger, and S. Schubert.** 2007. The salmochelin siderophore receptor IroN contributes to invasion of urothelial cells by extraintestinal pathogenic *Escherichia coli* in vitro. Infect Immun **75:**3183-7.
17. **Fischbach, M. A., H. Lin, D. R. Liu, and C. T. Walsh.** 2006. How pathogenic bacteria evade mammalian sabotage in the battle for iron. Nat Chem Biol **2:**132-8.
18. **Fischbach, M. A., H. Lin, D. R. Liu, and C. T. Walsh.** 2005. In vitro characterization of IroB, a pathogen-associated C-glycosyltransferase. Proc Natl Acad Sci U S A **102:**571-6.
19. **Fischbach, M. A., H. Lin, L. Zhou, Y. Yu, R. J. Abergel, D. R. Liu, K. N. Raymond, B. L. Wanner, R. K. Strong, C. T. Walsh, A. Aderem, and K. D. Smith.** 2006. The pathogen-associated *iroA* gene cluster mediates bacterial evasion of lipocalin 2. Proc Natl Acad Sci U S A **103:**16502-7.
20. **Foster, J. W., and H. K. Hall.** 1992. Effect of *Salmonella typhimurium* ferric uptake regulator (*fur*) mutations on iron- and pH-regulated protein synthesis. J Bacteriol **174:**4317-23.
21. **Foster, J. W., Y. K. Park, I. S. Bang, K. Karem, H. Betts, H. K. Hall, and E. Shaw.** 1994. Regulatory circuits involved with pH-regulated gene expression in *Salmonella typhimurium*. Microbiology **140 (Pt 2):**341-52.
22. **Goetz, D. H., M. A. Holmes, N. Borregaard, M. E. Bluhm, K. N. Raymond, and R. K. Strong.** 2002. The neutrophil lipocalin NGAL is a bacteriostatic agent that interferes with siderophore-mediated iron acquisition. Mol Cell **10:**1033-43.
23. **Griffiths, E.** 1999. Iron in Biological Systems, p. 1-26. *In* G. E. Bullen J.J. (ed.), Iron and Infection - Molecular, Physiological and Clinical Aspects. John Wiley & sons.
24. **Griffiths, E., and P. Williams.** 1999. The iron uptake systems of pathogenic bacteria, fungi and protozoa, p. 87-212. *In* G. E. Bullen J.J. (ed.), Iron and Infection - Molecular, Physiological and Clinical Aspects, 2nd ed. ed. John Wiley & Sons.
25. **Gross, W. G.** 1994. Diseases Due to *Escherichia coli* in Poultry, p. 237-259. *In* C. L. Gyles (ed.), *E.coli* in Domestic Animals & Humans. CAB International.
26. **Grozdanov, L., C. Raasch, J. Schulze, U. Sonnenborn, G. Gottschalk, J. Hacker, and U. Dobrindt.** 2004. Analysis of the genome structure of the nonpathogenic probiotic *Escherichia coli* strain Nissle 1917. J Bacteriol **186:**5432-41.

27. **Hantke, K., G. Nicholson, W. Rabsch, and G. Winkelmann.** 2003. Salmochelins, siderophores of *Salmonella enterica* and uropathogenic *Escherichia coli* strains, are recognized by the outer membrane receptor IroN. Proc Natl Acad Sci U S A **100:**3677-82.
28. **Johnson, T. J., S. J. Johnson, and L. K. Nolan.** 2006. Complete DNA sequence of a ColBM plasmid from avian pathogenic *Escherichia coli* suggests that it evolved from closely related ColV virulence plasmids. J Bacteriol **188:**5975-83.
29. **Johnson, T. J., K. E. Siek, S. J. Johnson, and L. K. Nolan.** 2006. DNA sequence of a ColV plasmid and prevalence of selected plasmid-encoded virulence genes among avian *Escherichia coli* strains. J Bacteriol **188:**745-58.
30. **Kanamaru, S., H. Kurazono, S. Ishitoya, A. Terai, T. Habuchi, M. Nakano, O. Ogawa, and S. Yamamoto.** 2003. Distribution and genetic association of putative uropathogenic virulence factors *iroN*, *iha*, *kpsMT*, *ompT* and *usp* in *Escherichia coli* isolated from urinary tract infections in Japan. J Urol **170:**2490-3.
31. **Kaper, J. B., J. P. Nataro, and H. L. Mobley.** 2004. Pathogenic *Escherichia coli*. Nat Rev Microbiol **2:**123-40.
32. **Konopka, K., and J. B. Neilands.** 1984. Effect of serum albumin on siderophore-mediated utilization of transferrin iron. Biochemistry **23:**2122-7.
33. **Lamarche, M. G., C. M. Dozois, F. Daigle, M. Caza, R. Curtiss, 3rd, J. D. Dubreuil, and J. Harel.** 2005. Inactivation of the *pst* system reduces the virulence of an avian pathogenic *Escherichia coli* O78 strain. Infect Immun **73:**4138-45.
34. **Lepine, F., E. Deziel, S. Milot, and L. G. Rahme.** 2003. A stable isotope dilution assay for the quantification of the Pseudomonas quinolone signal in *Pseudomonas aeruginosa* cultures. Biochim Biophys Acta **1622:**36-41.
35. **Leveille, S., M. Caza, J. R. Johnson, C. Clabots, M. Sabri, and C. M. Dozois.** 2006. Iha from an *Escherichia coli* urinary tract infection outbreak clonal group A strain is expressed in vivo in the mouse urinary tract and functions as a catecholate siderophore receptor. Infect Immun **74:**3427-36.
36. **Lin, H., M. A. Fischbach, D. R. Liu, and C. T. Walsh.** 2005. In vitro characterization of salmochelin and enterobactin trilactone hydrolases IroD, IroE, and Fes. J Am Chem Soc **127:**11075-84.
37. **Marrs, C. F., L. Zhang, and B. Foxman.** 2005. *Escherichia coli* mediated urinary tract infections: are there distinct uropathogenic *E. coli* (UPEC) pathotypes? FEMS Microbiol Lett **252:**183-90.
38. **Negre, V. L., S. Bonacorsi, S. Schubert, P. Bidet, X. Nassif, and E. Bingen.** 2004. The siderophore receptor IroN, but not the high-pathogenicity island or the hemin receptor ChuA, contributes to the bacteremic step of *Escherichia coli* neonatal meningitis. Infect Immun **72:**1216-20.
39. **Nelson, A. L., J. M. Barasch, R. M. Bunte, and J. N. Weiser.** 2005. Bacterial colonization of nasal mucosa induces expression of siderocalin, an iron-sequestering component of innate immunity. Cell Microbiol **7:**1404-17.
40. **Nelson, A. L., A. J. Ratner, J. Barasch, and J. N. Weiser.** 2007. Interleukin-8 secretion in response to aferric enterobactin is potentiated by siderocalin. Infect Immun **75:**3160-8.

41. **Pagano, A., P. Giannoni, A. Zambotti, D. Sanchez, M. D. Ganfornina, G. Gutierrez, N. Randazzo, R. Cancedda, and B. Dozin.** 2004. Phylogeny and regulation of four lipocalin genes clustered in the chicken genome: evidence of a functional diversification after gene duplication. Gene **331:**95-106.
42. **Payne, S. M., and A. R. Mey.** 2004. Pathogenic *Escherichia coli*, *Shigella*, and *Salmonella*, p. 199-239. *In* J. H. Crosa, A. R. Mey, and S. M. Payne (ed.), Iron Transport in Bacteria. ASM Press, Washington, D. C.
43. **Pourbakhsh, S. A., M. Boulianne, B. Martineau-Doize, C. M. Dozois, C. Desautels, and J. M. Fairbrother.** 1997. Dynamics of *Escherichia coli* infection in experimentally inoculated chickens. Avian Dis **41:**221-33.
44. **Provence, D. L., and R. Curtiss, 3rd.** 1992. Role of *crl* in avian pathogenic *Escherichia coli*: a knockout mutation of *crl* does not affect hemagglutination activity, fibronectin binding, or curli production. Infect Immun **60:**4460-7.
45. **Rabsch, W., U. Methner, W. Voigt, H. Tschape, R. Reissbrodt, and P. H. Williams.** 2003. Role of receptor proteins for enterobactin and 2,3-dihydroxybenzoylserine in virulence of *Salmonella enterica*. Infect Immun **71:**6953-61.
46. **Ratledge, C., and L. G. Dover.** 2000. Iron metabolism in pathogenic bacteria. Annu Rev Microbiol **54:**881-941.
47. **Restieri, C., G. Garriss, M. C. Locas, and C. M. Dozois.** 2007. Autotransporter-encoding sequences are phylogenetically distributed among *Escherichia coli* clinical isolates and reference strains. Appl Environ Microbiol **73:**1553-62.
48. **Rodriguez-Siek, K. E., C. W. Giddings, C. Doetkott, T. J. Johnson, M. K. Fakhr, and L. K. Nolan.** 2005. Comparison of *Escherichia coli* isolates implicated in human urinary tract infection and avian colibacillosis. Microbiology **151:**2097-110.
49. **Rodriguez-Siek, K. E., C. W. Giddings, C. Doetkott, T. J. Johnson, and L. K. Nolan.** 2005. Characterizing the APEC pathotype. Vet Res **36:**241-56.
50. **Ron, E. Z.** 2006. Host specificity of septicemic *Escherichia coli*: human and avian pathogens. Curr Opin Microbiol **9:**28-32.
51. **Russo, T. A., U. B. Carlino, A. Mong, and S. T. Jodush.** 1999. Identification of genes in an extraintestinal isolate of *Escherichia coli* with increased expression after exposure to human urine. Infect Immun **67:**5306-14.
52. **Russo, T. A., and J. R. Johnson.** 2003. Medical and economic impact of extraintestinal infections due to *Escherichia coli*: focus on an increasingly important endemic problem. Microbes Infect **5:**449-56.
53. **Russo, T. A., and J. R. Johnson.** 2000. Proposal for a new inclusive designation for extraintestinal pathogenic isolates of *Escherichia coli*: ExPEC. J Infect Dis **181:**1753-4.
54. **Russo, T. A., C. D. McFadden, U. B. Carlino-MacDonald, J. M. Beanan, T. J. Barnard, and J. R. Johnson.** 2002. IroN functions as a siderophore receptor and is a urovirulence factor in an extraintestinal pathogenic isolate of *Escherichia coli*. Infect Immun **70:**7156-60.
55. **Schubert, S., B. Picard, S. Gouriou, J. Heesemann, and E. Denamur.** 2002. Yersinia high-pathogenicity island contributes to virulence in *Escherichia coli* causing extraintestinal infections. Infect Immun **70:**5335-7.

56. **Sorsa, L. J., S. Dufke, J. Heesemann, and S. Schubert.** 2003. Characterization of an *iroBCDEN* gene cluster on a transmissible plasmid of uropathogenic *Escherichia coli*: evidence for horizontal transfer of a chromosomal virulence factor. Infect Immun **71:**3285-93.
57. **Torres, A. G., P. Redford, R. A. Welch, and S. M. Payne.** 2001. TonB-dependent systems of uropathogenic *Escherichia coli*: aerobactin and heme transport and TonB are required for virulence in the mouse. Infect Immun **69:**6179-85.
58. **Valdebenito, M., B. Bister, R. Reissbrodt, K. Hantke, and G. Winkelmann.** 2005. The detection of salmochelin and yersiniabactin in uropathogenic *Escherichia coli* strains by a novel hydrolysis-fluorescence-detection (HFD) method. Int J Med Microbiol **295:**99-107.
59. **Valdebenito, M., A. L. Crumbliss, G. Winkelmann, and K. Hantke.** 2006. Environmental factors influence the production of enterobactin, salmochelin, aerobactin, and yersiniabactin in *Escherichia coli* strain Nissle 1917. Int J Med Microbiol **296:**513-20.
60. **Welch, R. A., V. Burland, G. Plunkett, 3rd, P. Redford, P. Roesch, D. Rasko, E. L. Buckles, S. R. Liou, A. Boutin, J. Hackett, D. Stroud, G. F. Mayhew, D. J. Rose, S. Zhou, D. C. Schwartz, N. T. Perna, H. L. Mobley, M. S. Donnenberg, and F. R. Blattner.** 2002. Extensive mosaic structure revealed by the complete genome sequence of uropathogenic *Escherichia coli*. Proc Natl Acad Sci U S A **99:**17020-4.
61. **Williams, K. P.** 2003. Traffic at the tmRNA gene. J Bacteriol **185:**1059-70.
62. **Zhu, M., M. Valdebenito, G. Winkelmann, and K. Hantke.** 2005. Functions of the siderophore esterases IroD and IroE in iron-salmochelin utilization. Microbiology **151:**2363-72.

TABLE 1: Bacterial strains and plasmids used for this study

Bacterial strains and plasmids	Genotype and phenotype[a]	Reference or source
Bacterial strains		
χ7122	Avian pathogenic, O78 :K80 :H9, *gyrA*, Nal^R	(44)
χ7304	Δ*iroBCDEN ::nptII* Δ*iucABCD iutA ::xylE*, Km^R, Nal^R	(13)
DH5α	F- (Δ80d *lacZ*ΔM15) Δ(*lacZYA-argF*)U169 *endA1 recA1 hsdR17*(r_K-m_K+) *deoR thi*-1 *supE44 gyrA96 relA1* -	Bethesda Research Laboratories
Plasmids		
pACYC184	p15A replicon, Cm^R, Tc^R	(6)
pBC SK (-)	ColE1 origin, Cm^R	Stratagene
pYA3661	pACYC184 :: *iroBCDEN*, Cm^R	(13)
pIJ33	pACYC184 :: *iroN*, Cm^R	This study
pIJ34	pACYC184 :: *iroBCDE*, Cm^R	This study
pIJ37	pACYC184 :: *iroBDEN*, Cm^R	This study
pIJ53	pACYC184 :: *iroB*, Cm^R	This study
pIJ121	pACYC184 :: *iroBC*, Cm^R	This study
pIJ135	pACYC184 :: *iroBCN*, Cm^R	This study
pIJ136	pACYC184 :: *iroBCEN*, Cm^R	This study
pIJ137	pACYC184 :: *iroBCDN*, Cm^R	This study

a- Cm:chloramphenicol, Km : kanamycin Nal: nalidixic acid.

TABLE 2: Distribution of *iro* genes among avian pathogenic *E. coli* (APEC) and avian fecal commensal isolates according to lethality class.

Lethality class	*E. coli* isolates			
	APEC		Avian fecal commensal	
	Total no. isolates	No. *iro*-positive isolates [a] (%)	Total no. isolates	No. *iro*-positive isolates [a] (%)
LC1[b]	222	203 (91) [c]	1	1 (100)
LC2	38	24 (63)	12	6 (50)
LC3	38	17 (45)	19	3 (16)
Total	**298**	**244 (82)** [d]	**32**	**10 (31)**

[a] Positive PCR amplification of the *iroB* and *iroN* genes.

[b] Lethality classes (LC) were defined by lethality in 1-day-old chicks as follows: LC1, 50% lethal dose (LD50) < 10^8 CFU; LC2, LD50 ≥ 10^8 CFU; LC3, not lethal at ≥ 10^8 CFU. (14)

[c] *iro* sequences were significantly associated with APEC isolates from LC1 as compared to APEC isolates from LC2 or LC3 ($P < 0.0001$) using Fisher's exact test.

[d] *iro* sequences were significantly associated with APEC isolates relative to environmental isolates ($P < 0.0001$) using Fisher's exact test.

TABLE 3: Score based evaluation of gross lesions in organs of infected chickens

E. coli strain	Mean lesion score ± SEM [a]	
	Air sacs [b]	Liver and Heart [c]
χ7122	2.7 ± 0.2	3.2 ± 0.3
χ7304 (Δ*iro* Δ*iucABCiutA*)	1.5 ± 0.4 *	0.8 ± 0.3 **
χ7304 pYA3661 (*iroBCDEN*)	2.8 ± 0.3	3.2 ± 0.2
χ7304 pIJ34 (*iroBCDE*)	1.6 ± 0.4 *	1.3 ± 0.5 *
χ7304 pIJ37 (*iroBDEN*)	1.4 ± 0.3 **	1.0 ± 0.2 **
χ7304 pIJ135 (*iroBCN*)	1.4 ± 0.3 **	0.8 ± 0.1 **
χ7304 pIJ136 (*iroBCEN*)	1.9 ± 0.3	1.4 ± 0.1 **
χ7304 pIJ137 (*iroBCDN*)	2.7 ± 0.3	2.4 ± 0.4

[a] Lesion scores are presented as the mean of values attributed to gross lesions of airsacculitis and combined lesions of perihepatitis/ and perihepatitis as described in (33).

[b] Mean lesion scores for airsacculitis in both caudal thoracic air sacs.

[c] Combined lesion scoring values for pericarditis and perihepatitis. Statistical differences compared with the wild-type strain using the two-tailed Mann Whitney test are noted: * ($P < 0.05$) ** ($P < 0.001$)

Table 4: Mean concentrations (μM) of salmochelins detected in culture supernatants.[a]

Strain (genotype)	Mono-glucosylated molecules				Di-glucosylated molecules			Tri-glucosylated molecules	
	MGE	Linear MGE	S1	SX	DGE (S4)	Linear DGE (S2)	S5	TGE	Linear TGE
χ7122	1.7 ± 0.28	1.1 ± 0.11	5.1 ± 0.12	9.8 ± 0.33	0.31 ± 0.03	1.1 ± 0.02	0.45 ± 0.02	N.D.	N.D.
χ7304[b]	N.D.	N.D.	N.D.	N.D.	N.D.	N.D.	N.D.	N.D.	N.D.
χ7304 pYA3661 (*iroBCDEN*)[b]	**0.22 ± 0.02**	**0.14 ± 0.03**	**9.2 ± 0.94**	**31.0 ± 4.4**	**0.06 ± 0.004**	**2.9 ± 0.07**	**1.7 ± 0.18**	N.D.	N.D.
χ7304 pIJ34 (*iroBCDE*)[c]	**0.09 ± 0.01**	0.07 ± 0.01	8.6 ± 1.1	26.1 ± 3.9	**0.04 ± 0.005**	**8.8 ± 0.98**	1.5 ± 0.23	N.D.	0.06 ± 0.01
χ7304 pIJ137 (*iroBCDN*)[c]	**0.17 ± 0.001**	**0.22 ± 0.01**	9.9 ± 0.55	20.4 ± 1.1	**0.42 ± 0.02**	**22.7 ± 1.1**	1.5 ± 0.05	0.04 ± 0.001	0.19 ± 0.01
χ7304 pIJ136 (*iroBCEN*)[c]	**0.09 ± 0.01**	**0.06 ± 0.01**	**4.0 ± 0.33**	19.6 ± 1.8	**0.23 ± 0.02**	**5.6 ± 0.94**	1.7 ± 0.09	N.D.	0.04 ± 0.004
χ7304 pIJ53 (*iroB*)[c]	N.D.	N.D.	**0.04 ± 0.001**	N.D.	N.D.	N.D.	N.D.	N.D.	N.D.
χ7304 pIJ121 (*iroBC*)[c]	**0.09 ± 0.01**	N.D.	**1.3 ± 0.02**	**3.2 ± 0.26**	**0.52 ± 0.02**	**5.4 ± 0.12**	**0.43 ± 0.02**	0.25 ± 0.01	0.13 ± 0.01
χ7304 pIJ135 (*iroBCN*)[c]	**0.13 ± 0.01**	**0.04 ± 0.002**	**1.1 ± 0.04**	**3.5 ± 0.40**	**0.46 ± 0.01**	**5.1 ± 0.03**	**0.46 ± 0.04**	0.29 ± 0.01	0.15 ± 0.01
χ7304 pIJ37 (*iroBDEN*)[c]	N.D.	N.D.	**1.3 ± 0.1**	31.7 ± 3.5	N.D.	**0.71 ± 0.07**	**0.05 ± 0.005**	N.D.	N.D.

[a] Values represent the means ± the standard error of the mean of at least three independently grown cultures. Bold values indicate significant differences ($P < 0.05$) using a two-tailed unpaired t test. N.D. indicates the molecule was not detected in samples.

[b] Statistical differences were determined by using χ7122 as the reference strain.

[c] Statistical differences were determined by using χ7304 pYA3661 (*iroBCDEN*) as the reference.

Table 5: Mean concentrations (μM) of enterobactin related molecules detected in culture supernatants.[a]

Strain (genotype)	Enterobactin	$(DHBS)_3$	$(DHBS)_2$	DHBS
χ7122	12.1 ± 3.4	25.3 ± 4.6	33.1 ± 4.7	11.6 ± 1.2
χ7304[b]	**62.9 ± 7.2**	**62.7 ± 6.2**	**86.6 ± 9.3**	**25.9 ± 3.9**
χ7304 pYA3661 (*iroBCDEN*)[b]	**1.5 ± 0.16**	**1.9 ± 0.25**	**9.6 ± 1.01**	**27.1 ± 3.7**
χ7304 pIJ34 (*iroBCDE*)[c]	**0.9 ± 0.07**	**0.9 ± 0.11**	10.9 ± 1.9	20.8 ± 3.1
χ7304 pIJ137 (*iroBCDN*)[c]	**3.8 ± 0.14**	**5.1 ± 0.23**	**22.2 ± 0.9**	**13.9 ± 0.8**
χ7304 pIJ136 (*iroBCEN*)[c]	**0.6 ± 0.06**	**0.8 ± 0.12**	8.6 ± 0.57	**15.0 ± 1.3**
χ7304 pIJ53 (*iroB*)[c]	1.6 ± 0.35	**0.6 ± 0.10**	**0.5 ± 0.01**	N.D.
χ7304 pIJ121 (*iroBC*)[c]	**3.7 ± 0.20**	**2.9 ± 0.09**	10.7 ± 0.4	**1.6 ± 0.10**
χ7304 pIJ135 (*iroBCN*)[c]	**4.6 ± 0.36**	**3.9 ± 0.29**	11.8 ± 0.5	**2.6 ± 0.15**
χ7304 pIJ37 (*iroBDEN*)[c]	**2.7 ± 0.25**	**3.7 ± 0.35**	**15.3 ± 1.5**	**8.2 ± 1.12**

[a] Values represent the means ± the standard error of the mean of at least three independently grown cultures. Bold values indicate significant differences ($P < 0.05$) using a two-tailed unpaired t test. N.D. indicates the molecule was not detected in samples

[b] Statistical differences were determined by using χ7122 as the reference strain.

[c] Statistical differences were determined by using χ7304 pYA3661 (*iroBCDEN*) as the reference strain

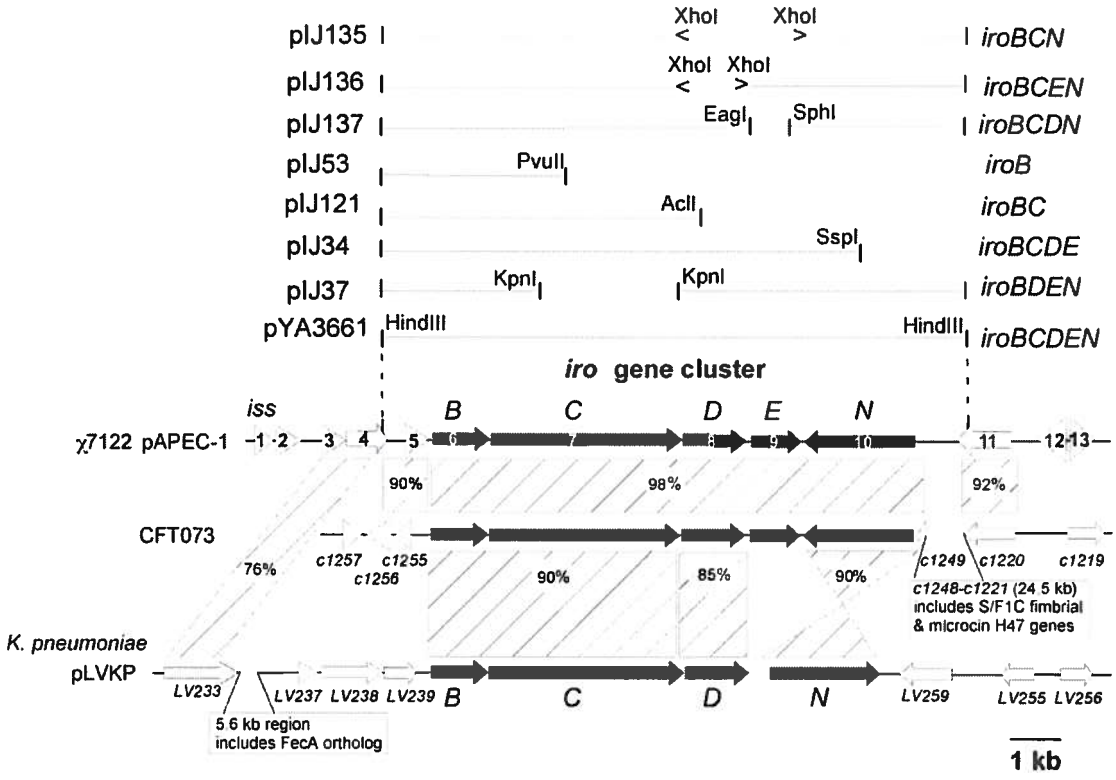

Fig. 1. Schematic diagram of the region comprising the iro locus and flanking sequences encoded on plasmid pAPEC-1 of APEC strain χ7122. Numbers within arrows correspond to designated open reading frames (ORFs) within the sequence (Accession no. AF449498). Black arrows indicate the *iro* genes. Nucleotide identities between segments of the χ7122 *iro* encoding region and those of UPEC strain CFT073 (Acc. no. AE014075; (60)) and *Klebsiella pneumoniae* plasmid pLVKP (Acc. no. AY378100; (9)) are illustrated within boxed segments, with numbers representing the % nucleotide identity between a segment. Additional sequences of CFT073 and pLVKP that are absent from the pAPEC-1 region are illustrated with diagonal lines and described in text boxes. Plasmid constructs described in the text are illustrated above the pAPEC-1 encoded *iro* locus region. Primers used to generate clones by PCR are indicated with the symbol > (for sense primer) or < (for antisense primer). Corresponding restriction endonuclease sites used to generate the plasmids are indicated. See text in materials and methods for details.

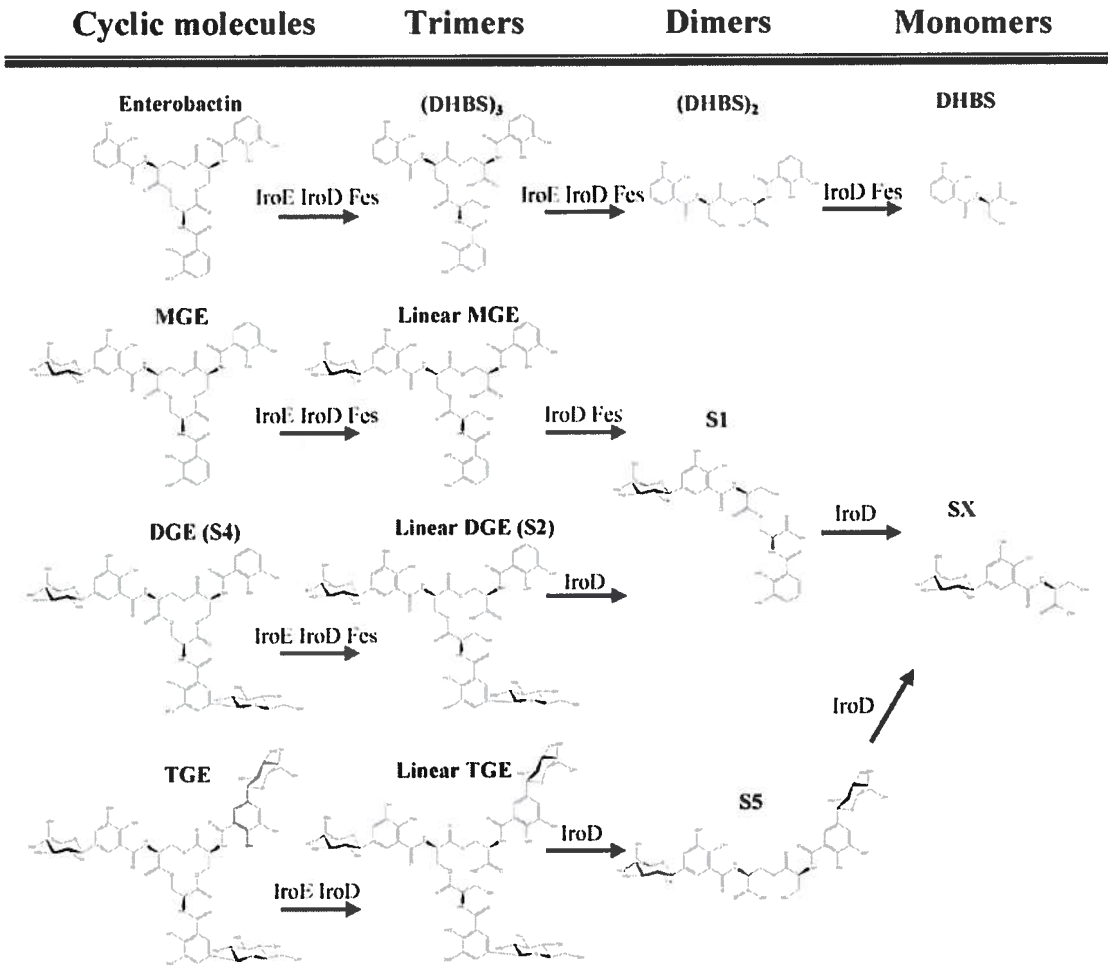

Fig. 2. Scheme showing molecular structures of each the catecholate siderophores that were analysed. Enzymes predicted to play a role in processing of salmochelins, enterobactin, or DHBS derivatives based on biochemical studies of Lin *et al.*(36), and Zhu *et al.* (62) are indicated.

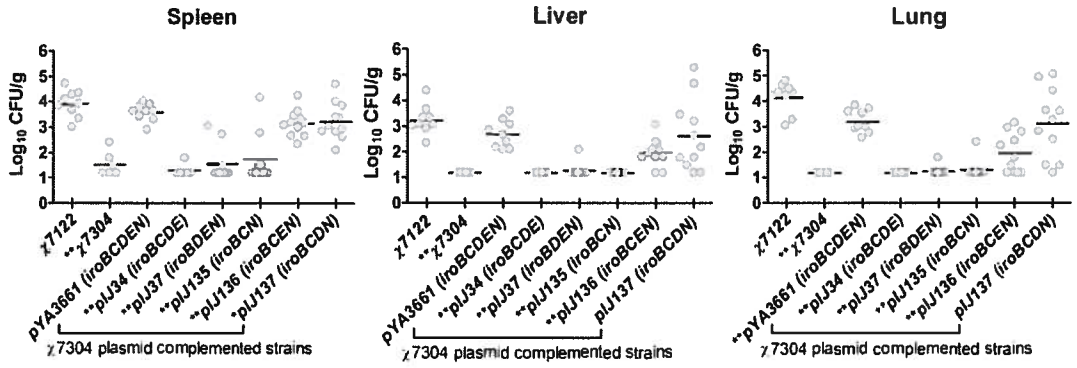

Fig. 3. Bacterial numbers present in the lungs, spleens, and livers of chickens infected with wild-type APEC strain χ7122, isogenic mutant derivatives and *iro* plasmid complemented strains. Data points represent bacterial counts from tissues isolated from different chickens (n = 5-11) 48 h post-infection. Horizontal bars represent the median bacterial colony-forming units. Statistical differences compared with the wild-type strain are noted: * ($P < 0.05$); ** ($P < 0.01$) using the two-tailed Mann Whitney test.

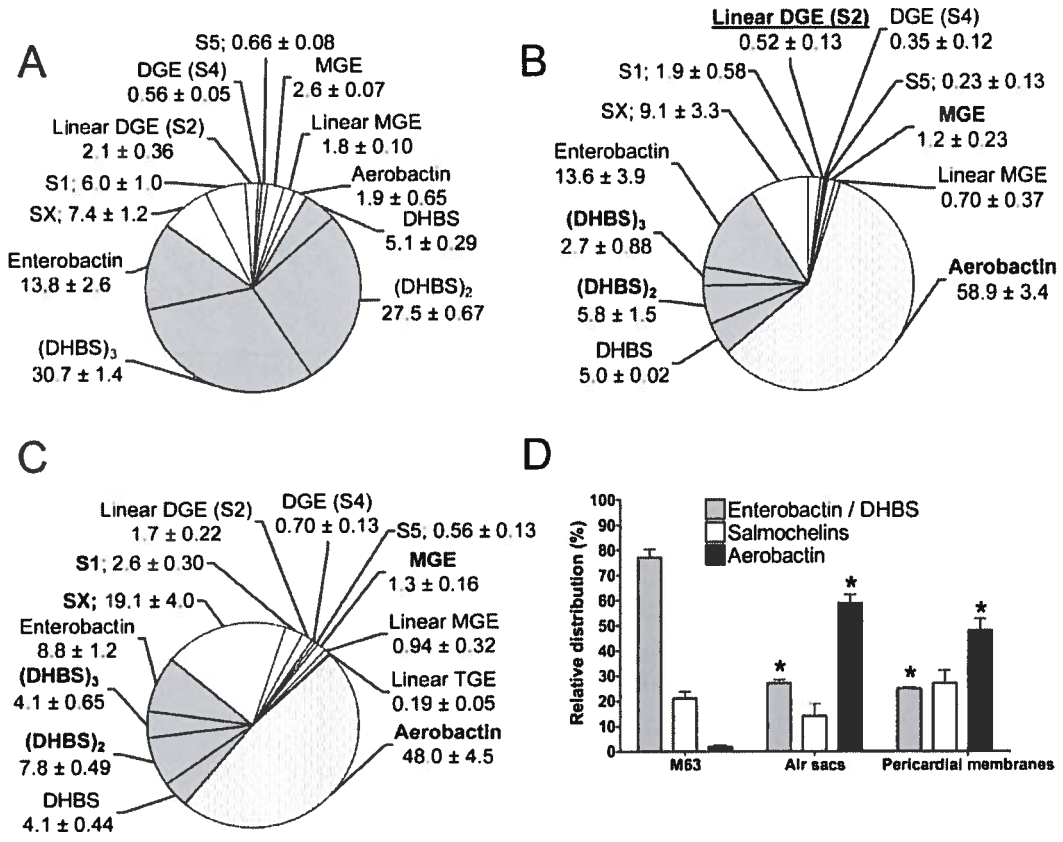

Fig. 4: Mean distribution of siderophores produced by wild-type APEC χ7122 in iron-poor M63 medium (A) and in air sacs (B) and pericardia (C) of infected chickens. The error values are the standard errors of the means. Bold values indicate significant differences of the same molecule as compared to levels present in iron-poor M63 medium. The underlined value indicates a significant difference between the air sacs and the pericardial membrane. (D) Relative total % distribution of siderophores belonging to each siderophore group. * indicates a significant difference of the same group of siderophore between the *in vivo* and *in vitro* conditions. ($P < 0.05$) using the unpaired t-test.

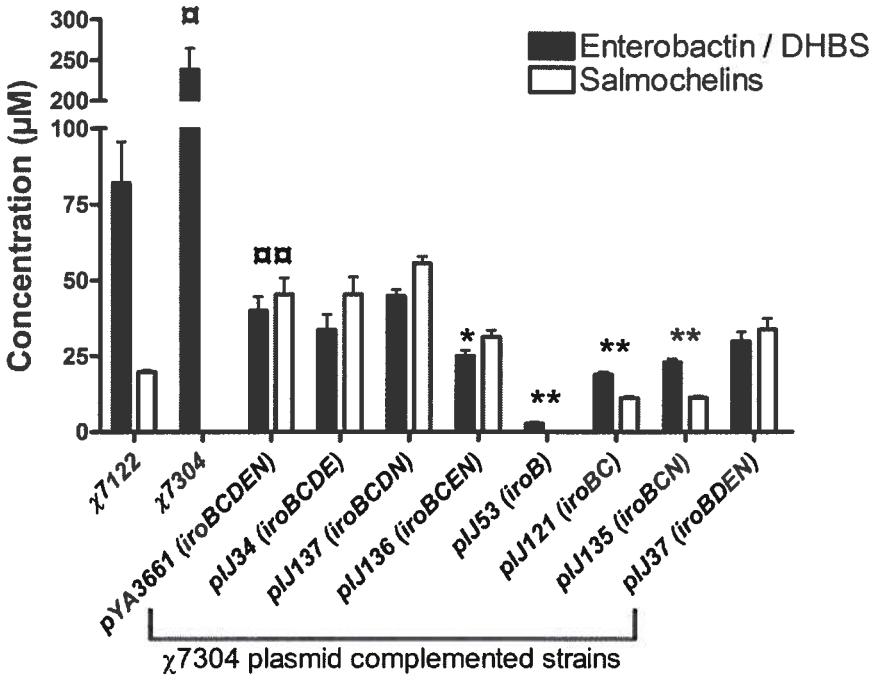

Fig. 5: Mean concentrations of enterobactin and DHBS (Enterobactin/DHBS) molecules and salmochelins detected in culture supernatants. The amount of each molecule was normalized with the internal standard and quantities were summed up according to the related siderophore group: salmochelins or enterobactin and non-glucosylated DHBS-derivatives (Enterobactin/DHBS). Error bars represent the standard errors of the means. ¤ indicates a significant difference between the total enterobactin/DHBS molecules produced by strain χ7304 compared to χ7122. ¤¤ indicates a significant difference between the total enterobactin / DHBS molecules and total salmochelins produced by strain χ7304 (pYA3661) compared to χ7122. * indicates a significant difference between the total enterobactin/DHBS molecules produced compared to χ7304 (pYA3661). ** indicates a significant difference between the total enterobactin/DHBS molecules and salmochelins produced compared to χ7304 (pYA3661) ($P < 0.05$).

Article #2

Secretion, but not overall synthesis, of catecholate siderophores contributes to virulence of extra-intestinal pathogenic *Escherichia coli*.

Mélissa Caza, François Lépine and Charles M. Dozois.
Soumis à Molecular Microbiology (19/07/2010)

A) Contribution de l'étudiante

1- L'étude présentée dans l'article soumis à Molecular Microbiology, avait pour objectifs de déterminer l'importance de la synthèse et la sécrétion des sidérophores catécholates pour la virulence de la souche χ7122 dans le modèle d'infection septicémique aviaire. Les résultats ont démontré que les molécules non- et mono-glucosylées sont préférentiellement sécrétées par EntS, tandis que les molécules di- et tri-glucosylées sont sécrétées par IroC. La sécrétion des sidérophores catécholates est un mécanisme important pour la virulence de la souche, puisque l'inhibition de la sécrétion de ces molécules diminue l'aptitude physiologique (fitness) des bactéries lorsque le fer est limité. Bien que la sécrétion des sidérophores catécholates soit dépendante de la synthèse de l'entérobactine, ce dernier n'est pas requis pour la virulence de la souche, seulement si un deuxième système de sidérophore, tel que l'aérobactine, est toujours fonctionnel.

2- L'étude a été réalisée en utilisant une approche multidisciplinaire regroupant des techniques de génétique bactérienne, un modèle d'infection septicémique aviaire, ainsi que de la chromatographie en phase liquide couplée à la spectrométrie de masse.

3- Avec l'aide des directeurs de recherches, la candidate a réalisé toutes les étapes de conceptions et réalisations des expériences, ainsi qu'à l'écriture du manuscrit.

B) Résumé de l'article:

Les *Escherichia coli* pathogènes extra-intestinaux (ExPEC) utilisent des sidérophores pour acquérir le fer pendant une infection. L'entérobactine et les salmochélines sont des sidérophores catécholates produits par certaines souches ExPEC et autres entérobactéries

pathogènes. Des mutants de synthèse et de sécrétion des sidérophores de la souche aviaire ExPEC χ7122 ont été testés dans un modèle d'infection aviaire. Une baisse significative des comptes bactériens dans les organes et dans le sang des poulets infectés par les souches mutantes pour la synthèse de l'entérobactine et de l'aérobactine ainsi que les souches mutantes pour les gènes *entS* et *entSiroC* a été obtenues. Une baisse du compte bactérien dans le sang des poulets infectés par le mutant Δ*iroC* a également été obtenue. De plus, le mutant Δ*entD*, ne produisant que l'aérobactine, a gardé sa pleine virulence, et la perte du gène *entD* dans un mutant Δ*entS*Δ*iroC* a rétabli la virulence de la souche. La quantification par LC-MS/MS des sidérophores des mutants défectueux en sécrétion a démontré que la perte du gène *entS* nuit à la sécrétion de l'entérobactine et de l'entérobactine mono-glucosylée, tandis que la perte du gène *iroC* empêche la sécrétion des molécules di- et tri-glucosylée d'entérobactine. La perte d'*entS* et/ou *iroC* produit une accumulation intracellulaire et une augmentation de la sécrétion des sidérophores monomériques. Les mutants Δ*entS* et/ou Δ*iroC* établissent moins efficacement une infection dans le modèle d'infection mixte. En contrepartie, les mutants de synthèse des sidérophores catécholates (Δ*entD* et Δ*iroB*) ont causé une infection aussi bien que la souche sauvage dans ce modèle d'infection mixte. Ces résultats montrent que EntS et IroC effectuent la sécrétion des sidérophores catécholate et que le rôle de ces exportateurs pour la virulence des souches ExPEC est dépendant de la synthèse de l'entérobactine, qui n'est elle–même pas requise si d'autres sidérophores, tels que l'aérobactine, sont fonctionnels.

Secretion, but not overall synthesis, of catecholate siderophores contributes to virulence of extra-intestinal pathogenic *Escherichia coli*.

Running title: Role of catecholate siderophore export for ExPEC virulence

Mélissa Caza, François Lépine and Charles M. Dozois*

INRS-Institut Armand-Frappier, Laval, Québec, CANADA

*Corresponding author:
Charles M. Dozois
Canada Research Chair in Infectious Bacterial Diseases
INRS-Institut Armand-Frappier
531 boul. des Prairies
Laval, Québec, CANADA H7V 1B7
Phone : 450.687.5010 ext. 4221 Fax : 450.686.5501
E-mail : charles.dozois@iaf.inrs.ca

Summary

Extra-intestinal pathogenic *Escherichia coli* (ExPEC) use siderophores to sequester iron during infection. Enterobactin and salmochelins are catecholate siderophores produced by some ExPEC strains and other pathogenic enterobacteria. Siderophore export and synthesis mutants of avian ExPEC strain χ7122 were tested in a chicken infection model. In single-strain infections, siderophore-negative (Δ*entD*Δ*iuc*), Δ*entS*, and Δ*entS*Δ*iroC* export mutants were attenuated in tissues and blood, whereas the Δ*iroC* export mutant was only attenuated in blood. Interestingly, the Δ*entD* mutant, producing only aerobactin, retained full virulence, and loss of *entD* in the Δ*entS*Δ*iroC* mutant restored virulence. LC-MS/MS quantification of siderophores in export mutants demonstrated that loss of *entS* impaired enterobactin and mono-glucosylated enterobactin secretion, whereas loss of *iroC* impaired di- and tri-glucosylated enterobactin secretion. Loss of *entS* and/or *iroC* resulted in intracellular accumulation and increased secretion of siderophore monomers. Catecholate siderophore export mutants also demonstrated decreased fitness in a co-challenge infection model. By contrast, catecholate siderophore synthesis mutants (Δ*entD* and Δ*iroB*) competed as well as the wild-type strain. Results establish that EntS and IroC mediate specific export of catecholate siderophores and the role of these exporters for ExPEC virulence is contingent on enterobactin synthesis, which is not required when other siderophores like aerobactin are functional.

Introduction

In humans and animals, iron is sequestered in ferritins, heme compounds and glycoproteins, such as transferrins, lactoferrins and ovotransferrins, making iron virtually unavailable for bacteria (Ratledge, 2007, Ratledge & Dover, 2000). Pathogenic bacteria have developed several high-affinity iron chelating siderophore systems to overcome this iron scarcity in the host (Andrews *et al.*, 2003, Ratledge & Dover, 2000). Catecholate siderophores, such as enterobactin (enterochelin) and salmochelins are produced by many pathogenic enterobacteria including *Escherichia coli*, *Salmonella* spp. and *Klebsiella* spp. and salmochelins have been reported to contribute to virulence (Dozois *et al.*, 2003, Crouch *et al.*, 2008, Bachman *et al.*, 2009). Enterobactin, a cyclic trimer of 2,3-dihydroxybenzoyl serine (DHBS), can capture ferric iron from host proteins, due to its superior binding strength (Brock *et al.*, 1983, O'Brien & Gibson, 1970, Pollack & Neilands, 1970, Brock *et al.*, 1991). However, enterobactin can be sequestered by the host innate defense protein neutrophil-gelatinase-associated lipocalin (NGAL, also called lipocalin 2 or siderocalin), hence preventing bacterial acquisition of host iron via enterobactin (Flo *et al.*, 2004, Goetz *et al.*, 2002). Glucosylation of enterobactin is a bacterial virulence mechanism to circumvent sequestration of catecholate siderophores by NGAL (Fischbach *et al.*, 2006). Modification of enterobactin is mediated by the IroB glucosyltransferase, encoded on the *iroBCDEN* gene cluster, and leads to synthesis of glycosylated derivatives termed salmochelins (Bister *et al.*, 2004). Addition of glucose molecules on catechol moieties of enterobactin results in synthesis of monoglucosylated enterobactin (MGE), diglucosylated enterobactin (DGE or S4) or triglucosylated enterobactin (TGE) (Fischbach *et al.*, 2005), although MGE and DGE are the predominant trimeric salmochelins that have been identified in bacterial cultures (Caza *et al.*, 2008, Crouch et al., 2008). Other salmochelins (SX, S1 and S5) and enterobactin derivative molecules include linear trimers, dimers and monomers of DHBS, some of which may function as siderophores and contribute to virulence (Methner *et al.*, 2008, Hantke, 1990, Hantke *et al.*, 2003).

Previous reports demonstrated that salmochelin synthesis and/or uptake via the outer membrane siderophore receptor IroN contributes to ExPEC virulence (Caza et al., 2008,

Russo *et al.*, 2002, Negre *et al.*, 2004). In the avian pathogenic *E. coli* (APEC) strain χ7122, loss of both the aerobactin and salmochelin encoding systems resulted in an avirulent strain that produced enterobactin but that was unable to colonize extraintestinal sites in the chicken infection model (Dozois et al., 2003). These results, suggested that enterobactin alone is inadequate for systemic survival of this avian ExPEC strain. While synthesis of salmochelins is inherently dependent on the enterobactin metabolic pathway, secretion of these siderophores, at least enterobactin and DGE (S4) has been shown to be specifically mediated by EntS and IroC respectively (Crouch et al., 2008, Furrer *et al.*, 2002). IroC is also required for virulence of *Salmonella enterica* serovar Typhimurium, which produces both enterobactin and salmochelin siderophores (Crouch et al., 2008). In the current report, we investigated the role of catecholate siderophore synthesis and the specific and combined roles of EntS and IroC for secretion of enterobactin and salmochelins in *E. coli* χ7122, a well characterized virulent avian ExPEC strain that produces these siderophores and the unrelated hydroxamate siderophore aerobactin.

Results

Role of siderophore synthesis for the virulence of strain χ7122.

Avian pathogenic *E. coli* strain χ7122 produces the hydroxamate siderophore aerobactin and thirteen known catecholate siderophore molecules: four belong to the enterobactin group and nine glucosylated derivatives comprise the salmochelins (Caza et al., 2008). Earlier studies have shown that salmochelin and aerobactin systems are required for the virulence of χ7122 in a chicken sepsis model of infection, and that expression of the enterobactin system alone is not sufficient for bacterial infection (Caza et al., 2008, Dozois et al., 2003). However, the direct role of enterobactin synthesis for the virulence of the APEC strain has not been investigated. The specific role of enterobactin synthesis was determined using a Δ*entD* derivative of χ7122 (QT163). *entD* encodes the phosphopantetheinyl transferase required for enterobactin synthesis. This mutant did not produce catecholate siderophores, neither enterobactin nor salmochelins, but still produced aerobactin. Despite loss of the catecholate siderophores, in the chicken infection model strain the Δ*entD* was present in blood and tissues at levels similar to the wild-type strain (Fig.1). Gross lesion scores were also similar to those in chickens infected with the wild-type strain (Table 1). These results indicate that abrogation of catecholate siderophore synthesis in ExPEC strain χ7122 does not reduce systemic virulence.

As aerobactin has previously been shown to contribute to virulence of strain χ7122 (Dozois et al., 2003), we assessed the cumulative roles of the aerobactin and catecholate siderophores for virulence. The Δ*entD*::*kan* allele was introduced into Δ*iuc*Δ*iutA* strain χ7300 resulting in strain QT1294. QT1294 produced no siderophore following growth on chrome azurol S (CAS) plates (Schwyn & Neilands, 1987) and as expected, it was highly attenuated, as very few bacteria were present in blood or tissues ($P<0.01$) (Fig.1). We also observed minimal lesions in tissues of infected chickens (Table 1). Complementation of the siderophore negative mutant (Δ*entD*Δ*iuc*) with plasmid pIJ70 encoding *entD* restores full virulence of the strain and gross lesions in tissues of infected chickens as compared to the wild type (Fig. 1 and Table 1). In addition, unlike the Δ*entD* strain, the Δ*entD*Δ*iuc* mutant demonstrated growth inhibition in medium containing the host iron-

sequestering protein, conalbumin (ovotransferrin) (Fig.2B). Individual loss of production of either salmochelins (Δ*iroB*) or aerobactin (Δ*iucABCD*) was also assessed, and these mutants demonstrated only a modest reduction in virulence in blood and tissues (Supp. Fig. 1) and confirmed our previous results on the role of salmochelins and aerobactin systems for the virulence of the strain χ7122 (Dozois et al., 2003). Taken together, these results suggest that aerobactin, enterobactin and salmochelins are the only siderophores produced by strain χ7122 and that aerobactin alone can fully compensate for the loss of catecholate siderophores and mediate sufficient iron acquisition *in vivo*.

Role of *entS* and *iroC* genes for χ7122 virulence.

Mutants in siderophore export of strain χ7122 Δ*entS*, Δ*iroC* and Δ*entS*Δ*iroC* were assessed in the chicken infection model. All siderophore export mutants demonstrated significantly decreased numbers in the blood at all time points (Fig. 3). The Δ*entS* mutant also demonstrated significantly reduced bacterial numbers in visceral organs ($P<0.05$). By contrast, the Δ*iroC* mutant was present in visceral organs at levels comparable to the wild-type. The combined loss of *entS* and *iroC* resulted in the greatest attenuation, as this strain demonstrated very low numbers from blood, and demonstrated the most significant decrease in bacterial numbers in visceral organs ($P<0.01$) (Fig. 3). Gross lesion scores were also significantly reduced in the Δ*entS*Δ*iroC* mutant, whereas they were not significantly reduced in chickens infected with either the Δ*entS* or Δ*iroC* mutants (Table 1). Complementation of the Δ*entS* and Δ*iroC* mutants resulted in a full regain of virulence in chickens and in gross lesion scores (Fig. 4 and Table 1). The Δ*entS*Δ*iroC* mutant (Δ*entS*Δ*iroC* + *entS iroC*) was also complemented, and demonstrated a complete regain in the blood, although inferior bacterial counts were obtained in the liver and the spleen of infected chickens (Fig. 4). Gross lesions scores in pericardial and liver tissues were also less marked for the Δ*entS*Δ*iroC* complemented mutant (Table 1). Despite its capacity to produce aerobactin, the Δ*entS*Δ*iroC* mutant also demonstrated a growth lag in the presence of conalbumin, which was complemented by re-introduction of either *entS* and/or *iroC* (Fig. 2 B). Hence, loss of catecholate exporters, even when aerobactin is produced, resulted in decreased virulence and a decreased capacity to cope with host iron sequestering proteins such as conalbumin. These results also suggest that for strain

χ7122, the EntS transporter is more critical for virulence than IroC. This result was not expected, as other studies have shown that EntS specifically mediates enterobactin export (Furrer et al., 2002, Crouch et al., 2008) and was not important for *Salmonella* virulence (Crouch et al., 2008). In addition, the results of the infection studies using an enterobactin synthesis mutant, described above, demonstrated that production of this siderophore was not required for virulence when the strain contained a functional aerobactin system.

Secretion of catecholate siderophores by EntS and IroC.

In order to explain the decreased virulence of the siderophore export mutants, we investigated the effect of loss of these exporters on the secretion of catecholate siderophores. Liquid chromatography coupled to mass spectrometry (LC-MS/MS) analyses was performed on culture supernatants to determine the quantities of each siderophore molecule secreted by export mutants grown in iron-poor minimal medium.

The Δ*entS* mutant secreted 5.04-fold less cyclic enterobactin, 2.77-fold less DHBS trimer and 1.79-fold less DHBS dimer (Fig.5 A and B). Moreover, secretion of monoglucosylated enterobactin molecules: i.e. the salmochelins MGE and linear MGE, was also impaired in the Δ*entS* mutant. Specifically, the Δ*entS* mutant demonstrated a 5.66-fold and 2.78-fold reduction in MGE and linear MGE-secretion respectively (Fig. 5C). Hence, overall in strain χ7122 export of both enterobactin and monoglucosylated salmochelins is dependent on the EntS pump. Conversely, in the absence of EntS, levels of degraded molecules such as salmochelins S5, S1, SX and DHBS monomer were increased by 1.83-fold, 3.17-fold, 2.09-fold and 2.35-fold respectively in supernatants of the *entS* mutant (Fig.5 B, D and E), suggesting a robust degradation of cyclic molecules that are blocked in this mutant. Single-copy complementation of the *entS* gene restored siderophore secretion to levels similar to the wild-type strain (Fig.5 A, B and C). Tri- and di-glucosylated salmochelin levels in supernatants were not affected by an *entS* mutation (Fig.5 D and F).

The Δ*iroC* mutant did not secrete any detectable TGE molecules and secreted reduced quantities of di-glucosylated salmochelins: i.e. DGE, linear DGE and S5 by 1.96-fold,

3.39-fold and 2.31-fold, respectively (Fig. 6 A and B). Single-copy complementation of the *iroC* gene restored siderophore secretion to levels similar to the wild-type strain (Fig.6 A and B). These results demonstrated that export of tri-glucosylated salmochelins only occurs by IroC and that di-glucosylated salmochelin secretion is facilitated by IroC. Moreover, secretion of mono-glucosylated salmochelins, i.e. MGE, linear MGE, S1 and SX, were not altered by a Δ*iroC* mutation (Fig.6 C and D). Concentrations of enterobactin and its derivative products were increased in supernatants of the Δ*iroC* mutant by 1.33-fold to 1.62-fold (Fig.6 E and F). Such results suggest an efficient secretion of non-glucosylated molecules by EntS in the absence of the IroC export pump.

Loss of both EntS and IroC export pumps eliminated the secretion of salmochelins TGE, linear TGE and DGE (S4) and greatly reduced secretion of linear DGE, S5, MGE and linear MGE (Fig. 7 A, B and C). These results confirmed that secretion of mono- and di-glucosylated salmochelins occurs only through EntS and/or IroC, and that in the absence of one exporter, the remaining pump can serve as an auxillary transporter for some of these glucosylated substrates. Complementation of the double mutant with either *entS* or *iroC* demonstrated that secretion of di-glucosylated salmochelins by EntS and mono-glucosylated salmochelin by IroC can occur in the absence of their principal exporter (Fig. 7) Enterobactin, DHBS trimers (or linear enterobactin) and dimers and salmochelin S1 were all significantly reduced but still present in the Δ*entS*Δ*iroC* mutant, suggesting that other transporters in strain χ7122 might export these molecules (Fig.7 D, E and F). SX and DHBS monomers were also significantly higher in the Δ*entS*Δ*iroC* mutant, suggesting an increase in processing of cyclic siderophores into smaller molecules may occur to export these products from the cell in the absence of the EntS or IroC transporters (Fig.7 E and F). Complementation of *entS* and *iroC* restored secretion of all siderophore molecules to levels similar to those of the wild-type strain (Fig. 7).

Abrogation of catecholate siderophore synthesis restores virulence of a Δ*entS*Δ*iroC* strain.

Since the Δ*entD* enterobactin synthesis mutant was as virulent as the wild-type parent (Fig. 1) whereas the siderophore export mutants were attenuated (Fig. 3), we wondered

whether attenuation of the secretion mutants might be caused by the inability of these mutants to secrete several forms of endogenously synthesized siderophores, resulting in a fitness disadvantage *in vivo* for these mutants. To address this question, we tested whether virulence of the Δ*entS*Δ*iroC* export mutant could be restored by inactivation of catecholate siderophore synthesis. The Δ*entD*Δ*entS*Δ*iroC* strain demonstrated a significant regain in virulence; as bacterial numbers recovered from blood at 24 h and 48 h and from the spleen and liver were similar to the wild-type strain (Fig. 8). Loss of *entD* in the Δ*entS*Δ*iroC* mutant also restored the growth rate to wild-type levels in the presence of conalbumin (Fig. 2B). These results suggest that abolition of catecholate siderophore synthesis counterbalances the negative effect of lacking the catecholate siderophore export pumps, and that virulence of the strain, which contains a fully functional aerobactin system, is therefore restored.

Co-challenge infections with siderophore synthesis and export mutants.

As shown in figure 8, deletion of siderophore synthesis in the Δ*entS*Δ*iroC* mutant restored virulence in our chicken infection model and growth in vitro in the presence of conalbumin, suggesting that blocking catecholate siderophore secretion impairs general fitness when iron is limited. The EntS and IroC export pumps were shown to contribute to systemic infection of avian ExPEC strain χ7122 in the single-strain infection model, and their absence severely impaired secretion of catecholate siderophore molecules. We therefore investigated whether the inability to secrete several forms of catecholate siderophores by the Δ*entS* and/or Δ*iroC* mutants could potentially be bypassed by *in trans* complementation of siderophores secreted by a wild-type strain during a co-infection, since the export mutants all contain functional siderophore receptors and import systems. Co-challenges were performed by infecting chickens with equal quantities of a virulent Δ*lac* derivative and each mutant strain. Bacterial counts of the siderophore or transport mutant were determined directly by plate dilutions and differential plate counts on MacConkey agar. The enterobactin synthesis Δ*entD* mutant competed efficiently against the challenge strain, as bacterial counts recovered from infected tissues were similar for both strains (Fig. 9 A), confirming that catecholate siderophore synthesis is not a prerequisite for competitive fitness of strain χ7122. Further,

the salmochelin synthesis, (Δ*iroB*) mutant, which demonstrated reduced virulence in the single-strain infection model (Supp. Fig. 1), was *in trans* complemented in the co-challenge infection model (Fig. 9 B). Hence, mutants defective for synthesis of catecholate siderophores were as fit as the siderophore-producing challenge strain in the co-challenge model. By contrast, in co-challenge experiments the Δ*entS* and/or Δ*iroC* siderophore export mutants were outcompeted by the challenge strain (Fig 9 C, D and E). The reduced fitness of the siderophore export mutants could potentially be due to the impaired capacity of these mutants to secrete endogenous catecholate siderophores. To test this possibility the Δ*entD*Δ*entS*Δ*iroC* was assessed in the competitive infection model, and results indicate that this mutant was also significantly outcompeted during co-challenge (Fig 9 F). Taken together, these results demonstrate that attenuated siderophore synthesis mutants can readily compete with siderophore producing strains in co-challenge experiments, since these synthesis mutants can utilize the siderophores as effectively as the siderophore-producing strains. By contrast, both the Δ*entS*Δ*iroC* and Δ*entD*Δ*entS*Δ*iroC* siderophore export mutants were outcompeted by a catecholate siderophore producing strain. These results suggest that for the export mutants, the reduced capacity to secrete catecholate siderophores that are either synthesized *de novo* or imported from exogenous sources during co-challenge is largely responsible for the reduced fitness or virulence of these strains.

***In vitro* co-cultures demonstrate a reduced fitness for the secretion mutants with and without endogenous catecholate siderophore synthesis.**

As the chicken co-infection model showed a competitive disadvantage for siderophore secretion mutants against a WT strain, *in vitro* co-cultures of strains were assessed in order to determine if similar effects could be observed *in vitro*. To conduct these assays, all strains used, including the competitor strain, were aerobactin-negative (Δ*iucABCD*) to demonstrate the specific role of catecholate siderophores or their secretion for competitive fitness. The Δ*entS* and Δ*iroC* secretion mutants as well as the siderophore synthesis mutant (Δ*entD*) were not outcompeted in an iron-poor medium with conalbumin, as the competitive indices were superior to or close to one (Fig. 10). The ability of the siderophore-negative mutant (Δ*entD*Δ*iuc*) to grow and compete in low-iron

medium indicates that *trans* complementation of catecholate siderophores rescues growth, since this mutant is unable to grow in this medium in pure culture (Fig.2 B). However, the double Δ*entS*Δ*iroC* mutant was severely outcompeted in vitro by the competitor strain at each time point, suggesting that the inability to secrete catecholate siderophores is a fitness disadvantage. Endogenous siderophore synthesis was indeed partially responsible for this phenotype; as competitive fitness of a siderophore synthesis and secretion negative (Δ*iuc*Δ*entD*Δ*entS*Δ*iroC)* strain was still reduced. This result suggests that exogenous uptake of catecholate siderophores occurs in this strain but re-secretion of partially degraded forms of catecholate siderophores through EntS and IroC may contribute to bacterial fitness.

Intracellular detection and quantification of siderophores.

Mass spectrometry analysis of culture supernatants from the siderophore export mutants demonstrated a significant decrease in the presence of larger siderophore molecules (trimers and dimers) and an increased level of monomers (DHBS and SX) compared to the wild-type strain. This suggested that siderophore export-defective strains could potentially be accumulating catecholate siderophores intracellularly. The intracellular concentrations of siderophores in secretion mutants were measured and quantified by LC-MS/MS. Strain χ7122 showed considerable quantities of cyclic enterobactin, DHBS trimer, dimer and monomer, as well as salmochelins S1 and SX (Table 2). Cyclic and linear trimeric salmochelins were not detected from the cell-associated siderophore extracts of either the wild-type or mutant strains. For the Δ*entS* mutant, compared to the wild-type strain, concentrations of enterobactin and DHBS dimer were 2.26-fold and 2.52-fold lower respectively; whereas there were substantial increases in DHBS (8.50-fold increase), and SX (4.30-fold) levels (Table 2). Quantities of cell-associated siderophore monomers were also greatly increased for the Δ*iroC* and Δ*entS*Δ*iroC* mutants. SX concentrations were 69.67-fold and 108.99-fold greater in the Δ*iroC* and Δ*entS*Δ*iroC* mutant respectively. DHBS monomer concentrations were 3.06-fold and 6.11-fold higher in the Δ*iroC* and Δ*entS*Δ*iroC* mutant respectively (Table 2). These results indicate that there is an increased cellular accumulation of monomeric siderophores, suggesting that greater processing of larger molecules into salmochelin SX

and DHBS occurs in the absence of the IroC and/or EntS export pumps. Enterobactin and its linear form, which were efficiently secreted by the Δ*iroC* mutant, were respectively 2.28-fold and 2.12-fold higher in the Δ*iroC* mutant. However, cumulative loss of the EntS and IroC pumps resulted in decreased levels of enterobactin that were similar to levels present in the Δ*entS* mutant (Table 2). Moreover, intracellular concentrations of salmochelin S1 and DHBS dimer were also significantly lower in the Δ*entS*Δ*iroC* mutant (Table 2). These data correlate well with the secretion data, and confirm that in the absence of the dedicated export pumps, catecholate siderophores, which cannot be exported, are degraded into smaller molecules prior to export.

Discussion

Since its discovery in 1970, enterobactin has been extensively studied, and is one of the best characterized bacterial siderophore systems. A number of publications have reported that the enterobactin system contributes to bacterial virulence of enterobacterial pathogens including *Escherichia coli, Salmonella* Typhimurium and *Salmonella* Typhi (Furman *et al.*, 1994, Gorbacheva *et al.*, 2001, Methner et al., 2008, Yancey *et al.*, 1979, Rabsch *et al.*, 2003); whereas others have asserted the opposite (Bearson *et al.*, 2008, Benjamin *et al.*, 1985, Tsolis *et al.*, 1996, Torres *et al.*, 2001). The subsequent discovery of salmochelin siderophores which contribute to the virulence of pathogenic enterobacteria (Caza et al., 2008, Crouch et al., 2008, Dozois et al., 2003, Negre et al., 2004, Russo et al., 2002, Bachman et al., 2009) and whose synthesis is intrinsically linked to the enterobactin pathway has lead to a reassessment of whether or not enterobactin is a virulence factor. In the current report, our results demonstrate that enterobactin synthesis is not implicated in the virulence of strain χ7122, since loss of enterobactin synthesis did not significantly reduce systemic infection and the development of lesions associated with colibacillosis in the chicken infection model. The aerobactin system compensated for the loss of catecholate siderophore synthesis, although inactivation of all siderophore systems severely impaired virulence of the strain, indicating that siderophores are critical for virulence in this natural host model of systemic infection. These results are consistent with the fact that enterobactin molecules are sequestered by NGAL (lipocalin 2) and that glucosylation of enterobactin impedes

this NGAL-mediated sequestration (Goetz et al., 2002, Fischbach et al., 2006). Several lipocalins have been identified in chickens, and one of these host proteins could function in avian innate host defense, similarly to the mammalian NGAL orthologues (Pagano *et al.*, 2004). It has been demonstrated that NGAL loaded with apo-enterobactin, and not salmochelin, triggers the secretion of the proinflammatory chemokine interleukin-8; suggesting that NGAL loaded with afferic enterobactin may initiate a proinflammatory response at the mammalian respiratory mucosa, alerting the host of potentially harmful bacteria (Bachman et al., 2009, Nelson *et al.*, 2007). In the avian host, enterobactin must be modified into salmochelins to contribute to the virulence of ExPEC strain χ7122 (Supp. Fig. 1) (Dozois et al., 2003) and the generation of salmochelins efficiently circumvents the avian innate host defenses that neutralize enterobactin and may trigger an inflammatory response.

Salmochelin synthesis requires glucosylation by IroB, and efficient secretion of salmochelins has been shown to be dependent on the IroC exporter (Caza et al., 2008, Crouch et al., 2008). Hence, the IroC transporter was expected to play a major role for the virulence of the avian ExPEC strain χ7122. However, results from infection experiments indicated that the Δ*iroC* mutant was only attenuated in the bloodstream of animals; whereas mutation of the EntS tranporter alone or in combination with IroC, was more critical for systemic virulence. An extensive quantitative analysis of siderophores secreted by the Δ*entS* and Δ*iroC* mutants was performed by mass spectrometry and revealed that the EntS export pump efficiently secreted non-glucosylated and mono-glucosylated enterobactin molecules. Further, secretion of di-glucosylated salmochelins was also mediated by EntS in the absence of the IroC exporter. By contrast, IroC mediated secretion of di- and tri-glucosylated salmochelins, and effectively exported mono-glycosylated enterobactin in the absence of EntS. However, IroC did not effectively mediate transport of enterobactin, DHBS trimers and dimers. Taken together, these results suggest that for ExPEC strain χ7122 secretion of enterobactin and mono-glucosylated salmochelins by EntS is more critical for virulence than secretion of di- and tri-glucosylated salmochelins by IroC.

These results are however in disagreement with previous studies with either *E. coli* strain χ7122 or *Salmonella enterica* serovar Typhimurium, which demonstrated that IroC is a major exporter of salmochelins and that this exporter plays an important role for virulence (Crouch et al., 2008, Caza et al., 2008). The level of glucosylated molecules produced and secreted by different bacteria, as well as whether or not they produce additional siderophores, may explain these discrepancies. Quantification of siderophores secreted by strain χ7122 demonstrates that the levels of mono-glucosylated and di-glucosylated salmochelin molecules are similar. However, introduction of the *iro* gene cluster on a medium-copy number plasmid to an aerobactin-negative and salmochelin-negative derivative of strain χ7122 resulted in increased glucosylation of salmochelins and a corresponding reduction of mono-glucosylated molecules (Caza et al., 2008). In this context, to complement the attenuated aerobactin-negative and salmochelin-negative strain, the presence of the *iroC* gene as part of the *iro* locus was shown to be critical (Caza et al., 2008). Interestingly, the level of glucosylation of salmochelins varies among ExPEC strains. For instance strain CFT073 secretes equal amounts of di-glucosylated and mono-glucosylated salmochelins, strain CP9 secretes 1.58-times more di-glucosylated than mono-glucosylated salmochelins, and strain 536 secretes 1.54-times more monoglucosylated than di-glucosylated salmochelins (Caza et al., unpublished results). Further, analysis of supernatants of *S. enterica* serovar Typhimurium (*S.* Typhimurium) strains LT2 and UK1, demonstrated that di-glucosylated salmochelins are secreted 1.90-fold and 1.79-fold greater than mono-glycosylated salmochelins (unpublished results). These differences in glucosylation among pathogenic strains and the preferential secretion of different salmochelins by the EntS and IroC transporters according to their level of glucosylation may explain the role of these exporters for the virulence of specific strains or different pathogenic enterobacteria. Moreover, since Crouch et *al.* demonstrated in *S.* Typhimurium strain 14028s that EntS only secreted enterobactin and no salmochelins, we wondered whether any differences in amino acid composition between EntS from *S.* Typhimurium or *E. coli* χ7122 could contribute to differences in secretion of catecholate siderophore molecules. The genes encoding EntS from *S. enterica* strains 14028s and LT2 are identical and exhibit 90% amino acid identity to EntS of *E. coli* χ7122. The *entS* gene from *S.* Typhimurium strain LT2 was cloned and

integrated into the *lacZYA* chromosomic region of the Δ*entS*Δ*iroC* mutant of χ7122. LC-MS/MS analysis of culture supernatants indicated that EntS from LT2 efficiently mediated secretion of mono-glucosylated salmochelins and enterobactin, as well as the export of minor quantities of DGE and linear DGE in absence of IroC (Supp. Fig. 2).

Given that secretion of catecholate siderophores by EntS and IroC is critical for systemic virulence of strain χ7122 although the synthesis of these siderophores is not needed when the aerobactin system is functional, we showed that abrogation of catecholate siderophore synthesis in the Δ*entS*Δ*iroC* secretion mutant restored the virulence of the strain. In fact, this mutant relies entirely on the aerobactin system for siderophore-mediated iron acquisition. This highlights the importance of multiple independent iron acquisition systems for the virulence of certain pathogenic bacteria such as ExPEC CFT073 and CP9 as well as *Klebsiella pneumoniae*. By contrast, *S.* Typhimurium produces only enterobactin and salmochelins, and inactivation of these systems impairs growth in iron-restricted medium and reduced virulence in mice (Crouch et al., 2008).

In trans complementation of catecholate siderophores was assessed in co-challenge infection experiments (Fig. 9). Exogenous siderophore uptake provided by a siderophore-producing challenge strain complemented the salmochelin synthesis (Δ*iroB*) mutant *in vivo*. However, *trans* complementation was not effective for any of the siderophore secretion mutants, including the catecholate siderophore synthesis/secretion mutant; suggesting that catecholate siderophores originating from either endogenous or exogenous sources can interfere with virulence/fitness of the ExPEC siderophore export mutants. *In vitro* co-cultures demonstrate a reduced fitness for the secretion mutants with and without endogenous catecholate siderophore synthesis. The significantly high intracellular accumulation of degraded catecholate siderophores, SX and DHBS, in the cell-associated and supernatant fractions of the Δ*entS*Δ*iroC* mutant suggest that in the absence of exporters multimeric siderophores from either exogenous or endogenous sources accumulate within the cell and must be completely degraded to monomers before release. These results also suggest a model in which catecholate siderophores may undergo multiple cycling mediated by secretion through EntS and IroC, with partial

degradation at each cycle, until full degradation into monomers may be achieved (Fig. 10). This brings new insight regarding the potential importance of cycling and importation of linear and processed catecholate siderophores, by outer membrane siderophore receptors such as Cir and Iha, which have been shown to play a role in the virulence of *S.* Typhimurium (Rabsch et al., 2003) and UPEC strain UCB34 respectively (Leveille *et al.*, 2006). Inhibition of the secretion of multimeric siderophores necessitates complete degradation to monomers, resulting in inefficient cycling of siderophores and the subsequent decreased capacity to obtain iron during infection, especially if no other siderophore system is encoded by the bacteria.

Taken together, this study demonstrated that EntS and IroC mediate specific export of catecholate siderophores, and that these exporters are critical for systemic virulence even when other efficient iron uptake systems such as aerobactin are present. Further, the role of these exporters for ExPEC virulence was conditional on enterobactin synthesis, which in itself is not required when other siderophore systems such as aerobactin are functional.

Experimental procedures

Bacterial strains, plasmids, media and growth conditions. Bacterial strains and plasmids used in this study are listed in Tables 3 and 4. For bacterial culture, Luria-Bertani (LB) broth and Tryptic Soy Agar (Difco Laboratories, Detroit, MI) were routinely used. For infection experiments, strain χ7122 and derivatives were grown in brain heart infusion (BHI) broth (Difco). For production and detection of catecholate siderophores, bacteria were grown at 37°C for 17 h in iron-poor M63-glycerol minimal medium as described in (Caza et al., 2008). Growth curves of strains were assessed in iron-poor M63-glycerol minimal with or without added conalbumin (ovotransferrin) (1mg/ml) in triplicate using a Bioscreen C Automated Microbiology Growth Curve Analysis System (Growth Curves U.S.A.). Nalidixic acid, kanamycin, chloramphenicol and carbenicillin were used at a final concentration of 40 μg ml^{-1}.

Generation of bacterial strains. All oligonucleotide primers used for the cloning of genes or generation of mutants are presented in Supplemental Table 1. Mutation of the

entD gene in strains χ7122, χ7300 and QT1931 was obtained by the λ red recombinase method developed by (Datsenko & Wanner, 2000). Briefly, the *entD'-kan-'entD* allele amplified from pKD4 with primers CMD60 and CMD61 was introduced into χ7122 (pKD46), χ7300 (pKD46) and QT1931 (pKD46) by electroporation. Potential Δ*entD* mutants were selected by growth on kanamycin, and loss of plasmid pKD46 was assessed by sensitivity to carbenicillin. Δ*entD* mutants, QT163 (χ7122 Δ*entD*), QT1294 (χ7300 Δ*entD*) and QT2598 (QT1931 Δ*entD*) were subsequently confirmed by PCR with primers CMD63 and CMD60. Mutations of the *entS* and *iroC* genes in χ7122 were obtained by allelic exchange with suicide plasmid pIJ69 and pIJ167, respectively. The backbone of these suicide plasmids is pMEG-375, which is a *sacB*-based allelic exchange plasmid (Dozois et al., 2003). Briefly, the *entS* gene was amplified by PCR from genomic DNA of χ7122 with primers CMD98 and CMD99 and cloned into the *Hin*dIII site of plasmid pIJ47 resulting in pIJ62. pIJ47 is a pBC II SK+ derivative which has lost the *Hin*cII restriction site following digestion with *Sal*I and *Xho*I. pIJ62 was digested with *Hin*cII, deleting 369 bp of *entS*. A kanamycin cassette, flanked by FRT sites, from pKD4 was introduced into the *Hin*cII site creating pIJ64. This construct was digested with *Ssp*I and the Δ*ents*::*kan* allele was cloned into the *Sma*I site of pMEG-375, generating suicide plasmid pIJ69. Plasmid pIJ167 was produced by cloning a *Bss*HII fragment containing an inactivated *iroC* gene from pIJ37 (Caza et al., 2008) into the *Asc*I site of suicide vector pMEG-375. The suicide plasmids pIJ69 and pIJ167 were introduced in strain χ7122 and the corresponding mutants QT279 (Δ*entS*::*kan*) and QT1299 (Δ*iroC*) were obtained by homologous recombination-mediated allelic exchange. The FRT-kanamycin cassette present in the Δ*entS* mutant was removed with FLP helper plasmid pCP20; generating strain QT1185 (Δ*entS*). The Δ*entS*Δ*iroC* mutant, QT1931, was produced by allelic exchange replacement of the *iroC* gene in strain QT1185 using suicide plasmid pIJ167. The deletion of *iroB* was obtained as follows. First, the *iroB* gene was deleted from pIJ121 by inverse PCR using primers CMD75 and CMD690 which each contain a *Xho*I site. The PCR fragment containing the plasmid pACYC184 was digested with *Xho*I and then ligated, creating pIJ173, which contained the *iroB* promoter and the *iroC* gene. This P_{iroB}-*iroC* construct was then amplified by PCR with CMD771 and CMD773 and cloned at the *Xba*I site of pMEG-375, creating suicide vector pIJ205, and was used for allelic

exchange mutagenesis. The mutation of the *iucABCD* allele in the wild type strain (QT2576) and several mutants (QT51, QT163, QT1185, QT1299, QT1931, QT2598) was generated as follows. The *iucABCD* gene was deleted from pABN5 by inverse PCR using primers CMD1328 and CMD1329 and ligation of the PCR fragment was achieved, creating plasmid pIJ339. This plasmid was then digested with *Sal*I and *Avr*II and the *iucA'-iucD'* fragment was cloned into vector pBluescript II SK+ at *Sal*I and *Xba*I sites, generating plasmid pIJ345. pIJ345 was digested with *BssH*II and the *iucA'-iucD'* fragment was then cloned into pMEG-375 suicide vector at the *Asc*I site, creating plasmid pIJ346. All suicide plasmids were introduced in strains of interest by conjugation using strain 17-1 □ *pir* as the donor strain and double homologous recombination was selected for by growing cells in the presence of sucrose.

Plasmid complementation of mutant QT1294 (Δ*entD*Δ*iucABCD*Δ*iutA*) was achieved by transformation with plasmid pIJ70, which encodes the *entD* gene with its native promoter. First the *fes fepA entD* region was amplified by PCR with primers CMD62 and CMD63 from χ7122 and cloned onto vector pACYC184 at the *Hind*III site, generating plasmid pIJ36. This plasmid was then digested with *Ale*I and *Nru*I enzyme in order to remove the *fes* genes and was self-ligated, creating plasmid pIJ66. This template was then used for inverse PCR with primers CMD125 and CMD126, which contain an *Xho*I site, to remove the *fepA* gene and to obtain the *entD* gene with its native promoter by self-ligation of the fragment, generating pIJ70.

Complementation of the *entS* and *iroC* mutants was achieved by integrating *entS* and/or *iroC* into the chromosome within the *lacZYA* operon. A template for *lacZYA* integration was created from plasmid pRS415 (Simons *et al.*, 1987) Inverse PCR using primers CMD870 and CMD871 was used to delete part of the *lacZYA* operon and introduced a *Pac*I site flanked by 500 pb of *lacZ'* and '*lacA* which was termed pIJ220. Moreover, a FRT-kanamycin resistance gene was cloned into the *Sac*I site of pBluescript II SK+. Using primers CMD843 and CMD844, the FRT-kanamycin resistance cassette was digested and cloned at the *Pac*I site of pIJ220, generating pIJ224. The *lacZ'-kan*-MCS-'*lacA* fragment was then amplified by PCR using primers CMD1033 and CMD1034 and

cloned into the *Avr*II site of plasmid pIJ264, generating plasmid pIJ266. pIJ264 is pBluescript II SK+ lacking the MCS, *lacZ*□ and fl packaging regions and was generated by inverse PCR using primers CMD1084 and CMD1085 and ligated using the introduced *Avr*II sites.

The *entS* gene with its promoter was amplified from pIJ62 with primers CMD1038 and CMD1039 and cloned into the *Not*I site of the MCS of plasmid pIJ266, generating plasmid pIJ284. Digestion of pIJ284 with *Avr*II results in a *lacZ*'-Km-*entS-lacA*' fragment, which was introduced into QT1185 (pKD46) using the Datsenko and Wanner protocol (Datsenko & Wanner, 2000), creating strain QT2274. The *lacZ*'-Km-*entS-lacA*' fragment was also cloned at the *Xba*I site of pMEG-375, generating pIJ288. This suicide plasmid was used to complement the Δ*entS*Δ*iroC* mutant by double cross-over integration of the Km-*entS* construct into the *lacZYA* operon, generating strain QT2310. Complementation of the *iroC* gene was also obtained similarly; the *iroC* gene from pIJ173 was cloned into the MCS *Not*I site of pIJ266 by PCR amplification using primers CMD1038 and CMD1040, creating plasmid pIJ276. This construct was then digested with *Avr*II and the *lacZ*'-Km-*iroC-lacA'* fragment was inserted into the *Xba*I site of pMEG-375, generating plasmid pIJ286. Integration of the complement allele into the Δ*iroC* and Δ*entS*Δ*iroC* mutant strains was achieved by double cross-over homologous recombination, producing strain QT2309 and QT2762 respectively. Complementation of the Δ*entS*Δ*iroC* mutant with both the *entS* and *iroC* alleles was achieved as follows. First the *entS* gene from pIJ62 was cloned into pIJ173 at the *Hin*dIII site, creating pIJ233. A fragment containing *entS* and *iroC* alleles was then amplified with primers CMD1038 and CMD1040 and cloned into the *Not*I site of pIJ266, creating plasmid pIJ347. pIJ347 was then digested with *Avr*II and the *lacZ*'-Km-*entS-iroC-lacA'* fragment was inserted into the *Xba*I site of pMEG-375, generating plasmid pIJ373. Integration of pIJ373 into QT1931 was achieved by double cross-over homologous recombination, producing strain QT2761. Selected colonies were grown on MacConkey agar with kanamycin and Lac- clones were verified by PCR.

***In vitro* co-cultures experiments.** Overnight cultures in M63-glycerol of strains were harvested and adjusted for an OD_{600nm} of 1.0. Co-inoculation of the wild type strain (QT2736 Δ*lac*Δ*iucABCD*) and the mutants were achieved by 1/1000 dilution of the adjusted cultures into M63-glycerol with 1 mg/ml of conalbumin. Bacterial counts (CFU/ml) of the mixed cultures were assessed at 0, 4, 8 and 24 h by serial dilution and plating onto MacConkey agar plates. Biological triplicates were performed for each co-culture assay.

Experimental infections of chickens via the air sacs. For infection studies, 3-week-old White Leghorn specific-pathogen-free chickens (Canadian Food Inspection Agency, Ottawa, Canada) were inoculated in the right thoracic air sac with 0.1 ml of a bacterial inoculum grown overnight in BHI broth (10^7 CFU for mono-infections and a mix of 5.0 X 10^6 CFU of each strain for co-infections). Experimental infections and the lesion scoring were carried out as previously described in (Caza et al., 2008) and in (Sabri *et al.*, 2008).

Analysis of siderophores from culture supernatants and whole cells. Supernatants of 17 h cultures were obtained following centrifugation of bacterial cells at 3200 X *g* for 15 minutes and were filtered on 0.2 µm membranes. Bacterial pellets from 10 ml cultures were washed once with M63 medium, disrupted with 1 ml of ethanol and centrifuged again at 16100 X *g*. 1 ml of ethanol extracts and aliquots of supernatant were then prepared in 5 % vol/vol formic acid and 0.12 ng/ml of 5,6,7,8-tetradeutero-3,4-dihydroxy-2-heptylquinoline was added as an internal control (Lepine *et al.*, 2003). Each strain was cultured in triplicate and a sample of each culture supernatant was analyzed by liquid chromatography coupled to a mass spectrometer (LC-MS/MS).

Liquid chromatography / Mass spectrometry analyses. Multiple reaction monitoring (MRM) analyses were performed using an Agilent HP 1100 HPLC (Agilent Canada, Mississauga, ON) coupled to a Micromass QuattroII spectrometer (Micromass Canada) and also a Waters 2795 Alliance HT coupled to a Micromass Quattro Premier XE spectrometer (Micromass MS Technologies) as described in (Caza et al., 2008).

Statistical analyses. Statistical analyses were performed using the Prism 4.0b software package (GraphPad Software, San Diego, CA, USA).

ACKNOWLEDGEMENTS

M.C. was funded by scholarships from the "Fondation Armand-Frappier" and the Swine infectious disease research center-"Centre de recherche en infectiologie porcine" (CRIP). Funding for this project was provided by a discovery grant to CMD from the Natural Sciences and Engineering Research Council of Canada (NSERC), and infrastructure funding from the Canadian Foundation for Innovation (CFI).

References

Andrews, S. C., A. K. Robinson & F. Rodriguez-Quinones, (2003) Bacterial iron homeostasis. *FEMS Microbiol Rev* **27**: 215-237.

Bachman, M. A., V. L. Miller & J. N. Weiser, (2009) Mucosal lipocalin 2 has pro-inflammatory and iron-sequestering effects in response to bacterial enterobactin. *PLoS Pathog* **5**: e1000622.

Bearson, B. L., S. M. Bearson, J. J. Uthe, S. E. Dowd, J. O. Houghton, I. Lee, M. J. Toscano & D. C. Lay, Jr., (2008) Iron regulated genes of *Salmonella enterica* serovar Typhimurium in response to norepinephrine and the requirement of fepDGC for norepinephrine-enhanced growth. *Microbes Infect* **10**: 807-816.

Benjamin, W. H., Jr., C. L. Turnbough, Jr., B. S. Posey & D. E. Briles, (1985) The ability of *Salmonella* Typhimurium to produce the siderophore enterobactin is not a virulence factor in mouse typhoid. *Infect Immun* **50**: 392-397.

Bindereif, A. & J. B. Neilands, (1983) Cloning of the aerobactin-mediated iron assimilation system of plasmid ColV. *J Bacteriol* **153**: 1111-1113.

Bister, B., D. Bischoff, G. J. Nicholson, M. Valdebenito, K. Schneider, G. Winkelmann, K. Hantke & R. D. Sussmuth, (2004) The structure of salmochelins: C-glucosylated enterobactins of *Salmonella enterica*. *Biometals* **17**: 471-481.

Brock, J. H., M. G. Pickering, M. C. McDowall & A. G. Deacon, (1983) Role of antibody and enterobactin in controlling growth of *Escherichia coli* in human milk and

acquisition of lactoferrin- and transferrin-bound iron by *Escherichia coli*. *Infect Immun* **40**: 453-459.

Brock, J. H., P. H. Williams, J. Liceaga & K. G. Wooldridge, (1991) Relative availability of transferrin-bound iron and cell-derived iron to aerobactin-producing and enterochelin-producing strains of *Escherichia coli* and to other microorganisms. *Infect Immun* **59**: 3185-3190.

Caza, M., F. Lepine, S. Milot & C. M. Dozois, (2008) Specific roles of the *iroBCDEN* genes in virulence of an avian pathogenic *Escherichia coli* O78 strain and in production of salmochelins. *Infect Immun* **76**: 3539-3549.

Chang, A. C. & S. N. Cohen, (1978) Construction and characterization of amplifiable multicopy DNA cloning vehicles derived from the P15A cryptic miniplasmid. *J Bacteriol* **134**: 1141-1156.

Crouch, M. L., M. Castor, J. E. Karlinsey, T. Kalhorn & F. C. Fang, (2008) Biosynthesis and IroC-dependent export of the siderophore salmochelin are essential for virulence of *Salmonella enterica* serovar Typhimurium. *Mol Microbiol* **67**: 971-983.

Datsenko, K. A. & B. L. Wanner, (2000) One-step inactivation of chromosomal genes in *Escherichia coli* K-12 using PCR products. *Proc Natl Acad Sci U S A* **97**: 6640-6645.

de Lorenzo, V. & K. N. Timmis, (1994) Analysis and construction of stable phenotypes in gram-negative bacteria with Tn5- and Tn10-derived minitransposons. *Methods Enzymol* **235**: 386-405.

Dozois, C. M., F. Daigle & R. Curtiss, 3rd, (2003) Identification of pathogen-specific and conserved genes expressed in vivo by an avian pathogenic *Escherichia coli* strain. *Proc Natl Acad Sci U S A* **100**: 247-252.

Fischbach, M. A., H. Lin, D. R. Liu & C. T. Walsh, (2005) In vitro characterization of IroB, a pathogen-associated C-glycosyltransferase. *Proc Natl Acad Sci U S A* **102**: 571-576.

Fischbach, M. A., H. Lin, L. Zhou, Y. Yu, R. J. Abergel, D. R. Liu, K. N. Raymond, B. L. Wanner, R. K. Strong, C. T. Walsh, A. Aderem & K. D. Smith, (2006) The

pathogen-associated *iroA* gene cluster mediates bacterial evasion of lipocalin 2. *Proc Natl Acad Sci U S A* **103**: 16502-16507.

Flo, T. H., K. D. Smith, S. Sato, D. J. Rodriguez, M. A. Holmes, R. K. Strong, S. Akira & A. Aderem, (2004) Lipocalin 2 mediates an innate immune response to bacterial infection by sequestrating iron. *Nature* **432**: 917-921.

Furman, M., A. Fica, M. Saxena, J. L. Di Fabio & F. C. Cabello, (1994) *Salmonella typhi* iron uptake mutants are attenuated in mice. *Infect Immun* **62**: 4091-4094.

Furrer, J. L., D. N. Sanders, I. G. Hook-Barnard & M. A. McIntosh, (2002) Export of the siderophore enterobactin in *Escherichia coli*: involvement of a 43 kDa membrane exporter. *Mol Microbiol* **44**: 1225-1234.

Goetz, D. H., M. A. Holmes, N. Borregaard, M. E. Bluhm, K. N. Raymond & R. K. Strong, (2002) The neutrophil lipocalin NGAL is a bacteriostatic agent that interferes with siderophore-mediated iron acquisition. *Mol Cell* **10**: 1033-1043.

Gorbacheva, V. Y., G. Faundez, H. P. Godfrey & F. C. Cabello, (2001) Restricted growth of ent(-) and tonB mutants of *Salmonella enterica* serovar Typhi in human Mono Mac 6 monocytic cells. *FEMS Microbiol Lett* **196**: 7-11.

Hantke, K., (1990) Dihydroxybenzoylserine--a siderophore for *E. coli*. *FEMS Microbiol Lett* **55**: 5-8.

Hantke, K., G. Nicholson, W. Rabsch & G. Winkelmann, (2003) Salmochelins, siderophores of *Salmonella enterica* and uropathogenic *Escherichia coli* strains, are recognized by the outer membrane receptor IroN. *Proc Natl Acad Sci U S A* **100**: 3677-3682.

Lamarche, M. G., C. M. Dozois, F. Daigle, M. Caza, R. Curtiss, 3rd, J. D. Dubreuil & J. Harel, (2005) Inactivation of the pst system reduces the virulence of an avian pathogenic *Escherichia coli* O78 strain. *Infect Immun* **73**: 4138-4145.

Lepine, F., E. Deziel, S. Milot & L. G. Rahme, (2003) A stable isotope dilution assay for the quantification of the Pseudomonas quinolone signal in Pseudomonas aeruginosa cultures. *Biochim Biophys Acta* **1622**: 36-41.

Leveille, S., M. Caza, J. R. Johnson, C. Clabots, M. Sabri & C. M. Dozois, (2006) Iha from an *Escherichia coli* urinary tract infection outbreak clonal group A strain is

expressed in vivo in the mouse urinary tract and functions as a catecholate siderophore receptor. *Infect Immun* **74**: 3427-3436.

Lymberopoulos, M. H., S. Houle, F. Daigle, S. Leveille, A. Bree, M. Moulin-Schouleur, J. R. Johnson & C. M. Dozois, (2006) Characterization of Stg fimbriae from an avian pathogenic *Escherichia coli* O78:K80 strain and assessment of their contribution to colonization of the chicken respiratory tract. *J Bacteriol* **188**: 6449-6459.

McClelland, M., K. E. Sanderson, J. Spieth, S. W. Clifton, P. Latreille, L. Courtney, S. Porwollik, J. Ali, M. Dante, F. Du, S. Hou, D. Layman, S. Leonard, C. Nguyen, K. Scott, A. Holmes, N. Grewal, E. Mulvaney, E. Ryan, H. Sun, L. Florea, W. Miller, T. Stoneking, M. Nhan, R. Waterston & R. K. Wilson, (2001) Complete genome sequence of *Salmonella enterica* serovar Typhimurium LT2. *Nature* **413**: 852-856.

Methner, U., W. Rabsch, R. Reissbrodt & P. H. Williams, (2008) Effect of norepinephrine on colonisation and systemic spread of *Salmonella enterica* in infected animals: role of catecholate siderophore precursors and degradation products. *Int J Med Microbiol* **298**: 429-439.

Negre, V. L., S. Bonacorsi, S. Schubert, P. Bidet, X. Nassif & E. Bingen, (2004) The siderophore receptor IroN, but not the high-pathogenicity island or the hemin receptor ChuA, contributes to the bacteremic step of *Escherichia coli* neonatal meningitis. *Infect Immun* **72**: 1216-1220.

Nelson, A. L., A. J. Ratner, J. Barasch & J. N. Weiser, (2007) Interleukin-8 secretion in response to aferric enterobactin is potentiated by siderocalin. *Infect Immun* **75**: 3160-3168.

O'Brien, I. G. & F. Gibson, (1970) The structure of enterochelin and related 2,3-dihydroxy-N-benzoylserine conjugates from *Escherichia coli*. *Biochim Biophys Acta* **215**: 393-402.

Pagano, A., P. Giannoni, A. Zambotti, D. Sanchez, M. D. Ganfornina, G. Gutierrez, N. Randazzo, R. Cancedda & B. Dozin, (2004) Phylogeny and regulation of four lipocalin genes clustered in the chicken genome: evidence of a functional diversification after gene duplication. *Gene* **331**: 95-106.

Pollack, J. R. & J. B. Neilands, (1970) Enterobactin, an iron transport compound from *Salmonella typhimurium*. *Biochem Biophys Res Commun* **38**: 989-992.

Provence, D. L. & R. Curtiss, 3rd, (1992) Role of crl in avian pathogenic *Escherichia coli*: a knockout mutation of *crl* does not affect hemagglutination activity, fibronectin binding, or Curli production. *Infect Immun* **60**: 4460-4467.

Rabsch, W., U. Methner, W. Voigt, H. Tschape, R. Reissbrodt & P. H. Williams, (2003) Role of receptor proteins for enterobactin and 2,3-dihydroxybenzoylserine in virulence of *Salmonella enterica*. *Infect Immun* **71**: 6953-6961.

Ratledge, C., (2007) Iron metabolism and infection. *Food Nutr Bull* **28**: S515-523.

Ratledge, C. & L. G. Dover, (2000) Iron metabolism in pathogenic bacteria. *Annu Rev Microbiol* **54**: 881-941.

Russo, T. A., C. D. McFadden, U. B. Carlino-MacDonald, J. M. Beanan, T. J. Barnard & J. R. Johnson, (2002) IroN functions as a siderophore receptor and is a urovirulence factor in an extraintestinal pathogenic isolate of *Escherichia coli*. *Infect Immun* **70**: 7156-7160.

Sabri, M., M. Caza, J. Proulx, M. H. Lymberopoulos, A. Bree, M. Moulin-Schouleur, R. Curtiss, 3rd & C. M. Dozois, (2008) Contribution of the SitABCD, MntH, and FeoB metal transporters to the virulence of avian pathogenic *Escherichia coli* O78 strain chi7122. *Infect Immun* **76**: 601-611.

Schwyn, B. & J. B. Neilands, (1987) Universal chemical assay for the detection and determination of siderophores. *Anal Biochem* **160**: 47-56.

Simons, R. W., F. Houman & N. Kleckner, (1987) Improved single and multicopy lac-based cloning vectors for protein and operon fusions. *Gene* **53**: 85-96.

Torres, A. G., P. Redford, R. A. Welch & S. M. Payne, (2001) TonB-dependent systems of uropathogenic *Escherichia coli*: aerobactin and heme transport and TonB are required for virulence in the mouse. *Infect Immun* **69**: 6179-6185.

Tsolis, R. M., A. J. Baumler, F. Heffron & I. Stojiljkovic, (1996) Contribution of TonB- and Feo-mediated iron uptake to growth of *Salmonella typhimurium* in the mouse. *Infect Immun* **64**: 4549-4556.

Yancey, R. J., S. A. Breeding & C. E. Lankford, (1979) Enterochelin (enterobactin): virulence factor for *Salmonella typhimurium*. *Infect Immun* **24**: 174-180.

TABLE 1 : Score based evaluation of gross lesions in organs of infected chickens

E. coli strain	Mean lesion score ± SEM [a]	
	Air sacs [b]	Liver and Heart [c]
χ7122	3.1 ± 0.1	3.5 ± 0.1
Δ*entD*	2.9 ± 0.3	3.0 ± 0.3
Δ*entD*Δ*iuc*	0.7 ± 0.2*	1.0 ± 0.2*
Δ*entD*Δ*iuc* + *entD*	3.3 ± 0.2	3.6 ± 0.2
Δ*entS*	2.7 ± 0.2	2.9 ± 0.3
Δ*entS* + *entS*	2.7 ± 0.2	3.1 ± 0.2
Δ*iroC*	2.9 ± 0.2	3.3 ± 0.2
Δ*iroC* + *iroC*	2.9 ± 0.2	3.0 ± 0.3
Δ*entS* Δ*iroC* (DM)	2.0 ± 0.3*	1.7 ± 0.3*
DM + *entS iroC*	2.9 ± 0.3	2.7 ± 0.3 *
Δ*entD*Δ*entS*Δ*iroC*	2.9 ± 0.3	2.6 ± 0.2*¤

[a] Lesion scores are presented as the mean of values attributed to gross lesions of airsacculitis and combined lesions of pericarditis and perihepatitis as described in (Lamarche *et al.*, 2005)

[b] Mean lesion scores for airsacculitis in both caudal thoracic air sacs.

[c] Combined lesion scoring values for pericarditis and perihepatitis. Statistical differences compared with the wild-type strain using the two-tailed Mann Whitney test are noted: * ($P<0.01$) and ¤ indicates a significant difference between the double mutant (DM) Δ*entS* Δ*iroC* and the Δ*entD*Δ*entS*Δ*iroC* mutant ($P<0.05$).

Table 2: Intracellular concentrations of catecholate siderophores in *E. coli* χ7122 and siderophore export mutants

Strain	Intracellular concentrations (nM) of catecholate siderophores[a]					
	Trimers		Dimers		Monomers	
	Ent	$(DHBS)_3$	$(DHBS)_2$	S1	SX	DHBS
χ7122	19.9 ± 2.1	6.5 ± 0.9	90.5 ± 1.1	12.1 ± 1.5	7.8 ± 0.5	44.3 ± 3.9
Δ*entS*	**8.8 ± 1.3**	4.6 ± 0.9	**35.9 ± 2.7**	28.1 ± 3.5	**33.5 ± 1.5**	**376.5 ± 38.3**
Δ*iroC*	**45.3 ± 4.0**	**13.8 ± 2.0**	**44.1 ± 6.4**	26.3 ± 3.4	**543.4 ± 77.7**	**135.4 ± 10.9**
Δ*entS*Δ*iroC*	**8.8 ± 1.8**	3.8 ± 0.4	**19.5 ± 2.3**	**1.9 ± 0.3**	**850.1 ± 89.5**	**270.7 ± 43.0**

[a] Intracellular concentrations (nM) of catecholate siderophores extracted from bacterial pellets of wild-type and secretion mutants. Bold numbers indicate a significant statistical difference in siderophore concentrations between the mutant and the wild-type strain ($P<0.01$) using the two-tailed unpaired *t* test.

Table 3: Bacterial strains used for this study

Bacterial strains	Genotype [a]	Source
χ7122	Avian pathogenic, O78 :K80 :H9, *gyrA*, Nal^R	(Provence & Curtiss, 1992)
χ7300	χ7122 Δ*iucABCD*Δ*iutA*	(Dozois et al., 2003)
LT2	*Salmonella* Typhimurium LT2	(McClelland *et al.*, 2001)
S17 λpir	*hsdR pro recA* RP4-2-Tc::Mu-Km::Tn7 + lysogenic λ *pir*	(de Lorenzo & Timmis, 1994)
QT51	χ7122 Δ*lacZYA* (markerless) Nal^R	(Lymberopoulos *et al.*, 2006)
QT163	χ7122 Δ*entD*::*kan*, Nal^R, Km^R	This study
QT279	χ7122 Δ*entS*::*kan*, Nal^R, Km^R	This study
QT1294	χ7300 Δ*entD*::*kan*, Nal^R, Km^R	This study
QT1468	χ7122 Δ*iroB* (markerless) Nal^R	This study
QT1185	χ7122 Δ*entS*::FRT Nal^R	This study
QT1195	χ7300 Δ*entS*:: *kan,* Nal^R, Km^R	This study
QT1299	χ7122 Δ*iroC* (markerless) Nal^R	This study
QT1300	χ7300 Δ*iroC* (markerless) Nal^R	This study
QT1931	QT1185 Δ*iroC* (markerless) Nal^R	This study
QT2274	QT1185 :: *kan-entS* integrated into *lacZYA*, Nal^R, Km^R	This study
QT2309	QT1299:: pIJ286, *iroC* integrated into *lacZYA*, Nal^R, Km^R	This study
QT2310	QT1931:: pIJ288, *entS* integrated into *lacZYA,* Nal^R, Km^R	This study
QT2471	QT1931:pIJ330, single copy of *entS* from *Salmonella* Typhimurium integrated into *lacZYA*, Nal^R, Km^R	This study
QT2576	χ7122 Δ*iucABCD*	This study
QT2598	QT1931 Δ*entD*::*kan*	This study
QT2734	QT1931 Δ*iucABCD*	This study
QT2736	QT51 Δ*iucABCD*	This study
QT2737	QT2598 Δ*iucABCD*	This study
QT2761	QT1931:: pIJ373, *entS iroC* integrated into *lacZYA,* Nal^R, Km^R	This study
QT2762	QT1931:: pIJ286, *iroC* integrated into *lacZYA*, Nal^R, Km^R	This study
QT2778	QT1294 pIJ70, Nal^R, Km^R, Cm^R	This study

[a]-Ap: amplicilin,Cm: chloramphenicol, Km : kanamycin Nal: nalidixic acid

Table 4: Plasmids used for this study

Plasmid	Characteristic [a]	Reference
pKD46	λ-Red recombinase plasmid Ts replicon; Ap^R	(Datsenko & Wanner, 2000)
pKD4	Template plasmid for the amplification of the *kan* cassette bordered by *FRT* sites	(Datsenko & Wanner, 2000)
pCP20	FLP helper plasmid Ts replicon; Ap^R Cm^R	(Datsenko & Wanner, 2000)
pABN5	pBR322 :: *iucABCD*, Ap^R	(Bindereif & Neilands, 1983)
pRS415	Operon fusion vector, *lacZYA*, Ap^R	(Simons et al., 1987)
pMEG-375	sacRB mobRP4 oriR6K, Cm^K, Ap^K	(Dozois et al., 2003)
pBC SK+	ColE1 origin; Cm^K	Stratagene
pBluescript II SK+	ColE1 origin, Ap^R	Stratagene
pACYC184	p15A replicon; Cm^R Tc^R	(Chang & Cohen, 1978)
pIJ36	pACYC184 :: *fes fepA entD*	This study
pIJ62	pBC SK+ :: *entS*, Cm^K	This study
pIJ64	pIJ62 with *entS* :: *kan*, Cm^K, Km^K	This study
pIJ66	pACYC184 :: *fepA entD*	This study
pIJ69	pMEG-375 with *entS* :: *kan* from pIJ64, Cm^K, Ap^K	This study
pIJ70	pACYC184 :: *entD*, Cm^K	This study
pIJ167	pMEG-375 :: Δ*iroC* from pIJ37, Cm^K, Ap^K	This study
pIJ173	pACYC184 :: P_{iroB} *iroC*, Cm^K	This study
pIJ205	pMEG-375 with P_{iroB} *iroC* from pIJ173, Cm^K, Ap^K	This study
pIJ233	pIJ173 with *entS* from pIJ62, Cm^K, Ap^K	This study
pIJ276	pBluescript II SK+ :: *lacz'-kan-iroC-lacA'* from pIJ173, Km^K, Ap^R	This study
pIJ284	pBluescript II SK+ :: *lacz'-kan-entS-lacA'*, from pIJ62, Km^K, Ap^R	This study
pIJ286	pMEG-375 :: *lacz'-kan-iroC-lacA'* from pIJ276 Km^K, Ap^K	This study
pIJ288	pMEG-375 :: *lacz'-kan-entS-lacA'* from pIJ284 Km^K, Ap^K	This study
pIJ327	pBluescript II SK+ :: *lacz'-kan-entS*$_{(LT2)}$-*lacA'*, Km^K, Ap^K	This study
pIJ330	pMEG-375 :: *lacz'-kan-entS* $_{(LT2)}$-*lacA'*, Km^K, Cm^K, Ap^K	This study
pIJ339	pABN5:: *iucA'-iucD'*, Ap^K	This study
pIJ345	pBluescript II Sk+ :: *iucA'-iucD'* from pIJ339, Ap^K	This study
pIJ346	pMEG-375 :: *iucA'-iucD'* from pIJ345, Cm^K, Ap^K	This study
pIJ347	pBluescript II SK+ :: *lacz'-kan-entS-iroC-lacA'*, from pIJ233, Km^R, Ap^R	This study
pIJ373	pMEG-375 :: *lacz'-kan-entS-iroC-lacA'* from pIJ347 Km^K, Ap^R	This study

[a]-Ap: amplicilin, Cm: chloramphenicol, Km : kanamycin Nal: nalidixic acid

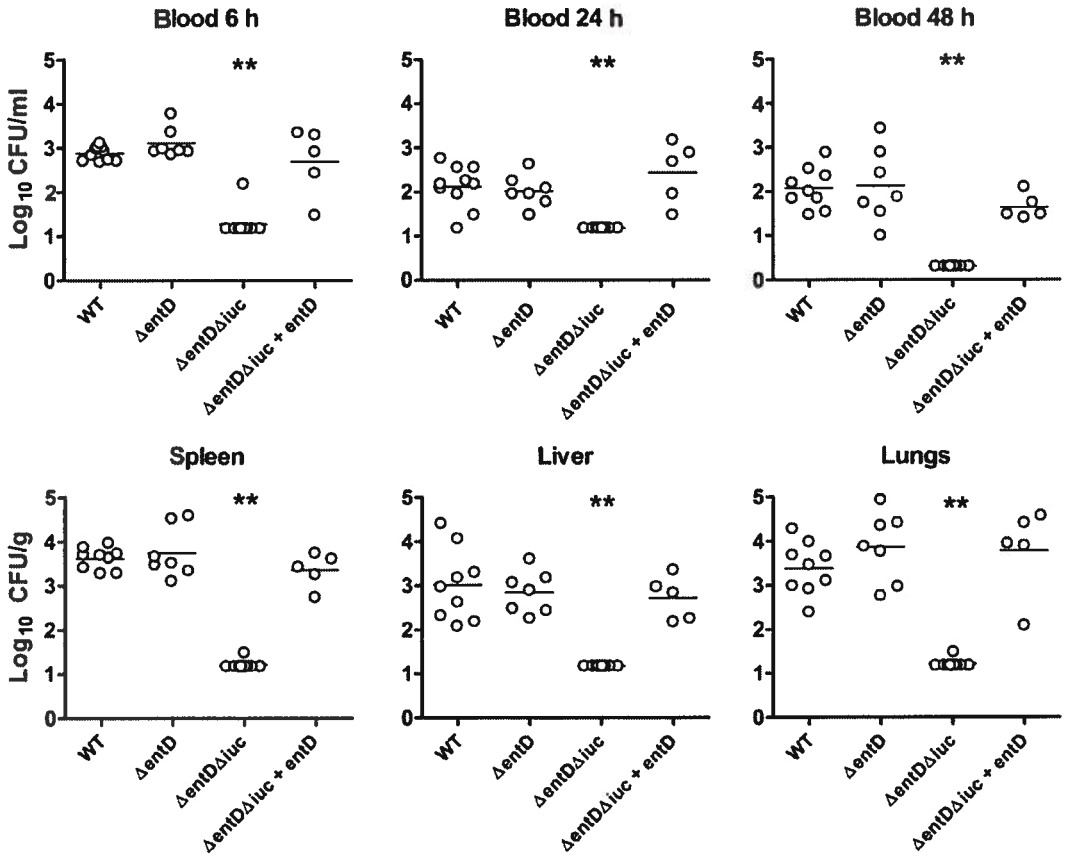

FIG 1. Bacterial numbers present in blood and tissues of chickens infected with wild-type APEC strain χ7122, siderophore synthesis mutants (QT163 and QT1294) and complemented strain (QT2778). Data points represent bacterial counts from different chickens (n=5-10) and horizontal bars represent the median bacterial colony-forming units. Statistical differences compared with the wild-type strain are noted: * (P<0.05), ** (P<0.01) using the two-tailed Mann Whitney test.

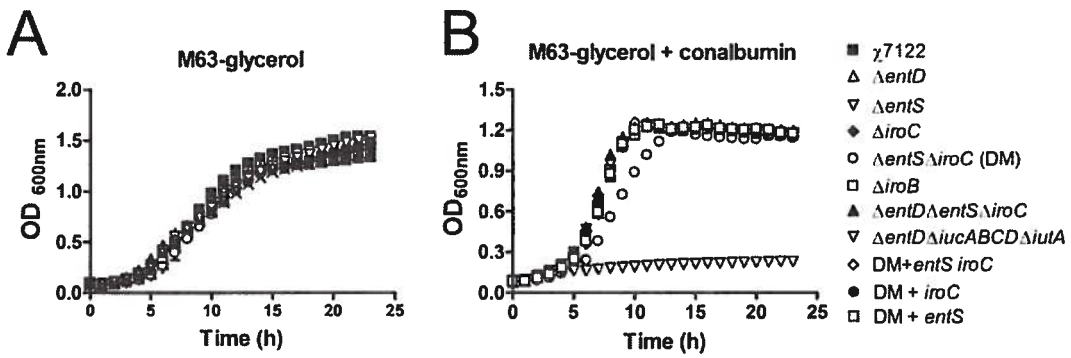

FIG.2: Growth curves of χ7122 (WT), derivative mutants and complemented strains cultured in **(A)** iron poor M63-glycerol or **(B)** iron poor M63-glycerol with conalbumin (B) at 37°C with agitation. Growth curves were obtained using a Bioscreen C apparatus. Biological samples in triplicate were evaluated.

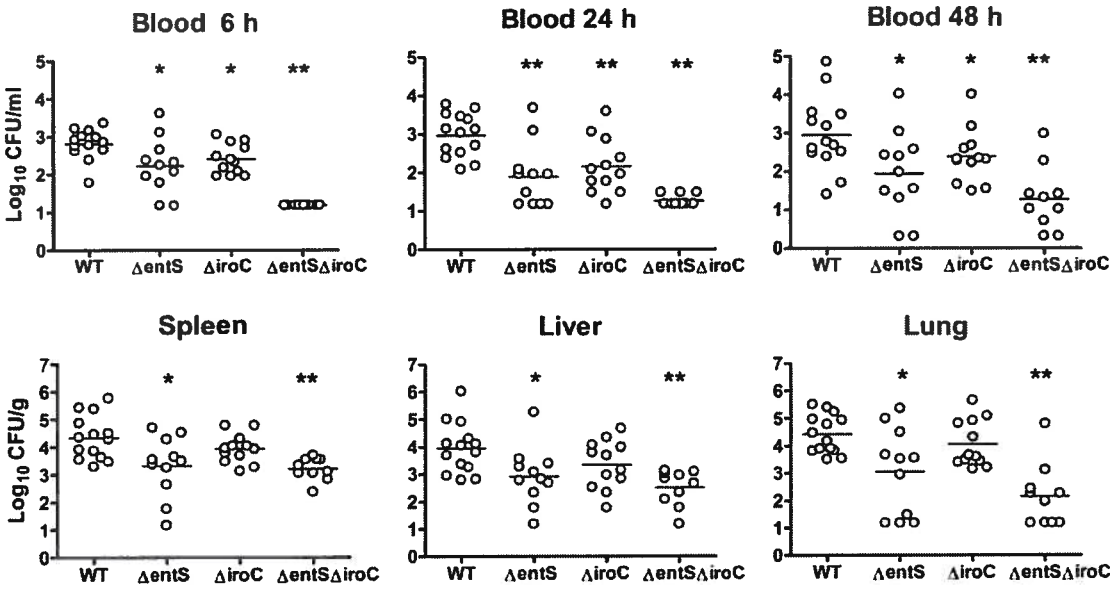

FIG. 3: Bacterial numbers present in blood and tissues of chickens infected with wild-type APEC strain χ7122 and catecholate siderophore secretion mutants. Data points represent bacterial counts from different chickens (n=10-14) and horizontal bars represent the median bacterial colony-forming units. Statistical differences compared with the wild-type strain are noted: * ($P < 0.05$); ** ($P < 0.01$) using the two-tailed Mann Whitney test.

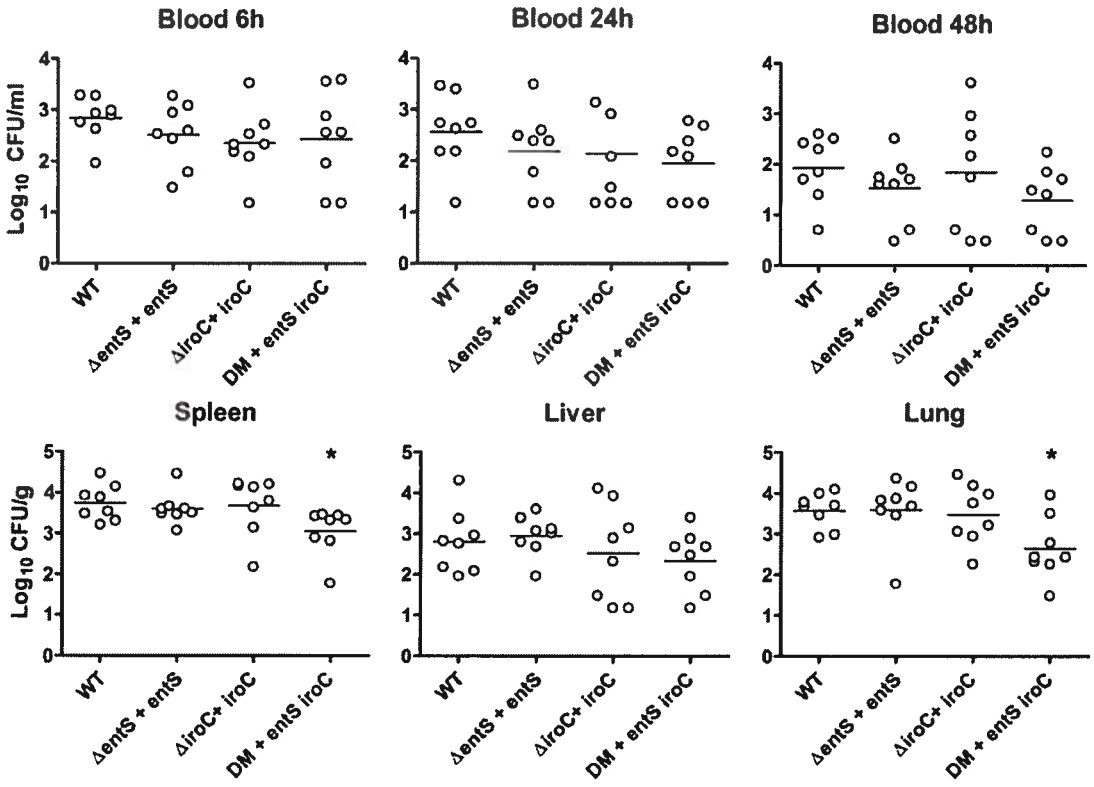

Fig. 4: Bacterial numbers present in blood and tissues of chickens infected with wild-type APEC strain χ7122 and complemented catecholate siderophore secretion mutants (QT2274, QT2309 and QT2761). Data points represent bacterial counts from different chickens (n=8) and horizontal bars represent the median bacterial colony-forming units. Statistical differences compared with the wild-type strain are noted: * ($P < 0.05$) using the two-tailed Mann Whitney test.

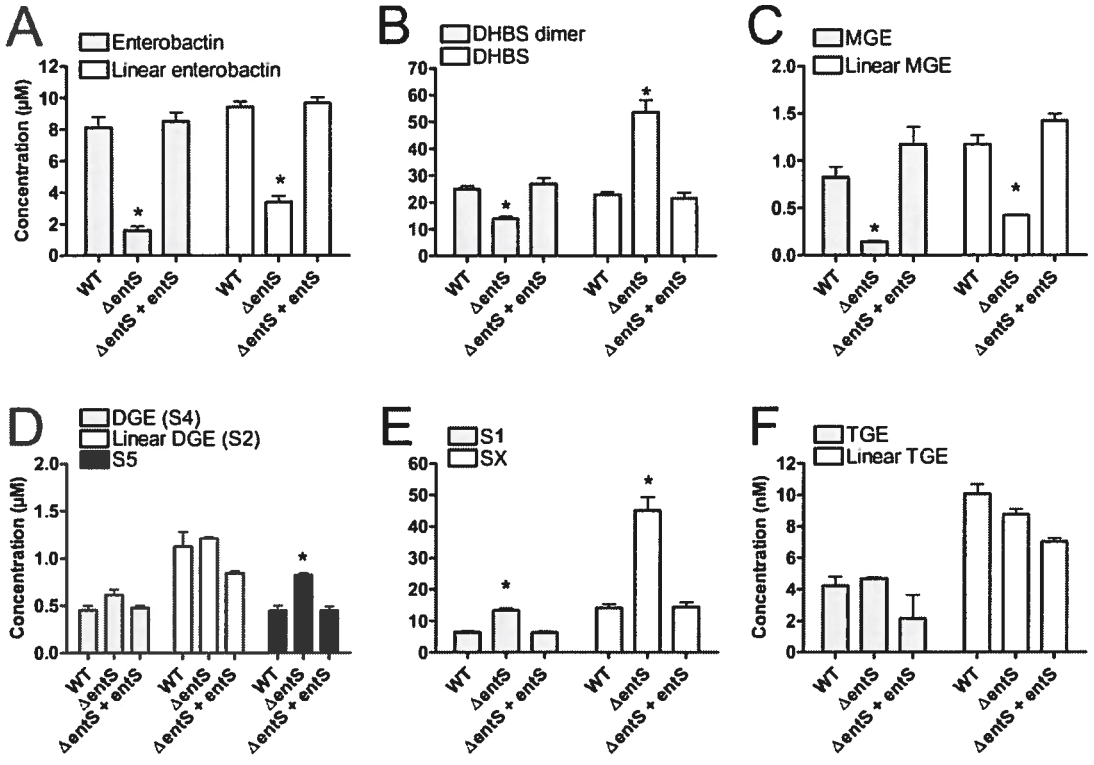

FIG. 5: Role of EntS for secretion of catecholate siderophores by *E. coli* strain χ7122. Concentrations of siderophores in the supernatants of the WT parent, a Δ*entS* mutant (QT1185) and its complemented derivative Δ*entS* + *entS* (QT2274) in M63-glycerol. Concentrations are [uM] except for TGE which is in [nM]. Mean values of at least 3 analyses of biological replicates and corresponding standard errors are presented. * indicates a significant statistical difference in siderophore concentrations between the mutant and the wild-type strain ($P<0.01$) using the two-tailed unpaired *t* test.

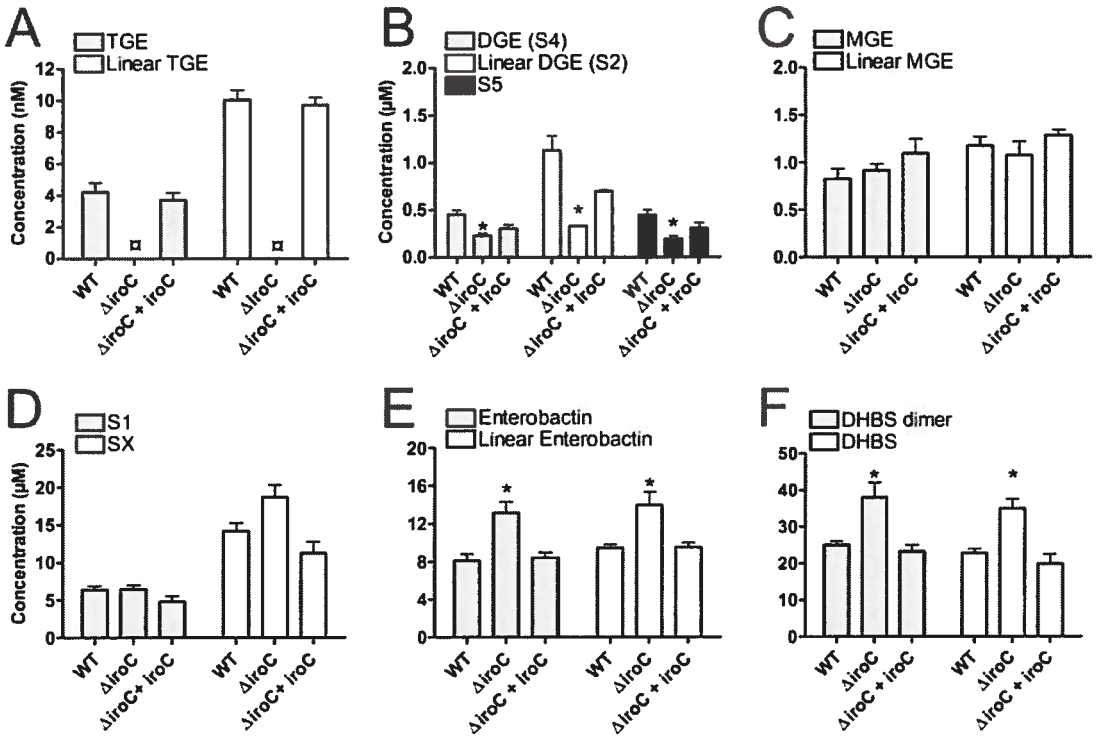

FIG.6: Role of IroC for secretion of catecholate siderophores by *E. coli* strain χ7122. Concentrations of siderophores secreted in supernatants of the wild-type (WT) parent, a Δ*iroC* mutant (QT1299) and its complement derivative (Δ*iroC* + *iroC*; QT2309) in M63-glycerol. Concentrations are in [μM] except for TGE, which is in [nM]. Mean values of at least 3 analyses of biological replicates and the standard error of the means are expressed. * indicates a significant statistical difference in siderophore concentrations between the mutant and the wild-type strain ($P<0.01$) using the two-tailed unpaired *t* test.

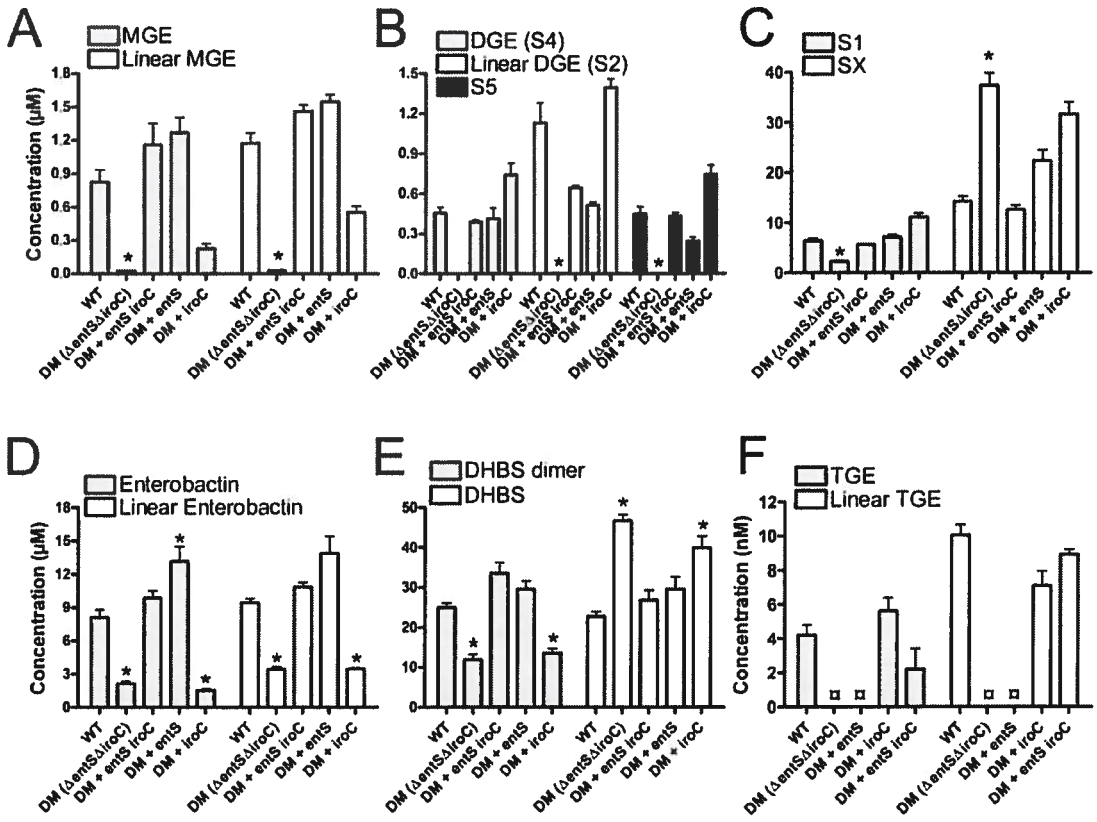

FIG 7: Combined Role of EntS and IroC for secretion of catecholate siderophores by *E. coli* strain χ7122. Concentrations of siderophores secreted in supernatant of the wild-type (WT) strain, a Δ*entS*Δ*iroC* double mutant (DM) (QT1931) and its complemented derivatives DM + *entS iroC* (QT2761), DM + *entS* (QT2310) and DM + *iroC* (QT2762) in M63-glycerol. Concentrations are in [uM] except for TGE, which is in [nM]. Means values of at least 3 analyses of biological replicates and the standard error of the mean are expressed. * indicates a significant statistical difference in siderophore concentrations between the mutant and the wild type strain ($P<0.01$) using the two-tailed unpaired *t* test.

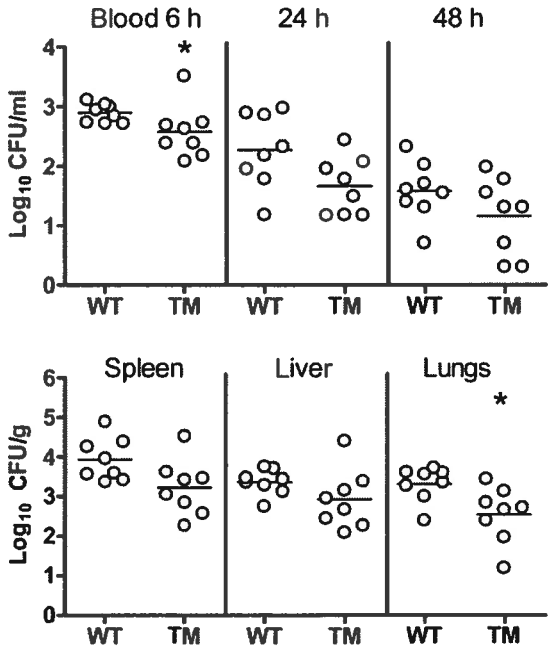

FIG 8: Abrogation of catecholate siderophore synthesis restores virulence of a Δ*entS*Δ*iroC* strain. Bacterial counts recovered from blood and tissues of infected chickens with wild-type and a Δ*entD*Δ*entS*Δ*iroC* triple mutant (TM) (QT2598) in a single-strain infection experiment. Data points represent bacterial numbers from different chickens (n=8). Horizontal bars represent the median bacterial colony-forming units. Statistical differences compared with the wild-type strain are noted * ($P<0.05$) using the two-tailed Mann Whitney test.

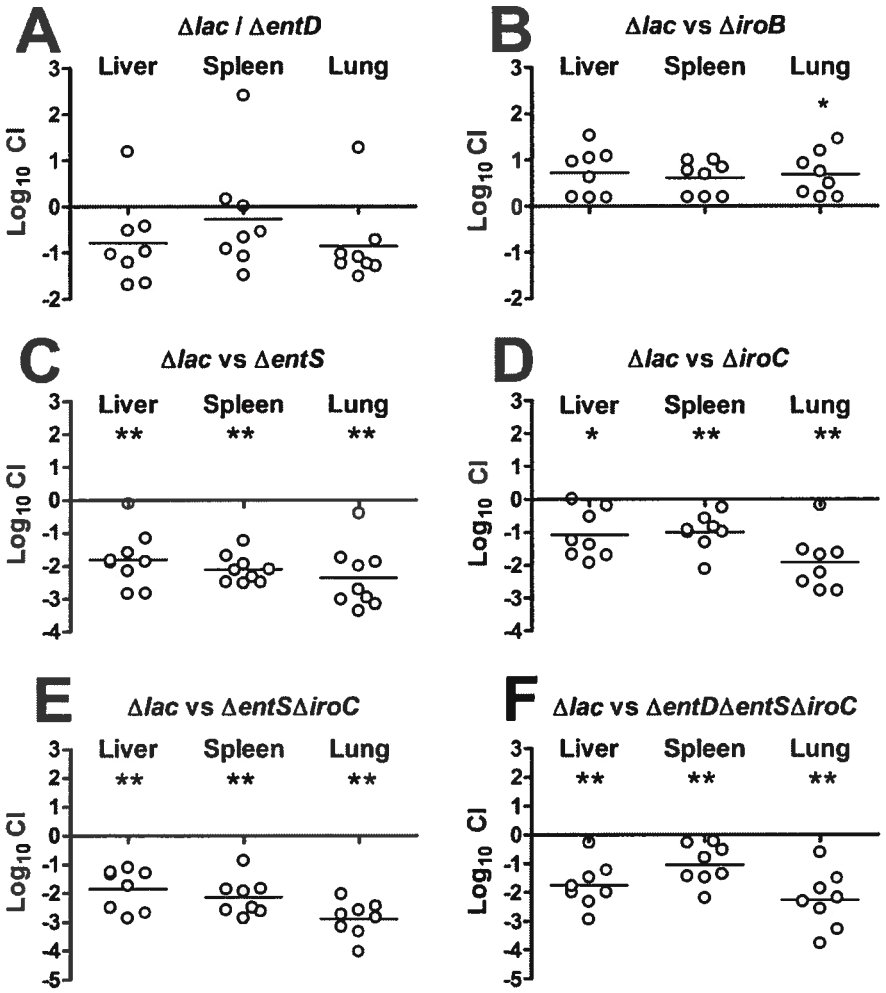

FIG. 9: Competitive fitness of catecholate siderophore synthesis and exports mutants in a co-challenge infection model. The $\log_{10}$ competitive index (CI) values from organs of infected chickens challenged simultaneously with virulent Δ*lac* strain QT51 and siderophore synthesis (QT163, QT1468 and QT2598) and export mutants (QT1185, QT1299, QT1931 and QT2598) are indicated. Data points represent individual $\log_{10}$ CI values from different chickens (n= 8). Horizontal bars represent the median $\log_{10}$ CI value. Statistical differences * (P<0.05) and ** (P<0.01) indicated were determined using the two-tailed Wilcoxon signed rank test.

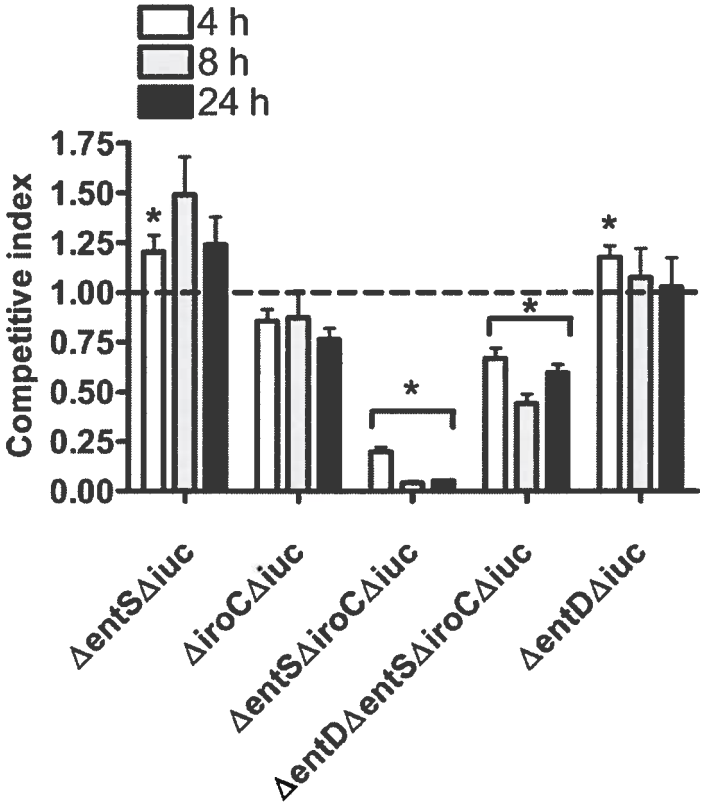

FIG. 10 : In vitro co-culture experiments. Competitive fitness of catecholate siderophore synthesis and exports mutants in M63-glycerol with conalbumin. Bacterial counts were obtained on MacConkey agar plates at 0, 4, 8 and 24 h. The $\log_{10}$ competitive index (CI) values from serial dilution bacterial counts of the Δ*lac*Δ*iucABCD* competitor strain QT2736 co-cultured with either the siderophore synthesis-negative mutant (QT1294) and export mutants (QT1195, QT1300, QT2734 and QT2737) are indicated. The histogram bars represent the individual $\log_{10}$ CI values from different co-culture experiments (n=3) with the standard deviation. Statistical differences * (P<0.01) indicated were determined using the two-tailed Wilcoxon signed rank test.

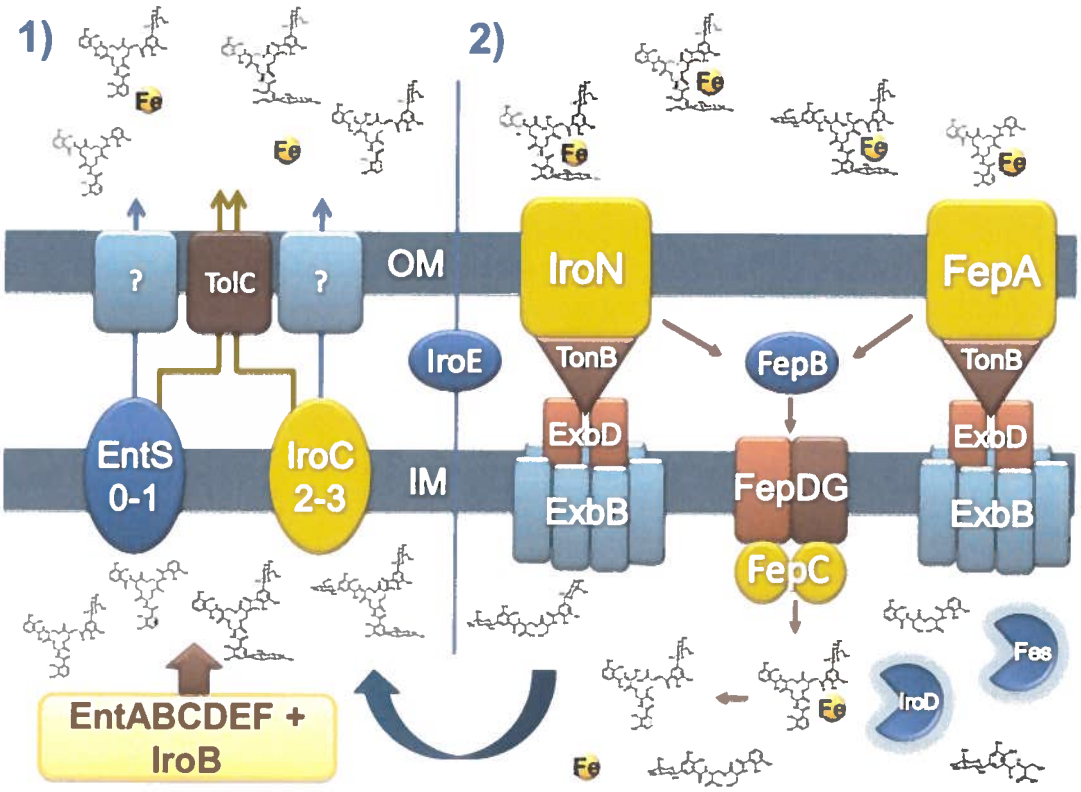

FIG. 11: Scheme of enterobatin and salmochelins systems (**1**) synthesis by EntABCDEF and IroB and secretion through the inner membrane by EntS (non- and mono-glucosylated enterobactin) and IroC (di- and tri-glucosylated enterobactin) and outer membrane by TolC or other (?) proteins and (**2**) uptake by outer membrane receptor IroN (salmochelins) and FepA (enterobactin), transmembrane passage through ABC transporter FepBDGC, degradation by Fes, IroD and IroE and re-secretion (cycling) of processed molecules (curved blue arrow).

Supp. Table 1: Primers used in this study

Primer	Sequence	Used for plasmid construct
CMD60	5'-GTCTCGAATATGGTCGATATGAAAACTACGCATACCTCGTGTAGGCTGGAGCTGCTTC-3'	
CMD61	5'-GCGAATCGTACCAGATGTTGTCAATTAATCGTGTTGCATATGAATATCCTCCTTAGTTCC-3'	
CMD62	5'-AGAAGCTTTGTTGCGGCCACAGAC-3' (*Hin*dIII)	pIJ36
CMD63	5'-ACAAGCTTTACACTTTCGCCCGT-3' (*Hin*dIII)	pIJ36
CMD75	5'-CGCTCGAGAAAATCCCTCTCCGCTTGA-3' (*Xho*I)	pIJ173
CMD98	5'-GCAAAGCTTGCTCCGGCGTTCACGCCAAG-3' (*Hin*dIII)	pIJ62
CMD99	5'-ACAAGCTTGTTTATGCGCTGGGAACCGAG-3' (*Hin*dIII)	pIJ62
CMD125	5'-GAACTCGAGATTGTTTTATTCCTGCATTTTTGC-3' (*Xho*I)	pIJ66
CMD126	5'-GAACTCGAGGATGCTAACGTCAGATTGTTGAC-3'(*Xho*I)	pIJ66
CDM690	5'-CACTCGAGCTTCATGATAATCATATGCCA-3' (*Xho*I)	pIJ173
CMD771	5'-CTAGCGTCTAGACAACCTGACCTGGAATC-3' (*Xba*I)	pIJ205
CMD773	5'- ATTCTGCATCTAGACCTCCTATGCCGCTGT-3' (X*ba*I)	pIJ205
CMD843	5'-CGCTTAATTAAACTCACTATAGGGCGAATTG-3' (*Pac*I)	pIJ224
CMD844	5'-GCTTAATTAACCCTCACTAAAGGGAACAAA-3' (*Pac*I)	pIJ224
CMD870	5'-AGGTTAATTAAGTCGCTTAAGCAATCAATG-3'(*Pac*I)	pIJ220
CMD871	5'-ATCTTAATTAAAGCGAGTGGCAACATGGA-3'(*Pac*I)	pIJ220
CMD1033	5'-CTGACCTAGGTGACGATACTACCCGCGCCA-3' (*Avr*II)	pIJ266
CMD1034	5'-AGTCCCTAGGGGTGCGCAGCCTGAATGGC-3'(*Avr*II)	pIJ266
CMD1038	5'-CAGAGCAAGAGCGGCCGCGCAGACCAAAACGATCT-3' (*Not*I)	pIJ276, pIJ284 & pIJ347
CMD1039	5'-CGCTAGCAGCGCGGCCGCGTGACTGGCGATGCTGTC-3'(*Not*I)	pIJ284
CMD1040	5'-GCCCGGCTCCAGCGGCCGCGACGCAACGCGG-3'(*Not*I)	pIJ276 & pIJ347
CMD1084	5'-ATCATGGTCCTAGGTGTTTCCTGTGTGAAATTG-3'(*Avr*II)	pIJ264
CMD1085	5'-TTTCGGCCTAGGGGTTAAAAAATGAGCTGAT-3'(*Avr*II)	pIJ264
CMD1328	5'-CCACCGTTTTGAAGTTCTGAG-3'	pIJ339
CMD1329	5'-GGGAACAGCCATTGATTGTC-3'	pIJ339

Supplemental figures

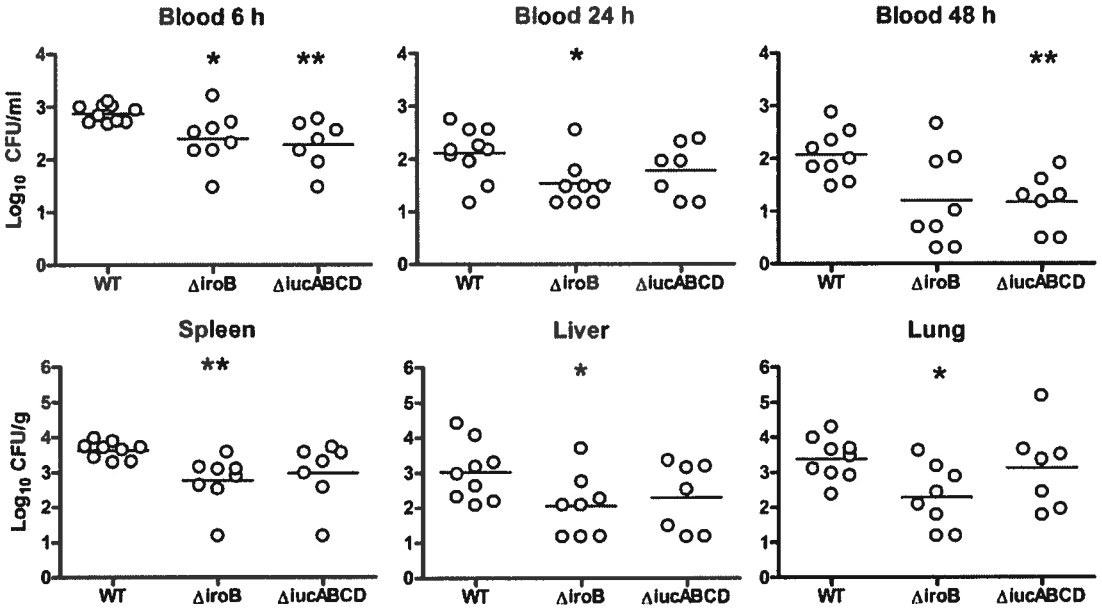

Supp. FIG 1. Bacterial numbers present in blood and tissues of chickens infected with wild-type APEC strain χ7122, siderophore synthesis mutants (QT1468 and QT2576). Data points represent bacterial counts from different chickens (n=7-10) and horizontal bars represent the median bacterial colony-forming units. Statistical differences compared with the wild-type strain are noted: * (P<0.05), ** (P<0.01) using the two-tailed Mann Whitney test

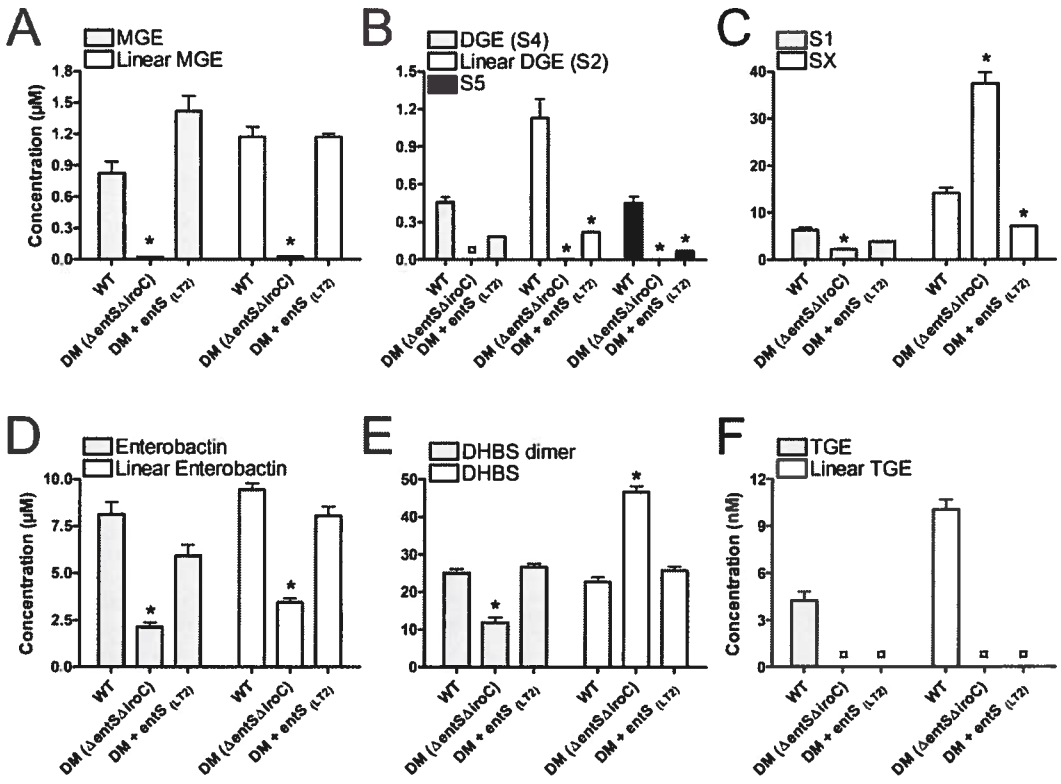

Supp. Fig.2 : Role of EntS from *S. enterica* serovar Typhimurium strain LT2 for secretion of catecholate siderophores. Concentrations of siderophores in the supernatants of the WT strain χ7122, a Δ*entS*Δ*iroC* mutant (QT1931, designated DM) and its complemented derivative DM+ *entS* $_{(LT2)}$ (QT2471) in M63-glycerol. The *entS* gene from *S.* Typhimurium strain LT2 was integrated into the *lacZYA* operon of strain QT1931 and designated DM + *entS* $_{(LT2)}$. Concentrations are in [uM] except for TGE which is in [nM]. Mean values of at least 3 analyses of biological replicates and corresponding standard errors are presented. * indicates a significant statistical difference in siderophore concentrations between the mutant and the wild-type strain.

Article #3

Siderophore esterases IroD and Fes are involved in the biosynthesis of salmochelins and contribute to virulence of an avian extra-intestinal pathogenic *Escherichia coli* strain χ7122.

Mélissa Caza, François Lépine and Charles M. Dozois.
Article en préparation

A) Contribution de l'étudiante

1- L'étude décrite dans ce manuscript en préparation tente de démontrer un nouveau rôle des estérases IroD et Fes dans la biosynthèse des salmochélines et pour la virulence de la souche χ7122. Bien qu'il ait été déjà établi que les estérases Fes et IroD dégradent les sidérophores catécholates, l'absence de ces deux gènes résulte en une inhibition de la synthèse des salmochélines. De plus, la complémentation plasmidique des gènes *fes* et *iroD* fonctionnels rétablit la production des salmochélines, seulement si le site actif est intact. Aussi, la perte des deux estérases affecte la virulence de la souche χ7122 dans le modèle d'infection septicémique aviaire, suggérant un rôle important de ces estérases pour la biosynthèse et la dégradation des sidérophores catécholates lors d'une infection systémique.

2- L'étude a été réalisée en utilisant une approche multidisciplinaire regroupant des techniques de génétique bactérienne et de biologie moléculaire, un modèle d'infection septicémique aviaire, ainsi que de la chromatographie en phase liquide couplée à la spectrométrie de masse.

3- L'étudiante a réalisé, avec l'aide de ses directeurs de recherche, toutes les étapes de conceptions et réalisations des expériences, ainsi que l'écriture du manuscrit.

B) Résumé de l'article:

Plusieurs souches d'*Escherichia coli* pathogène extra-intestinal (ExPEC) et autres entérobactéries pathogènes synthétisent les salmochélines, qui sont des formes

glucosylées du sidérophore entérobactine. Les estérases Fes, IroD et IroE dégradent les salmochélines et l'entérobactine, afin de libérer le fer nécessaire à la croissance bactérienne. Dans cette étude, nous démontrons que les estérases Fes et IroD sont requises pour la biosynthèse des salmochélines et qu'elles contribuent à la virulence de la souche ExPEC aviaire χ7122. Les mutants de la souche χ7122 contenant des mutations simples ou combinées des gènes *fes*, *iroD* et *iroE* ont été testés dans le modèle d'infection systémique aviaire. Les résultats des infections ont révélé que les mutants Δ*fes* et/ou Δ*iroD* n'établissent pas efficacement une infection systémique, puisqu'ils sont retrouvés en moins grand nombre que la souche sauvage dans les organes et le sang des animaux infectés. Les analyses en chromatographie liquide couplée au spectromètre de masse (LC-MS/MS) des mutants Δ*fes*Δ*iroD* et Δ*fes*Δ*iroD*Δ*iroE* démontrent une élimination quasi complète de la détection des salmochélines dans les surnageants. Des analyses quantitatives de PCR avec transcriptase inverse en temps réel (qRT-PCR) ont démontré qu'il n'y a pas de différence significative de l'expression des gènes *iroB*, *iroC*, *iroN* et *entF* entre le triple mutant Δ*fes*Δ*iroD*Δ*iroE* et la souche sauvage. Un immunobuvardage de type Western indique que la glucosyltransférase des salmochélines IroB est aussi produite à des niveaux similaires par les souches sauvage et mutante. Une complémentation du triple mutant Δ*fes*Δ*iroD*Δ*iroE* a été accomplie en introduisant des plasmides à copie multiple encodant pour les gènes *fes* et *iroD* fonctionnels et inactivés dans le site actif des estérases, $GX_1\underline{S}X_2G$. Les analyses en LC-MS/MS des surnageants de cultures de ces mutants complémentés démontrent une production faible des salmochélines en présence des gènes *fes* et *iroD* fonctionnels, mais une inhibition de production en présence des ces gènes dont le site actif a été muté. De plus, l'introduction de plasmides à copie multiple encodant différente combinaison des gènes *iroBCDEN* chez le triple mutant Δ*fes*Δ*iroD*Δ*iroE* a rétablie la concentration extracellulaire des salmochélines à des niveaux similaires à la souche sauvage. En somme, les résultats démontrent un rôle critique des estérases Fes et IroD dans la virulence et la nécessité des estérases Fes et IroD pour la dégradation et la biosynthèse des salmochélines.

Siderophore esterases IroD and Fes are involved in the biosynthesis of salmochelins and contribute to virulence of an avian extra-intestinal pathogenic *Escherichia coli* strain χ7122.

Running title: Esterases are required for salmochelin synthesis and virulence

Mélissa Caza, François Lépine and Charles M. Dozois*

INRS-Institut Armand-Frappier, Laval, Québec, CANADA

*Corresponding author:

Charles M. Dozois

Canada Research Chair in Infectious Bacterial Diseases

INRS-Institut Armand-Frappier

531 boul. des Prairies

Laval, Québec, CANADA H7V 1B7

Phone : 450.687.5010 ext. 4221 Fax : 450.686.5501

E-mail : charles.dozois@iaf.inrs.ca

ABSTRACT

Many extra-intestinal pathogenic *Escherichia coli* strains (ExPEC) and other pathogenic enterobacteria synthesize salmochelins, which are glucosylated forms of the siderophore enterobactin. The esterases Fes, IroD and IroE degrade salmochelins and enterobactin to release iron for bacterial utilization. In this study, we demonstrate that the esterases Fes and IroD are required for the biosynthesis of salmochelins and that these esterases contribute to virulence of an avian ExPEC strain χ7122. Mutants of strain χ7122 containing single and combined mutations of *fes*, *iroD* and *iroE* genes were tested in an avian systemic infection model. Infection results indicate that the Δ*fes* and/or Δ*iroD* mutants are less able to establish an infection similar to the wild type as demonstrated by inferior bacterial counts recovered from blood and organs of infected chickens. Liquid chromatography coupled to mass spectrometry analyses of the Δ*fes*Δ*iroD* and Δ*fes*Δ*iroD*Δ*iroE* mutants revealed a significant decrease of salmochelins molecules in supernatants. Quantitative real-time reverse transcriptase-PCR (qRT-PCR) analyses and western blot against the salmochelin glucosyltransferase IroB demonstrate no differences in genes expression of *iroB*, *iroC*, *iroN* and *entF* and similar protein levels of IroB in the triple mutant (Δ*fes*Δ*iroD*Δ*iroE*) compared to the wild-type strain. LC-MS/MS analyses of supernatants of complemented triple mutant with multiple copy plasmids encoding *fes* and *iroD* genes with functional and inactivated esterase catalytic site $GX_1\underline{S}X_2G$ indicates that *fes* and *iroD* slightly restores salmochelin production, although salmochelin production is not reinstate if Fes and IroD catalytic site is inactivated. Introduction of multiple copy plasmids encoding several *iro* genes combinations into the triple mutant reinstate extracellular concentration of salmochelins at levels similar to the wild type

strain. Taken together, our results demonstrate the critical role of the esterases Fes and IroD for the virulence of an avian ExPEC strain and also the requirement of these esterases for salmochelin degradation and biosynthesis.

INTRODUCTION

The ability of a bacterial pathogen to invade and proliferate within host tissues results from multiple complex interactions occurring between the bacteria and its host. Iron availability is a critical element for the establishment of an infection by many pathogenic bacteria for which iron is an essential element (Andrews *et al.*, 2003, Ratledge & Dover, 2000). In mammals and birds, iron is sequestered by host proteins, such as transferrin, lactoferrin and conalbumin (ovotransferrin), and can prevent toxicity due to iron-mediated generation of reactive oxygen species (Ratledge & Dover, 2000). In the host, free Fe^{3+} concentrations are estimated to be 10^{-18} M, whereas bacterial iron requirements are estimated to be from 10^{-7} to 10^{-5} M (Andrews et al., 2003, Raymond *et al.*, 2003). To overcome such an iron deficit, some bacteria produce and secrete Fe^{3+}-chelating molecules, called siderophores, which scavenge iron from their environment (Crosa & Walsh, 2002). Enteric bacteria, such as *Escherichia coli*, *Salmonella enterica* and *Klebsiella pneumoniae,* synthesize the siderophore enterobactin (Ent), a 2,3-dihydroxybenzoylserine (DHBS) macrolactone which can be glucosylated to produced salmochelins (Bister *et al.*, 2004, Fischbach *et al.*, 2005, Hantke *et al.*, 2003, Bachman *et al.*, 2009). Glucosylation of enterobactin is a virulence strategy to circumvent siderophore capture by the host innate immunity protein siderocalin (also named NGAL or lipocalin 2), which inhibits enterobactin-mediated bacterial growth during infection (Fischbach *et al.*, 2006b, Goetz *et al.*, 2002, Bachman et al., 2009). Further, salmochelins more effectively promoted bacterial growth than enterobactin in the presence of serum albumin (Bister et al., 2004). Enterobactin glucosylation by IroB can occur three times, generating cyclic salmochelins MGE, DGE and TGE (Fischbach et al., 2005). Degradation of cyclic

salmochelins by esterases Fes, IroD or IroE generates linear MGE, linear DGE, linear TGE, S5, S1 and SX (Lin *et al.*, 2005, Zhu *et al.*, 2005). The degradation of these iron loaded-catecholate siderophores (enterobactin and salmochelins) are required for iron release into bacterial cytoplasm, since an *E. coli* K-12 *fes* mutant showed growth deficiency on iron limited media with and without addition of purified enterobactin and salmochelin DGE (Zhu et al., 2005). Similarly, Vinella and co-workers have reported that an *E. coli* K-12 Δ*fes* mutant has a growth deficit on iron rich media, which can be circumvent by deletion of enterobactin synthesis gene *entB* (Vinella *et al.*, 2005). Our group demonstrated the importance of *iroBCDN* genes involved in salmochelin synthesis, processing and transport for the virulence of avian pathogenic *E. coli* strain χ7122 in an avian model of systemic infection (Caza *et al.*, 2008, Dozois *et al.*, 2003). Herein, we demonstrate that the esterases Fes and IroD are required for the biosynthesis and degradation of salmochelins and that these esterases contribute to virulence.

MATERIAL & METHODS

Bacterial strains, media and growth conditions. Bacterial strains and plasmids used are presented in Table 1. APEC strain χ7122 is an O78:K80:H9 strain isolated from the liver of a diseased turkey (Provence & Curtiss, 1992). LB broth (Difco Laboratories, Detroit, MI) was routinely used for growing *E. coli* strains. For infection studies, strain χ7122 and derivatives were grown in brain heart infusion (BHI) broth (Difco). For production and detection of catecholate siderophores, bacteria were grown at 37°C for 17 h in iron-poor M63-glycerol minimal medium as described (Caza et al., 2008). Nalidixic acid, kanamycin and chloramphenicol were added at a final concentration of 30 μg ml^{-1}.

Mutagenesis. Mutation of *fes* and *iroE* in χ7122 was generated by homologous recombination using the lambda red recombinase method (Datsenko & Wanner, 2000). The *fes*::*kat* allele from *E. coli* K-12 BW25113 JWK0576_4 (Baba *et al.*, 2006) was amplified with *Taq* DNA polymerase (New England Biolabs) using primers CMD252 and CMD 253 and introduced into χ7122 (pKD46), generating strain QT817. The kanamycin resistance gene, which is flanked by *FRT* sites, was then removed through FLP recombinase-mediated excision using plasmid pCP20 (Datsenko & Wanner, 2000), creating strain QT1198. The *iroE*::cat amplicon was obtained using primers CMD526 and CDM527 and specific amplification of the *cat* gene from pKD3 (Datsenko & Wanner, 2000) and deletion of *iroE* in χ7122 (pKD46) and in QT817 (pKD46) was achieved, generating strain QT1179 and QT1206, respectively. Deletion of *iroD* and *iroDE* was achieved by conventional allelic exchange with suicide plasmids pIJ200 (Δ*iroD*) and pIJ269 (Δ*iroDE*). The backbone of plasmid pIJ200 is pMEG-375 (Dozois *et al.*, 2000) in

which a PCR fragment from pIJ136 (Caza et al., 2008) containing *iroC and iroE* gene region from which *iroD* had been deleted was amplified with primers CMD773 and CMD774 and cloned into the XbaI site of the vector. Plasmid pIJ269 is also a derivative of pMEG-375 in which the *iroBCN* genes from pIJ135 (Caza et al., 2008) were cloned into the XbaI and BamHI sites of the vector. The allelic exchanges were realized as described in (Dozois et al., 2000) in strains χ7122 and QT1198 (Δ*fes::FRT*) producing strains QT1448 (Δ*iroD*), QT1967 (Δ*fes* Δ*iroD*), QT2083 (Δ*iroDE*) and QT2084 (Δ*fes* Δ*iroDE*). All mutants were confirmed by PCR.

Construction of plasmids. Enzymes used for generation of constructs were purchased from New England Biolabs and Fermentas. For PCR-generated fragments, Elongase DNA polymerase (Invitrogen) and Herculase II Fusion DNA Polymerase (Stratagene) were used. Plasmid constructs were derived from pIJ34 which carries the *iroBCDE* operon of APEC strain χ7122 cloned at the HindIII and EcoRV sites of vector pACYC184 (Caza et al., 2008). Plasmid pIJ48 was created by amplification of a segment of pIJ34 with primers CMD75 and CMD76, which each contain a XhoI site. The amplified product containing the *iroB* promoter and the *iroDE* genes as well as the vector backbone was ligated resulting in pIJ48. Plasmid pIJ52 is a derivative of pIJ48 in which *iroE* was removed by digesting pIJ48 with SnaBI and SmaI and recircularized with ligase. Plasmid pIJ54 was produced by amplifying a PCR fragment of pIJ34 with primers CMD75 and CMD79, which each contain a XhoI site. The amplified product containing the *iroB* promoter and the *iroE* gene and the vector backbone were ligated resulting in pIJ54. pIJ35 which encodes the *fes fepA entD* genes was generated by amplification of

χ7122 genomic DNA using primers CMD62 and CMD63 and the PCR fragment was cloned at the HindIII site of pACYC184. Plasmid pIJ35 was then digested with EcoRV, removing *fepA* and *entD* and the *fes*-containing vector was religated, resulting in pIJ285.

Site directed mutagenesis of pIJ285 was achieved by a two-step PCR procedure to generate nucleotide substitutions of the *fes* gene corresponding to a S255A switch. Plasmid pIJ285 was amplified initially with primers CMD1090 and CMD81 and with primers CMD1091 and CMD83 generating two fragments containing the nucleotide substitutions of the *fes* gene. A second PCR was performed on a mixture of these two fragments using primers CMD81 and CMD83, and the amplicon was digested and cloned into pACYC184 at the HindIII and EcoRV sites, creating pIJ304. Similarly, plasmid pIJ52 was amplified with primers CMD1092 and CMD81 and with primers CMD1093 and CMD1040, which generated two fragments containing the desired nucleotide changes and a final fragment was produced with primers CMD81 and CMD1040 and cloned at the HindIII and BamHI sites of pACYC184. This construction, pIJ311, encodes for *iroD* with a S291A substitution. Both plasmids pIJ304 and pIJ311 were sequenced and contained no additional mutations.

Experimental infection of chickens via the air sacs. Experimental infections were carried out as previously described (Caza et al., 2008, Sabri *et al.*, 2008).

Quantification of siderophores from culture supernatants by liquid chromatography coupled to a mass spectrometer. Siderophores were detected by direct analysis of

supernatants and quantified as described (Caza et al., 2008). Multiple reaction monitoring (MRM) analyses were performed on a Waters 2795 Alliance HT coupled to a Micromass Quattro Premier XE spectrometer (Micromass MS Technologies).

Quantitative real-time reverse transcriptase-PCR (qRT-PCR). For expression analysis of the salmochelin and enterobactin encoding genes, the *iroBCN* and *entF* transcripts of the wild type and triple esterase mutant strain were analyzed following growth in M63-glycerol for 3 h at 37°C with agitation. Cultures were pelleted by centrifugation for 5 min at room temperature, and RNA was extracted from whole bacterial cells using TRIzol reagent according to the manufacturer instructions (Invitrogen). A 10-fold dilution was performed in TRIzol, followed by RNA extraction. RNA was treated twice with DNase using the DNA-free kit (Ambion) to eliminate any genomic DNA. RNA concentrations were determined using a NanoDrop 1000 apparatus (NanoDrop Technologies, Wilmington, DE), and 0.1 µg/ml of total RNA was used. Real-time PCR was done using the IScript™ One-Step RT-PCR kit with SYBR® Green (Bio-Rad) according to the manufacturer guidelines and a Rotor-Gene 3000 real-time PCR apparatus (Corbett Research, Sydney, Australia). The *gapA* gene was used as a housekeeping control (Fitzmaurice *et al.*, 2004) . Three biological samples were tested and each qRT-PCR run was done in duplicate and for each reaction, the calculated threshold cycle (*C*t) was normalized to the *C*t of the *gapA* gene amplified from the corresponding sample. The fold-change was calculated using the $2^{-\Delta\Delta Ct}$ method (Schmittgen *et al.*, 2000).

Preparation of IroB-specific antisera. CPGEVAKSLITMVQKG a purified peptide corresponding to the C-terminal portion of IroB, was coupled to keyhole limpet hemocyanin and used to immunize two New Zealand White rabbits. Peptide synthesis and IroB antiserum production were provided by New England Peptide, Inc.

Western blotting. Whole cell extracts were obtained from 17 h M63-glycerol cultures, for which cell density was adjusted to OD_{600} 1.0. Cultures were centrifuged and proteins from pellets were extracted with BugBuster™ (Novagen). Proteins were separated by sodium dodecyl sulfate (SDS)-12% polyacrylamide gel electrophoresis minigels as previously described by (Laemmli, 1970). Proteins were transferred to nitrocellulose membranes (Bio-Rad) using a Mini Trans-Blot electrophoretic cell (Bio-Rad) for 60 min at 100 V. The membrane was blocked with StartingBlock supplemented with 0.05% Tween 20 (Pierce). Incubations with primary (1:5,000) and secondary (1:25,000) antibodies were carried out for 1 h respectively at room temperature. SuperSignal West Pico chemiluminescent substrate (Pierce) was used for detection.

RESULTS

Role of esterases for the virulence of strain χ7122. To determine the importance of catecholate siderophore degradation by esterases Fes, IroD and IroE, single and multiple esterase mutants were generated and tested in a chicken systemic infection model. The enterobactin esterase Δ*fes* mutant demonstrated decreased numbers in the blood at 24 and 48 h post-infection and in liver, spleen and lungs (figure 1). The Δ*iroD* mutant was even more attenuated than the Δ*fes* mutant with decreased bacterial counts in all visceral organs and in blood at all time points (figure 2). Inactivation of the periplasmic hydrolase IroE had no effect on virulence of the strain, since similar bacterial counts were obtained as compared to the wild type strain (figure 2), suggesting that IroE does not play a major role during systemic infection. The combined loss of esterases in strain χ7122 was expected to result in more marked attenuation than either the Δ*fes* or Δ*iroD* mutants individually. However, a Δ*fes*Δ*iroD* mutant infection results were actually less pronounced when compared to the single esterase mutants (figure 2). Furthermore, the triple Δ*fes*Δ*iroDE* (TM) mutant was no more attenuated than Δ*fes*Δ*iroD* mutant and was more virulent than the Δ*iroD* mutant as it was present in increased numbers in the bloodstream liver and lungs. These results confirmed that the periplasmic hydrolase IroE is not required for virulence of χ7122 under these conditions and that combined loss of esterases lead to a less marked decrease in virulence when compared to either of the single *fes* or *iroD* mutants. To further investigate these differences in virulence, siderophore production in culture supernatants of esterase mutants was assessed by LC-MS/MS.

Esterase Fes is required for the degradation of cyclic enterobactin and salmochelin MGE. Culture supernatants analyzed by LC-MS/MS revealed a 3.5-fold increase in cyclic enterobactin in the supernatant of the *fes* mutant as compared to supernatants of the wild-type strain χ7122 (figure 3A). Trimers and dimers of DHBS were also increased in the *fes* mutant, whereas the amount of DHBS monomer was similar to the wild-type strain (figure 3 A and B). Loss of Fes also altered salmochelin levels. Indeed, a *fes* mutation increased mono-glycosylated enterobactin molecules (MGE) by 1.8-fold, whereas levels of linear MGE were similar to the wild-type (Figure 3C). Conversely, production of di-glycosylated salmochelins (DGE and linear DGE) and tri-glycosylated salmochelins (TGE and linear TGE) as well as degraded forms of salmochelins, S5, S1 and SX, was greatly reduced in culture supernatants of the *fes* mutant (Figure 3 D, E and F). Overall, loss of *fes* increased levels of enterobactin molecules and diminished salmochelin production (Figure 3 G and H). This suggest that in absence of Fes, iron acquisition through iron loaded- enterobactin and salmochelin MGE does not occur and these molecules are re-secreted and accumulates in the supernatant, while iron acquisition through iron-loaded di- and tri-glucosylated salmochelins is achieved by degradation of these molecules into salmochelins S1 and SX by other esterases, likely IroD. The decrease of salmochelin S1 and SX observed can be explained by the fact that these molecules are also generated by degradation of mono-glucosylated salmochelins, which is restrained in a Δ*fes* mutant. These results are in accordance with previous biochemical reports demonstrating the role of Fes for hydrolysis of enterobactin into trimers, dimers and monomers of 2,3-dihydroxybenzoylserine and salmochelin MGE into linear MGE (Winkelmann *et al.*, 1994, Lin et al., 2005, Brickman & McIntosh, 1992).

Esterase IroD is required for the degradation of enterobactin and salmochelins. Enterobactin and its derivatives concentration are reduced in the supernatants of a Δ*iroD* mutant compared to the wild-type strain. In fact, a 3.4-fold and 2.1-fold decrease of DHBS monomer and trimer were obtained, while a mild reduction of DHBS dimer and cyclic enterobactin were observed (figure 3 A and B). Salmochelin concentrations were also altered in the absence of IroD. With the exception of TGE and linear TGE, all salmochelin concentrations were greatly diminished (figure 3C, D, E and F), making an overall reduction of salmochelin production of 3.7-fold (figure 3 G). Since esterase activity of IroD was already reported in biochemical reports made by other groups (Lin et al., 2005, Zhu et al., 2005), reduction of linear and degraded forms of salmochelins was expected. However, reduced levels of cyclic salmochelins MGE and DGE were unexpected (figure 3 C and D).

Periplasmic hydrolase IroE is not required for degradation of catecholate siderophore. While significant variations of monomers and trimers of DHBS concentrations occurred, the total amount of enterobactin derivatives as well as cyclic enterobactin and DHBS dimer were fairly similar to those of strain χ7122 (figure 3A, B and H). Even if salmochelins S1 and linear MGE were less abundant in supernatants of an *iroE* mutant, overall total salmochelins and other individual glucosylated molecule concentrations were not significantly affected (Figure 3 C , E and G). However, loss of *iroE* did significantly increased TGE and linear TGE concentration in supernatants (figure 3 F), while concentrations of di-glycosylated salmochelins were similar to the wild type strain (figure 3 D). Reminiscent of Fes and IroD, IroE was also characterized as a periplasmic hydrolase that efficiently cleaves one ester bond of cyclic enterobactin and

salmochelin molecules generating trimeric linear molecules (Lin et al., 2005, Zhu et al., 2005). Our results also support the fact that IroE cleaves only one ester bond resulting in production of trimeric linear MGE and DHBS, as concentration of these molecules are significantly reduced in culture supernatant of the *iroE* mutant. Our results also suggest that IroE cleave efficiently salmochelin TGE. Consequently, molecules derived from linear trimers and salmochelin TGE, such as monomers of DHBS and salmochelin S1 are also less abundant (Figure 3B and E). Overall, mutation of *iroE* did not drastically affect enterobactin and salmochelin degradation (figure 3 G and H), because efficient esterase Fes and IroD are still functional in the single mutant Δ*iroE*.

Cumulative losses of esterase Fes and IroD impair salmochelin synthesis. LC-MS/MS analyses of single esterase mutant supernatants suggested that cytoplasmic esterase IroD and Fes more extensively degrade catecholate siderohores into monomers of DHBS and salmochelin S1 than IroE. Whereas of either mutation of *fes* or *iroD* diminished salmochelin production, mutations of both esterases nearly inhibited synthesis of salmochelins completely, without inhibiting production of non-glycosylated molecules (figure 3 G and H). Only trace amounts of salmochelins MGE, linear MGE, S1 and SX were detected in supernatant of the Δ*fes*Δ*iroD* mutant or the Δ*fes*Δ*iroD*Δ*iroE* triple mutant (figure 3 C and E). Concentration of cyclic enterobactin was unchanged in the Δ*fes*Δ*iroD* mutant compared to strain χ7122, although DHBS trimers and dimers were increased to levels similar to the Δ*fes* mutant (figure 3A and B). Levels of non-glycosylated siderophores were also diminished in supernatants of the Δ*fes*Δ*iroD*Δ*iroE* triple mutant, although cyclic enterobactin concentration was comparable to the wild type strain (Figure 3A and H). These results suggest that esterase activity is required for the

production of salmochelins or that loss of esterases may result in regulatory feedback inhibition of salmochelin glucosyltransferase IroB production or *iroB* gene expression.

Inhibition of salmochelin synthesis is not due to regulatory feed-back inhibition or a post-translational inhibition of IroB. To test either possibility, we first determined if expression of salmochelin synthesis and secretion genes is altered in the triple esterase mutant. Real-time PCR (RT-PCR) experiments performed on *iroB*, *iroC*, *iroN* and on enterobactin synthesis gene *entF* indicated no differential gene expression (figure 4 A). Moreover, a western blot was performed on total cell lysates with anti-IroB antiserum. As shown in figure 4B, IroB protein is produced at similar levels in both the wild-type strain and triple esterase mutant whereas as IroB is not detected in the Δ*iroB* mutant. These experiments confirm that regulatory feed-back inhibition on *iroB* expression or protein production is not responsible for loss of production of salmochelins in the Δ*fes*Δ*iroD*Δ*iroE* triple esterase mutant.

Serine-esterase activity of IroD and Fes is required for the synthesis of salmochelins. To confirm that esterases are required for the production of salmochelins, we re-introduced the esterase genes cloned onto a mid-copy number plasmid to the Δ*fes*Δ*iroD*Δ*iroE* triple mutant and performed LC-MS/MS analysis on culture supernatants. Complementation of the Δ*fes*Δ*iroD*Δ*iroE* triple esterase mutant with plasmids encoding functional IroD, Fes and IroE partially restored salmochelin production, even though wild-type concentrations were not attained (figure 5 A). However, no tri-glucosylated molecules were detected. LC-MS/MS analysis of the

mutant complemented with *iroD* revealed an overall regain in salmochelin synthesis (figure 5A) and all remaining salmochelins were detected in an *iroD* complemented mutant (figure 5B, C and D). Complementation with plasmid encoding both *iroD* and *iroE* restored production of salmochelin more efficiently (figure 5A) and all salmochelins were produced by this complemented mutant (figure 5B, C and D). However, introduction of *iroE* alone in the triple mutant only slightly increased salmochelin MGE, linear MGE, S1 and SX production but not di-glucosylated molecules (figure 5B, C and D). By contrast, complementation with *fes* re-established synthesis of salmochelins DGE, MGE, linear MGE, S1 and SX, although at levels much lower than the *iroD* and *iroDE* complemented strains (figure 5B, C and D). These results support the requirement of cytoplasmic esterases for salmochelin production.

Catalytic activity of IroD and Fes are required for Fe^{3+}-salmochelin degradation (Lin et al., 2005, Zhu et al., 2005). We wanted to determine if this esterase active site domain is also mandatory for salmochelin synthesis. The esterase active site, $GX_1\underline{S}X_2G$ contains a serine that is essential for catalytic activity (Larsen *et al.*, 2006). We replaced the active site serine with an alanine in the plasmids encoding either IroD or Fes. LC-MS/MS analysis of culture supernatants of the Δ*fes*Δ*iroD*Δ*iroE* triple esterase mutant complemented with non-active Fes or IroD encoding plasmids confirmed the importance of an intact esterase catalytic site for salmochelin synthesis, as plasmids encoding the S>A substituted esterases demonstrate very low levels of salmochelin production (figure 5 A, B, C and D)

Complementation with stochiometric expression of IroB and IroD restores salmochelin production. Complementation of the Δ*fes*Δ*iroD*Δ*iroE* triple esterase mutant

with plasmids encoding the complete IroA cluster restored production of diglucosylated salmochelins and derivatives (S1 and SX) at levels similar to wild-type strain (figure 6 B and D). LC-MS/MS analysis of the triple mutant complemented with the *iroBCDEN* genes (pIJ20) revealed an overall regain in salmochelin synthesis of 1.6-fold as compared to the wild-type strain χ7122 (figure 6A). Even if salmochelin SX is the main molecule detected from a 17 h culture supernatant, concentrations of salmochelin S1 were similar to wild-type and salmochelins S5, DGE and linear DGE were also produced in considerable amounts (figure 6B and D). Moreover, introduction of *iroBCDN* genes (pIJ137) increased synthesis of salmochelins S5, linear DGE and SX at equivalent concentrations as the wild type strain (figure 6B and D). The regain in salmochelin synthesis was not attained in the absence of *iroD*, since *iroBCEN* complemented mutant produced only small amounts of S5, MGE, linear MGE, S1 and SX and did not synthesize DGE and linear DGE. However, *iroE* contributed to salmochelin S5 production, given that in an *iroBCN* complemented mutant no di-glucosylated salmochelins were detected (figure 6B). Taken together, these results strongly suggest that salmochelin production requires gene dosage of the *iroB* and *iroD* genes encoding the salmochelin glucosyltransferase and esterase respectively.

DISCUSSION

Glucosylation of catechol siderophores is a new feature of the extentively studied iron acquisition system enterobactin. This modification of enterobactin into salmochelins allows pathogenic *E. coli* to evade siderophore capture by the host innate immunity protein NGAL (lipocalin 2 or siderocalin) (Fischbach *et al.*, 2006a, Fischbach et al., 2006b, Flo *et al.*, 2004). Glucosylation of only one catechol moiety (salmochelin MGE) is sufficient to create a steric burden with siderocalin, making its capture impossible (Fischbach et al., 2006b). This evasion is one of the strategies that allows iron acquisition by pathogenic bacteria from the host, since salmochelins maintain a ferric iron acquisition rate similar to enterobactin (Luo *et al.*, 2006). We have demonstrated that the salmochelin-encoding *iro* gene cluster, *iroBCDN*, contributes to the virulence of APEC strain χ7122 in a chicken sepsis model (Caza et al., 2008, Dozois et al., 2003).

Salmochelins can be produced in vitro in a consecutive manner with purified IroB and cyclic enterobactin, with accumulation of MGE prior to conversion into salmochelin DGE, followed by TGE (Fischbach et al., 2005). Glucosylation of DHBS monomer is also not possible, reinforcing the fact that intact enterobactin is the relevant substrate for IroB (Fischbach et al., 2005). We tested whether cyclic enterobactin or degraded/linear DHBS molecules could be recycled and transformed into salmochelin by an *entA* mutant of χ7122, deficient in 2,3-dihydroxybenzoate (2,3-DHB) formation (Sakaitani *et al.*, 1990). Results obtained demonstrated that only 2,3-dihydroxybenzoic acid (DHBA), a precursor of enterobactin, can be converted into enterobactin and salmochelin suggesting that enterobactin and degraded products cannot be recycled for the production of salmochelins (supp. fig 1).

Degradation/linearization of salmochelins and enterobactin is achieved through cytoplasmic esterase Fes, IroD and also by the periplasmic hydrolase IroE (Bister et al., 2004, Fischbach et al., 2005, Hantke et al., 2003, Lin et al., 2005, Zhu et al., 2005). The degradation of iron-bound enterobactin and salmochelins is required for iron release. The Fes esterase preferentially cleaves iron-loaded enterobactin and mono-glucosylated molecules and that IroD efficiently degrades iron-bound enterobactin and salmochelins MGE, DGE and TGE (Lin et al., 2005). The kinetic parameters of Fes and IroD revealed that these enzymes have a stronger catalytic activity (k_{cat}) for apo-enterobactin/salmochelins than its holo equivalent form, but saturation concentrations of the substrates (K_M) are higher for apo-forms than holo-forms, resulting in a better catalytic efficiency (k_{cat}/K_M) of Fes and IroD for iron-loaded siderophores (Lin et al., 2005). On the other hand, the role of the periplasmic hydrolase IroE functions is to linearize cyclic apo-salmochelin and enterobactin (Lin et al., 2005, Luo et al., 2006). In this study, we have demonstrated that linearization of salmochelin and enterobactin by IroE is not required for the virulence of strain χ7122. By contrast, mutation of either of the cytoplasmic esterases, IroD or Fes significantly reduced virulence of the strain in an avian systemic infection model. LC-MS/MS analyses suggest that degradation of enterobactin was reduced in the absence of Fes as greater amounts of cyclic enterobactin and linear trimer were present in supernatants of the Δ*fes* strain. This observation was not expected, since degradation of enterobactin has previously been shown to also occur through IroD (Lin et al., 2005). Interestingly, loss of Fes also resulted in an overall decrease of salmochelin production. Similarly, a decrease of salmochelin concentrations was noted in absence of esterase IroD. These reductions in salmochelin synthesis may

also explain the attenuation of virulence of the mutant strains. However, the combined losses of both esterases alleviated the attenuation of virulence to a certain degree despite the marked decreased in salmochelin production, suggesting that degradation of iron-loaded salmochelins as well as enterobactin is more critical for virulence than salmochelin synthesis. These phenotypes are maintained in a Δ*fes*Δ*iroD*Δ*iroE* triple esterase mutant, confirming that IroE is ancillary for the pathogenesis of the strain and that IroD and Fes are required for salmochelin synthesis.

The restoration of salmochelin synthesis in the Δ*fes*Δ*iroD*Δ*iroE* triple esterase mutant by complementation with plasmids encoding Fes, IroD and IroE demonstrated their role in the synthesis of salmochelins. IroD complementation restored more efficiently salmochelin production than Fes and the combination of IroDE was even better than IroD alone. However, addition of Fes and IroE alone demonstrate a weak restoration of salmochelin synthesis in a triple mutant. This observation suggests that IroD functions as the primary esterase for salmochelin synthesis and that Fes and IroE may play auxiliary roles. The fact that the catalytic sites of Fes and IroD are required for regain of salmochelin production, since very little salmochelin amount were detected in catalytic deficient *fes* and *iroD* plasmids, suggests that linearization of apo-enterobactin in the cytoplasm may be required for addition of glucoses on catechol moieties before or after cyclotrimerization.

Furthermore, complementation with plasmids encoding stochiometric levels of IroB and IroD (pIJ20 or pIJ137) restored production of di-glucosylated salmochelins (linear DGE and S5) and degraded derivatives (S1 and SX) at levels similar to the wild type strain.

Taken together, these results strongly suggest an interaction between IroB and IroD for salmochelin synthesis.

ACKNOWLEDGEMENTS

M.C. was funded by scholarships from the "Fondation Armand-Frappier" and the Swine infectious disease research center-"Centre de recherche en infectiologie porcine" (CRIP). Funding for this project was provided by a discovery grant to CMD from the Natural Sciences and Engineering Research Council of Canada (NSERC), and infrastructure funding from the Canadian Foundation for Innovation (CFI).

REFERENCES

Andrews, S. C., A. K. Robinson & F. Rodriguez-Quinones, (2003) Bacterial iron homeostasis. *FEMS Microbiol Rev* **27**: 215-237.

Baba, T., T. Ara, M. Hasegawa, Y. Takai, Y. Okumura, M. Baba, K. A. Datsenko, M. Tomita, B. L. Wanner & H. Mori, (2006) Construction of *Escherichia coli* K-12 in-frame, single-gene knockout mutants: the Keio collection. *Mol Syst Biol* **2**: 2006 0008.

Bachman, M. A., V. L. Miller & J. N. Weiser, (2009) Mucosal lipocalin 2 has pro-inflammatory and iron-sequestering effects in response to bacterial enterobactin. *PLoS Pathog* **5**: e1000622.

Bister, B., D. Bischoff, G. J. Nicholson, M. Valdebenito, K. Schneider, G. Winkelmann, K. Hantke & R. D. Sussmuth, (2004) The structure of salmochelins: C-glucosylated enterobactins of *Salmonella enterica*. *Biometals* **17**: 471-481.

Brickman, T. J. & M. A. McIntosh, (1992) Overexpression and purification of ferric enterobactin esterase from *Escherichia coli*. Demonstration of enzymatic hydrolysis of enterobactin and its iron complex. *J Biol Chem* **267**: 12350-12355.

Caza, M., F. Lepine, S. Milot & C. M. Dozois, (2008) Specific roles of the *iroBCDEN* genes in virulence of an avian pathogenic *Escherichia coli* O78 strain and in production of salmochelins. *Infect Immun* **76**: 3539-3549.

Chang, A. C. & S. N. Cohen, (1978) Construction and characterization of amplifiable multicopy DNA cloning vehicles derived from the P15A cryptic miniplasmid. *J Bacteriol* **134**: 1141-1156.

Crosa, J. H. & C. T. Walsh, (2002) Genetics and assembly line enzymology of siderophore biosynthesis in bacteria. *Microbiol Mol Biol Rev* **66**: 223-249.

Datsenko, K. A. & B. L. Wanner, (2000) One-step inactivation of chromosomal genes in *Escherichia coli* K-12 using PCR products. *Proc Natl Acad Sci U S A* **97**: 6640-6645.

Dozois, C. M., F. Daigle & R. Curtiss, 3rd, (2003) Identification of pathogen-specific and conserved genes expressed in vivo by an avian pathogenic *Escherichia coli* strain. *Proc Natl Acad Sci U S A* **100**: 247-252.

Dozois, C. M., M. Dho-Moulin, A. Bree, J. M. Fairbrother, C. Desautels & R. Curtiss, 3rd, (2000) Relationship between the Tsh autotransporter and pathogenicity of avian *Escherichia coli* and localization and analysis of the Tsh genetic region. *Infect Immun* **68**: 4145-4154.

Fischbach, M. A., H. Lin, D. R. Liu & C. T. Walsh, (2005) In vitro characterization of IroB, a pathogen-associated C-glycosyltransferase. *Proc Natl Acad Sci U S A* **102**: 571-576.

Fischbach, M. A., H. Lin, D. R. Liu & C. T. Walsh, (2006a) How pathogenic bacteria evade mammalian sabotage in the battle for iron. *Nat Chem Biol* **2**: 132-138.

Fischbach, M. A., H. Lin, L. Zhou, Y. Yu, R. J. Abergel, D. R. Liu, K. N. Raymond, B. L. Wanner, R. K. Strong, C. T. Walsh, A. Aderem & K. D. Smith, (2006b) The pathogen-associated *iroA* gene cluster mediates bacterial evasion of lipocalin 2. *Proc Natl Acad Sci U S A* **103**: 16502-16507.

Fitzmaurice, J., M. Glennon, G. Duffy, J. J. Sheridan, C. Carroll & M. Maher, (2004) Application of real-time PCR and RT-PCR assays for the detection and quantitation of VT 1 and VT 2 toxin genes in *E. coli* O157:H7. *Mol Cell Probes* **18**: 123-132.

Flo, T. H., K. D. Smith, S. Sato, D. J. Rodriguez, M. A. Holmes, R. K. Strong, S. Akira & A. Aderem, (2004) Lipocalin 2 mediates an innate immune response to bacterial infection by sequestrating iron. *Nature* **432**: 917-921.

Goetz, D. H., M. A. Holmes, N. Borregaard, M. E. Bluhm, K. N. Raymond & R. K. Strong, (2002) The neutrophil lipocalin NGAL is a bacteriostatic agent that interferes with siderophore-mediated iron acquisition. *Mol Cell* **10**: 1033-1043.

Hantke, K., G. Nicholson, W. Rabsch & G. Winkelmann, (2003) Salmochelins, siderophores of *Salmonella enterica* and uropathogenic *Escherichia coli* strains, are recognized by the outer membrane receptor IroN. *Proc Natl Acad Sci U S A* **100**: 3677-3682.

Laemmli, U. K., (1970) Cleavage of structural proteins during the assembly of the head of bacteriophage T4. *Nature* **227**: 680-685.

Larsen, N. A., H. Lin, R. Wei, M. A. Fischbach & C. T. Walsh, (2006) Structural characterization of enterobactin hydrolase IroE. *Biochemistry* **45**: 10184-10190.

Lin, H., M. A. Fischbach, D. R. Liu & C. T. Walsh, (2005) In vitro characterization of salmochelin and enterobactin trilactone hydrolases IroD, IroE, and Fes. *J Am Chem Soc* **127**: 11075-11084.

Luo, M., H. Lin, M. A. Fischbach, D. R. Liu, C. T. Walsh & J. T. Groves, (2006) Enzymatic tailoring of enterobactin alters membrane partitioning and iron acquisition. *ACS Chem Biol* **1**: 29-32.

Provence, D. L. & R. Curtiss, 3rd, (1992) Role of *crl* in avian pathogenic *Escherichia coli*: a knockout mutation of *crl* does not affect hemagglutination activity, fibronectin binding, or Curli production. *Infect Immun* **60**: 4460-4467.

Ratledge, C. & L. G. Dover, (2000) Iron metabolism in pathogenic bacteria. *Annu Rev Microbiol* **54**: 881-941.

Raymond, K. N., E. A. Dertz & S. S. Kim, (2003) Enterobactin: an archetype for microbial iron transport. *Proc Natl Acad Sci U S A* **100**: 3584-3588.

Sabri, M., M. Caza, J. Proulx, M. H. Lymberopoulos, A. Bree, M. Moulin-Schouleur, R. Curtiss, 3rd & C. M. Dozois, (2008) Contribution of the SitABCD, MntH, and FeoB metal transporters to the virulence of avian pathogenic *Escherichia coli* O78 strain chi7122. *Infect Immun* **76**: 601-611.

Sakaitani, M., F. Rusnak, N. R. Quinn, C. Tu, T. B. Frigo, G. A. Berchtold & C. T. Walsh, (1990) Mechanistic studies on trans-2,3-dihydro-2,3-dihydroxybenzoate dehydrogenase (Ent A) in the biosynthesis of the iron chelator enterobactin. *Biochemistry* **29**: 6789-6798.

Schmittgen, T. D., B. A. Zakrajsek, A. G. Mills, V. Gorn, M. J. Singer & M. W. Reed, (2000) Quantitative reverse transcription-polymerase chain reaction to study mRNA decay: comparison of endpoint and real-time methods. *Anal Biochem* **285**: 194-204.

Vinella, D., C. Albrecht, M. Cashel & R. D'Ari, (2005) Iron limitation induces SpoT-dependent accumulation of ppGpp in *Escherichia coli*. *Mol Microbiol* **56**: 958-970.

Winkelmann, G., A. Cansier, W. Beck & G. Jung, (1994) HPLC separation of enterobactin and linear 2,3-dihydroxybenzoylserine derivatives: a study on mutants of *Escherichia coli* defective in regulation (fur), esterase (fes) and transport (fepA). *Biometals* **7**: 149-154.

Zhu, M., M. Valdebenito, G. Winkelmann & K. Hantke, (2005) Functions of the siderophore esterases IroD and IroE in iron-salmochelin utilization. *Microbiology* **151**: 2363-2372.

Table 1: Bacterial strains and plasmids used for this study

Bacterial strain and plasmid	Genotype	Source
	Bacterial strains	
χ7122	Avian pathogenic *E. coli*, O78 :K80 :H9, *gyrA*, Nal^r	(Provence & Curtiss, 1992)
QT1179	χ7122 Δ*iroE*::*cat*, Nal^r, Cm^r	This study
QT1198	χ7122 Δ*fes*::*FRT*, Nal^r	This study
QT1206	χ7122 Δ*fes*::*FRT* Δ*iroE*::cat, Nal^r, Cm^r	This study
QT1448	χ7122 Δ*iroD*, Nal^r	This study
QT1967	χ7122 Δ*fes*::*FRT* Δ*iroD*, Nal^r	This study
QT2083	χ7122 Δ*iroD* Δ*iroE*, Nal^r	This study
QT2084	χ7122 Δ*fes*::*FRT* Δ*iroD* Δ*iroE*, Nal^r	This study
	Plasmids	
pMEG-375	*sacRB mobRP4 ori*R6K. Cm^r, Ap^r	Megan Health (St. Louis, MO)
pACYC184	p15A replicon cloning vector, Cm^r, Tc^r	(Chang & Cohen, 1978)
pKD46	Lambda-Red recombinase plasmid Ts replicon, Ap^r	(Datsenko & Wanner, 2000)
pCP20	FLP helper plasmid Ts replicon, Cm^r, Ap^r	(Datsenko & Wanner, 2000)
pKD4	Template plasmid for amplification of *kan* bordered by *FRT* sites	(Datsenko & Wanner, 2000)
pIJ48	*iroDE* with p*iroB* of χ7122 cloned into pACYC184	This study
pIJ52	*iroD* with p*iroB* of χ7122 cloned into pACYC184	This study
pIJ54	*iroE* with p*iroB* of χ7122 cloned into pACYC184	This study
pIJ285	*fes* from χ289 cloned into pACYC184	This study
pIJ304	*fes* S255A from pIJ285	This study
pIJ311	*iroD* S291A from pIJ52	This study
pYA3661 or pIJ20	*iroBCDEN* from χ7122 cloned into pACYC184	(Dozois et al., 2003)
pIJ135	*iroBCN* from χ7122 cloned into pACYC184	(Caza et al., 2008)
pIJ136	*iroBCEN* from χ7122 cloned into pACYC184	(Caza et al., 2008)
pIJ137	*iroBCDN* from χ7122 cloned into pACYC184	(Caza et al., 2008)

Table 2: Primers used in this study

Primer	Sequence
CMD252	5'-CCAGTAAGCTTCCAGCCACTGCTGGCAGGA-3'
CMD253	5'-GGATGAAGCTTCTTGTTCATTGTTTTATTC-3'
CMD526	5'-ATGTATGCCCGCGAGTATCGCTCAACACGCCCGCATAA AGCGATTTTCTTTCCGTGTAGGCTGGAGCTGCTTC-3'
CMD527	5'-TTAGTGGCTTAACTCATGACAACCTGCTGTGTAATTTGC GTTTTCACCACTGCATATGAATATCCTCCTTAG-3'
CMD773	5'-ATTCTGCATCTAGACCTCCTATGCCGCTGT-3'
CMD774	5'-CATCATTCTAGACGTAGTGTTTCAGGC-3'
CMD75	5'-CGCTCGAGAAAATCCCTCTCCGCTTGA-3'
CMD76	5'-ACCTCGAGATAGTTACTGGACACGTAA-3'
CMD79	5'-GTTTACTCGAGGGTTGAGTTGACCCAC-3'
CMD62	5'AGAAGCTTTGTTGCGGCCACAGAC-3'
CMD63	5'-ACAAGCTTTACACTTTCGCCCGT-3'
CMD1090	5'-GCCGGGCAGGCTTTTGGTGGGCTGTCCG-3'
CMD1091	5'-CGGACAGCCCACCAAAAGCCTGCCCGGC-3'
CMD1092	5'-GCTGGCCGGGCAGGCCCTCGGCGGGATCAG-3'
CMD1093	5'-CTGATCCCGCCGAGGGCCTGCCCGGCCAGC-3'
CMD81	5'-TCAGAGCAAGAGATTACGCGCAGAC-3'
CMD83	5'-GTCCATTCCGACAGCATCGCCAGTCACT-3'
CMD1040	5'-GCCCGGCTCCAGCGGCCGCGACGCAACGCGG-3'

Real-Time - PCR Primer	Sequence
CMD958	5′-GAGAGAAGGCCCGAGCGTAAACGTCTGCTG-3′
CMD959	5′-TGGCAGAATCCATAACCCAGGCGATTAGAT-3′
CMD960	5′-GATCTGGCATCGTTTCTGGTTATCGCACAG-3′
CMD961	5′-CCGTCCCGTCCTCCATCTGTGAACGGGTGT-3′
CMD962	5′-CGACGCTTATCGCGGTTCCACTCTGCACCAA-3′
CMD963	5′-CTGAGTTCCTGGCGAACCAGCGGCGAGCTT-3′
CMD964	5′-CGCTGGTGGCAGAACAAGCGGCAAAAACA-3′
CMD965	5′-CAGATTCGCCAGCGCCACCACCTGCTCGC-3′
CMD966	5′-AATGGGACGAAGTTGGTGTTGACGTTGTCG-3′
CMD967	5′-ACTTTCTTCGCACCAGCGGTGATGTGTTTA-3′

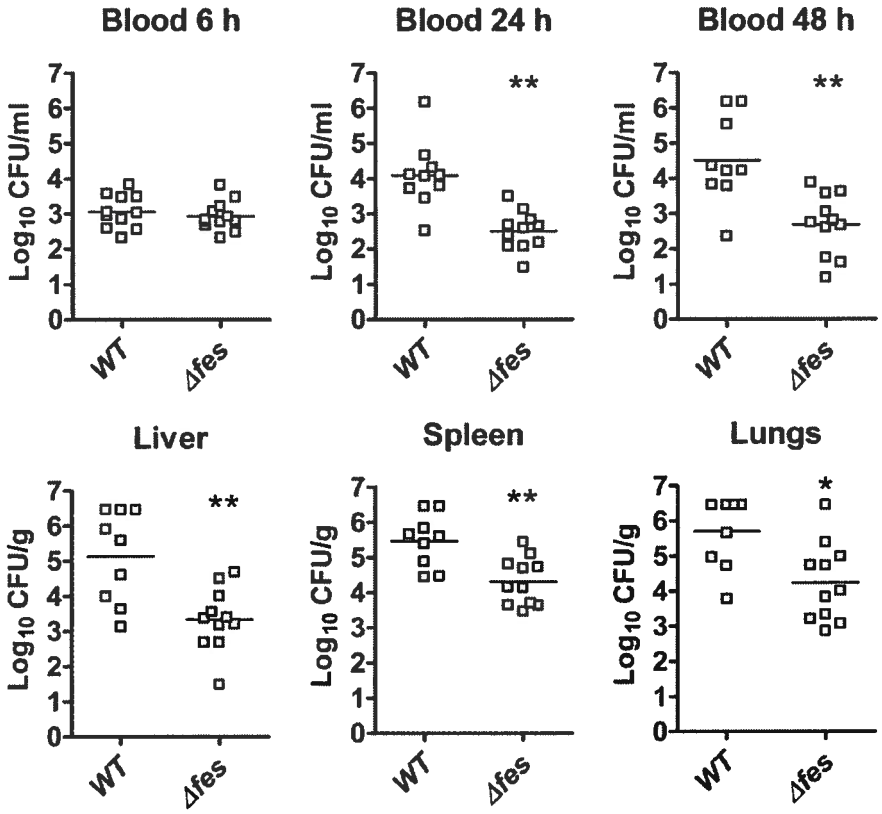

Figure 1: Bacterial numbers present in the blood and deeper tissues of infected chickens. Data points represent bacterial counts from different chickens (n = 9 to 11). Horizontal bars represent the median bacterial CFU. Statistical differences compared with wild-type strain are noted: * $P < 0.05$ and ** $P < 0.001$, using the two-tailed Mann-Whitney test.

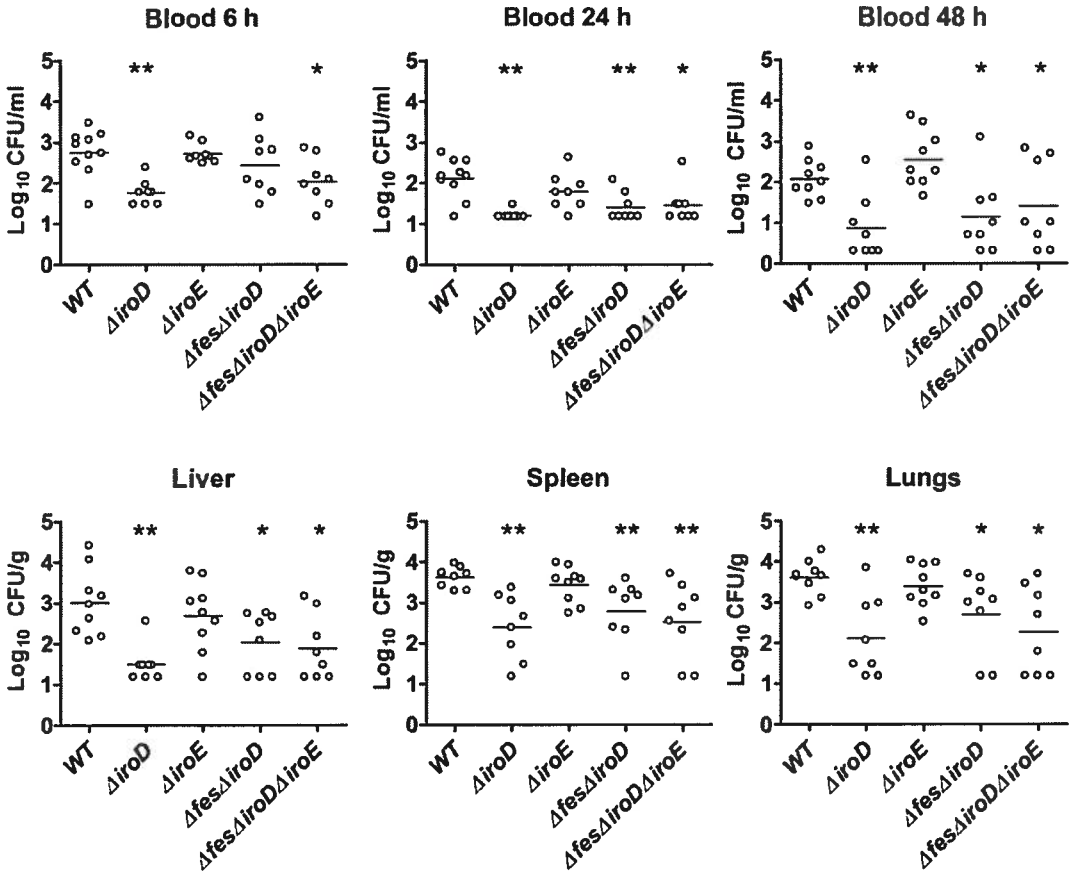

Figure 2: Bacterial numbers present in the blood and deeper tissues of infected chickens. Data points represent bacterial counts from different chickens (n = 8 to 10). Horizontal bars represent the median bacterial CFU. Statistical differences compared with wild-type strain are noted: * $P < 0.05$ and ** $P < 0.001$, using the two-tailed Mann-Whitney test.

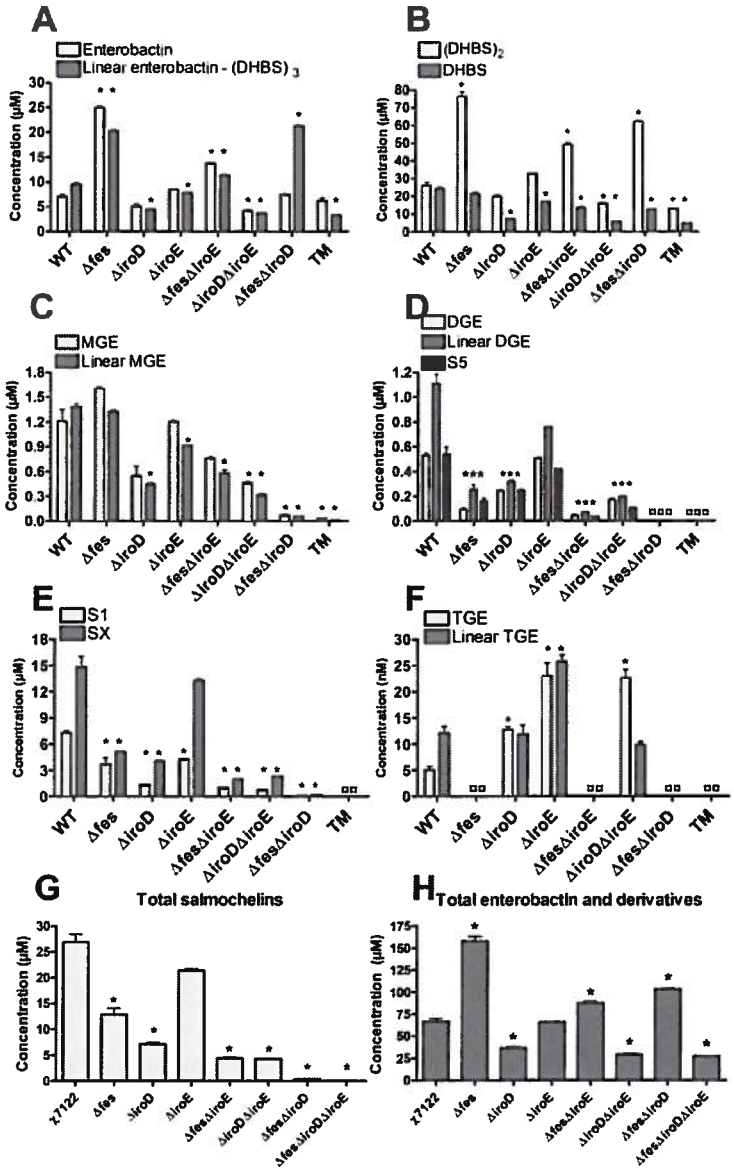

Figure 3: Mean concentrations of catecholate siderophores in supernatants of strains grown in M63-glycerol for 17h at 37°C. The amount of each molecule was normalized with the internal standard of 5,6,7,8-tetradeutero-3,4-dihydroxy-2-heptylquinoline. Error bars represent the standard errors of the means of biological triplicates. Statistical differences compared with wild-type strain are noted: * $P < 0.01$ using a two-tailed unpaired *t* test. ¤ indicates that molecules were not detected.

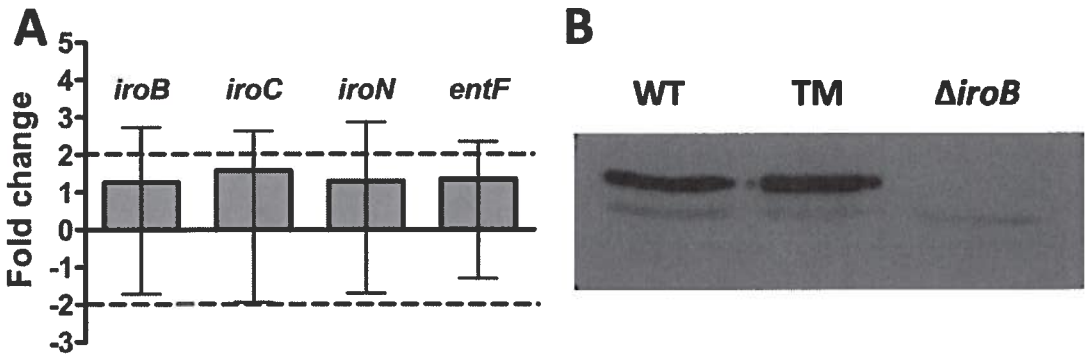

Figure 4: A) Fold-change of expression of *iroBCN* and *entF* from wild-type strain χ7122 and Δ*fes*Δ*iroD*Δ*iroE* triple esterase mutant (TM) grown in M63-glycerol as determined by real-time PCR. Errors bars represent standard deviations of the mean of biological triplicates. B) Western blot against IroB on total cell lysates of χ7122, Δ*fes*Δ*iroDE* triple esterase mutant (TM) and a Δ*iroB* mutant, used as a negative control.

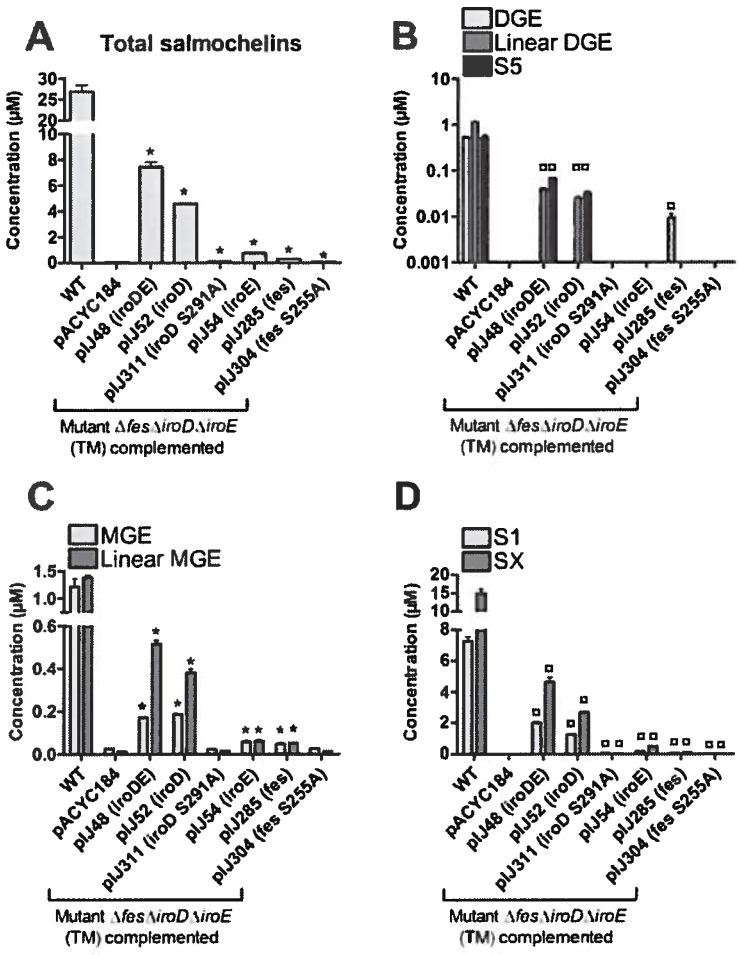

Figure 5: Mean concentrations of salmochelins in culture supernatants of the Δ*fes*Δ*iroD*Δ*iroE* triple esterase mutant (TM) complemented with empty vector (pACYC184) or with plasmids encoding functional *iroD* (pIJ52) or *fes* (pIJ285) and active site mutated *iroD* S291A (pIJ311) and *fes* S255A (pIJ304). The amount of each molecule was normalized with the internal standard of 5,6,7,8-tetradeutero-3,4-dihydroxy-2-heptylquinoline. Error bars represent the standard errors of the means of biological triplicates. Statistical differences compared with the triple mutant complemented with pACYC184 strain are noted: * $P < 0.01$ using a two-tailed unpaired *t* test. ¤ indicates that molecules were detected in the complemented mutant but absent in TM (pACYC184).

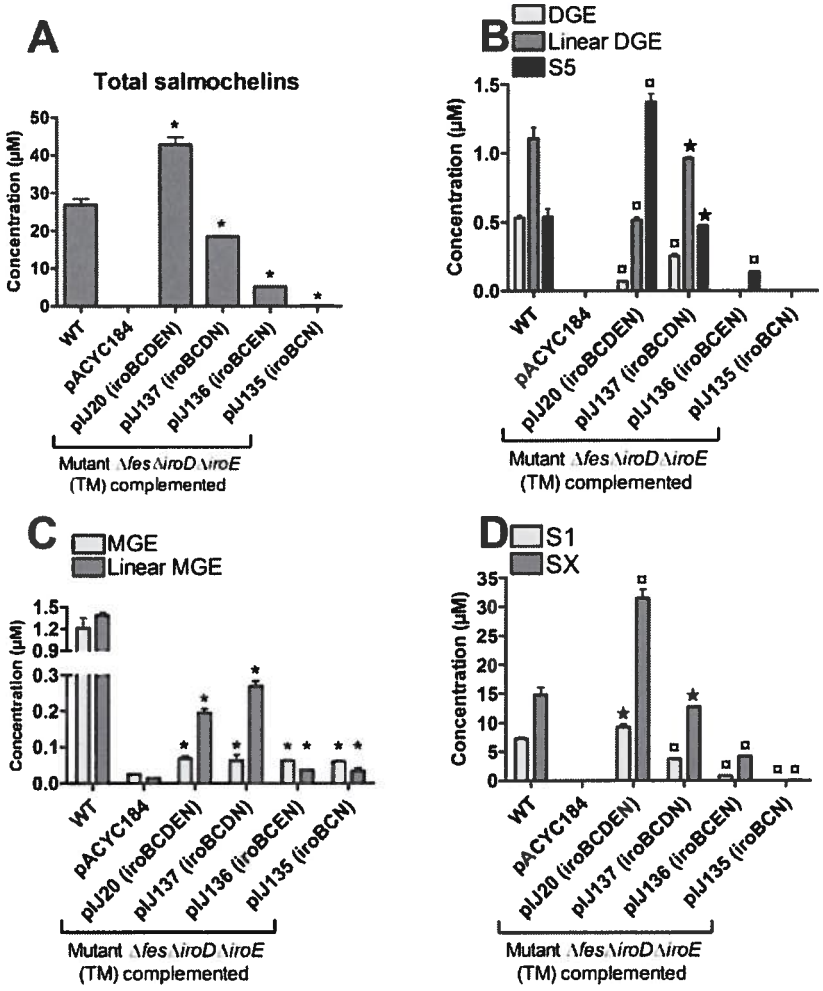

Figure 6: Mean concentrations of salmochelins in culture supernatants of the Δ*fes*Δ*iroD*Δ*iroE* triple esterase mutant (TM) complemented with empty vector (pACYC184) or with plasmids encoding the iroA cluster and derivatives. The amount of each molecule was normalized with the internal standard of 5,6,7,8-tetradeutero-3,4-dihydroxy-2-heptylquinoline. Error bars represent the standard errors of the means of biological triplicates. Data noted ★ indicates concentration of salmochelin is similar to the wild-type and that there are no statistical differences. Statistical differences compared with triple mutant complemented with pACYC184 strain are noted: * $P < 0.01$ using a two-tailed unpaired *t* test. ¤ indicates that molecules were detected in complemented mutant but absent in TM (pACYC184).

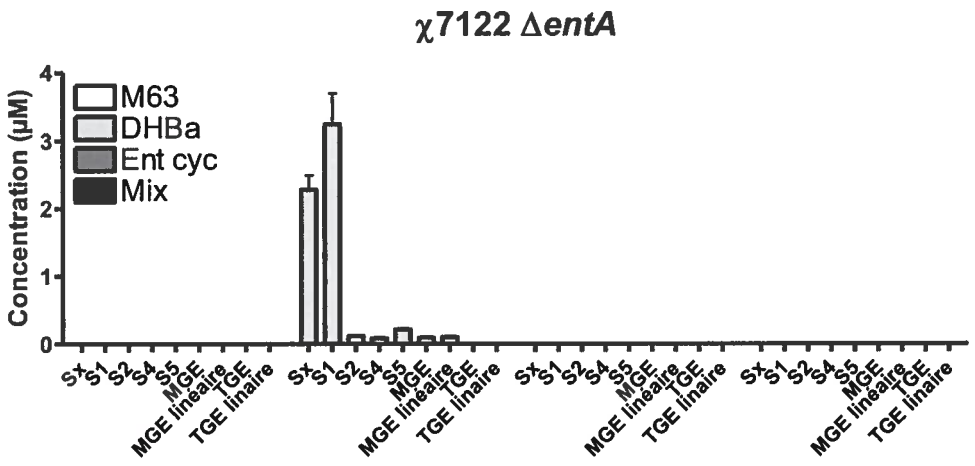

Supplemental figure 1 : Quantification of salmochelins by LC-MS/MS in supernatant of an Δ*entA* mutant grown in iron poor M63-glycerol with addition of either DHBa (33 µM), purified enterobactin (33 µM) or a mix of purified enterobactin related compound (33 µM). Biological triplicates was assessed.

Résultats supplémentaires

1) Le taux relatif de glucosylation de l'entérobactine chez les entérobactéries.

Puisque l'importance des transporteurs IroC et EntS pour la virulence des souches ExPEC aviaire χ7122 et *S.* Typhimurium 14028s est différent, une hypothèse suggéré dans l'article portant sur la sécrétion des sidérophores catécholates présenté dans cette thèse (page 95-139) fut que le taux relatif de glucosylation de l'entérobactine peut varier entre les deux souches. La quantification par LC-MS/MS des différentes molécules a été réalisée pour plusieurs autres entérobacties afin de valider cette hypothèse. Le taux relatif de glucosylation de l'entérobactine varie effectivement entre les souches ExPEC et *S. enterica*. En fait, les sidérophores catécholates de la souche ExPEC χ7122 sont peu ou pas glucosylés, puisque 21,3 % des molécules totales ne sont pas glucosylées, 2,6 % des molécules possèdent seulement un glucose et seulement 1,2 % des molécules sont di-glucosylées (Tableau 1). Or, cette quantification relative n'est pas conservée parmi les souches, puisque la souche ExPEC CP9 et les souches de *S.* Typhimurium, *S.* Stanleyville et *S.* Cholerasuis sécrètent plus de salmochélines di-glucosylées que de mono-glucosylée (Tableau 1). Ceci suggère que le taux de glucosylation de l'entérobactine est spécifique à la bactérie et que l'opéron encodant les gènes *iroBCDE* est probablement régulé différemment chez ces bactéries.

Tableau 1 : Taux relatif moyen (%) des molécules non-, mono- et di-glucosylées par rapport à la concentration totale des sidérophores catécholates sécrétées par la souche*.

Souches	Ent/Ent linéaire	MGE/MGE linéaire	DGE/DGE linéaire
***E. coli* (ExPEC)**			
χ7122	21.3 ± 2.9	**2.6 ± 0.9**	1.2 ± 0.4
CFT073	9.7 ± 2.3	1.7 ± 0.1	1.7 ± 0.04
CP9	9.0 ± 0.9	1.5 ± 0.1	**2.4 ± 0.1**
536	11.1 ± 1.1	**2.0 ± 0.2**	1.3 ± 0.2
***S.* Typhimurium**			
SR-11	7.9 ± 2.2	1.3 ± 0.01	**2.9 ± 0.2**
UK1	13.1 ± 2.4	1.8 ± 0.1	**3.3 ± 0.2**
LT2	8.3 ± 2.4	1.4 ± 0.1	**2.7 ± 0.1**
S. Stanleyville	6.8 ± 2.4	1.6 ± 0.2	**2.6 ± 0.1**
S. Cholerasuis	16.9 ± 2.8	2.6 ± 0.004	**3.2 ± 0.1**

* Les salmochélines TGE et TGE linéaire représentent moins de 0.1 % des sidérophores de type catécholate sécrétés par les souches après 17 h de culture en M63-glycérol à 37°C. Toutes les souches cultivées dans le M63-glycérol ont atteint la phase stationnaire et présentaient un DO_{600nm} d'au moins 1.0 après 17h de culture. Les analyses ont été réalisés tels que décrite dans Caza et al. [98].

2) TolC est impliqué dans la sécrétion de sidérophores catécholates

Pendant l'étude sur la sécrétion des sidérophores catécholates de la souche χ7122, une étude publié par Bleuel et ses collaborateurs [197] a rapporté que chez la souche *E. coli* W3110 non-pathogène, la sécrétion de l'entérobactine à travers les deux membranes était réalisé d'abord par le transporteur de la membrane interne EntS et ensuite par la protéine tunnel de la membrane externe TolC [197]. L'analyse des surnageants de culture par HPLC a démontré qu'un mutant Δ*fur*Δ*tolC* ne sécrète plus autant d'entérobactine cyclique qu'un mutant Δ*fur*, bien qu'il sécrète relativement autant de monomère, dimère et trimère de DHBS [197]. Ainsi, la délétion du gène *tolC* chez χ7122 a été réalisée par la

méthode développée par Datsenko et Wanner [334]; et la quantification des sidérophores catécholates sécrétées a été exécutée par LC-MS/MS selon la méthode décrite dans Caza et al.[98].

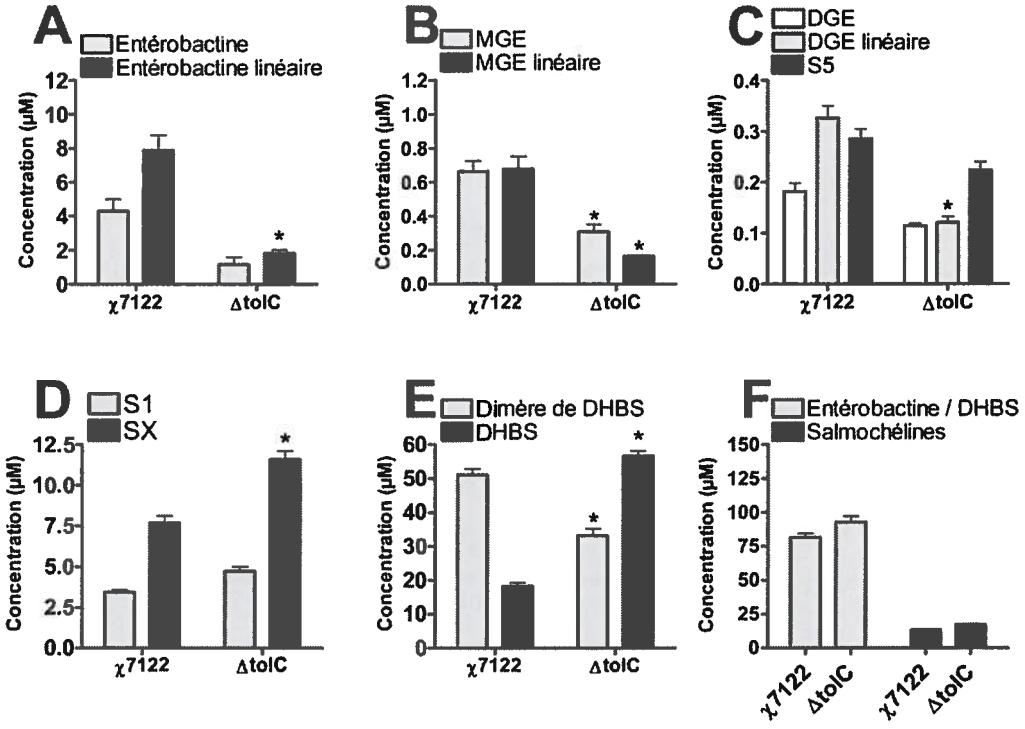

Figure 1 : Concentrations moyennes des sidérophores catécholates des souches χ7122 et du mutant Δ*tolC* cultivées dans le milieu M63-glycérol pendant 17h à 37°C. La barre d'erreur représente l'erreur standard de la moyenne des triplicatas biologiques. Les différences statistiques par rapport à la souche sauvage χ7122 sont notées : * $P < 0.01$ selon le test *t* bilatéral non-apparié.

Les résultats de la figure 1 démontrent que la perte de la protéine TolC chez χ7122 diminue les concentrations d'entérobactine, d'entérobactine linéaire, de salmochéline MGE et MGE linéaire et DGE linéaire détectés dans le surnageant de culture (Figure 1 A, B et C). Par contre, les molécules de dimère et monomère de DHBS, ainsi que la salmochéline SX (Figure 1 D et E) sont retrouvées en plus grande quantité dans le surnageant de ce mutant, de façon à ce qu'au total, les concentrations des sidérophores

catécholates ne sont pas affectées par la perte de TolC (Figure 1 F). Ces données suggèrent que TolC participe à la sécrétion des molécules catécholates nécessitant déjà un transport facilité par EntS et IroC, tel que démontré dans le deuxième article de ce document (page 95-139).

3) Le système de transport de type ABC des sidérophores catécholates

Suite à la synthèse et à la sécrétion, les sidérophores complexés à des atomes de fer, doivent être internalisés par la bactérie pour que cette dernière acquière les quantités de fer nécessaire à sa croissance et prolifération. Un transporteur de type ABC spécifique, comprenant un récepteur et un transporteur de la membrane interne, est requis pour l'internalisation des sidérophores. Puisque le récepteur des salmochélines, IroN, a été caractérisé au même moment que la découverte des salmochélines [24] et qu'il est un facteur de virulence de la souche UPEC CP9 [259], la caractérisation du récepteur IroN chez χ7122 a été réalisée brièvement. Un mutant Δ*iroN* a été réalisé dans la souche χ7122 par la méthode décrite par Datsenko et Wanner [334]. La quantification des sidérophores catécholates dans le surnageants du mutant Δ*iroN* a seulement révélé une augmentation significative de l'entérobactine (Figure 2 C), suggérant que ce dernier est moins bien internalisé par la bactérie en absence du récepteur IroN. La concentration des autres molécules n'est pas altérée par l'absence de IroN.

Suite à l'internalisation des sidérophores par le récepteur de la membrane externe, le transport du complexe fer-sidérophore jusqu'au cytoplasme bactérien nécessite un transporteur de la membrane interne spécifique. Il est connu que le transport du périplasme au cytoplasme de l'entérobactine est assuré par le complexe FepDGC [220, 221] et puisqu'aucun gène *iro* ne semblait coder pour un transporteur de la membrane interne, il fut donc logique de vérifier si le transporteur de l'entérobactine sert aussi au transport des salmochélines. Ainsi, une mutation dans le gène *fepC* fut réalisée par la méthode décrite par Datsenko et Wanner [334]. L'analyse en LC-MS/MS du surnageant de culture de la souche mutante Δ*fepC* démontre une diminution des molécules non-, mono- et di-glucosylées, ainsi que leurs formes linéaires (Figure 2 A, B et C), et une

augmentation des molécules de dégradations, telles que le monomère et dimère de DHBS et les salmochélines S1 et SX (Figure 2 D et E), ce qui contribue à l'augmentation générale de la concentration totale des salmochélines dans le surnageant de culture (Figure 2 F). De plus, l'élimination de l'hydrolase périplasmique IroE chez le mutant Δ*fepC* augmente la concentration extracellulaire des molécules d'entérobactine, MGE et MGE linéaire par rapport au mutant Δ*fepC*, ainsi qu'un rétablissement des concentrations des molécules di-glucosylées et dégradées à des niveaux similaires à la souche sauvage (Figure 2 A, B, C, D et E). Au total, cette mutation supplémentaire a diminué la concentration des molécules d'entérobactine, mais rétabli la concentration des salmochélines (Figure 2 F).

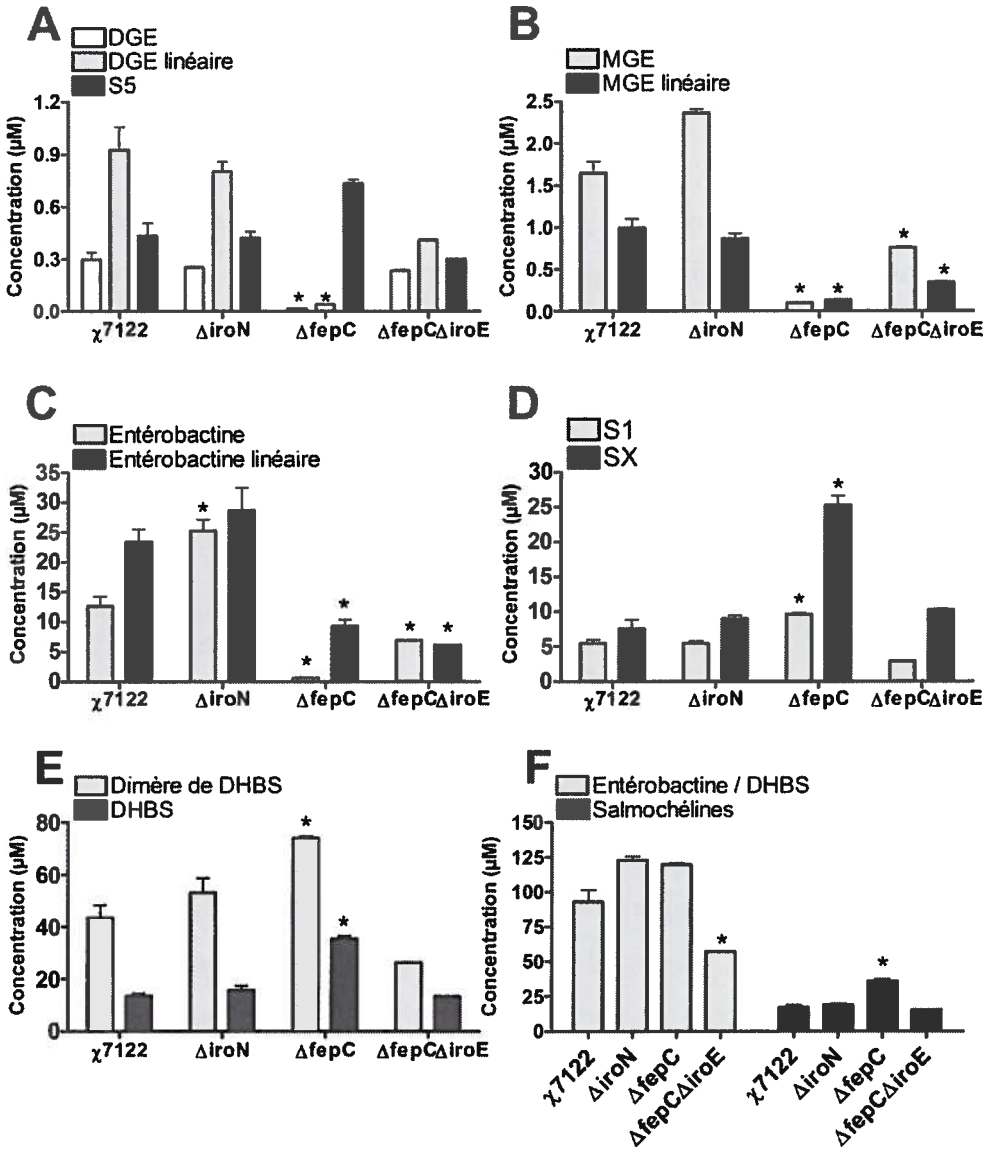

Figure 2 : Concentrations moyennes des sidérophores catécholates des souches χ7122 et dérivées isogéniques cultivées dans le milieu M63-glycérol pendant 17h à 37°C. La barre d'erreur représente l'erreur standard de la moyenne des triplicatas biologiques. Les différences statistiques par rapport à la souche sauvage χ7122 sont notées : * $P < 0.01$ selon le test *t* bilatéral non-apparié.

4) La croissance des bactéries mutantes pour les estérases *fes*, *iroD* et *iroE* en présence de conalbumine.

La croissance des souches mutantes pour la dégradation des sidérophores catécholates a été mesurée en milieu minimal M63 en présence et absence de conalbumine, qui est une protéine aviaire de haute affinité pour le fer, servant ici de chélateur de fer du milieu de culture (Figure 3) [8]. Les différents mutants de dégradation (Δ*fes*, Δ*iroD*, Δ*iroE*) individuels ou en combinaison, ainsi que mutant de synthèses des sidérophores catécholates et aérobactine (Δ*entD*Δ*iro*Δ*iuc*) ne présentent pas de défaut majeur de croissance en milieu minimal M63-glycérol (Figure 3 A et C). Il est à noter que les courbes des souches possédant une mutation Δ*iroE* ne sont pas présentées dans la figure 3 A et B, puisque cette mutation n'a aucun effet sur la croissance de toutes les différentes souches mutantes dans le milieu M63-glycérol avec ou sans conalbumine. Par exemple, un double mutant Δ*iroD*Δ*iroE* présente une courbe identique au mutant Δ*iroD*. Par ailleurs, l'ajout de conalbumine empêche la croissance du triple mutant de synthèse des sidérophores (Δ*entD*Δ*iro*Δ*iuc*) et diminue grandement celle du mutant Δ*fes*Δ*iroD* (Figure 3 B et D). Bien que le système de l'aérobactine soit toujours fonctionnel chez cette souche, la mutation des estérases Fes et IroD cause un délai de croissance considérable. Ce délai est toutefois levé s'il y a inhibition de la synthèse des sidérophores catécholates par l'introduction d'une mutation du gène *entA* chez la souche Δ*fes*Δ*iroD* (Figure 3 B). Bien que les salmochélines ne soient pas synthétisées chez le mutant Δ*fes*Δ*iroD*, cette absence de synthèse des salmochélines n'est pas attribuable au délai de croissance observé du mutant Δ*fes*Δ*iroD*, puisqu'un mutant Δ*iroA* ne présente pas de délai de croissance en présence de conalbumine (Figure 3 D).

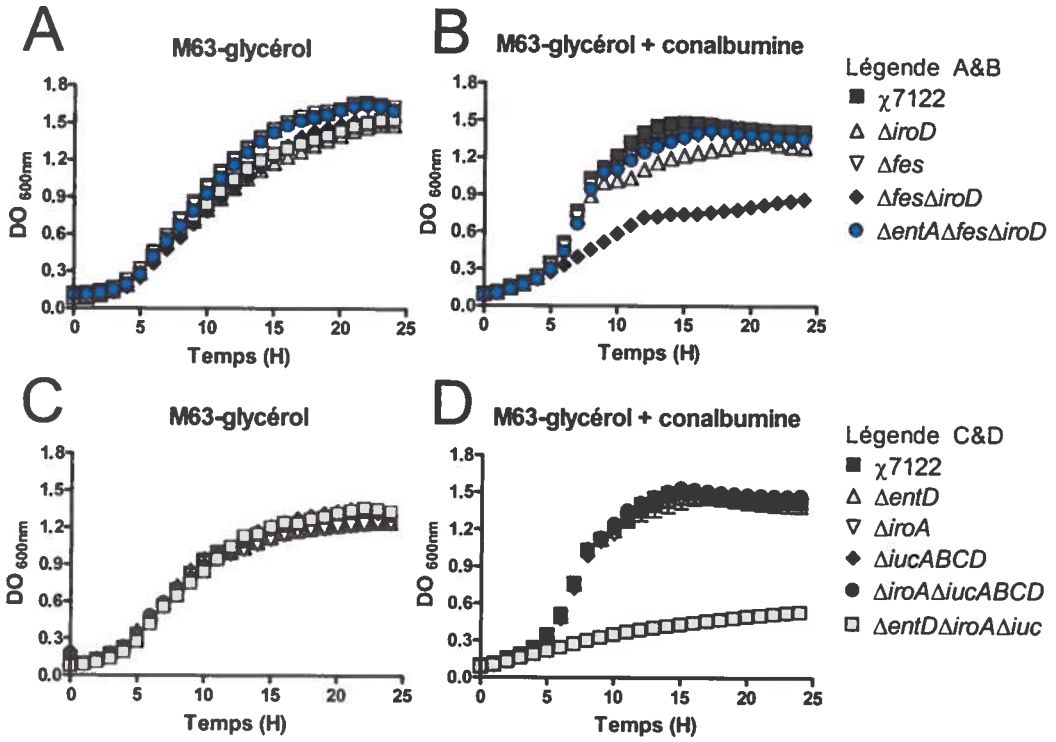

Figure 3 : Courbes de croissance des souches χ7122, des mutants de dégradation (Δ*fes* et/ou Δ*iroD*) (A et B) et des mutants de synthèse des sidérophores (Δ*entD*, Δ*iroA* et/ou Δ*iucABCD*) (C et D) effectuées à 37°C avec agitation dans le milieu minimal M63-glycérol avec ou sans 1mg/ml conalbumine. La densité optique a été mesurée sur des triplicatas biologiques à 600nm en utilisant un Bioscreen C.

5) La quantification relatives des sidérophores catécholates, aérobactine et yersiniabactine chez les entérobactéries pathogènes

Lors de l'étude du locus *iroA* chez la souche χ7122, nous avons développé une méthode de quantification des sidérophores catécholates, ainsi que l'aérobactine par chromatographie liquide couplée à la spectrométrie de masse. Cette méthode a par la suite été modifiée pour y ajouter la détection de la yersiniabactine. Cet ajout a été réalisé à la suite d'une collaboration avec le Dr. Michael Bachman du laboratoire du Dr. Jeffrey Weiser de l'Université de Pennsylvanie. Ces derniers travaillent sur la relation entre les sidérophores produits par des souches de *Klebsiella pneumoniae* pathogènes et leurs

séquestrations par le NGAL retrouvé dans le tractus respiratoire humain et murin [25]. Cette collaboration a mené à l'élaboration d'un manuscrit en préparation (Annexe IV).

Brièvement, la yersiniabactine est un sidérophore de type phénolate d'abord caractérisé chez *Yersinia enterocolitica* et ensuite retrouvé chez plusieurs entérobactéries dont *Yersinia pestis*, *Yersinia pseudotuberculosis*, *Klebsiella pneumoniae* et *E. coli* [335-338]. La production de ce sidérophore, qui possède une affinité pour le fer ferrique de l'ordre de ~ $4X10^{36}$ M^{-1}, est encodé par quatre opérons qui font partie de l'îlot de haute pathogénicité (High-pathogenicity island ou HPI) retrouvé chez les souches de *Yersinia* hautement pathogène [339, 340]. En fait, ces quatre opérons codent pour la biosynthèse (*irp1*, *irp2*, *ybtETU*), le transport (*ybtSXQP, fyuA*) et la régulation de la yersiniabactine (*ybtA*) [123, 336]. De plus, les gènes de synthèse ou de transport de la yersiniabactine sont requis pour la virulence de *Y. pestis* [142, 341], des souches ExPEC [97] et *K. pneumonia* [25, 338].

La détection de la yersiniabactine se fait en enregistrant les ions de transitions spécifiques de l'ion pseudomoléculaire à l'ion fille 482>295 *m/z*. Aussi, l'acide formique n'a pas été ajouté aux échantillons des souches de *Klebsiella* afin de prévenir la dégradation de la yersiniabactine. Puisque les molécules d'aérobactine et de yersiniabactine n'ont pas été purifiées, seule la distribution relative et la quantification arbitraire par le biais de l'aire sous la courbe déterminé par l'appareil de spectrométrie de masse sont utilisées pour comparer les quantités de chacun des sidérophores produits.

Ainsi, la distribution relative des sidérophores à partir de surnageants de culture de plusieurs souches ExPEC, *S. enterica* et de *K. pneumoniae* a été réalisée (Tableau 2). Les souches cliniques de *Klebsiella pneumoniae* provenant du tractus urinaire (KP33-36), respiratoire (KP30, KP56-58) et gatro-intestinal (KP102, KP76-78) possèdent une diversité de systèmes de sidérophores et une variabilité de production relative. Certaines souches, dont KP102 et KP78, synthétisent à la fois les quatre sidérophores à l'étude, mais dans des proportions très différentes (Tableau 2).

Tableau 2 : Quantification relative des sidérophores (%) produits par différentes entérobactéries cultivées dans le milieu minimal M63-glycérol à 37°C pendant 17h

Bactérie	Entérobactine	Salmochélines	Aérobactine	Yersiniabactine
Escherichia coli				
χ7122	69.0 ± 2.2	23.4 ± 1.9	7.7 ± 0.4	-
CFT073	53.4 ± 2.1	37.1 ± 1.5	9.0 ± 2.2	-
CP9	55.5 ± 1.4	44.5 ± 1.4	-	-
536	21.0 ± 0.6	31.7 ± 0.8	-	47.3 ± 1.4
Salmonella enterica				
S. Typhimurium UK1	55.2 ± 2.0	44.8 ± 2.0	-	-
S. Typhimurium SR11	50.6 ± 1.5	49.4 ± 1.5	-	-
S. Typhimurium LT2	50.2 ± 2.8	49.8 ± 2.8	-	-
S. Stanleyville	55.8 ± 1.3	44.2 ± 1.3	-	-
S. Cholerasuis	60.7 ± 1.8	39.3 ± 1.8	-	-
S. Typhi χ3744	100 ± 0	0 ± 0	-	-
S. Typhi Ty2	95.8 ± 0.8	4.2 ± 0.8	-	-
S. Typhi SARBB63	84.6 ± 2.2	15.4 ± 2.2	-	-
S. Typhi SARBB64	92.6 ± 1.0	7.4 ± 1.0	-	-
S. Paratyphi A	99.6 ± 0.02	0.4 ± 0.02	-	-
Klebsiella pneumoniae				
KPPR1	39.3 ± 3.6	40.8 ± 3.8	-	20.0 ± 7.3
KP33	58.8 ± 5.3	-	-	41.2 ± 5.3
KP34	74.4 ± 4.5	0.2 ± 0.02	-	25.4 ± 4.5
KP35	100 ± 0	-	-	-
KP36	100 ± 0	-	-	-
KP30	100 ± 0	-	-	-
KP56	100 ± 0	-	-	-
KP57	92.4 ± 2.3	-	-	7.6 ± 2.3
KP58	100 ± 0	-	-	-
KP76	100 ± 0	-	-	-
KP77	100 ± 0	-	-	-
KP78	26.4 ± 1.4	9.6 ± 0.4	62.1 ± 1.3	1.9 ± 0.2
KP102	1.0 ± 0.2	0.2 ± 0.02	86.3 ± 3.6	12.5 ± 3.4

- : signifie que le sidérophore n'a été détecté dans le surnageant de culture. Toutes les souches ont atteints une DO d'au moins 1.0 après 17h de culture et les analyses ont été effectués selon Caza et al., 2008 [98]

Tel que décrit au tableau 2, les souches de *S.* Typhimurium testées produisent les sidérophores de type catécholates, soit l'entérobactine et les salmochélines, et ce, à des niveaux relatifs similaires. Cependant, il est intéressant de constater que l'expression des salmochélines chez les souches de *S.* Typhi et Paratyphi est relativement plus basse que chez les souches de *S.* Typhimurium. Pourtant, ces souches possèdent bel et bien le locus IroA fonctionnel, mais ce dernier semble être régulé différemment. D'ailleurs, l'ajout d'acides casaminés déferrés induit la synthèse de toutes les salmochélines chez la souche *S.* Typhi Ty2 sans affecter la production d'entérobactine, telle que le démontre la quantification extracellulaire des sidérophores catécholates de la souche cultivée en présence et en absence de acides casaminés déferés (Figure 4).

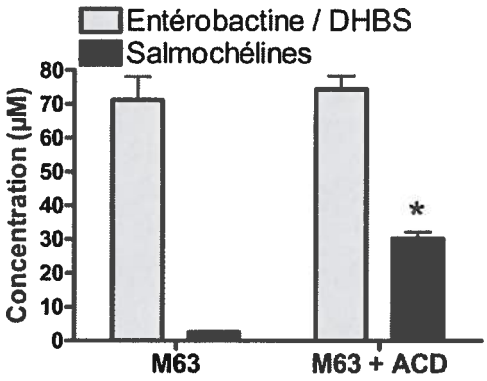

Figure 4 : Concentration (µM) de sidérophores catécholates produits par la souche S. Typhi Ty2 en milieu M63-glycérol en présence et absence d'acides casaminés déférés (ACD) (30µl/ml). Les différences statistiques entre la présence et l'absence d'acide casaminés déférés sont notées * ($P < 0.01$) selon le test *t* bilatéral et non-apparié. Les données présentent la moyenne et l'erreur standard de la moyenne de triplicatas biologiques.

Finalement, la production des sidérophores en présence de conalbumine a été quantifiée chez la souche χ7122 par LC-MS/MS. Les résultats démontrent que l'ajout de conalbumine au milieu de culture M63-glycérol augmente considérablement la synthèse de l'aérobactine et diminue celle des sidérophores catécholates (Figure 5).

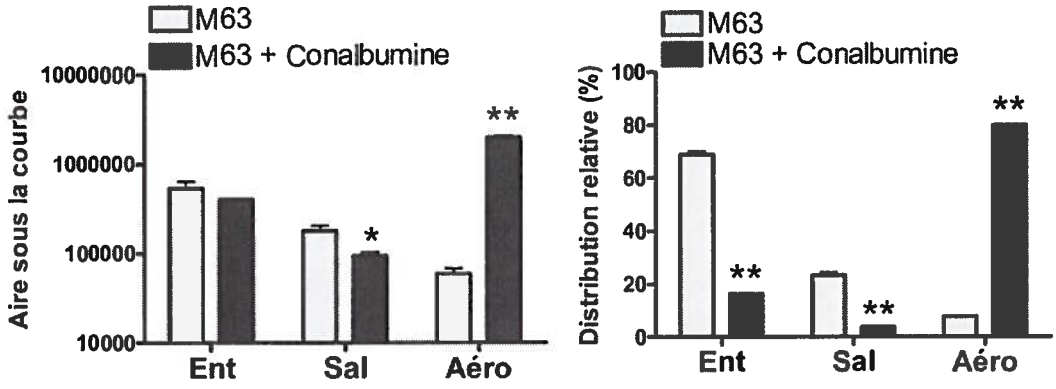

Figure 5 : Quantification arbitraire et relative de l'entérobactine (Ent) / DHBS, des salmochélines (Sal) et de l'aérobactine (Aéro) de la souche χ7122 cultivée en milieu M63-glycérol et en M63-glycérol + 1 mg/ml de conalbumine. Les différences statistiques entre la présence et l'absence de conalbumine pour chaque sidérophore sont notées * ($P < 0.05$), ** ($P < 0.01$) selon le test *t* bilatérale et non-apparié. Les données présentent la moyenne et l'erreur standard de la moyenne de triplicatas biologiques.

Discussion

1) La caractérisation des gènes iroBCDEN

L'étude des gènes *iroBCDEN* chez la souche pathogène aviaire χ7122 débuta par la découverte de l'ARNm du gène *iroC* exprimé lors d'une infection septicémique chez le poulet par la méthode de capture sélective de séquences transcrites (SCOTS) [16]. La découverte de ce gène bactérien transcrit *in vivo* mena à la délétion complète du locus *iroA*, ce qui atténua la virulence de la souche. De plus, les séquences des gènes *iutA* et *iucD*, qui font partie du locus *iucABCDiutA* codant pour l'aérobactine, furent également repêchées par la méthode SCOTS; et la délétion de ces gènes atténua également la virulence de la souche pathogène. Aussi, la délétion des deux loci affecta grandement le potentiel infectieux de la souche, puisque cette souche colonisa très faiblement les organes internes des animaux. Or, l'introduction d'un plasmide codant pour les gènes *iroBCDEN* dans la souche dont les locus *iroA* et *iucABCDiutA* furent mutés fut suffisante pour redonner à cette souche la capacité de coloniser le foie des animaux [16]. Ainsi, il fut démontré que les gènes *iroBCDEN* participaient à la virulence de la souche χ7122. Peu de temps après, on identifia les gènes *iroBCDEN* responsables de la synthèse (IroB) et du transport (IroN) des salmochélines chez *Salmonella* [24]. Cette découverte aida grandement à élucider le rôle de chacun des gènes *iroBCDEN* pour la synthèse, le transport et la dégradation des salmochélines.

L'étude de l'importance de chacun des gènes *iroBCDEN* pour la virulence de la souche χ7122 a été réalisée en utilisant l'approche de la complémentation plasmidique. L'insertion des diverses combinaisons de gènes *iro* sur des plasmides dans la souche atténuée n'exprimant plus l'aérobactine, ni les salmochélines a permis de mettre en lumière les rôles essentiels des gènes *iroBCDN* et ainsi de caractériser la fonction de chacun lorsque le locus est surexprimé.

1.1 La synthèse des salmochélines

Tout d'abord, la glucosyltransferase IroB est la seule enzyme responsable de l'ajout de glucoses sur les groupements catécholates de l'entérobactine, puisqu'une mutation du gène *iroB* abolit la formation de salmochéline et, par le fait même, atténue la virulence de

la souche lorsque celle-ci se retrouve chez le poulet. Ceci confirma l'importance de la glucolysation de l'entérobactine pour la virulence de la souche χ7122. De plus, lors d'une infection mixte avec la souche sauvage, le mutant Δ*iroB* survie aussi bien que la souche sauvage, suggérant que cette dernière fournit les salmochélines nécessaires à la survie de la souche mutante *in vivo*. Ceci démontra alors qu'une complémentation *in trans* des sidérophores peut avoir lieu lors d'une infection mixte. Par ailleurs, la surexpression d'*iroB* seul chez un mutant Δ*iroA* ne résulta pas en la détection de salmochéline dans les surnageants de culture; la combinaison minimale de gènes *iro* requise est composée des gènes *iroBC*.

Les études biochimiques publiées par le groupe du Dr. Christopher T. Walsh démontrent que IroB est la seule enzyme nécessaire à l'ajout de glucose sur l'entérobactine [244]. De plus, le seul substrat accepté par IroB est bel et bien l'entérobactine cyclique. Des essais de glucolysation à partir du DHBS purifié et de l'enzyme IroB purifié a démontré un piètre taux de glucosylation [244]. Des essais chez la bactérie à partir de DHBS purifié, d'entérobactine cyclique, de surnageant de culture et de co-cultures ont été aussi effectué par notre groupe et celui de Klaus Hantke [243] et ont tous démontré une impossibilité à produire des salmochélines, suggérant fortement que le substrat accepté par IroB est l'entérobactine cyclique.

Or, l'étude démontré dans le troisième article de ce document (page140-175) démontre que les estérases Fes et IroD sont également requises pour la production des salmochélines, puisque leur mutation affecte la détection des salmochélines dans les surnageants de culture. De plus, la réintroduction sur plasmide à copie multiple des gènes codant pour Fes et IroD a démontré un rétablissement partiel de la synthèse des salmochélines et un rétablissement quasi complet par l'introduction des gènes *iroBCDN* sur plasmide. Ceci suggère que le retour de la synthèse des salmochélines peut avoir lieu sans l'estérase Fes, si *iroB* et *iroD* sont exprimés en grande quantité sur le même plasmide et ce, à des niveaux similaires. De plus, le site actif d'*iroD* et *fes* semble nécessaire au processus de synthèse des salmochélines. Le rôle exact de ces deux

enzymes lors de la synthèse des salmochélines reste à élucider, toutefois, la formation d'un complexe IroB-IroD et/ou Fes est plausible.

1.2 La sécrétion de l'entérobactine et des salmochélines

Le gène *iroC* sembla d'abord essentiel pour la virulence de la souche χ7122, puisque la complémentation plasmidique avec les gènes *iroBDEN* fut insuffisante pour permettre à la souche Δ*iroA*Δ*iucABCD*Δ*iutA* à retrouver sa capacité virulente. Aussi, les analyses des surnageants de culture ont démontré une diminution significative de la sécrétion des salmochélines cycliques et linéaires chez cette souche; en plus d'augmenter grandement la quantité de monomères de salmochélines.

Une caractérisation plus exhaustive de la sécrétion des salmochélines par IroC et par EntS fut réalisée dans le cadre de la deuxième étude portant sur la sécrétion des sidérophores de types catécholates produits par la souche χ7122. L'approche utilisée dans cette étude fut de muter les gènes *iroC* et *entS*, afin de déterminer l'effet de leur perte sur la virulence de la souche ainsi que sur la sécrétion des sidérophores. Tel que démontré par Crouch et ses collaborateurs [223], IroC sécrète à la fois les salmochélines et l'entérobactine, tandis que EntS ne sécrète que l'entérobactine chez la souche *S.* Typhimurium 14028s [223]. Or, la distribution relative des sidérophores effectués dans leur étude ne porta que sur les salmochélines DGE, S1 et SX et sur les molécules d'entérobactine cyclique, du dimère et du monomère de DHBS sécrétés dans le milieu de culture [223]. La sécrétion des autres salmochélines, MGE, MGE linéaire, DGE linéaire, TGE, TGE linéaire et S5, ainsi que le trimère linéaire d'entérobactine, par EntS, IroC ou autre n'a pas été démontrée. Ainsi, lors de l'étude sur la sécrétion des sidérophores catécholates chez χ7122, la quantification de toutes les formes de salmochélines et entérobactine a été effectuée à partir des surnageants de cultures des souches mutantes, et ce, afin d'obtenir une meilleure compréhension des mécanismes de sécrétions de ces sidérophores. La quantification des sidérophores sécrétés dans le milieu de culture a d'ailleurs permis de démontrer que les molécules non- et mono-glucosylées sont transportées par EntS et que les di- et tri-glucosylées sont exportées par IroC.

Cette séparation moléculaire ajoute à la compréhension de l'importance des transporteurs pour la virulence de la souche χ7122. En effet, une mutation du gène *entS* affecte plus profondément la capacité infectieuse de la souche que la perte du transporteur IroC dans le modèle d'infection septicémique aviaire. Ceci est d'ailleurs contraire à ce qui a été trouvé par Crouch *et al.* [223] puisque, la virulence de *S.* Typhimurium est plus affectée en l'absence d'*iroC* que d'*entS*. Cette différence s'explique, d'abord par la nature des bactéries et des modèles animaux, mais aussi par le taux relatif de glucosylation de l'entérobactine qui varie entre les souches ExPEC et *S. enterica* (Section Résultat, Tableau I). Ceci suggère que le taux de glucosylation de l'entérobactine est spécifique à la bactérie et que l'opéron encodant les gènes *iroBCDE* est probablement régulé différemment chez ces bactéries. Ainsi, puisque le taux de glucosylation de l'entérobactine est différent à travers les souches pathogènes pour une même condition de croissance, l'importance des transporteurs EntS et IroC ou autres peut varier selon la prédominance des molécules synthétisées. Néanmoins, la sécrétion des molécules synthétisées est un élément commun pour la virulence des souches *E. coli* χ7122 et *S.* Typhimurium 14028s dans leur modèle d'infection animal respectif.

De plus, Bleuel et ses collaborateur on publié en 2005 une étude démontrant le rôle de TolC pour la sécrétion de l'entérobactine [197]. Ils ont démontré que chez *E. coli* W3110 non-pathogène que la sécrétion de l'entérobactine à travers les deux membranes était probablement un processus réalisé en deux étapes, dont la première nécessitait le transporteur EntS et la deuxième, la protéine tunnel de la membrane externe TolC [197]. L'évaluation du rôle de TolC pour la sécrétion des sidérophores catécholates par la souche χ7122 a donc été réalisée. Les résultats obtenues par l'analyses du surnageant de culture par LC-MS/MS d'un mutant Δ*tolC* de χ7122 suggèrent que TolC joue est requis pour la sécrétion des molécules cycliques et linéaires, tels que l'entérobactine, les salmochélines MGE et DGE, ainsi que leurs formes trimériques linéaires (Section Résultat, Figure 1). Cependant, le mécanisme exact de la sécrétion des sidérophores catécholates par le biais de EntS-TolC et de IroC-TolC restent encore à démontrer à ce jour.

1.3 L'internalisation des sidérophores catécholates par IroN et FepDGC

Tel que démontré dans le premier article de cette thèse (p53-94), la complémentation de la souche Δ*iroA*Δ*iucABCD*Δ*iutA* avec le plasmide codant pour les gènes *iroBCDE* n'est pas suffisante pour rétablir la virulence de la souche mutante lors d'une infection septicémique chez le poulet. Ceci suggère que la présence du récepteur est requise *in vivo* lorsque le système Iro est surexprimé. De plus, les analyses en LC-MS/MS ont démontré une faible variation entre les quantités de sidérophores catécholates totales détectées entre la souche Δ*iroA*Δ*iucABCD*Δ*iutA* complémentée avec les gènes *iroBCDEN* ou *iroBCDE*. Cependant, une diminution des molécules DGE, MGE, MGE linéaire, entérobactine et entérobactine linéaire et une augmentation des salmochélines TGE linéaire et DGE linéaire ont été observés en absence du récepteur IroN. Ce profil de concentration de sidérophores est d'ailleurs similaire à celui obtenu de la souche Δ*iroA*Δ*iucABCD*Δ*iutA* complémentée par les gènes *iroBC*. L'augmentation des molécules DGE linéaire et TGE linéaire dans les surnageants de culture en absence du récepteur IroN indique que ces molécules sont probablement internalisées par ce dernier. D'ailleurs, la salmochéline DGE linéaire (S2) est majoritairement captée par IroN, bien que FepA et Cir puissent également contribuer à l'internalisation [24]. De plus, la diminution en concentration des molécules non- et mono-glucosylées en absence d'IroN, peut s'expliquer par le fait que la bactérie, qui ne possède plus l'aérobactine, doit acquérir le fer nécessaire à sa croissance par l'internalisation des molécules catécholates via d'autres récepteurs de sidérophores, tels que FepA et/ou Cir.

Par ailleurs, la simple mutation du gène *iroN* chez la souche χ7122 affecte peu le profil des sidérophores catécholates, mis à part une augmentation significative de l'entérobactine (Section Résultat, Figure 2). Cette augmentation de l'entérobactine dans le surnageant en absence d'IroN confirment ce que Baumler et ses collaborateurs [238] ont démontré, soit que le récepteur IroN peut capter et internaliser l'entérobactine. Ces données suggèrent aussi que la présence des autres récepteurs de sidérophores catécholates tels que FepA, Cir et Iha et celui de l'aérobactine IutA peut compenser la perte du récepteur IroN dans un milieu de culture pauvre en fer.

De plus, l'internalisation des sidérophores jusqu'au cytoplasme bactérien nécessite un transporteur de la membrane interne. Les résultats des analyses en LC-MS/MS des surnageants de culture du mutant Δ*fepC* suggèrent que le transporteur de la membrane interne FepDGC transporte l'entérobactine et les salmochéline. Une délétion de FepC bloque l'entrée des sidérophores dans le périplasme et en présence de l'hydrolase périplasmique IroE, ce dernier dégrade les molécules cycliques et linéaires, expliquant l'augmentation des molécules SX, S1, dimère et monomère de DHBS (Section Résultat, Figure 2). L'addition de la mutation Δ*iroE* chez le mutant Δ*fepC* démontre le rôle de l'estérase périplasmique IroE. Les résultats des analyses du surnageant de culture par LC-MS/MS du double mutant Δ*fepC*Δ*iroE* démontrent un regain général des sidérophores cyclique par rapport au mutant Δ*fepC*.

Puisque l'absence de FepC et IroE n'empêche pas la détection des molécules cycliques et linéaires dans le surnageant de culture, et ce même en présence des récepteurs de sidérophores, on peut émettre l'hypothèse que les sidérophores peuvent être internalisés au niveau du périplasme bactérien et par conséquent doivent être sécrétés à nouveau en absence d'un transporteur de la membrane interne spécifique. D'ailleurs, il a été démontré récemment que l'internalisation du complexe ^{55}Fe-entérobactine par FepA, requiert les protéines FepBDGC pour l'internalisation complète du complexe, sans quoi le complexe sera sécrété à nouveau du périplasme vers l'extérieur par TolC [224]. Un mécanisme similaire pourrait avoir lieu pour les salmochélines.

1.4 La dégradation des sidérophores par Fes, IroD et IroE

La dégradation des salmochélines et de l'entérobactine par les estérases Fes, IroD et IroE a fait l'objet de la troisième étude de ce document (page 140-175). Tel que démontré précédemment, les estérases cytoplasmiques Fes et IroD présentent une double fonction pour la dégradation des sidérophores, ainsi que pour leur synthèse et contribuent individuellement et en combinaison à la virulence de la souche χ7122 pour l'établissement d'une infection dans le modèle aviaire. Quant à l'hydrolase périplasmique

IroE, elle linéarise les molécules dans l'espace périplasmique, fonction qui est accessoire pour la virulence de la souche.

La croissance des souches mutantes pour la dégradation des sidérophores catécholates a été mesurée en milieu minimal M63 en présence et absence de conalbumine. La présence de conalbumine dans le milieu de croissance ralentit la croissance du double mutant Δ*fes*Δ*iroD* et ce délai de croissance est levé à l'ajout d'une mutation *entA* qui inhibe ainsi la synthèse des sidérophores catécholates (Section Résultat, Figure 3).Ce phénotype de rétablissement de la croissance en absence de synthèse est similaire que celui observé chez le double mutant de sécrétion Δ*entS*Δ*iroC*, tel que démontré dans le deuxième article de ce document (page 95-139). L'inhibition de la synthèse des sidérophores catécholates rend la délétion des systèmes de transport et de dégradation inutile, en ce sens que leur absence n'empêche plus le bon fonctionnement du mécanisme d'acquisition du fer par les systèmes de sidérophores de types catécholates. Ceci n'aurait d'ailleurs probablement pas d'incidence sur la virulence d'une bactérie pathogène, si bien sûr, un système de sidérophore auxiliaire et non apparenté, tel que l'aérobactine, est présent chez cette bactérie.

Ainsi, les résultats suggèrent que l'absence des estérases Fes et IroD diminue l'aptitude de la souche à acquérir le fer par l'entérobactine en présence de conalbumine, bien que le système de l'aérobactine soit fonctionnel. Ceci ajoute à l'importance de la fonction de dégradation des estérases Fes et IroD pour le bon fonctionnement des systèmes de sidérophores catécholates.

1.5 Modèle proposé des mécanismes d'action des sidérophores catécholates chez χ7122

L'étude des gènes *iroBCDEN* responsable de la synthèse, de la sécrétion et de la dégradation des sidérophores catécholates chez χ7122 a permis de mettre en lumière l'interdépendance des systèmes de l'entérobactine et des salmochélines, ainsi que le rôle complémentaire de l'aérobactine, pour l'acquisition du fer lors d'une infection chez les espèces aviaires. Le modèle proposé ci-dessous met en place le mécanisme d'action des

sidérophores catécholates tel que démontré au cours de cette étude, ainsi que par plusieurs groupes de recherches [24, 197, 223, 229, 238, 244].

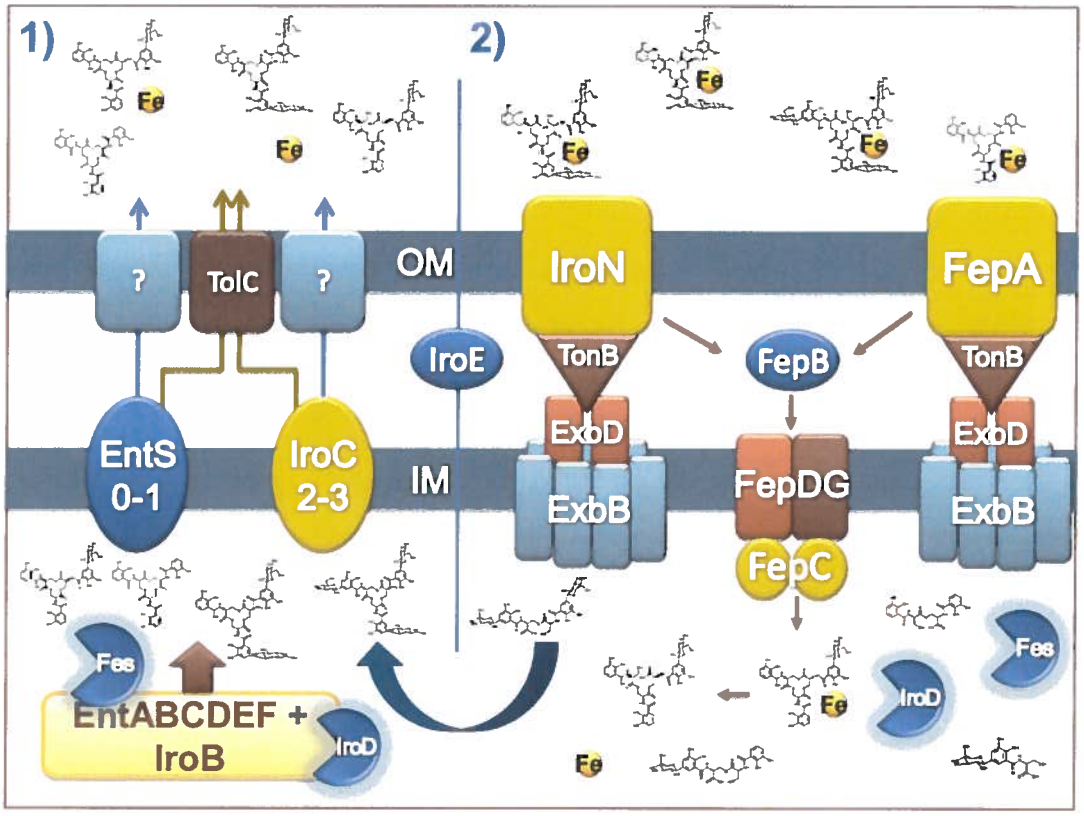

Figure 1 : Modèle proposé des mécanismes d'actions des sidérophores catécholates. 1) Synthèse de l'entérobactine et des salmochélines par EntABCDEF et IroBD; et sécrétion à travers la membrane interne des molécules non- et mono-glucosylées par EntS et des molécules di- et tri-glucosylées par IroC. La sécrétion de ces molécules à travers la membrane externe se fait par TolC et/ou un partenaire inconnu (?). 2) Internalisation par les récepteurs de la membrane externe IroN (salmochélines) et FepA (entérobactine et possiblement salmochélines mono-glucosylées), passage à travers la membrane interne par le transporteur ABC FepBDGC, dégradation des molécules par Fes, IroD et IroE et re-sécrétion des molécules dégradées (flèche incurvée bleu).

2) La production des sidérophores catécholates, aérobactine et yersiniabactine chez les entérobactéries pathogènes.

La production des divers sidérophores connus chez les entérobactéries varient considérablement selon l'espèce bactérienne, mais aussi selon la souche. Cette variabilité peut s'expliquer par divers facteurs, dont la spécificité d'hôte (humain vs animal), mais aussi par la niche d'infection spécifique (tractus respiratoire vs tractus urinaire) et où l'efficacité de certains sidérophores peut être augmentée. Un criblage plus exhaustif d'une collection de souches pathogènes pourrait mener à une corrélation entre la production d'un sidérophore spécifique et un groupe de souche partageant la même niche d'infection. C'est d'ailleurs le résultat de l'étude faite en collaboration avec les Dr. Michael Bachman et Jeffrey Weiser. L'étude menée auprès de 132 isolats clinique de *K.pneumoniae* démontre une corrélation entre de la production de la yersiniabactine et les souches de *K. pneumoniae* isolées du tractus respiratoire des patients atteints de pneumonie (Annexe IV).

Une régulation différentielle des gènes encodant pour les différentes composantes des systèmes de sidérophores peut également être à l'origine de cette variabilité moléculaire. Quelques études ont d'ailleurs démontré l'utilité des sidérophores catécholates et de l'aérobactine en fonction du milieu dans lequel les bactéries devaient acquérir le fer. Par exemple, l'aérobactine semble plus efficace pour acquérir le fer dans le sérum humain et en présence d'albumine que l'entérobactine, bien que la glucosylation de ce dernier aide à la croissance bactérienne en présence d'albumine [243, 276, 277]. De plus, l'entérobactine est nécessaire à la croissance bactérienne en présence de norépinephrine et les salmochélines sont requises pour contrecarrer l'effet bactériostatique du NGAL [26, 296, 297]. Ceci suggère qu'une production différentielle des sidérophores peut subvenir en fonction des conditions de culture ou selon les différentes niches de l'hôte.

Un exemple récent de modulation de la synthèse de l'entérobactine chez la souche *E. coli* MG1655 par les acides aminés cystéine et sérine fait d'ailleurs l'objet d'une étude en

collaboration avec le laboratoire du Dr. Éric Massé. L'étude maintenant publiée démontre en fait que le petit ARN régulateur RyhB est requis pour la synthèse de l'entérobactine, puisque l'absence du régulateur empêche l'inhibition de la sérine acétyltransférase CysE et ainsi promeut la conversion de la sérine en *O*-acetyl-L-sérine. Cette conversion est en fait la première étape de la synthèse de la cystéine [172]. Ainsi, puisque la synthèse de l'entérobactine nécessite la sérine, la conversion de celle-ci en cystéine en l'absence de RyhB diminue grandement la quantité d'entérobactine produite.

La régulation du locus IroA chez *S.* Typhi Ty2 semble également être différents des autre souches. La production des salmochélines chez la souche *S.* Typhi Ty2 et Paratyphi est relativement basse par rapport aux autres souches de *S. enterica* (Section Résultat, Tableau 2). Cependant, l'ajout d'acides casaminés déferrés augmente considérablement la concentration extracellulaire des salmochélines (Section Résultat, Figure 4). Une étude plus approfondie sur la régulation du locus IroA par les acides aminés et/ou les protéines de l'hôte chez les souches de *S. enterica* serait une avenue intéressante à explorer.

Un autre exemple de régulation différentielle a été identifié dans le premier article de ce document (page 53-94). La distribution relative de l'aérobactine augmente au détriment de l'entérobactine lorsque la souche χ7122 se retrouve dans les tissus d'un animal. Ce changement indique que plusieurs conditions de l'hôte modulent l'expression de ces molécules. D'ailleurs, l'ajout de conalbumine au milieu de culture M63-glycérol augmente considérablement la synthèse de l'aérobactine et diminue celle des sidérophores catécholates (Section Résultat, Figure 5). L'ajout de la conalbumine au milieu de culture module de façon similaire l'expression de l'entérobactine et l'aérobactine lorsque la bactérie se retrouve dans les tissus des poulets. Cependant, la présence de conalbumine diminue la synthèse des salmochélines; diminution qui n'est pas observée *in vivo*. De plus, tel que démontré précédemment, la croissance en présence de la conalbumine est dépendante des systèmes de sidérophores, sans quoi, la souche ne se multiplie pas. Ceci suggère que bien que la conalbumine module la production des sidérophores, la production d'au moins un type de sidérophore est requise pour la

croissance bactérienne; ce qui est très différent d'une infection septicémique dans le modèle aviaire, où les salmochélines ou l'aérobactine, mais pas l'entérobactine, sont nécessaires à l'établissement de l'infection.

Autrement dit, plusieurs facteurs de l'hôte peuvent venir interférer dans la production des sidérophores, dont la présence de conalbumine, lorsque la bactérie se retrouve chez le poulet. Aussi, quelques protéines homologues au NGAL dont Ex-FABP, CALβ et CALγ et C8GC, ont été retrouvées chez le poulet [342] et pourraient jouer un rôle similaire à celui-ci, et ainsi séquestrer l'entérobactine produit par la souche χ7122. Les défenses naturelles de l'hôte dont le rôle est de séquestrer le fer libre ou complexé à des sidérophores justifient en quelque sorte la variété, le nombre et la modulation de l'expression des systèmes d'obtentions du fer présent chez de nombreuses bactéries pathogènes.

3) Conclusions

L'évaluation de l'importance des trois systèmes d'acquisition du fer ferrique exprimé chez la souche ExPEC aviaire χ7122 lors d'une infection systémique chez le poulet a permis de mettre en lumière les rôles individuels et combinés de ces sidérophores pour la virulence de la souche. *À priori*, la présence des trois systèmes de sidérophores chez la souche χ7122 semble redondante; cependant l'étude de ces sidérophores dans la virulence a démontré une interrelation étroite entre les systèmes de sidérophores catécholates et une capacité infectieuse maintenue en présence de l'aérobactine. L'étude détaillée de la synthèse, de la sécrétion et de la dégradation des salmochélines, ainsi que des interrelations entre les systèmes de l'entérobactine et des salmochélines a permis de mettre en évidence les mécanismes de virulence nécessaire pour l'établissement d'une infection dans le modèle septicémique aviaire. Bien que ce modèle d'infection expérimentale surpasse l'étape de colonisation trachéale, l'utilisation de l'hôte naturel, le poulet, pour l'étude de la virulence de la souche χ7122 renforce les conclusions tirées de cette étude.

Perspectives

En guise de perspectives à cette étude des systèmes de sidérophores chez la souche ExPEC aviaire χ7122, le premier objectif serait de démontrer le rôle exacte des enzymes IroD et Fes pour la biosynthèse des salmochélines. La démonstration de la formation d'un complexe entre IroB et IroD et/ou Fes serait souhaitable et plausible à l'aide d'une expérience de co-immunoprécipitation. Cette donné augmenterait grandement la valeur des résultats obtenus jusqu'à présent.

Une étude plus approfondit sur les mécanismes exactes de TolC pour la sécrétion des sidérophores catécholates pourraient également être intéressante. L'analyse des surnageant des cultures par LC-MS/MS de doubles et triples mutants des gènes entS, iroC et iroE chez un mutant ΔtolC devrait facilité la compréhension du rôle précis de TolC pour la sécrétion de ces molécules.

De plus, la présence de plusieurs facteurs de l'hôte ou de l'environnement nutritionnel semble moduler l'expression des sidérophores selon les souches pathogènes. Cette variabilité de la production de ces sidérophores selon les souches pathogènes indique qu'une régulation et/ou modulation de ces systèmes doit avoir lieu. Les quelques données préliminaires exposées dans ce travail pourraient d'ailleurs faire partie d'un projet de recherche visant l'étude de la régulation de la production des sidérophores par les entérobactéries pathogènes en fonction de leur niche d'infection chez l'hôte (intestinal, tractus urinaire ou respiratoire). Ces études basées sur les interactions hôtes-pathogènes devraient mettre en lumière les mécanismes qui régissent la modulation de la production des sidérophores chez les bactéries pathogènes.

Finalement, le développement d'un vaccin utilisant des souches aviaire de sérogroupe O78, O1 et O2, dont l'atténuation de la virulence réside en l'élimination des gènes iroBCDE et/ou iucABCD est en cours. En fait, ce vaccin sera constitué de souches mutées dans les systèmes de synthèse des sidérophores salmochélines et aérobactine et dont les récepteurs de la membrane externe seront intacts, afin de préserver le caractère immunogène de la bactérie. De plus, ces mutations ont été réalisées sans l'introduction de gènes de résistance à des antibiotiques afin d'éviter des risques de transferts à d'autres

bactéries présents dans la flore normale des animaux, et ainsi causer une éventuelle résistance naturelle à ces antibiotiques. Par ailleurs, les souches atténuées par la délétion des gènes de sécrétion (entS et iroC) et de dégradation (fes et iroD) des sidérophores catécholates auraient pu être des bons candidats vaccinaux; cependant ces souches présentent un risque de rétablissement de la virulence si une mutation spontanée survient dans les gènes de synthèse de l'entérobactine, puisque l'aérobactine est toujours fonctionnelle chez ces souches. Le but du vaccin avec des souches atténuées est d'offrir une protection immunitaire aux jeunes poussins contre les principaux sérogroupes de souches APEC causant la colibacillose aviaire tout en évitant l'introduction de gènes de résistance aux antibiotiques. Ceci aura pour conséquences une augmentation de la survie des poulets d'élevage, une diminution de l'utilisation d'antibiotiques dans les élevages, un meilleur rendement pour l'industrie avicole et, éventuellement, une diminution du risque zoonotique potentiel des infections extra-intestinales à E. coli en provenance des poulets de consommation.

Références

1. Welch, R.A., *The Genus Escherichia*, in *The Prokaryotes*, S.N. York, Editor. 2006: New York. p. 60-71.
2. Bonacorsi, S. and E. Bingen, *Molecular epidemiology of Escherichia coli causing neonatal meningitis.* Int J Med Microbiol, 2005. **295**(6-7): p. 373-81.
3. Johnson, J.R. and T.A. Russo, *Molecular epidemiology of extraintestinal pathogenic (uropathogenic) Escherichia coli.* Int J Med Microbiol, 2005. **295**(6-7): p. 383-404.
4. Schade, A.L. and L. Caroline, *Raw Hen Egg White and the Role of Iron in Growth Inhibition of Shigella Dysenteriae, Staphylococcus Aureus, Escherichia Coli and Saccharomyces Cerevisiae.* Science, 1944. **100**(2584): p. 14-15.
5. Bullen, J.J., L.C. Leigh, and H.J. Rogers, *The effect of iron compounds on the virulence of Escherichia coli for guinea-pigs.* Immunology, 1968. **15**(4): p. 581-8.
6. Kochan, I., *The role of iron in bacterial infections, with special consideration of host-tubercle bacillus interaction.* Curr Top Microbiol Immunol, 1973. **60**: p. 1-30.
7. Andrews, S.C., A.K. Robinson, and F. Rodriguez-Quinones, *Bacterial iron homeostasis.* FEMS Microbiol Rev, 2003. **27**(2-3): p. 215-37.
8. Evans, R.W.C., J.B. Joannou, C.L. Sharma, N.D., *Iron Proteins*, in *Iron and Infection - Molecular, Physiological and Clinical Aspects*, J.J.a.G. Bullen, E., Editor. 1999, John Wiley & Sons Ltd: West Sussex. p. 27-87.
9. Ratledge, C. and L.G. Dover, *Iron metabolism in pathogenic bacteria.* Annu Rev Microbiol, 2000. **54**: p. 881-941.
10. Aisen, P. and E.B. Brown, *The iron-binding function of transferrin in iron metabolism.* Semin Hematol, 1977. **14**(1): p. 31-53.
11. Bullen, J.J., H.J. Rogers, and E. Griffiths, *Role of iron in bacterial infection.* Curr Top Microbiol Immunol, 1978. **80**: p. 1-35.
12. Braun, V. and M. Braun, *Iron transport and signaling in Escherichia coli.* FEBS Lett, 2002. **529**(1): p. 78-85.
13. Raymond, K.N., E.A. Dertz, and S.S. Kim, *Enterobactin: an archetype for microbial iron transport.* Proc Natl Acad Sci U S A, 2003. **100**(7): p. 3584-8.
14. Faraldo-Gomez, J.D. and M.S. Sansom, *Acquisition of siderophores in gram-negative bacteria.* Nat Rev Mol Cell Biol, 2003. **4**(2): p. 105-16.
15. Miethke, M. and M.A. Marahiel, *Siderophore-based iron acquisition and pathogen control.* Microbiol Mol Biol Rev, 2007. **71**(3): p. 413-51.
16. Dozois, C.M., F. Daigle, and R. Curtiss, 3rd, *Identification of pathogen-specific and conserved genes expressed in vivo by an avian pathogenic Escherichia coli strain.* Proc Natl Acad Sci U S A, 2003. **100**(1): p. 247-52.
17. Warner, P.J., et al., *ColV plasmid-specific aerobactin synthesis by invasive strains of Escherichia coli.* Infect Immun, 1981. **33**(2): p. 540-5.
18. Williams, P.H., *Novel iron uptake system specified by ColV plasmids: an important component in the virulence of invasive strains of Escherichia coli.* Infect Immun, 1979. **26**(3): p. 925-32.

19. Torres, A.G., et al., *TonB-dependent systems of uropathogenic Escherichia coli: aerobactin and heme transport and TonB are required for virulence in the mouse.* Infect Immun, 2001. **69**(10): p. 6179-85.
20. Rogers, H.J., *Iron-binding catechols and virulence in Escherichia coli.* Infect Immun, 1973. **7**(3): p. 438-44.
21. Furman, M., et al., *Salmonella typhi iron uptake mutants are attenuated in mice.* Infect Immun, 1994. **62**(9): p. 4091-4.
22. Benjamin, W.H., Jr., et al., *The ability of Salmonella typhimurium to produce the siderophore enterobactin is not a virulence factor in mouse typhoid.* Infect Immun, 1985. **50**(2): p. 392-7.
23. Rabsch, W., et al., *Role of receptor proteins for enterobactin and 2,3-dihydroxybenzoylserine in virulence of Salmonella enterica.* Infect Immun, 2003. **71**(12): p. 6953-61.
24. Hantke, K., et al., *Salmochelins, siderophores of Salmonella enterica and uropathogenic Escherichia coli strains, are recognized by the outer membrane receptor IroN.* Proc Natl Acad Sci U S A, 2003. **100**(7): p. 3677-82.
25. Bachman, M.A., V.L. Miller, and J.N. Weiser, *Mucosal lipocalin 2 has pro-inflammatory and iron-sequestering effects in response to bacterial enterobactin.* PLoS Pathog, 2009. **5**(10): p. e1000622.
26. Fischbach, M.A., et al., *The pathogen-associated iroA gene cluster mediates bacterial evasion of lipocalin 2.* Proc Natl Acad Sci U S A, 2006. **103**(44): p. 16502-7.
27. Nelson, A.L., et al., *Interleukin-8 secretion in response to aferric enterobactin is potentiated by siderocalin.* Infect Immun, 2007. **75**(6): p. 3160-8.
28. Prescott, H., Klein, *Microbiologie.* 2 ed. 1995, Bruxelle: DeBoeck Université. 1014.
29. Kaper, J.B., J.P. Nataro, and H.L. Mobley, *Pathogenic Escherichia coli.* Nat Rev Microbiol, 2004. **2**(2): p. 123-40.
30. Farthing, M.J., *Bugs and the gut: an unstable marriage.* Best Pract Res Clin Gastroenterol, 2004. **18**(2): p. 233-9.
31. Dozois, C.M. and R. Curtiss, 3rd, *Pathogenic diversity of Escherichia coli and the emergence of 'exotic' islands in the gene stream.* Vet Res, 1999. **30**(2-3): p. 157-79.
32. Dobrindt, U., *(Patho-)Genomics of Escherichia coli.* Int J Med Microbiol, 2005. **295**(6-7): p. 357-71.
33. Hacker, J. and J.B. Kaper, *Pathogenicity islands and the evolution of microbes.* Annu Rev Microbiol, 2000. **54**: p. 641-79.
34. Nataro, J.P. and M.M. Levine, *Escherichia coli Diseases in Humans*, in *Escherichia coli in Domestic Animals & Humans*, C.C. Gyles, Editor. 1994, CAB International. p. 285-333.
35. Nataro, J.P. and J.B. Kaper, *Diarrheagenic Escherichia coli.* Clin Microbiol Rev, 1998. **11**(1): p. 142-201.
36. McDaniel, T.K., et al., *A genetic locus of enterocyte effacement conserved among diverse enterobacterial pathogens.* Proc Natl Acad Sci U S A, 1995. **92**(5): p. 1664-8.

37. Jerse, A.E., et al., *A genetic locus of enteropathogenic Escherichia coli necessary for the production of attaching and effacing lesions on tissue culture cells.* Proc Natl Acad Sci U S A, 1990. **87**(20): p. 7839-43.
38. Tzipori, S., et al., *Role of a 60-megadalton plasmid and Shiga-like toxins in the pathogenesis of infection caused by enterohemorrhagic Escherichia coli O157:H7 in gnotobiotic piglets.* Infect Immun, 1987. **55**(12): p. 3117-25.
39. Caprioli, A., et al., *Enterohaemorrhagic Escherichia coli: emerging issues on virulence and modes of transmission.* Vet Res, 2005. **36**(3): p. 289-311.
40. Nataro, J.P., et al., *Aggregative adherence fimbriae I of enteroaggregative Escherichia coli mediate adherence to HEp-2 cells and hemagglutination of human erythrocytes.* Infect Immun, 1992. **60**(6): p. 2297-304.
41. Henderson, I.R., et al., *Characterization of pic, a secreted protease of Shigella flexneri and enteroaggregative Escherichia coli.* Infect Immun, 1999. **67**(11): p. 5587-96.
42. Fasano, A., et al., *Shigella enterotoxin 1: an enterotoxin of Shigella flexneri 2a active in rabbit small intestine in vivo and in vitro.* J Clin Invest, 1995. **95**(6): p. 2853-61.
43. Savarino, S.J., et al., *Enteroaggregative Escherichia coli elaborate a heat-stable enterotoxin demonstrable in an in vitro rabbit intestinal model.* J Clin Invest, 1991. **87**(4): p. 1450-5.
44. Eslava, C., et al., *Pet, an autotransporter enterotoxin from enteroaggregative Escherichia coli.* Infect Immun, 1998. **66**(7): p. 3155-63.
45. Navarro-Garcia, F., et al., *In vitro effects of a high-molecular-weight heat-labile enterotoxin from enteroaggregative Escherichia coli.* Infect Immun, 1998. **66**(7): p. 3149-54.
46. Hicks, S., D.C. Candy, and A.D. Phillips, *Adhesion of enteroaggregative Escherichia coli to pediatric intestinal mucosa in vitro.* Infect Immun, 1996. **64**(11): p. 4751-60.
47. Bilge, S.S., et al., *Molecular characterization of a fimbrial adhesin, F1845, mediating diffuse adherence of diarrhea-associated Escherichia coli to HEp-2 cells.* J Bacteriol, 1989. **171**(8): p. 4281-9.
48. Echeverria, P., O. Sethabutr, and C. Pitarangsi, *Microbiology and diagnosis of infections with Shigella and enteroinvasive Escherichia coli.* Rev Infect Dis, 1991. **13 Suppl 4**: p. S220-5.
49. Russo, T.A. and J.R. Johnson, *Medical and economic impact of extraintestinal infections due to Escherichia coli: focus on an increasingly important endemic problem.* Microbes Infect, 2003. **5**(5): p. 449-56.
50. Stamm, W.E. and T.M. Hooton, *Management of urinary tract infections in adults.* N Engl J Med, 1993. **329**(18): p. 1328-34.
51. Yamamoto, S., *Molecular epidemiology of uropathogenic Escherichia coli.* J Infect Chemother, 2007. **13**(2): p. 68-73.
52. Watt, S., et al., *Escherichia coli strains from pregnant women and neonates: intraspecies genetic distribution and prevalence of virulence factors.* J Clin Microbiol, 2003. **41**(5): p. 1929-35.
53. Johnson, J.R. and T.A. Russo, *Extraintestinal pathogenic Escherichia coli: "the other bad E coli".* J Lab Clin Med, 2002. **139**(3): p. 155-62.

54. Dho-Moulin, M. and J.M. Fairbrother, *Avian pathogenic Escherichia coli (APEC).* Vet Res, 1999. **30**(2-3): p. 299-316.
55. Gross, W.G., *Diseases Due to Escherichia coli in Poultry*, in *Escherichia coli in Domestic Animals and Humans*, C.L. Gyles, Editor. 1994, CAB International: Wallingford. p. 237-261.
56. La Ragione, R.M. and M.J. Woodward, *Virulence factors of Escherichia coli serotypes associated with avian colisepticaemia.* Res Vet Sci, 2002. **73**(1): p. 27-35.
57. White, D.G., et al., *Clonal relationships and variation in virulence among Escherichia coli strains of avian origin.* Microb Pathog, 1993. **14**(5): p. 399-409.
58. Dozois, C.M., et al., *Relationship between the Tsh autotransporter and pathogenicity of avian Escherichia coli and localization and analysis of the Tsh genetic region.* Infect Immun, 2000. **68**(7): p. 4145-54.
59. RAIZO. *Revue d'épidémiosurveillance animale du Réseau d'alerte et d'informantion zoosanitaire (RAIZO), Bilan 2008.* 2008; Available from: http://www.mapaq.gouv.qc.ca/NR/rdonlyres/890464CC-3DFA-494A-8BAE-F18C52C54B96/0/Raizo2009WEB_low.pdf.
60. Besser, C.C.G.a.T.E., *Escherichia coli Septicaemia in Calves*, in *Escherichia coli in Domestic Animal and Humans*, G. C.L, Editor. 1994, CAB International: Wallingford. p. 75-91.
61. Ngeleka, J.M.F.a.M., *Extraintestinal Escherichia coli Infections in Pigs*, in *Escherichia coli in Domestic Animals and Humans*, G. C.L, Editor. 1994, CAB International: Wallingford. p. 221-237.
62. Hodgson, J.C., *Diseases Due to Escherichia coli in Sheep*, in *Escherichia coli in Domestic Animal and Humans*, G. C.L, Editor. 1994, CAB International: Wallingford. p. 221-237.
63. Shpigel, N.Y., S. Elazar, and I. Rosenshine, *Mammary pathogenic Escherichia coli.* Curr Opin Microbiol, 2008. **11**(1): p. 60-5.
64. Fairbrother, J.M.N., M., *Extraintestinal Escherichia coli Infecgtions in Pigs*, in *Escherichia coli in Domestic Animals and Humans*, C.L. Gyles, Editor. 1994, CAB International: Wallingford. p. 221-237.
65. Ewers, C., et al., *Avian pathogenic, uropathogenic, and newborn meningitis-causing Escherichia coli: how closely related are they?* Int J Med Microbiol, 2007. **297**(3): p. 163-76.
66. Johnson, T.J., et al., *Examination of the source and extended virulence genotypes of Escherichia coli contaminating retail poultry meat.* Foodborne Pathog Dis, 2009. **6**(6): p. 657-67.
67. Moulin-Schouleur, M., et al., *Extraintestinal pathogenic Escherichia coli strains of avian and human origin: link between phylogenetic relationships and common virulence patterns.* J Clin Microbiol, 2007. **45**(10): p. 3366-76.
68. Johnson, T.J., et al., *Comparison of extraintestinal pathogenic Escherichia coli strains from human and avian sources reveals a mixed subset representing potential zoonotic pathogens.* Appl Environ Microbiol, 2008. **74**(22): p. 7043-50.
69. Ochman, H. and R.K. Selander, *Standard reference strains of Escherichia coli from natural populations.* J Bacteriol, 1984. **157**(2): p. 690-3.

70. Dziva, F. and M.P. Stevens, *Colibacillosis in poultry: unravelling the molecular basis of virulence of avian pathogenic Escherichia coli in their natural hosts.* Avian Pathol, 2008. **37**(4): p. 355-66.
71. Moulin-Schouleur, M., et al., *Common virulence factors and genetic relationships between O18:K1:H7 Escherichia coli isolates of human and avian origin.* J Clin Microbiol, 2006. **44**(10): p. 3484-92.
72. Mora, A., et al., *Extraintestinal pathogenic Escherichia coli O1:K1:H7/NM from human and avian origin: detection of clonal groups B2 ST95 and D ST59 with different host distribution.* BMC Microbiol, 2009. **9**: p. 132.
73. Ewers, C., et al., *Intestine and environment of the chicken as reservoirs for extraintestinal pathogenic Escherichia coli strains with zoonotic potential.* Appl Environ Microbiol, 2009. **75**(1): p. 184-92.
74. Rodriguez-Siek, K.E., et al., *Comparison of Escherichia coli isolates implicated in human urinary tract infection and avian colibacillosis.* Microbiology, 2005. **151**(Pt 6): p. 2097-110.
75. Vincent, C., et al., *Food reservoir for Escherichia coli causing urinary tract infections.* Emerg Infect Dis, 2010. **16**(1): p. 88-95.
76. Johnson, J.R., et al., *Antimicrobial-resistant and extraintestinal pathogenic Escherichia coli in retail foods.* J Infect Dis, 2005. **191**(7): p. 1040-9.
77. Schierack, P., et al., *ExPEC-typical virulence-associated genes correlate with successful colonization by intestinal E. coli in a small piglet group.* Environ Microbiol, 2008. **10**(7): p. 1742-51.
78. Butaye, P., L.A. Devriese, and F. Haesebrouck, *Antimicrobial growth promoters used in animal feed: effects of less well known antibiotics on gram-positive bacteria.* Clin Microbiol Rev, 2003. **16**(2): p. 175-88.
79. Gyles, C.L., *Antimicrobial resistance in selected bacteria from poultry.* Anim Health Res Rev, 2008. **9**(2): p. 149-58.
80. Hammerum, A.M. and O.E. Heuer, *Human health hazards from antimicrobial-resistant Escherichia coli of animal origin.* Clin Infect Dis, 2009. **48**(7): p. 916-21.
81. Bonnet, C., et al., *Pathotype and antibiotic resistance gene distributions of Escherichia coli isolates from broiler chickens raised on antimicrobial-supplemented diets.* Appl Environ Microbiol, 2009. **75**(22): p. 6955-62.
82. Maynard, C., et al., *Heterogeneity among virulence and antimicrobial resistance gene profiles of extraintestinal Escherichia coli isolates of animal and human origin.* J Clin Microbiol, 2004. **42**(12): p. 5444-52.
83. Ramchandani, M., et al., *Possible animal origin of human-associated, multidrug-resistant, uropathogenic Escherichia coli.* Clin Infect Dis, 2005. **40**(2): p. 251-7.
84. Cortes, P., et al., *Isolation and characterization of potentially pathogenic antimicrobial-resistant Escherichia coli strains from chicken and pig farms in Spain.* Appl Environ Microbiol, 2010. **76**(9): p. 2799-805.
85. Johnson, J.R., et al., *Isolation and molecular characterization of nalidixic acid-resistant extraintestinal pathogenic Escherichia coli from retail chicken products.* Antimicrob Agents Chemother, 2003. **47**(7): p. 2161-8.

86. Dobrindt, U., et al., *S-Fimbria-encoding determinant sfa(I) is located on pathogenicity island III(536) of uropathogenic Escherichia coli strain 536.* Infect Immun, 2001. **69**(7): p. 4248-56.
87. Roberts, J.A., et al., *The Gal(alpha 1-4)Gal-specific tip adhesin of Escherichia coli P-fimbriae is needed for pyelonephritis to occur in the normal urinary tract.* Proc Natl Acad Sci U S A, 1994. **91**(25): p. 11889-93.
88. Marre, R. and J. Hacker, *Role of S- and common-type I-fimbriae of Escherichia coli in experimental upper and lower urinary tract infection.* Microb Pathog, 1987. **2**(3): p. 223-6.
89. Connell, I., et al., *Type 1 fimbrial expression enhances Escherichia coli virulence for the urinary tract.* Proc Natl Acad Sci U S A, 1996. **93**(18): p. 9827-32.
90. Johnson, J.R., et al., *The IrgA homologue adhesin Iha is an Escherichia coli virulence factor in murine urinary tract infection.* Infect Immun, 2005. **73**(2): p. 965-71.
91. Leveille, S., et al., *Iha from an Escherichia coli urinary tract infection outbreak clonal group A strain is expressed in vivo in the mouse urinary tract and functions as a catecholate siderophore receptor.* Infect Immun, 2006. **74**(6): p. 3427-36.
92. La Ragione, R.M., A.R. Sayers, and M.J. Woodward, *The role of fimbriae and flagella in the colonization, invasion and persistence of Escherichia coli O78:K80 in the day-old-chick model.* Epidemiol Infect, 2000. **124**(3): p. 351-63.
93. Welch, R.A., et al., *Haemolysin contributes to virulence of extra-intestinal E. coli infections.* Nature, 1981. **294**(5842): p. 665-7.
94. Rippere-Lampe, K.E., et al., *Mutation of the gene encoding cytotoxic necrotizing factor type 1 (cnf(1)) attenuates the virulence of uropathogenic Escherichia coli.* Infect Immun, 2001. **69**(6): p. 3954-64.
95. Khan, N.A., et al., *Cytotoxic necrotizing factor-1 contributes to Escherichia coli K1 invasion of the central nervous system.* J Biol Chem, 2002. **277**(18): p. 15607-12.
96. Guyer, D.M., et al., *Sat, the secreted autotransporter toxin of uropathogenic Escherichia coli, is a vacuolating cytotoxin for bladder and kidney epithelial cells.* Infect Immun, 2002. **70**(8): p. 4539-46.
97. Schubert, S., et al., *Yersinia high-pathogenicity island contributes to virulence in Escherichia coli causing extraintestinal infections.* Infect Immun, 2002. **70**(9): p. 5335-7.
98. Caza, M., et al., *Specific roles of the iroBCDEN genes in virulence of an avian pathogenic Escherichia coli O78 strain and in production of salmochelins.* Infect Immun, 2008. **76**(8): p. 3539-49.
99. Russo, T.A., U.B. Carlino, and J.R. Johnson, *Identification of a new iron-regulated virulence gene, ireA, in an extraintestinal pathogenic isolate of Escherichia coli.* Infect Immun, 2001. **69**(10): p. 6209-16.
100. Sabri, M., et al., *Contribution of the SitABCD, MntH, and FeoB metal transporters to the virulence of avian pathogenic Escherichia coli O78 strain chi7122.* Infect Immun, 2008. **76**(2): p. 601-11.
101. Sabri, M., S. Houle, and C.M. Dozois, *Roles of the extraintestinal pathogenic Escherichia coli ZnuACB and ZupT zinc transporters during urinary tract infection.* Infect Immun, 2009. **77**(3): p. 1155-64.

102. Lamarche, M.G., et al., *Inactivation of the pst system reduces the virulence of an avian pathogenic Escherichia coli O78 strain.* Infect Immun, 2005. **73**(7): p. 4138-45.
103. Lloyd, A.L., et al., *Uropathogenic Escherichia coli Suppresses the host inflammatory response via pathogenicity island genes sisA and sisB.* Infect Immun, 2009. **77**(12): p. 5322-33.
104. Kim, K.S., et al., *The K1 capsule is the critical determinant in the development of Escherichia coli meningitis in the rat.* J Clin Invest, 1992. **90**(3): p. 897-905.
105. Buckles, E.L., et al., *Role of the K2 capsule in Escherichia coli urinary tract infection and serum resistance.* J Infect Dis, 2009. **199**(11): p. 1689-97.
106. Mellata, M., et al., *Role of virulence factors in resistance of avian pathogenic Escherichia coli to serum and in pathogenicity.* Infect Immun, 2003. **71**(1): p. 536-40.
107. Russo, T., et al., *The O4 specific antigen moiety of lipopolysaccharide but not the K54 group 2 capsule is important for urovirulence of an extraintestinal isolate of Escherichia coli.* Infect Immun, 1996. **64**(6): p. 2343-8.
108. Culham, D.E., et al., *Osmoregulatory transporter ProP influences colonization of the urinary tract by Escherichia coli.* Microbiology, 1998. **144 (Pt 1)**: p. 91-102.
109. Wang, Y. and K.S. Kim, *Role of OmpA and IbeB in Escherichia coli K1 invasion of brain microvascular endothelial cells in vitro and in vivo.* Pediatr Res, 2002. **51**(5): p. 559-63.
110. Badger, J.L., et al., *Application of signature-tagged mutagenesis for identification of escherichia coli K1 genes that contribute to invasion of human brain microvascular endothelial cells.* Infect Immun, 2000. **68**(9): p. 5056-61.
111. Huang, S.H., et al., *Identification and characterization of an Escherichia coli invasion gene locus, ibeB, required for penetration of brain microvascular endothelial cells.* Infect Immun, 1999. **67**(5): p. 2103-9.
112. Hoffman, J.A., et al., *Escherichia coli K1 aslA contributes to invasion of brain microvascular endothelial cells in vitro and in vivo.* Infect Immun, 2000. **68**(9): p. 5062-7.
113. Li, G., et al., *Identification of genes required for avian Escherichia coli septicemia by signature-tagged mutagenesis.* Infect Immun, 2005. **73**(5): p. 2818-27.
114. Li, G., et al., *Characterization of a yjjQ mutant of avian pathogenic Escherichia coli (APEC).* Microbiology, 2008. **154**(Pt 4): p. 1082-93.
115. Kulkarni, R., et al., *Roles of putative type II secretion and type IV pilus systems in the virulence of uropathogenic Escherichia coli.* PLoS One, 2009. **4**(3): p. e4752.
116. Allsopp, L.P., et al., *UpaH is a newly identified autotransporter protein that contributes to biofilm formation and bladder colonization by uropathogenic Escherichia coli CFT073.* Infect Immun, 2010. **78**(4): p. 1659-69.
117. Cirl, C., et al., *Subversion of Toll-like receptor signaling by a unique family of bacterial Toll/interleukin-1 receptor domain-containing proteins.* Nat Med, 2008. **14**(4): p. 399-406.
118. Griffiths, E., *Iron in Biological Systems*, in *Iron and Infection*, J.J.a.G. Bullen, E., Editor. 1999, John Wiley & Sons Ltd: West Sussex. p. 1-26.

119. Halliwell, B. and J.M. Gutteridge, *Oxygen toxicity, oxygen radicals, transition metals and disease.* Biochem J, 1984. **219**(1): p. 1-14.
120. Bullen, J., et al., *Sepsis: the critical role of iron.* Microbes Infect, 2000. **2**(4): p. 409-15.
121. Harrison, P.M. and P. Arosio, *The ferritins: molecular properties, iron storage function and cellular regulation.* Biochim Biophys Acta, 1996. **1275**(3): p. 161-203.
122. Francis, J., J. Madinaveitia, and et al., *Isolation from acid-fast bacteria of a growth-factor for Mycobacterium johnei and of a precursor of phthiocol.* Nature, 1949. **163**(4140): p. 365.
123. Crosa, J.H. and C.T. Walsh, *Genetics and assembly line enzymology of siderophore biosynthesis in bacteria.* Microbiol Mol Biol Rev, 2002. **66**(2): p. 223-49.
124. Winkelmann, G., *Microbial siderophore-mediated transport.* Biochem Soc Trans, 2002. **30**(4): p. 691-6.
125. Ratledge, C., *Iron, mycobacteria and tuberculosis.* Tuberculosis (Edinb), 2004. **84**(1-2): p. 110-30.
126. O'Brien, I.G. and F. Gibson, *The structure of enterochelin and related 2,3-dihydroxy-N-benzoylserine conjugates from Escherichia coli.* Biochim Biophys Acta, 1970. **215**(2): p. 393-402.
127. Pollack, J.R. and J.B. Neilands, *Enterobactin, an iron transport compound from Salmonella typhimurium.* Biochem Biophys Res Commun, 1970. **38**(5): p. 989-92.
128. Harris, W.R.C., C.J. Cooper, S.R. Sofen, S.R. Avdeef, A.E. McArdle, J.V. Raymond, K.N., *Coordination chemistry of microbial iron transpont compounds. 19. Stability constants and electrochemical behavior of ferric enterobactin and model complexes.* Journal of the American Chemical Society, 1979(101:20): p. 6097-6104.
129. Neilands, J.B., *Siderophores: structure and function of microbial iron transport compounds.* J Biol Chem, 1995. **270**(45): p. 26723-6.
130. Oves-Costales, D., N. Kadi, and G.L. Challis, *The long-overlooked enzymology of a nonribosomal peptide synthetase-independent pathway for virulence-conferring siderophore biosynthesis.* Chem Commun (Camb), 2009(43): p. 6530-41.
131. Kupper, F.C., et al., *Photoreactivity of iron(III)-aerobactin: photoproduct structure and iron(III) coordination.* Inorg Chem, 2006. **45**(15): p. 6028-33.
132. Griffiths, E.W., P., *The Iron-uptake Systems of Pathogenic Bacteria, Fungi and Protozoa*, in *Iron and Infection - Molecular, Physiological and Clinical Aspects*, J.G. Bullen, E. , Editor. 1999, John Wiley & Sons Ltd: West Sussex. p. 87-213.
133. Wandersman, C. and I. Stojiljkovic, *Bacterial heme sources: the role of heme, hemoprotein receptors and hemophores.* Curr Opin Microbiol, 2000. **3**(2): p. 215-20.
134. Letoffe, S., V. Redeker, and C. Wandersman, *Isolation and characterization of an extracellular haem-binding protein from Pseudomonas aeruginosa that shares function and sequence similarities with the Serratia marcescens HasA haemophore.* Mol Microbiol, 1998. **28**(6): p. 1223-34.

135. Kammler, M., C. Schon, and K. Hantke, *Characterization of the ferrous iron uptake system of Escherichia coli.* J Bacteriol, 1993. **175**(19): p. 6212-9.
136. Bearden, S.W. and R.D. Perry, *The Yfe system of Yersinia pestis transports iron and manganese and is required for full virulence of plague.* Mol Microbiol, 1999. **32**(2): p. 403-14.
137. Janakiraman, A. and J.M. Slauch, *The putative iron transport system SitABCD encoded on SPI1 is required for full virulence of Salmonella typhimurium.* Mol Microbiol, 2000. **35**(5): p. 1146-55.
138. Angerer, A., S. Gaisser, and V. Braun, *Nucleotide sequences of the sfuA, sfuB, and sfuC genes of Serratia marcescens suggest a periplasmic-binding-protein-dependent iron transport mechanism.* J Bacteriol, 1990. **172**(2): p. 572-8.
139. Adhikari, P., et al., *The fbpABC locus of Neisseria gonorrhoeae functions in the periplasm-to-cytosol transport of iron.* J Bacteriol, 1996. **178**(7): p. 2145-9.
140. Katoh, H., et al., *Genes essential to iron transport in the cyanobacterium Synechocystis sp. strain PCC 6803.* J Bacteriol, 2001. **183**(9): p. 2779-84.
141. Kochan, I., J.T. Kvach, and T.I. Wiles, *Virulence-associated acquisition of iron in mammalian serum by Escherichia coli.* J Infect Dis, 1977. **135**(4): p. 623-32.
142. Bearden, S.W., J.D. Fetherston, and R.D. Perry, *Genetic organization of the yersiniabactin biosynthetic region and construction of avirulent mutants in Yersinia pestis.* Infect Immun, 1997. **65**(5): p. 1659-68.
143. Visser, M.B., et al., *Importance of the ornibactin and pyochelin siderophore transport systems in Burkholderia cenocepacia lung infections.* Infect Immun, 2004. **72**(5): p. 2850-7.
144. Sokol, P.A., et al., *Role of ornibactin biosynthesis in the virulence of Burkholderia cepacia: characterization of pvdA, the gene encoding L-ornithine N(5)-oxygenase.* Infect Immun, 1999. **67**(9): p. 4443-55.
145. Henderson, D.P. and S.M. Payne, *Vibrio cholerae iron transport systems: roles of heme and siderophore iron transport in virulence and identification of a gene associated with multiple iron transport systems.* Infect Immun, 1994. **62**(11): p. 5120-5.
146. Takase, H., et al., *Impact of siderophore production on Pseudomonas aeruginosa infections in immunosuppressed mice.* Infect Immun, 2000. **68**(4): p. 1834-9.
147. Pecqueur, L., et al., *Structural changes of Escherichia coli ferric uptake regulator during metal-dependent dimerization and activation explored by NMR and X-ray crystallography.* J Biol Chem, 2006. **281**(30): p. 21286-95.
148. Mills, S.A. and M.A. Marletta, *Metal binding characteristics and role of iron oxidation in the ferric uptake regulator from Escherichia coli.* Biochemistry, 2005. **44**(41): p. 13553-9.
149. Lavrrar, J.L. and M.A. McIntosh, *Architecture of a fur binding site: a comparative analysis.* J Bacteriol, 2003. **185**(7): p. 2194-202.
150. McHugh, J.P., et al., *Global iron-dependent gene regulation in Escherichia coli. A new mechanism for iron homeostasis.* J Biol Chem, 2003. **278**(32): p. 29478-86.
151. Boyer, A.E. and P.C. Tai, *Characterization of the cvaA and cvi promoters of the colicin V export system: iron-dependent transcription of cvaA is modulated by downstream sequences.* J Bacteriol, 1998. **180**(7): p. 1662-72.

152. Dubrac, S. and D. Touati, *Fur positive regulation of iron superoxide dismutase in Escherichia coli: functional analysis of the sodB promoter.* J Bacteriol, 2000. **182**(13): p. 3802-8.
153. Ellermeier, J.R. and J.M. Slauch, *Fur regulates expression of the Salmonella pathogenicity island 1 type III secretion system through HilD.* J Bacteriol, 2008. **190**(2): p. 476-86.
154. Escolar, L., J. Perez-Martin, and V. de Lorenzo, *Opening the iron box: transcriptional metalloregulation by the Fur protein.* J Bacteriol, 1999. **181**(20): p. 6223-9.
155. Masse, E. and S. Gottesman, *A small RNA regulates the expression of genes involved in iron metabolism in Escherichia coli.* Proc Natl Acad Sci U S A, 2002. **99**(7): p. 4620-5.
156. Masse, E., F.E. Escorcia, and S. Gottesman, *Coupled degradation of a small regulatory RNA and its mRNA targets in Escherichia coli.* Genes Dev, 2003. **17**(19): p. 2374-83.
157. Jacques, J.F., et al., *RyhB small RNA modulates the free intracellular iron pool and is essential for normal growth during iron limitation in Escherichia coli.* Mol Microbiol, 2006. **62**(4): p. 1181-90.
158. Masse, E., et al., *Small RNAs controlling iron metabolism.* Curr Opin Microbiol, 2007. **10**(2): p. 140-5.
159. Masse, E., C.K. Vanderpool, and S. Gottesman, *Effect of RyhB small RNA on global iron use in Escherichia coli.* J Bacteriol, 2005. **187**(20): p. 6962-71.
160. Nandal, A., et al., *Induction of the ferritin gene (ftnA) of Escherichia coli by Fe(2+)-Fur is mediated by reversal of H-NS silencing and is RyhB independent.* Mol Microbiol, 2010. **75**(3): p. 637-57.
161. Desnoyers, G., et al., *Small RNA-induced differential degradation of the polycistronic mRNA iscRSUA.* EMBO J, 2009. **28**(11): p. 1551-61.
162. Vecerek, B., I. Moll, and U. Blasi, *Control of Fur synthesis by the non-coding RNA RyhB and iron-responsive decoding.* EMBO J, 2007. **26**(4): p. 965-75.
163. Prevost, K., et al., *The small RNA RyhB activates the translation of shiA mRNA encoding a permease of shikimate, a compound involved in siderophore synthesis.* Mol Microbiol, 2007. **64**(5): p. 1260-73.
164. Gibson, F. and D.I. Magrath, *The isolation and characterization of a hydroxamic acid (aerobactin) formed by Aerobacter aerogenes 62-I.* Biochim Biophys Acta, 1969. **192**(2): p. 175-84.
165. Williams, P.H. and P.J. Warner, *ColV plasmid-mediated, colicin V-independent iron uptake system of invasive strains of Escherichia coli.* Infect Immun, 1980. **29**(2): p. 411-6.
166. Carbonetti, N.H. and P.H. Williams, *A cluster of five genes specifying the aerobactin iron uptake system of plasmid ColV-K30.* Infect Immun, 1984. **46**(1): p. 7-12.
167. de Lorenzo, V., et al., *Aerobactin biosynthesis and transport genes of plasmid ColV-K30 in Escherichia coli K-12.* J Bacteriol, 1986. **165**(2): p. 570-8.
168. de Lorenzo, V., et al., *Operator sequences of the aerobactin operon of plasmid ColV-K30 binding the ferric uptake regulation (fur) repressor.* J Bacteriol, 1987. **169**(6): p. 2624-30.

169. Thariath, A., et al., *Construction and biochemical characterization of recombinant cytoplasmic forms of the IucD protein (lysine:N6-hydroxylase) encoded by the pColV-K30 aerobactin gene cluster.* J Bacteriol, 1993. **175**(3): p. 589-96.
170. Coy, M., et al., *Isolation and properties of N epsilon-hydroxylysine:acetyl coenzyme A N epsilon-transacetylase from Escherichia coli pABN11.* Biochemistry, 1986. **25**(9): p. 2485-9.
171. de Lorenzo, V. and J.B. Neilands, *Characterization of iucA and iucC genes of the aerobactin system of plasmid ColV-K30 in Escherichia coli.* J Bacteriol, 1986. **167**(1): p. 350-5.
172. Karp, P.D., *EcoCyc - A member of the BioCyc database collection*. 2010, SRI International.
173. Koster, W. and V. Braun, *Iron (III) hydroxamate transport into Escherichia coli. Substrate binding to the periplasmic FhuD protein.* J Biol Chem, 1990. **265**(35): p. 21407-10.
174. Fecker, L. and V. Braun, *Cloning and expression of the fhu genes involved in iron(III)-hydroxamate uptake by Escherichia coli.* J Bacteriol, 1983. **156**(3): p. 1301-14.
175. Wooldridge, K.G., J.A. Morrissey, and P.H. Williams, *Transport of ferric-aerobactin into the periplasm and cytoplasm of Escherichia coli K12: role of envelope-associated proteins and effect of endogenous siderophores.* J Gen Microbiol, 1992. **138**(3): p. 597-603.
176. Burkhardt, R. and V. Braun, *Nucleotide sequence of the fhuC and fhuD genes involved in iron (III) hydroxamate transport: domains in FhuC homologous to ATP-binding proteins.* Mol Gen Genet, 1987. **209**(1): p. 49-55.
177. Hantke, K., *Regulation of ferric iron transport in Escherichia coli K12: isolation of a constitutive mutant.* Mol Gen Genet, 1981. **182**(2): p. 288-92.
178. Ozenberger, B.A., T.J. Brickman, and M.A. McIntosh, *Nucleotide sequence of Escherichia coli isochorismate synthetase gene entC and evolutionary relationship of isochorismate synthetase and other chorismate-utilizing enzymes.* J Bacteriol, 1989. **171**(2): p. 775-83.
179. Liu, J., et al., *Overexpression, purification, and characterization of isochorismate synthase (EntC), the first enzyme involved in the biosynthesis of enterobactin from chorismate.* Biochemistry, 1990. **29**(6): p. 1417-25.
180. Rusnak, F., et al., *Subcloning of the enterobactin biosynthetic gene entB: expression, purification, characterization, and substrate specificity of isochorismatase.* Biochemistry, 1990. **29**(6): p. 1425-35.
181. Liu, J., K. Duncan, and C.T. Walsh, *Nucleotide sequence of a cluster of Escherichia coli enterobactin biosynthesis genes: identification of entA and purification of its product 2,3-dihydro-2,3-dihydroxybenzoate dehydrogenase.* J Bacteriol, 1989. **171**(2): p. 791-8.
182. Sakaitani, M., et al., *Mechanistic studies on trans-2,3-dihydro-2,3-dihydroxybenzoate dehydrogenase (Ent A) in the biosynthesis of the iron chelator enterobactin.* Biochemistry, 1990. **29**(29): p. 6789-98.

183. Lipmann, F., et al., *Polypeptide synthesis on protein templates: the enzymatic synthesis of gramicidin S and tyrocidine.* Adv Enzymol Relat Areas Mol Biol, 1971. **35**: p. 1-34.
184. Marahiel, M.A., *Multidomain enzymes involved in peptide synthesis.* FEBS Lett, 1992. **307**(1): p. 40-3.
185. Marahiel, M.A., *Protein templates for the biosynthesis of peptide antibiotics.* Chem Biol, 1997. **4**(8): p. 561-7.
186. Gehring, A.M., K.A. Bradley, and C.T. Walsh, *Enterobactin biosynthesis in Escherichia coli: isochorismate lyase (EntB) is a bifunctional enzyme that is phosphopantetheinylated by EntD and then acylated by EntE using ATP and 2,3-dihydroxybenzoate.* Biochemistry, 1997. **36**(28): p. 8495-503.
187. Ehmann, D.E., et al., *The EntF and EntE adenylation domains of Escherichia coli enterobactin synthetase: sequestration and selectivity in acyl-AMP transfers to thiolation domain cosubstrates.* Proc Natl Acad Sci U S A, 2000. **97**(6): p. 2509-14.
188. Roche, E.D. and C.T. Walsh, *Dissection of the EntF condensation domain boundary and active site residues in nonribosomal peptide synthesis.* Biochemistry, 2003. **42**(5): p. 1334-44.
189. Rusnak, F., W.S. Faraci, and C.T. Walsh, *Subcloning, expression, and purification of the enterobactin biosynthetic enzyme 2,3-dihydroxybenzoate-AMP ligase: demonstration of enzyme-bound (2,3-dihydroxybenzoyl)adenylate product.* Biochemistry, 1989. **28**(17): p. 6827-35.
190. Frueh, D.P., et al., *Dynamic thiolation-thioesterase structure of a non-ribosomal peptide synthetase.* Nature, 2008. **454**(7206): p. 903-6.
191. Gehring, A.M., I. Mori, and C.T. Walsh, *Reconstitution and characterization of the Escherichia coli enterobactin synthetase from EntB, EntE, and EntF.* Biochemistry, 1998. **37**(8): p. 2648-59.
192. Guo, Z.F., et al., *Suppression of linear side products by macromolecular crowding in nonribosomal enterobactin biosynthesis.* Org Lett, 2008. **10**(4): p. 649-52.
193. Furrer, J.L., et al., *Export of the siderophore enterobactin in Escherichia coli: involvement of a 43 kDa membrane exporter.* Mol Microbiol, 2002. **44**(5): p. 1225-34.
194. Ozenberger, B.A., M.S. Nahlik, and M.A. McIntosh, *Genetic organization of multiple fep genes encoding ferric enterobactin transport functions in Escherichia coli.* J Bacteriol, 1987. **169**(8): p. 3638-46.
195. O'Brien, I.G., G.B. Cox, and F. Gibson, *Enterochelin hydrolysis and iron metabolism in Escherichia coli.* Biochim Biophys Acta, 1971. **237**(3): p. 537-49.
196. Hantke, K., *Dihydroxybenzoylserine--a siderophore for E. coli.* FEMS Microbiol Lett, 1990. **55**(1-2): p. 5-8.
197. Bleuel, C., et al., *TolC is involved in enterobactin efflux across the outer membrane of Escherichia coli.* J Bacteriol, 2005. **187**(19): p. 6701-7.
198. Misra, R. and V.N. Bavro, *Assembly and transport mechanism of tripartite drug efflux systems.* Biochim Biophys Acta, 2009. **1794**(5): p. 817-25.
199. Piddock, L.J., *Multidrug-resistance efflux pumps - not just for resistance.* Nat Rev Microbiol, 2006. **4**(8): p. 629-36.

200. Masi, M., et al., *Initial steps of colicin E1 import across the outer membrane of Escherichia coli.* J Bacteriol, 2007. **189**(7): p. 2667-76.
201. Wandersman, C. and P. Delepelaire, *TolC, an Escherichia coli outer membrane protein required for hemolysin secretion.* Proc Natl Acad Sci U S A, 1990. **87**(12): p. 4776-80.
202. Yamanaka, H., et al., *MacAB is involved in the secretion of Escherichia coli heat-stable enterotoxin II.* J Bacteriol, 2008. **190**(23): p. 7693-8.
203. Pierce, J.R. and C.F. Earhart, *Escherichia coli K-12 envelope proteins specifically required for ferrienterobactin uptake.* J Bacteriol, 1986. **166**(3): p. 930-6.
204. Lundrigan, M.D. and R.J. Kadner, *Nucleotide sequence of the gene for the ferrienterochelin receptor FepA in Escherichia coli. Homology among outer membrane receptors that interact with TonB.* J Biol Chem, 1986. **261**(23): p. 10797-801.
205. Buchanan, S.K., et al., *Crystal structure of the outer membrane active transporter FepA from Escherichia coli.* Nat Struct Biol, 1999. **6**(1): p. 56-63.
206. Murphy, C.K., V.I. Kalve, and P.E. Klebba, *Surface topology of the Escherichia coli K-12 ferric enterobactin receptor.* J Bacteriol, 1990. **172**(5): p. 2736-46.
207. Usher, K.C., et al., *The plug domain of FepA, a TonB-dependent transport protein from Escherichia coli, binds its siderophore in the absence of the transmembrane barrel domain.* Proc Natl Acad Sci U S A, 2001. **98**(19): p. 10676-81.
208. Pierce, J.R., C.L. Pickett, and C.F. Earhart, *Two fep genes are required for ferrienterochelin uptake in Escherichia coli K-12.* J Bacteriol, 1983. **155**(1): p. 330-6.
209. Heidinger, S., et al., *Iron supply to Escherichia coli by synthetic analogs of enterochelin.* J Bacteriol, 1983. **153**(1): p. 109-15.
210. Wookey, P. and H. Rosenberg, *Involvement of inner and outer membrane components in the transport of iron and in colicin B action in Escherichia coli.* J Bacteriol, 1978. **133**(2): p. 661-6.
211. Annamalai, R., et al., *Recognition of ferric catecholates by FepA.* J Bacteriol, 2004. **186**(11): p. 3578-89.
212. Nikaido, H. and E.Y. Rosenberg, *Cir and Fiu proteins in the outer membrane of Escherichia coli catalyze transport of monomeric catechols: study with beta-lactam antibiotics containing catechol and analogous groups.* J Bacteriol, 1990. **172**(3): p. 1361-7.
213. Larsen, R.A., T.E. Letain, and K. Postle, *In vivo evidence of TonB shuttling between the cytoplasmic and outer membrane in Escherichia coli.* Mol Microbiol, 2003. **49**(1): p. 211-8.
214. Letain, T.E. and K. Postle, *TonB protein appears to transduce energy by shuttling between the cytoplasmic membrane and the outer membrane in Escherichia coli.* Mol Microbiol, 1997. **24**(2): p. 271-83.
215. Higgs, P.I., R.A. Larsen, and K. Postle, *Quantification of known components of the Escherichia coli TonB energy transduction system: TonB, ExbB, ExbD and FepA.* Mol Microbiol, 2002. **44**(1): p. 271-81.
216. Higgs, P.I., P.S. Myers, and K. Postle, *Interactions in the TonB-dependent energy transduction complex: ExbB and ExbD form homomultimers.* J Bacteriol, 1998. **180**(22): p. 6031-8.

217. Larsen, R.A., M.G. Thomas, and K. Postle, *Protonmotive force, ExbB and ligand-bound FepA drive conformational changes in TonB.* Mol Microbiol, 1999. **31**(6): p. 1809-24.
218. Ferguson, A.D. and J. Deisenhofer, *TonB-dependent receptors-structural perspectives.* Biochim Biophys Acta, 2002. **1565**(2): p. 318-32.
219. Sprencel, C., et al., *Binding of ferric enterobactin by the Escherichia coli periplasmic protein FepB.* J Bacteriol, 2000. **182**(19): p. 5359-64.
220. Shea, C.M. and M.A. McIntosh, *Nucleotide sequence and genetic organization of the ferric enterobactin transport system: homology to other periplasmic binding protein-dependent systems in Escherichia coli.* Mol Microbiol, 1991. **5**(6): p. 1415-28.
221. Chenault, S.S. and C.F. Earhart, *Organization of genes encoding membrane proteins of the Escherichia coli ferrienterobactin permease.* Mol Microbiol, 1991. **5**(6): p. 1405-13.
222. Chenault, S.S. and C.F. Earhart, *Identification of hydrophobic proteins FepD and FepG of the Escherichia coli ferrienterobactin permease.* J Gen Microbiol, 1992. **138**(10): p. 2167-71.
223. Crouch, M.L., et al., *Biosynthesis and IroC-dependent export of the siderophore salmochelin are essential for virulence of Salmonella enterica serovar Typhimurium.* Mol Microbiol, 2008. **67**(5): p. 971-83.
224. Newton, S.M., et al., *Direct measurements of the outer membrane stage of ferric enterobactin transport: postuptake binding.* J Biol Chem, 2010. **285**(23): p. 17488-97.
225. Winkelmann, G., et al., *HPLC separation of enterobactin and linear 2,3-dihydroxybenzoylserine derivatives: a study on mutants of Escherichia coli defective in regulation (fur), esterase (fes) and transport (fepA).* Biometals, 1994. **7**(2): p. 149-54.
226. Langman, L., et al., *Enterochelin system of iron transport in Escherichia coli: mutations affecting ferric-enterochelin esterase.* J Bacteriol, 1972. **112**(3): p. 1142-9.
227. Greenwood, K.T. and R.K. Luke, *Enzymatic hydrolysis of enterochelin and its iron complex in Escherichia Coli K-12. Properties of enterochelin esterase.* Biochim Biophys Acta, 1978. **525**(1): p. 209-18.
228. Brickman, T.J. and M.A. McIntosh, *Overexpression and purification of ferric enterobactin esterase from Escherichia coli. Demonstration of enzymatic hydrolysis of enterobactin and its iron complex.* J Biol Chem, 1992. **267**(17): p. 12350-5.
229. Lin, H., et al., *In vitro characterization of salmochelin and enterobactin trilactone hydrolases IroD, IroE, and Fes.* J Am Chem Soc, 2005. **127**(31): p. 11075-84.
230. Berner, I., et al., *Identification of enterobactin and linear dihydroxybenzoylserine compounds by HPLC and ion spray mass spectrometry (LC/MS and MS/MS).* Biol Met, 1991. **4**(2): p. 113-8.
231. O'Brien, I.G., G.B. Cox, and F. Gibson, *Biologically active compounds containing 2,3-dihydroxybenzoic acid and serine formed by Escherichia coli.* Biochim Biophys Acta, 1970. **201**(3): p. 453-60.

232. Ernst, J.F., R.L. Bennett, and L.I. Rothfield, *Constitutive expression of the iron-enterochelin and ferrichrome uptake systems in a mutant strain of Salmonella typhimurium.* J Bacteriol, 1978. **135**(3): p. 928-34.
233. Brickman, T.J., B.A. Ozenberger, and M.A. McIntosh, *Regulation of divergent transcription from the iron-responsive fepB-entC promoter-operator regions in Escherichia coli.* J Mol Biol, 1990. **212**(4): p. 669-82.
234. Christoffersen, C.A., et al., *Regulatory architecture of the iron-regulated fepD-ybdA bidirectional promoter region in Escherichia coli.* J Bacteriol, 2001. **183**(6): p. 2059-70.
235. Hunt, M.D., G.S. Pettis, and M.A. McIntosh, *Promoter and operator determinants for fur-mediated iron regulation in the bidirectional fepA-fes control region of the Escherichia coli enterobactin gene system.* J Bacteriol, 1994. **176**(13): p. 3944-55.
236. Foster, J.W. and H.K. Hall, *Effect of Salmonella typhimurium ferric uptake regulator (fur) mutations on iron- and pH-regulated protein synthesis.* J Bacteriol, 1992. **174**(13): p. 4317-23.
237. Baumler, A.J., et al., *Identification of a new iron regulated locus of Salmonella typhi.* Gene, 1996. **183**(1-2): p. 207-13.
238. Baumler, A.J., et al., *IroN, a novel outer membrane siderophore receptor characteristic of Salmonella enterica.* J Bacteriol, 1998. **180**(6): p. 1446-53.
239. Chen, Y.T., et al., *Sequencing and analysis of the large virulence plasmid pLVPK of Klebsiella pneumoniae CG43.* Gene, 2004. **337**: p. 189-98.
240. Yang, F., et al., *Genome dynamics and diversity of Shigella species, the etiologic agents of bacillary dysentery.* Nucleic Acids Res, 2005. **33**(19): p. 6445-58.
241. Russo, T.A., et al., *Identification of genes in an extraintestinal isolate of Escherichia coli with increased expression after exposure to human urine.* Infect Immun, 1999. **67**(10): p. 5306-14.
242. Johnson, J.R., et al., *Molecular epidemiological and phylogenetic associations of two novel putative virulence genes, iha and iroN(E. coli), among Escherichia coli isolates from patients with urosepsis.* Infect Immun, 2000. **68**(5): p. 3040-7.
243. Bister, B., et al., *The structure of salmochelins: C-glucosylated enterobactins of Salmonella enterica.* Biometals, 2004. **17**(4): p. 471-81.
244. Fischbach, M.A., et al., *In vitro characterization of IroB, a pathogen-associated C-glycosyltransferase.* Proc Natl Acad Sci U S A, 2005. **102**(3): p. 571-6.
245. Wawszkiewicz, E.J. and H.A. Schneider, *Control of salmonellosis pacifarin biosynthesis by iron.* Infect Immun, 1975. **11**(1): p. 69-72.
246. Zhu, M., et al., *Functions of the siderophore esterases IroD and IroE in iron-salmochelin utilization.* Microbiology, 2005. **151**(Pt 7): p. 2363-72.
247. Luo, M., et al., *Enzymatic tailoring of enterobactin alters membrane partitioning and iron acquisition.* ACS Chem Biol, 2006. **1**(1): p. 29-32.
248. Lagos, R., et al., *Structure, organization and characterization of the gene cluster involved in the production of microcin E492, a channel-forming bacteriocin.* Mol Microbiol, 2001. **42**(1): p. 229-43.
249. Patzer, S.I., et al., *The colicin G, H and X determinants encode microcins M and H47, which might utilize the catecholate siderophore receptors FepA, Cir, Fiu and IroN.* Microbiology, 2003. **149**(Pt 9): p. 2557-70.

250. Azpiroz, M.F. and M. Lavina, *Involvement of enterobactin synthesis pathway in production of microcin H47.* Antimicrob Agents Chemother, 2004. **48**(4): p. 1235-41.
251. Poey, M.E., M.F. Azpiroz, and M. Lavina, *Comparative analysis of chromosome-encoded microcins.* Antimicrob Agents Chemother, 2006. **50**(4): p. 1411-8.
252. Thomas, X., et al., *Siderophore peptide, a new type of post-translationally modified antibacterial peptide with potent activity.* J Biol Chem, 2004. **279**(27): p. 28233-42.
253. Vassiliadis, G., et al., *Insight into siderophore-carrying peptide biosynthesis: enterobactin is a precursor for microcin E492 posttranslational modification.* Antimicrob Agents Chemother, 2007. **51**(10): p. 3546-53.
254. Vassiliadis, G., et al., *Isolation and characterization of two members of the siderophore-microcin family, microcins M and H47.* Antimicrob Agents Chemother, 2010. **54**(1): p. 288-97.
255. Nolan, E.M., et al., *Biosynthetic tailoring of microcin E492m: post-translational modification affords an antibacterial siderophore-peptide conjugate.* J Am Chem Soc, 2007. **129**(46): p. 14336-47.
256. Mercado, G., et al., *The production in vivo of microcin E492 with antibacterial activity depends on salmochelin and EntF.* J Bacteriol, 2008. **190**(15): p. 5464-71.
257. Strahsburger, E., et al., *Cooperative uptake of microcin E492 by receptors FepA, Fiu, and Cir and inhibition by the siderophore enterochelin and its dimeric and trimeric hydrolysis products.* Antimicrob Agents Chemother, 2005. **49**(7): p. 3083-6.
258. Duquesne, S., et al., *Microcins, gene-encoded antibacterial peptides from enterobacteria.* Nat Prod Rep, 2007. **24**(4): p. 708-34.
259. Russo, T.A., et al., *IroN functions as a siderophore receptor and is a urovirulence factor in an extraintestinal pathogenic isolate of Escherichia coli.* Infect Immun, 2002. **70**(12): p. 7156-60.
260. Rabsch, W., et al., *Salmonella typhimurium IroN and FepA proteins mediate uptake of enterobactin but differ in their specificity for other siderophores.* J Bacteriol, 1999. **181**(11): p. 3610-2.
261. Methner, U., et al., *Effect of norepinephrine on colonisation and systemic spread of Salmonella enterica in infected animals: role of catecholate siderophore precursors and degradation products.* Int J Med Microbiol, 2008. **298**(5-6): p. 429-39.
262. Anderson, M.T. and S.K. Armstrong, *The Bordetella bfe system: growth and transcriptional response to siderophores, catechols, and neuroendocrine catecholamines.* J Bacteriol, 2006. **188**(16): p. 5731-40.
263. Valvano, M.A. and J.H. Crosa, *Aerobactin iron transport genes commonly encoded by certain ColV plasmids occur in the chromosome of a human invasive strain of Escherichia coli K1.* Infect Immun, 1984. **46**(1): p. 159-67.
264. Valvano, M.A. and J.H. Crosa, *Molecular cloning, expression, and regulation in Escherichia coli K-12 of a chromosome-mediated aerobactin iron transport system from a human invasive isolate of E. coli K1.* J Bacteriol, 1988. **170**(12): p. 5529-38.

265. Bindereif, A. and J.B. Neilands, *Aerobactin genes in clinical isolates of Escherichia coli.* J Bacteriol, 1985. **161**(2): p. 727-35.
266. Carbonetti, N.H., et al., *Aerobactin-mediated iron uptake by Escherichia coli isolates from human extraintestinal infections.* Infect Immun, 1986. **51**(3): p. 966-8.
267. Lafont, J.P., et al., *Presence and expression of aerobactin genes in virulent avian strains of Escherichia coli.* Infect Immun, 1987. **55**(1): p. 193-7.
268. Opal, S.M., et al., *Aerobactin and alpha-hemolysin as virulence determinants in Escherichia coli isolated from human blood, urine, and stool.* J Infect Dis, 1990. **161**(4): p. 794-6.
269. Linggood, M.A., et al., *Incidence of the aerobactin iron uptake system among Escherichia coli isolates from infections of farm animals.* J Gen Microbiol, 1987. **133**(4): p. 835-42.
270. Johnson, J.R., et al., *Aerobactin and other virulence factor genes among strains of Escherichia coli causing urosepsis: association with patient characteristics.* Infect Immun, 1988. **56**(2): p. 405-12.
271. Dozois, C.M., et al., *pap-and pil-related DNA sequences and other virulence determinants associated with Escherichia coli isolated from septicemic chickens and turkeys.* Infect Immun, 1992. **60**(7): p. 2648-56.
272. Emery, D.A., et al., *Virulence factors of Escherichia coli associated with colisepticemia in chickens and turkeys.* Avian Dis, 1992. **36**(3): p. 504-11.
273. Vidotto, M.C., et al., *Virulence factors of avian Escherichia coli.* Avian Dis, 1990. **34**(3): p. 531-8.
274. Delicato, E.R., et al., *Virulence-associated genes in Escherichia coli isolates from poultry with colibacillosis.* Vet Microbiol, 2003. **94**(2): p. 97-103.
275. Williams, P.H. and N.H. Carbonetti, *Iron, siderophores, and the pursuit of virulence: independence of the aerobactin and enterochelin iron uptake systems in Escherichia coli.* Infect Immun, 1986. **51**(3): p. 942-7.
276. Konopka, K. and J.B. Neilands, *Effect of serum albumin on siderophore-mediated utilization of transferrin iron.* Biochemistry, 1984. **23**(10): p. 2122-7.
277. Konopka, K., A. Bindereif, and J.B. Neilands, *Aerobactin-mediated utilization of transferrin iron.* Biochemistry, 1982. **21**(25): p. 6503-8.
278. Der Vartanian, M., *Differences in excretion and efficiency of the aerobactin and enterochelin siderophores in a bovine pathogenic strain of Escherichia coli.* Infect Immun, 1988. **56**(2): p. 413-8.
279. Valdebenito, M., et al., *Environmental factors influence the production of enterobactin, salmochelin, aerobactin, and yersiniabactin in Escherichia coli strain Nissle 1917.* Int J Med Microbiol, 2006. **296**(8): p. 513-20.
280. Worsham, P.L. and J. Konisky, *Effect of growth temperature on the acquisition of iron by Salmonella typhimurium and Escherichia coli.* J Bacteriol, 1984. **158**(1): p. 163-8.
281. Rogers, H.J., *Iron-Binding Catechols and Virulence in Escherichia coli.* Infect Immun, 1973. **7**(3): p. 445-456.
282. Brock, J.H., et al., *Role of antibody and enterobactin in controlling growth of Escherichia coli in human milk and acquisition of lactoferrin- and transferrin-bound iron by Escherichia coli.* Infect Immun, 1983. **40**(2): p. 453-9.

283. Brock, J.H., et al., *Relative availability of transferrin-bound iron and cell-derived iron to aerobactin-producing and enterochelin-producing strains of Escherichia coli and to other microorganisms.* Infect Immun, 1991. **59**(9): p. 3185-90.
284. Griffiths, E. and J. Humphreys, *Isolation of enterochelin from the peritoneal washings of guinea pigs lethally infected with Escherichia coli.* Infect Immun, 1980. **28**(1): p. 286-9.
285. Snyder, J.A., et al., *Transcriptome of uropathogenic Escherichia coli during urinary tract infection.* Infect Immun, 2004. **72**(11): p. 6373-81.
286. Reigstad, C.S., S.J. Hultgren, and J.I. Gordon, *Functional genomic studies of uropathogenic Escherichia coli and host urothelial cells when intracellular bacterial communities are assembled.* J Biol Chem, 2007. **282**(29): p. 21259-67.
287. Kochan, I., J. Wasynczuk, and M.A. McCabe, *Effects of injected iron and siderophores on infections in normal and immune mice.* Infect Immun, 1978. **22**(2): p. 560-7.
288. Yancey, R.J., S.A. Breeding, and C.E. Lankford, *Enterochelin (enterobactin): virulence factor for Salmonella typhimurium.* Infect Immun, 1979. **24**(1): p. 174-80.
289. O'Brien, A.D., *Innate resistance of mice to Salmonella typhi infection.* Infect Immun, 1982. **38**(3): p. 948-52.
290. Fernandez-Beros, M.E., et al., *Immune response to the iron-deprivation-induced proteins of Salmonella typhi in typhoid fever.* Infect Immun, 1989. **57**(4): p. 1271-5.
291. Gorbacheva, V.Y., et al., *Restricted growth of ent(-) and tonB mutants of Salmonella enterica serovar Typhi in human Mono Mac 6 monocytic cells.* FEMS Microbiol Lett, 2001. **196**(1): p. 7-11.
292. Eriksson, S., et al., *Unravelling the biology of macrophage infection by gene expression profiling of intracellular Salmonella enterica.* Mol Microbiol, 2003. **47**(1): p. 103-18.
293. Bearson, B.L., et al., *Iron regulated genes of Salmonella enterica serovar Typhimurium in response to norepinephrine and the requirement of fepDGC for norepinephrine-enhanced growth.* Microbes Infect, 2008. **10**(7): p. 807-16.
294. Williams, P.H., et al., *Catecholate receptor proteins in Salmonella enterica: role in virulence and implications for vaccine development.* Vaccine, 2006. **24**(18): p. 3840-4.
295. Freestone, P.P., et al., *The mammalian neuroendocrine hormone norepinephrine supplies iron for bacterial growth in the presence of transferrin or lactoferrin.* J Bacteriol, 2000. **182**(21): p. 6091-8.
296. Burton, C.L., et al., *The growth response of Escherichia coli to neurotransmitters and related catecholamine drugs requires a functional enterobactin biosynthesis and uptake system.* Infect Immun, 2002. **70**(11): p. 5913-23.
297. Freestone, P.P., et al., *Involvement of enterobactin in norepinephrine-mediated iron supply from transferrin to enterohaemorrhagic Escherichia coli.* FEMS Microbiol Lett, 2003. **222**(1): p. 39-43.
298. Sandrini, S.M., et al., *Elucidation of the mechanism by which catecholamine stress hormones liberate iron from the innate immune defense proteins transferrin and lactoferrin.* J Bacteriol. **192**(2): p. 587-94.

299. Spencer, H., et al., *Genome-wide transposon mutagenesis identifies a role for host neuroendocrine stress hormones in regulating the expression of virulence genes in Salmonella.* J Bacteriol, 2010. **192**(3): p. 714-24.
300. Freestone, P.P., et al., *Growth stimulation of intestinal commensal Escherichia coli by catecholamines: a possible contributory factor in trauma-induced sepsis.* Shock, 2002. **18**(5): p. 465-70.
301. Baumler, A.J., F. Heffron, and R. Reissbrodt, *Rapid detection of Salmonella enterica with primers specific for iroB.* J Clin Microbiol, 1997. **35**(5): p. 1224-30.
302. Welch, R.A., et al., *Extensive mosaic structure revealed by the complete genome sequence of uropathogenic Escherichia coli.* Proc Natl Acad Sci U S A, 2002. **99**(26): p. 17020-4.
303. Chen, S.L., et al., *Identification of genes subject to positive selection in uropathogenic strains of Escherichia coli: a comparative genomics approach.* Proc Natl Acad Sci U S A, 2006. **103**(15): p. 5977-82.
304. Bauer, R.J., et al., *Molecular epidemiology of 3 putative virulence genes for Escherichia coli urinary tract infection-usp, iha, and iroN(E. coli).* J Infect Dis, 2002. **185**(10): p. 1521-4.
305. Johnson, J.R., et al., *Epidemiological correlates of virulence genotype and phylogenetic background among Escherichia coli blood isolates from adults with diverse-source bacteremia.* J Infect Dis, 2002. **185**(10): p. 1439-47.
306. Sorsa, L.J., et al., *Characterization of an iroBCDEN gene cluster on a transmissible plasmid of uropathogenic Escherichia coli: evidence for horizontal transfer of a chromosomal virulence factor.* Infect Immun, 2003. **71**(6): p. 3285-93.
307. Grozdanov, L., et al., *Analysis of the genome structure of the nonpathogenic probiotic Escherichia coli strain Nissle 1917.* J Bacteriol, 2004. **186**(16): p. 5432-41.
308. Mellata, M., J.W. Touchman, and R. Curtiss, *Full sequence and comparative analysis of the plasmid pAPEC-1 of avian pathogenic E. coli chi7122 (O78:K80:H9).* PLoS ONE, 2009. **4**(1): p. e4232.
309. Johnson, T.J., S.J. Johnson, and L.K. Nolan, *Complete DNA sequence of a ColBM plasmid from avian pathogenic Escherichia coli suggests that it evolved from closely related ColV virulence plasmids.* J Bacteriol, 2006. **188**(16): p. 5975-83.
310. Johnson, T.J., et al., *DNA sequence of a ColV plasmid and prevalence of selected plasmid-encoded virulence genes among avian Escherichia coli strains.* J Bacteriol, 2006. **188**(2): p. 745-58.
311. Bonacorsi, S., et al., *Molecular analysis and experimental virulence of French and North American Escherichia coli neonatal meningitis isolates: identification of a new virulent clone.* J Infect Dis, 2003. **187**(12): p. 1895-906.
312. Peigne, C., et al., *The plasmid of neonatal meningitis Escherichia coli strain S88 (O45:K1:H7) is closely related to avian pathogenic E. coli plasmids and is associated with high level bacteremia in neonatal rat meningitis model.* Infect Immun, 2009.
313. Vandekerchove, D., et al., *Virulence-associated traits in avian Escherichia coli: comparison between isolates from colibacillosis-affected and clinically healthy layer flocks.* Vet Microbiol, 2005. **108**(1-2): p. 75-87.

314. Schouler, C., et al., *Genomic subtraction for the identification of putative new virulence factors of an avian pathogenic Escherichia coli strain of O2 serogroup.* Microbiology, 2004. **150**(Pt 9): p. 2973-84.
315. Johnson, J.R., P. Delavari, and T.T. O'Bryan, *Escherichia coli O18:K1:H7 isolates from patients with acute cystitis and neonatal meningitis exhibit common phylogenetic origins and virulence factor profiles.* J Infect Dis, 2001. **183**(3): p. 425-34.
316. Ananias, M. and T. Yano, *Serogroups and virulence genotypes of Escherichia coli isolated from patients with sepsis.* Braz J Med Biol Res, 2008. **41**(10): p. 877-83.
317. Hejnova, J., et al., *Characterization of the flexible genome complement of the commensal Escherichia coli strain A0 34/86 (O83 : K24 : H31).* Microbiology, 2005. **151**(Pt 2): p. 385-98.
318. Zdziarski, J., et al., *Molecular basis of commensalism in the urinary tract: low virulence or virulence attenuation?* Infect Immun, 2008. **76**(2): p. 695-703.
319. Negre, V.L., et al., *The siderophore receptor IroN, but not the high-pathogenicity island or the hemin receptor ChuA, contributes to the bacteremic step of Escherichia coli neonatal meningitis.* Infect Immun, 2004. **72**(2): p. 1216-20.
320. Feldmann, F., et al., *The salmochelin siderophore receptor IroN contributes to invasion of urothelial cells by extraintestinal pathogenic Escherichia coli in vitro.* Infect Immun, 2007. **75**(6): p. 3183-7.
321. Russo, T.A., et al., *The Siderophore receptor IroN of extraintestinal pathogenic Escherichia coli is a potential vaccine candidate.* Infect Immun, 2003. **71**(12): p. 7164-9.
322. Walters, M.S. and H.L. Mobley, *Identification of uropathogenic Escherichia coli surface proteins by shotgun proteomics.* J Microbiol Methods, 2009. **78**(2): p. 131-5.
323. Alteri, C.J., et al., *Mucosal immunization with iron receptor antigens protects against urinary tract infection.* PLoS Pathog, 2009. **5**(9): p. e1000586.
324. Kjeldsen, L., et al., *Isolation and primary structure of NGAL, a novel protein associated with human neutrophil gelatinase.* J Biol Chem, 1993. **268**(14): p. 10425-32.
325. Berger, T., et al., *Lipocalin 2-deficient mice exhibit increased sensitivity to Escherichia coli infection but not to ischemia-reperfusion injury.* Proc Natl Acad Sci U S A, 2006. **103**(6): p. 1834-9.
326. Goetz, D.H., et al., *The neutrophil lipocalin NGAL is a bacteriostatic agent that interferes with siderophore-mediated iron acquisition.* Mol Cell, 2002. **10**(5): p. 1033-43.
327. Kjeldsen, L., J.B. Cowland, and N. Borregaard, *Human neutrophil gelatinase-associated lipocalin and homologous proteins in rat and mouse.* Biochim Biophys Acta, 2000. **1482**(1-2): p. 272-83.
328. Yan, L., et al., *The high molecular weight urinary matrix metalloproteinase (MMP) activity is a complex of gelatinase B/MMP-9 and neutrophil gelatinase-associated lipocalin (NGAL). Modulation of MMP-9 activity by NGAL.* J Biol Chem, 2001. **276**(40): p. 37258-65.

329. Kjeldsen, L., et al., *Structural and functional heterogeneity among peroxidase-negative granules in human neutrophils: identification of a distinct gelatinase-containing granule subset by combined immunocytochemistry and subcellular fractionation.* Blood, 1993. **82**(10): p. 3183-91.
330. Borregaard, N., et al., *Biosynthesis of granule proteins in normal human bone marrow cells. Gelatinase is a marker of terminal neutrophil differentiation.* Blood, 1995. **85**(3): p. 812-7.
331. Flo, T.H., et al., *Lipocalin 2 mediates an innate immune response to bacterial infection by sequestrating iron.* Nature, 2004. **432**(7019): p. 917-21.
332. Miethke, M. and A. Skerra, *Neutrophil gelatinase-associated lipocalin expresses antimicrobial activity by interfering with L-norepinephrine-mediated bacterial iron acquisition.* Antimicrob Agents Chemother, 2010. **54**(4): p. 1580-9.
333. Devireddy, L.R., et al., *A mammalian siderophore synthesized by an enzyme with a bacterial homolog involved in enterobactin production.* Cell, 2010. **141**(6): p. 1006-17.
334. Datsenko, K.A. and B.L. Wanner, *One-step inactivation of chromosomal genes in Escherichia coli K-12 using PCR products.* Proc Natl Acad Sci U S A, 2000. **97**(12): p. 6640-5.
335. Heesemann, J., et al., *Virulence of Yersinia enterocolitica is closely associated with siderophore production, expression of an iron-repressible outer membrane polypeptide of 65,000 Da and pesticin sensitivity.* Mol Microbiol, 1993. **8**(2): p. 397-408.
336. Pelludat, C., et al., *The yersiniabactin biosynthetic gene cluster of Yersinia enterocolitica: organization and siderophore-dependent regulation.* J Bacteriol, 1998. **180**(3): p. 538-46.
337. Koczura, R. and A. Kaznowski, *The Yersinia high-pathogenicity island and iron-uptake systems in clinical isolates of Escherichia coli.* J Med Microbiol, 2003. **52**(Pt 8): p. 637-42.
338. Lawlor, M.S., C. O'Connor, and V.L. Miller, *Yersiniabactin is a virulence factor for Klebsiella pneumoniae during pulmonary infection.* Infect Immun, 2007. **75**(3): p. 1463-72.
339. Carniel, E., I. Guilvout, and M. Prentice, *Characterization of a large chromosomal "high-pathogenicity island" in biotype 1B Yersinia enterocolitica.* J Bacteriol, 1996. **178**(23): p. 6743-51.
340. Perry, R.D., et al., *Yersiniabactin from Yersinia pestis: biochemical characterization of the siderophore and its role in iron transport and regulation.* Microbiology, 1999. **145 (Pt 5)**: p. 1181-90.
341. Fetherston, J.D., et al., *The yersiniabactin transport system is critical for the pathogenesis of bubonic and pneumonic plague.* Infect Immun, 2010. **78**(5): p. 2045-52.
342. Pagano, A., et al., *Phylogeny and regulation of four lipocalin genes clustered in the chicken genome: evidence of a functional diversification after gene duplication.* Gene, 2004. **331**: p. 95-106.

Annexe

Annexe I

Iha from an *Escherichia coli* UTI outbreak clonal group A strain is expressed *in vivo* in the mouse urinary tract and functions as a catecholate siderophore receptor.

Simon Léveillé, **Mélissa Caza**, James R. Johnson, Connie Clabots, Mourad Sabri and Charles M. Dozois **(2006)** ***Infection and Immunity*** **74:3427-36**

A) Contribution de l'étudiante

1- L'article publié dans Infection and Immunity, met en lumière la caractérisation du premier facteur de virulence, Iha, caractérisé chez la souche UCB34 du groupe clonage A causant des infections urinaires. Iha est une protéine de la membrane externe servant à la fois d'adhésine aux cellules épithéliales et de récepteur de molécules dégradées de l'entérobactine, en plus de contribuer à la virulence de la souche lors d'une infection ascendante du tractus urinaire (UTI) murin.

2- L'étude a été réalisée d'abord en utilisant la technique de capture sélective des séquences transcrites (SCOTS) afin de découvrir les gènes uniques à la souche UCB34 qui sont transcrits lors d'une UTI chez la souris. De plus, des techniques de génétique bactérienne, un modèle d'infection ascendant du tractus urinaire murin, des tests d'adhésions aux cellules épithéliales, des réactions de qRT-PCR en temps réel ainsi que des courbes de croissances et d'internalisation de l'entérobactine et de DHBS purifiés ont été réalisés au cours de cette étude.

3- L'étudiante a purifié l'entérobactine et les produits dégradés (DHBS) et a fait les clones pIJ68 et pIJ120.

B) Résumé de l'article:

Les facteurs de virulence d'*Escherichia coli* pathogène appartenant à un groupe clonal émergeant et disséminé associé aux infections du tractus urinaire (UTI), désigné provisoirement groupe clonal A (CGA), n'ont pas été investigué expérimentalement.

Nous avons utilisé un modèle murin d'infection ascendante du tractus urinaire avec un membre du groupe CGA, la souche UCB34, dans le but d'identifier des gènes spécifiques aux CGA contribuant à l'UTI. Le gène *iha* a été identifié comme étant exprimé par la souche UCB34 dans les reins de souris en utilisant la technique de capture sélective de séquences transcrites (SCOTS). Le gène *iha* de la souche UCB34 a démontré un phénotype de récepteur de sidérophores lorsqu'il a été cloné dans une souche d'*E. coli* K-12 n'exprimant plus aucun récepteur de sidérophores de type catécholate, tel que démontré par des expériences de croissance et d'internalisation du ^{55}Fe complexé à l'entérobactine ou à son dérivé linéaire, le 2,3-dihydroxybenzoylserine (DHBS). La promotion de la croissance par les sidérophores et Iha est un processus dépendant à TonB. La croissance et l'internalisation du fer ont été plus efficaces avec des dérivés linéaires de DHBS que de l'entérobactine purifié. Le phénotype rapporté d'adhérence aux cellules épithéliales conféré à l'expression d'*iha* sur un vecteur de clonage à multi-copie dans une souche *E. coli* K-12 faiblement adhérente a été confirmé d'être spécifique à *iha*, en comparaison avec d'autres gènes codant pour des récepteurs de sidérophores. L'expression d'*iha* est régulé par le régulateur Fur et par la disponibilité du fer, tel que démontré par des expériences de « RT-PCR » en temps réel. Dans une expérience d'infection en compétition utilisant le modèle d'UTI murin, la souche sauvage UCB34 infecta mieux que la souche isogénique mutante pour le gène *iha*. Ainsi, Iha représente un récepteur de sidérophores catécholates régulé par Fur qui exhibe un phénotype d'adhérence, en plus d'être le premier facteur de virulence identifié chez une souche CGA.

INFECTION AND IMMUNITY, June 2006, p. 3427–3436 Vol. 74, No. 6
0019-9567/06/$08.00+0 doi:10.1128/IAI.00107-06

Iha from an *Escherichia coli* Urinary Tract Infection Outbreak Clonal Group A Strain Is Expressed In Vivo in the Mouse Urinary Tract and Functions as a Catecholate Siderophore Receptor

Simon Léveillé,[1] Mélissa Caza,[1] James R. Johnson,[2] Connie Clabots,[2] Mourad Sabri,[1] and Charles M. Dozois[1]*

Institut National de la Recherche Scientifique, INRS-Institut Armand-Frappier, Laval, Québec, Canada,[1] and Medical Service, VA Medical Center, and Department of Medicine, University of Minnesota, Minneapolis, Minnesota[2]

Received 20 January 2006/Returned for modification 23 February 2006/Accepted 16 March 2006

Virulence factors of pathogenic *Escherichia coli* belonging to a recently emerged and disseminated clonal group associated with urinary tract infection (UTI), provisionally designated clonal group A (CGA), have not been experimentally investigated. We used a mouse model of ascending UTI with CGA member strain UCB34 in order to identify genes of CGA that contribute to UTI. *iha* was identified to be expressed by strain UCB34 in the mouse kidney using selective capture of transcribed sequences. *iha* from strain UCB34 demonstrated a siderophore receptor phenotype when cloned in a catecholate siderophore receptor-negative *E. coli* K-12 strain, as shown by growth promotion experiments and uptake of ^{55}Fe complexed to enterobactin or its linear 2, 3-dihydroxybenzoylserine (DHBS) siderophore derivatives. Siderophore-mediated growth promotion by Iha was TonB dependent. Growth and iron uptake were more marked with linear DHBS derivatives than with purified enterobactin. The reported phenotype of adherence to epithelial cells conferred by expressing *iha* from a multicopy cloning vector in a poorly adherent *E. coli* K-12 host strain was confirmed to be specific to *iha*, in comparison with other siderophore receptor genes. *iha* expression was regulated by the ferric uptake regulator Fur and by iron availability, as shown by real-time reverse transcriptase PCR. In a competitive infection experiment using the mouse UTI model, wild-type strain UCB34 significantly outcompeted an isogenic *iha* null mutant. Iha thus represents a Fur-regulated catecholate siderophore receptor that, uniquely, exhibits an adherence-enhancing phenotype and is the first described urovirulence factor identified in a CGA strain.

Urinary tract infections (UTIs) are one of the most frequent bacterial infections in industrialized countries, and *Escherichia coli* is the major causal agent (26, 61). Many virulence factors associated with extraintestinal pathogenic *E. coli* (ExPEC) strains, the distinctive strains that cause most UTIs, are important for establishing infection. These include adhesins, toxins, iron acquisition systems, and capsular antigens (11, 23, 25). Extraintestinal infections, including UTIs, are caused predominantly by *E. coli* isolates belonging to phylogenetic group B2 (60 to 70%), whereas the remaining cases are caused mostly by strains belonging to phylogenetic group D (8, 42, 66). Most research into the pathogenic mechanisms of ExPEC has focused on archetype strains, such as CFT073, J96, CP9, and 536, which all belong to group B2. Much less attention has been given to the virulence mechanisms of group D ExPEC strains, which represent the second most important cause of UTI after group B2 strains (8, 41, 66).

Recently, a multidrug-resistant clonal group, termed clonal group A (CGA), was identified as a cause of UTI outbreaks in California, Michigan, and Minnesota (46). It is now known that this clonal group is widespread and quite prevalent throughout the United States and is also widely prevalent, although to a lesser extent, in many other countries (40, 41, 46). This newly emerged clonal group was responsible for up to 50% of the trimethoprim-sulfamethoxazole-resistant isolates identified in some areas (27, 40, 41, 46). The prevalence of resistance to trimethoprim-sulfamethoxazole, which is a commonly used first-line antibiotic therapy for UTIs (61), is increasing (32), which emphasizes the importance of elucidating the virulence mechanisms of CGA. CGA strains derive from *E. coli* phylogenetic group D (41) and demonstrate a fairly conserved virulence gene profile. Specifically, CGA strains commonly contain the F16 *papA* allele and *papG* allele II encoding a major subunit and adhesin of P fimbriae, respectively, *iutA* encoding the aerobactin siderophore receptor, *kpsMT*II encoding group II capsule synthesis, and *traT* encoding a plasmid-associated exclusion protein, whereas they typically lack *sfa/foc* (S and F1C fimbriae), *afa/dra* (Dr family adhesins), *hly* (hemolysin), *cnf* (cytotoxic necrotizing factor), *iroN* (siderophore receptor), *iss* (serum resistance associated), and *malX* (pathogenicity island marker) (40, 46). Hence, although CGA strains can cause UTIs in healthy women, they lack many of the virulence-associated genes common to group B2 ExPEC strains.

In order to investigate potential genes that may contribute to the capacity of CGA strains to cause UTIs, we used CGA strain UCB34 in a mouse model of ascending UTI for the identification of genes that are expressed in vivo. We used the cDNA capture method selective capture of transcribed sequences (SCOTS) to recover bacterial transcripts from infected tissues (15, 18). This strategy resulted in the capture of *iha* transcripts during infection in the mouse kidney.

Iha was first described as an adhesin in an enterohemorrhagic *E. coli* O157:H7 strain and was named "IrgA homologue

* Corresponding author. Mailing address: INRS-Institut Armand-Frappier, 531 boul. des Prairies, Laval H7V 1B7, Québec, Canada. Phone: (450) 687-5010, ext. 4221. Fax: (450) 686-5501. E-mail: charles.dozois@iaf.inrs.ca.

TABLE 1. *E. coli* strains and plasmids

Strain or plasmid	Genotype (siderophore[s])[a]	Source or reference
E. coli K-12 strains		
DM1187	*lexA51 lexA3*	50
H5058	*aroB tsx malT cirA fepA fiu* (Ent[b])	5
MG1655	F$^-$ λ$^-$ *rph-1* (Ent)	9
ORN172	*thr-1 leu-6 thi-1* Δ(*argF-lac*)*U169 xyl-7 ara-13 mtl-2 gal-6 rspL tonA2 minA minB* Δ(*fimEACDFGH*)::*kan pilG1*	63
QC2517	MG1655 *recD190*::Tn*10* Δ*fur*::*cat* (Ent)	20
QT1272	H5058 Δ*tonB*::*kan* (Ent[b])	This study
Other *E. coli* strains		
QT686	UCB34 Δ*iha*::*tetAR*(B) (Ent, Aero, Ybt[c])	This study
QT796	UCB34 Δ*fur*::*cat* (Ent, Aero, Ybt[c])	This study
UCB34	O17/77 ExPEC CGA isolate (cystitis); possesses F16 *papA*, *papGII*, *iutA*, *kpsMT*II, *fyuA*, *ybte*, *iha*; lacks *sfa*/*foc*, *afa*/*dra*, *hly*, *cnf*, *iroN*, *iss*, *malX* (Ent, Aero, Ybt[c])	Amee Manges, 46
χ7122	Avian pathogenic *E. coli*, O78:K80:H9; *gyrA* Nal[r] (Ent, Aero, Sal)	52
Plasmids		
pACYC184	p15A ori; Tc[r] Cm[r]	14
pAMR18	*Vibrio cholerae* CA401 *irgA* in pACYC184	49
pBC SK+	ColE1 ori, Cm[r]	Stratagene, La Jolla, CA
pBR322	pMB1 ori; Ap[r] Tc[r]	10
pC6	*E. coli rrnB* operon in pBR322, Ap[r]	C. Squires
pCR2.1-TOPO	pUC ori; Ap[r] Km[r]	Invitrogen, Carlsbad, CA
pIJ68	MG1655 *fepA* in pACYC184, Cm[r]	This study
pIJ82	UCB34 *iha* in pCR2.1-TOPO; Ap[r] Km[r]	This study
pIJ83	*iha*::*tetAR*(B) in pACYC184, Cm[r]	This study
pIJ84	UCB34 *iha* in pACYC184, Cm[r]	This study
pIJ111	UCB34 *iha* in pBC SK+, Cm[r]	This study
pIJ120	χ7122 *iroN* in pBC SK+, Cm[r]	This study
pIJ122	MG1655 *fepA* in pBC SK+, Cm[r]	This study
pIJ123	*irgA* in pBC SK+, Cm[r]	This study
pIJ159	H5058 *tonB* in pBR322; Ap[r] Tc[r]	This study
pKD13	Rγ ori, FRT-flanked kanamycin resistance; Km[r] Ap[r]	16
pKD46	pSC101 Ts ori, *araBp-gam-bet-exo*, Ap[r]	16
pYA3442	*tetAR*(B) in pBSL86, Ap[r]	19

[a] Ap, ampicillin; Cm, chloramphenicol; Km, kanamycin; Tc, tetracycline; Ent, enterobactin; Aero, aerobactin; Sal, salmochelin; Ybt, yersiniabactin. The sidephores listed in parentheses are known siderophores produced.
[b] Only when supplemented with shikimate or dihydroxybenzoic acid.
[c] Possesses yersiniabactin genes, but no product was detected by mass spectrometry.

adhesin," based on its homology to the IrgA enterobactin siderophore receptor of *Vibrio cholerae* (49) and its ability to confer epithelial cell adherence capability to a nonadherent K-12 strain when expressed from a multicopy plasmid (60). More recently, Iha was determined to be a urovirulence factor for ExPEC strain CFT073 and its double *pap* mutant UPEC76, in a mouse UTI model (39). Despite its high homology to siderophore receptors, Iha has thus far been characterized functionally only as a putative adhesin. The prevalence of *iha* has been reported in a number of studies; overall, 37% to 55% of UTI isolates contained *iha* or closely related sequences (4, 39, 41, 43, 44). Certain studies have reported an epidemiological association of *iha* with *E. coli* isolates causing UTI and other extraintestinal diseases, compared to that with commensal fecal *E. coli* isolates (4, 30, 39, 41, 43, 44), whereas other reports did not establish such an association (4, 30). However, specifically among CGA isolates from UTIs, *iha* was present in 92% to 100% of the isolates tested (40, 41), suggesting that Iha might be partly responsible for the virulence of CGA.

The purpose of this study was to investigate the role of the in vivo-expressed *iha* gene from CGA strain UCB34 as a virulence factor in a mouse UTI coinfection model and to further assess its function and regulation in vitro.

MATERIALS AND METHODS

Bacterial and cell culture. The bacterial strains and plasmids used are presented in Table 1. UCB34 is an O17/77 CGA strain isolated from a 19-year-old woman with cystitis at the University of California, Berkeley (46). Bacteria were routinely grown in Luria-Bertani (LB) broth, tryptic soy agar, or nutrient broth (NB) (Gibco, Carlsbad, CA). M63 glucose minimal medium [13.6 g/liter KH_2PO_4, 2 g/liter $(NH_4)_2SO_4$, 1 mM $MgSO_4$, 0.1 mM $CaCl_2$, and 0.4% glucose, pH 7.4, adjusted with KOH] was used for growth promotion and uptake experiments. Antibiotics were used at 25 μg/ml for chloramphenicol and kanamycin, 10 μg/ml for tetracycline, and 40 μg/ml for carbenicillin. Siderophore production in M63 medium by strains H5058, MG1655, UCB34, QT686, and χ7122 was determined by liquid chromatography/mass spectrometry (LC/MS) (see below) (Table 1). T24 bladder (ATCC HTB-4) epithelial cells were grown in McCoy's 5a medium (modified) with 1.5 mM L-glutamine adjusted to contain 2.2 g/liter sodium bicarbonate and 25 mM HEPES and supplemented with 10% fetal bovine serum. 293 kidney (ATCC CRL-1573) epithelial cells were grown in Eagle's minimum essential medium with 2 mM L-glutamine and Earle's balanced salt solution, adjusted to contain 1.5 g/liter sodium bicarbonate, 0.1 mM nonessential amino acids, 1.0 mM sodium pyruvate, and 25 mM HEPES, and supplemented with 10% fetal bovine serum (Gibco).

SCOTS. Five female CBA/J mice (5 to 6 weeks old) were inoculated via a urethral catheter under nonrefluxing conditions as previously described (37, 38) with a bacterial suspension of UCB34 (approximately 3×10^8 CFU/g of mouse weight). After 24 h, infected tissues were harvested aseptically. Total RNA from the kidneys of the five infected mice was extracted using TRIzol reagent (Invitrogen, Carlsbad, CA). RNA samples were treated with DNase using the DNA-free kit (Ambion, Austin, TX) to remove genomic DNA contamination. Five 1-μg samples of each RNA were converted into cDNA by random priming with Superscript II reverse transcriptase (Invitrogen), followed by Klenow treatment (New England Biolabs, Ipswich, MA). Primers with a defined sequence at the 5′ end and random nonamers at the 3′ end (CMD115, 5′-GTGGTACCGC TCTCCGTCCGANNNNNNNNN-3′) were used for first- and second-strand cDNA syntheses. Samples were then pooled, and cDNA from each kidney was then amplified for 25 cycles by PCR using the defined primer. SCOTS was performed as previously described (15, 18). The initial capture round was performed with the five cDNA samples (corresponding to each kidney) in parallel. After the first round, the five cDNA samples were combined and two more rounds of capture were done. This procedure resulted in selection for cDNA corresponding to bacterial transcripts. In the second step of SCOTS, UCB34-specific transcripts (absent from *E. coli* K-12) were selectively enriched by performing three more rounds of capture while blocking for nonpathogenic transcripts using a 100-fold excess of *E. coli* MG1655 K-12 genomic DNA. Selected cDNA fragments were then cloned with a TA cloning kit (Invitrogen) and were sequenced.

Cloning the *iha*, *fepA*, *irgA*, *iroN*, and *tonB* genes. For cloning experiments, restriction enzymes and DNA modification enzymes were purchased from and used as recommended by New England Biolabs or Invitrogen. The *iha* gene from UCB34 was PCR amplified using Elongase (Invitrogen) with the following primers: CMD204, 5′-GGTGGAAATCCGCTTCTACAG-3′; and CMD205, 5′-TA ACGAAATCTCATTAGCGGATCG-3′. The amplified product was cloned in pCR2.1-Topo (Invitrogen), resulting in pIJ82. The *iha* gene was subcloned from pIJ82 following digestion with EcoRV and BamHI. Ligation of the *iha*-containing fragment into the same sites of cloning vectors pACYC184 and pBC SK+ generated plasmids pIJ84 and pIJ111, respectively. *fepA* from strain MG1655 was PCR amplified using Elongase with the following primers: CMD127, 5′-GCCAAG CTTCGCGCAATTCGAGGCG-3′; and CMD128, 5′-GAAAAGCTTAACCGCA GTCTGCGAGT-3′. The amplified product was digested with HindIII and was cloned into vectors pACYC184 and pBC SK+, generating plasmids pIJ68 and pIJ122, respectively. *irgA* from *Vibrio cholerae* CA401 was subcloned from plasmid pAMR18 (49) into pBC SK+ by using EcoRI, generating plasmid pIJ123. Plasmid pIJ120 was produced by cloning *iroN* from *E. coli* strain χ7122 into pBC SK+ at the HincII and XhoI sites. The PCR fragment was amplified with Elongase using primers CMD276 (5′-TACCGCAGTTTAAACAGGCTTTCAT AATTCTC-3′) and CMD277 (5′-CGCCCTCGAGACTACGATCAGAATGAT GCGGT-3′), which have a PmeI and a XhoI site, respectively, at their 5′ end. *tonB* from strain H5058 was PCR amplified using Phusion (Finnzymes, Finland) and primers CMD658 (5′-AAGGCCGAATTCAAAGTAAGGGTAATTACGC CAA-3′) and CMD659 (5′-CCTGTTGAATTCTAGTCAAAAGCCTCCGGTC GG-3′). The amplified product was digested with EcoRI and was cloned into vector pBR322, generating plasmid pIJ159.

Construction of *iha*, *fur*, and *tonB* mutants. A mutant *iha* allele was created as follows: a 1,154-bp PCR fragment of *iha* was generated using primers CMD200 (5′-GGGCGGGATCCTGAATATCATTACCAGA-3′) and CMD201 (5′-GTG CCGGATCCTTCCACACCATGCAAC-3′). The amplified product was digested with BamHI and was cloned in pACYC184, resulting in pIJ81. pIJ81 was digested with SacI, which introduced a 96-bp deletion in the middle of *iha*, and a *tetAR*(B) cassette derived from Tn*10* (obtained from pYA3442 [19]) was ligated into the SacI sites, resulting in pIJ83. The *iha*::*tetAR*(B) allele from pIJ83 was PCR amplified using primers CMD200 and CMD201 and was introduced into strain UCB34 by homologous recombination using the λ Red recombinase method (16). An *iha* mutant strain, designated QT686, was confirmed by PCR using external primers flanking the *iha* allele. QT686 demonstrated no difference in growth rate, plasmid profile, extended virulence profile (43), or pulsed-field gel electrophoresis restriction digest band pattern of genomic DNA compared with the wild-type parent. A *fur* mutant of strain UCB34 was created as follows: a Δ*fur*::*cat* allele derived from *E. coli* strain QC2517 (20) was amplified with primers CMD18 (5′-ATTCTAGACTGCTGCTGGGCATCCC-3′) and CMD19 (5′-ACTCTAGACACTCCGACATCCCAAGC-3′). The Δ*fur*::*cat*-containing amplicon was transferred to strain UCB34 by homologous recombination using the λ Red recombinase method (16), as the DNA region encompassing *fur* is highly conserved among different *E. coli* strains. The *fur* mutant of strain UCB34 was designated QT796. A *tonB* mutant of strain H5058 was created. Primers CMD656 (5′-ATTTAAAATCGAGACCTGGTTTTTCTACTGAAATGATTA TGACTTCAATGATTCCGGGGATCCGTCGACC-3′) and CMD657 (5′-CCT CCGGTCGGAGGCTTTTGACTTTCTGCTTACTGAATTTCGGTGGTGCC TGTAGGCTGGAGCTGCTTCG-3′) were used to create a Δ*tonB*::*kan* allele by PCR, using the kanamycin resistance cassette from pKD13. The regions underlined show homologies to pKD13, and the remaining 50 bp of each primer are homologous to DNA flanking *tonB*. Primers were designed from the sequence of *E. coli* K-12 strain MG1655. The Δ*tonB*::*kan*-containing amplicon was transferred to strain H5058 by homologous recombination using the λ Red recombinase method (16). A *tonB* mutant strain was designated QT1272 and was confirmed by PCR using external primers flanking the *tonB* allele (CMD658 and CMD659).

Purification of enterobactin and its by-products. Extraction was done using the method described by Young and Gibson (64) with slight modifications. MG1655 bacterial cells were grown for 18 h in M63 glucose minimal medium with 75 μM 2,2′-dipyridyl. Cells were pelleted, and the supernatant was retained. $FeCl_3$ (5 mM) was added to the supernatant, and samples were filtered. One liter of the clear supernatant was passed through a DE52 DEAE-cellulose column (Whatman, United Kingdom). The column was washed with water and eluted with 2.5 M NH_4Cl. Colored fractions were pooled, and a sample was taken for analysis by LC/MS. The siderophores were then acidified with HCl to pH 1.5, and three extractions with ethyl acetate were made. To remove any of the hydrolysis products of enterobactin, an additional extraction step with sodium phosphate buffer (0.1 M, pH 7) was done on the combined ethyl acetate extract. These extractions were then dehydrated with Na_2SO_4, evaporated, and resuspended in methanol for the sample containing both enterobactin and linear degradation products or in ethyl acetate for the purified enterobactin sample. Analysis by LC/MS revealed the presence of enterobactin and linear 2,3-dihydroxybenzoylserine (DHBS) trimers, dimers, and monomers at a proportion of 3:2:4:1, respectively, in the enterobactin and DHBS product mix. LC/MS analysis also revealed a highly purified enterobactin in the sample extracted with sodium phosphate buffer.

LC/MS. Analyses by LC/MS were performed by using an Agilent HP 1100 high-pressure liquid chromatograph with a C8 Luna Phenomenex 150-mm by 3-mm column at a flow rate of 400 μl/min, a linear gradient of water-acetonitrile with 1% acetic acid, and a Quattro II (Micromass, Canada) mass spectrometer in electrospray-positive mode. Catecholate siderophores were detected and quantified in full-scan mode between 150 to 1,200 *m/z*. Enterobactin and linear DHBS trimers, dimers, and monomers were detected at 670, 688, 465, and 242 *m/z*, respectively (7, 62). The relative quantification of each peak was done by integration of the area under the curve determined by the MassLynx software. The presence of other siderophores, such as aerobactin, salmochelins, and yersiniabactin, was determined from the M63 glucose culture supernatants of strains UCB34, QT686, MG1655, H5058, and χ7122 at 565, 627, and 483 *m/z*, respectively (28, 33, 35).

Growth in iron-limited medium. *E. coli* strain H5058 and derivatives were grown at 37°C with agitation in M63 glucose minimal medium supplemented with aromatic amino acids (20 mg/liter each of L-phenylalanine, L-tryptophan, and L-tyrosine), thiamine (1 mg/liter), appropriate antibiotics, and 50 μM 2,2′-dipyridyl. Enterobactin extracts with or without DHBS products (50 μM) were added to cultures, and bacterial growth was measured by spectrophotometry (an optical density at 600 nm [OD_{600}]) at each hour for 12 h. A final time point was taken at 24 h. Tests were performed in triplicate.

Siderophore-^{55}Fe uptake experiments. ^{55}Fe-radiolabeled siderophore uptake experiments were based on a protocol modified from that described by Sabri et al. (57) and Eisenhauer et al. (21). *E. coli* strain H5058 and derivatives were grown overnight at 37°C with agitation in supplemented M63 minimal medium (without dipyridyl). Cultures were adjusted to an OD_{600} of 0.5, corresponding to 10^8 CFU/ml, and were washed three times with equal volumes of nonsupplemented M63 medium. After the third wash, 50 μM 2,2′-dipyridyl was added to the cells and they were subsequently incubated at 37°C for 60 min without agitation. $^{55}Fe^{3+}$ isotope (PerkinElmer, Wellesley, MA) was complexed with enterobactin extracts with or without DHBS products in a 1:3 ratio and incubated for 10 min at room temperature with agitation. The ^{55}Fe-siderophore complex was added to bacterial cells at a 1-nmol/ml concentration, and samples were left to stand for 5 min at room temperature. Samples were centrifuged at 10,000 × *g* for 2 min, and pellets were washed three times with M63 medium and resuspended in 100 μl of M63 medium. A 2-ml volume of Optiphase scintillation cocktail was added to the resuspended cells, and scintillation was measured in a Beckman LS 1701 (Beckman, Fullerton, CA) scintillation counter on the 0 to 350 channels as suggested for ^{55}Fe by the supplier. All experiments were done in triplicate and controlled by using nonwashed cells with isotope-siderophore mix as a positive control and cells without isotope as a negative control. Statistical significance was calculated by an unpaired *t* test (two tailed).

Adherence assays. Quantitative adherence assays were performed essentially as described previously (22, 47). T24 or 293 epithelial cells were grown to confluence in 24-well plates. *E. coli* K-12 derivative ORN172 or ExPEC strain UCB34 and derivatives were grown on LB plates containing appropriate antibiotics and were resuspended in LB broth to an OD_{600} of approximately 0.5. Cells were washed twice with serum-free medium and were then incubated for 1 hour with 880 μl of fresh medium (with serum). Next, 20 μl of bacteria (approximately 3×10^7 CFU) was added to six wells per strain (multiplicity of infection, approximately 1/60 to 1/100), and bacteria-host cell contact was enhanced by a 5-min centrifugation at 600 × *g*. After 2 hours of incubation, three wells per strain were lysed by adding 100 μl of phosphate-buffered saline, pH 7.4, containing 1% (wt/vol) sodium deoxycholate. Lysates were then plated on LB agar with appropriate antibiotics. The bacteria present in these lysates represented total bacteria. Cells in the three other wells per strain were washed three times using serum-free medium and were then similarly lysed. Bacterial adherence was calculated as the number of bacteria after the washes divided by total bacteria. Statistical significance was calculated by an unpaired *t* test (two tailed).

Quantitative real-time reverse transcriptase (RT) PCR. For expression analysis in NB medium, UCB34 and the Δ*fur*::*cat* derivative strain QT796 were grown for 3 h at 37°C with agitation. Approximately 3×10^7 CFU were pelleted by centrifugation for 5 min at room temperature, and RNA was extracted from whole bacterial cells by using TRIzol reagent according to the manufacturer's instructions (Invitrogen). For cell culture conditions, bacterial cells were suspended in culture medium in the presence or absence of 293 epithelial cells as described above for the adherence assays. For bacteria-eukaryote cell interaction, no washes were done, medium was removed, and TRIzol was added to the wells. Bacteria without eukaryotic cells were harvested by centrifugation. A 10-fold dilution was performed in TRIzol, followed by RNA extraction. RNA was submitted to a second precipitation using lithium chloride (Ambion) and was treated twice with DNase using the DNA-free kit (Ambion) to eliminate any genomic DNA. RNA concentrations were determined using a NanoDrop 1000 apparatus (NanoDrop Technologies, Wilmington, DE), and 15 ng of total RNA was reverse transcribed in triplicate using random hexamers and Superscript II (Invitrogen). Real-time PCR was done using the Dynamo SYBR green qPCR kit (Finnzymes) according to the manufacturer's guidelines. Reactions (25 μl) were performed using 1 μl of cDNA template per reaction. A Rotor-Gene 3000 real-time PCR apparatus (Corbett Research, Sydney, Australia) was used. PCR conditions consisted of an initial incubation step for 15 min at 95°C, followed by 45 cycles for 20 s at 95°C, 20 s at 60°C, and 20 s at 72°C. Melting curve analyses were performed after each reaction to ensure amplification specificity. Differences (*n*-fold) in transcript were calculated using the relative comparison method, and amplification efficacies of each primer set were verified as previously described (2, 58). RNA levels were normalized by using *rpoD* as the control gene (3, 49, 67). Statistical significance was calculated on $\Delta\Delta C_T$ values (58) with a paired *t* test, and *P* values were all <0.0001. Primers used for real-time PCR analysis were CMD306 (5′-GGCTGAATCTGCAGGAAAGCAACA-3′) and CMD307 (5′-TGCAGGCTGACAGAATCATCCACA-3′) for *iha*, CMD308 (5′-AGCTGACTGACAGCACCATCGTAA-3′) and CMD309 (5′-AAACCTTGCGATATGTTCAGCGCC-3′) for *fepA*, and CMD310 (5′-TCATGAAGCTCTGCGTTGAGCAGT-3′) and CMD328 (5′-CAATTGCCGCGTTCAACCAGGTAT-3′) for *rpoD*.

Mouse infection experiment. Fifteen female CBA/J mice were coinfected with a mixed inoculum, consisting of the strain UCB34 and its isogenic *iha* mutant QT686 in equal proportions, using the same ascending UTI model used for SCOTS (37, 38). After 48 h, mice were euthanatized. Bacterial colonies recovered from tissues, urine, and the initial inoculum suspension were replica plated to LB agar plates with or without tetracycline to determine the relative proportion of wild-type UCB34 versus *iha* mutant QT686 in each sample. Data from postinfection cultures (output ratios) were normalized to the input ratios. Statistical differences were calculated with the Wilcoxon matched-pairs test (signed rank).

Nucleotide sequence accession number. The accession number of the complete nucleotide sequence of *iha* from strain UCB34 is DQ211582.

RESULTS

***iha* is expressed by CGA strain UCB34 during UTI.** In order to identify genes expressed in vivo by CGA strain UCB34, mice were infected in a UTI model. RNA was extracted from infected kidneys and was used for SCOTS. This technique of bacterial transcript capture allowed us to determine that *iha* from UCB34 was expressed in the mouse kidneys. The 470-bp SCOTS fragment clone that was identified by sequencing was identical to a portion of the *iha* gene from strain CFT073. By using primers derived from the CFT073 and EDL933 *iha* sequences, the *iha* gene and promoter region were amplified from genomic DNA of strain UCB34 and were cloned. *iha* from strain UCB34 is nearly identical to *iha* from strain CFT073, demonstrating only a single nonsynonymous nucleotide difference that results in a Gly^{565} to Ser^{565} substitution in the predicted peptide sequence. We identified a putative Fur box regulatory region located just 3′ of the predicted −35 region. In addition, a putative TonB box has already been identified at the beginning of Iha from strain EDL933 (60). The TonB box is also conserved in the predicted Iha proteins from strains UCB34 and CFT073.

Iha has previously been reported to share 53% similarity to the siderophore receptor IrgA from *Vibrio cholerae* (60). Additionally, new protein sequence homology searches showed that Iha demonstrates identity/similarity with a number of putative outer membrane receptors from recently completed genomes, as well as to characterized iron-regulated outer membrane proteins, such as Cir2A from *Yersinia pestis* and *Yersinia pseudotuberculosis* (73.2% similarity) (13, 17, 59), CfrA from *Campylobacter coli* and *Campylobacter jejuni* (54.5%) (31, 51), and BfrA from *Bordetella bronchiseptica* (50.7%) (6). Known siderophore receptors from *E. coli* that share identity/similarity with Iha include FepA (44.1%) (45) and IroN (44.2%) (55, 56). The percent similarities reported are Emboss pairwise alignments (full-length sequence alignments) obtained using Needle (European Bioinformatics Institute; http://www.ebi.ac.uk).

Iha from UCB34 functions as a siderophore receptor in *E. coli* K-12 strain H5058. Due to its similarity to other siderophore receptors, we wished to assess whether Iha from UCB34 was able to function as a siderophore receptor. First, growth promotion experiments in iron-limited minimal medium were done using the *E. coli* K-12 strain H5058. H5058 is an *aroB* mutant and is therefore not able to synthesize aromatic amino acids or enterobactin. Production of enterobactin by H5058 can be achieved only when the strain is supplemented with shikimate or dihydroxybenzoic acid, which are precursors of enterobactin (29). Strain H5058 is also defective in the uptake of enterobactin and enterobactin's DHBS derivatives, as it lacks the catecholate siderophore receptors FepA, Fiu, and Cir. It therefore grows poorly in iron-limited medium even when supplemented with shikimate or dihydroxybenzoic acid. Introduction of plasmid pIJ84 (*iha*) increased the growth of strain H5058 in iron-limited minimal medium supplemented with purified enterobactin compared to the negative control (vector only), although growth promotion was less marked than when complemented with the positive control plasmid pIJ68 (*fepA*) (Fig. 1). The addition of purified enterobactin to iron-limited medium promoted the growth of the *iha* clone up to 68% of the *fepA* clone (Fig. 1A), whereas the addition of extract that contained both enterobactin and DHBS products (trimers, dimers, and monomers) promoted the growth of the same clone to 78% of the *fepA*-complemented positive control (Fig. 1B). Further, from 6 h onward, growth of the *iha* clone, when supplemented with the enterobactin-DHBS mixture, was significantly greater ($P < 0.05$) than when supplemented with purified enterobactin alone. These results indicate that *iha* can

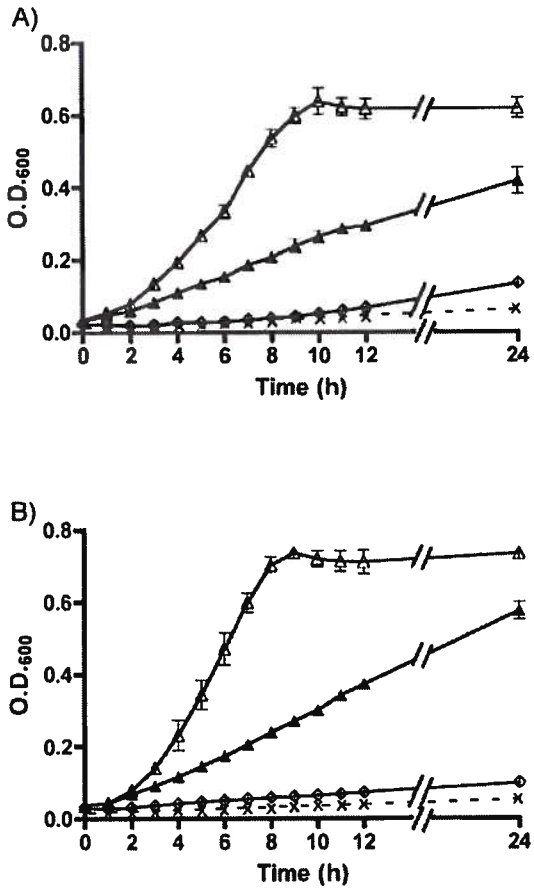

FIG. 1. Growth of *E. coli* K-12 catecholate siderophore receptor-negative strain H5058 containing a cloned copy of *iha* (pIJ84, ▲), *fepA* (pIJ68, △), or the control vector (pACYC184, ◇) in iron-limited minimal medium (M63 glucose) supplemented with 50 μM 2,2′-dipyridyl and 50 μM of purified enterobactin (A) or 50 μM of enterobactin and its DHBS breakdown products, trimers, dimers, and monomers (B). Growth of H5058 (pIJ84) expressing *iha* in medium without siderophore supplements is indicated (x) on dashed lines.

promote growth of a catecholate siderophore receptor-negative *E. coli* K-12 strain in iron-limited medium in the presence, but not the absence, of DHBS products, derivatives of enterobactin, and to a lesser extent, cyclic enterobactin, presumably by facilitating the uptake of iron coupled to these substances.

Siderophore-^{55}Fe complex uptake assays using strain H5058 containing plasmids carrying *iha* or *fepA*, or the control vector alone, were done to further investigate the role of Iha as a siderophore receptor. The *iha* clone mediated uptake of the cyclic enterobactin-^{55}Fe complex slightly, 1.96 ± 0.04 pmol/ml (mean ± standard deviation) compared to 1.28 ± 0.04 pmol/ml for the negative control. This uptake was minimal compared to that of the *fepA*-complemented positive control, i.e., 18.55 ± 0.09 pmol/ml (Fig. 2). By contrast, when a siderophore extract comprised of a mixture of enterobactin and its DHBS products was used for the uptake experiments, the *iha* clone demonstrated an increased uptake level of 10.9 ± 0.77 pmol/ml, compared to 16.4 ± 1.06 pmol/ml for the *fepA*-complemented positive control. These results correlate with the growth experiments and indicate that Iha functions as a catecholate siderophore receptor that demonstrates a greater specificity for linear enterobactin DHBS products than for tricyclic enterobactin. As Iha demonstrated a catecholate siderophore receptor function, we also compared the ability of ExPEC strain UCB34 or its isogenic Δ*iha* derivative QT686 to mediate the uptake of catecholate siderophores from the enterobactin-DHBS mixture. Interestingly, QT686 demonstrated a decreased transport capacity of 25.6% ± 2.6% compared to the wild-type parent ($P < 0.0001$). Taken together, these results support a role for Iha in the uptake of catecholate siderophores in both *E. coli* K-12 and ExPEC strain UCB34.

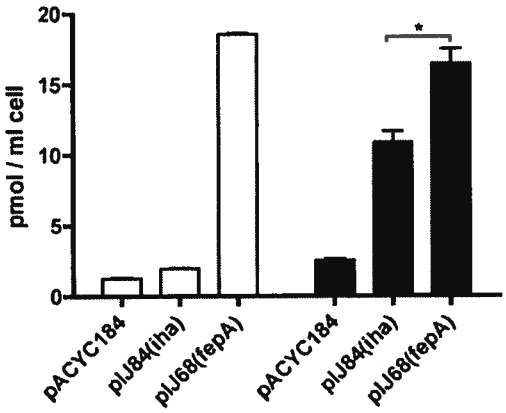

FIG. 2. Enterobactin-^{55}Fe transport of *E. coli* K-12 catecholate siderophore receptor-negative strain H5058 containing a cloned copy of *iha* (pIJ84), *fepA* (pIJ68), or the control vector (pACYC184) in iron-limited minimal medium (M63 glucose) supplemented with 50 μM 2,2′-dipyridyl using an enterobactin-^{55}Fe complex (white bars) or enterobactin and its DHBS products and ^{55}Fe (black bars). Compared to those for vector controls, values are significantly different ($P < 0.0001$). *, $P = 0.002$.

The *iha* siderophore receptor phenotype is *tonB* dependent. As gram-negative bacteria typically require the TonB-ExbB-ExbD energy complex to import siderophores into the cytoplasm (1, 12), we assessed whether the capacity of Iha to transport siderophores was dependent on the TonB complex. pIJ84 (*iha*), pIJ68 (*fepA*), and control vector pACYC184 were introduced into the H5058 *tonB* mutant strain QT1272. As expected, strains exhibited poor growth in iron-depleted minimal medium supplemented with enterobactin and its DHBS products, even when complemented with *fepA* or *iha* (Fig. 3A). However, introduction of a cloned copy of the *tonB* gene (pIJ159) into these strains restored growth of the *iha*- and *fepA*-complemented strain in the same medium (Fig. 3B), suggesting that siderophore transport by Iha is TonB dependent.

Iha from UCB34 promotes epithelial cell adherence in *E. coli* K-12 strain ORN172. In previous reports, introduction of Iha from strains EDL933 and CFT073, when cloned into a high-copy vector, conferred increased adherence of the poorly adhering *E. coli* K-12 *fim* mutant strain ORN172 to epithelial cells (39, 60). These results suggested that Iha may act directly (or indirectly) as an adhesin. As Iha shares sequence similarities with other siderophore receptors, this suggested (by extension) that other siderophore receptors also might promote adherence. Accordingly, we compared the adherence-enhancing phenotype of Iha with other siderophore receptors. Adhe-

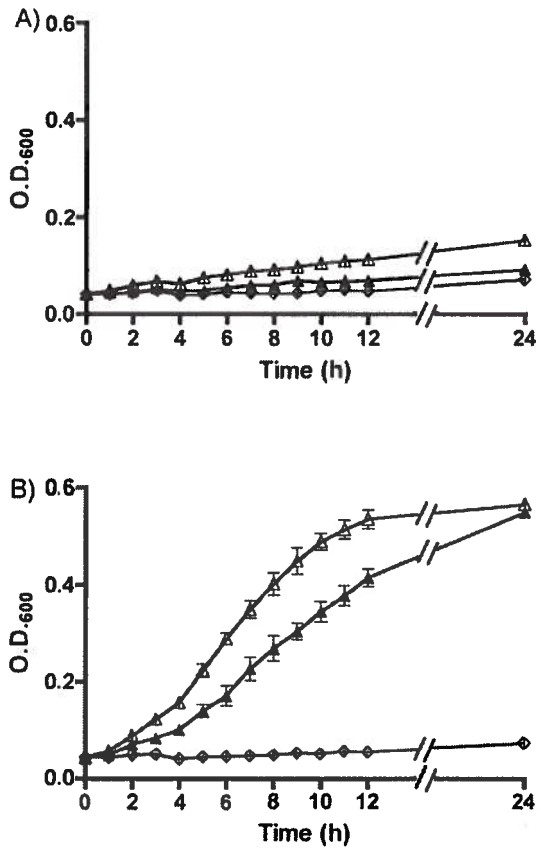

FIG. 3. Growth of *E. coli* K-12 catecholate siderophore receptor-negative Δ*tonB* H5058 strain QT1272 (A) or QT1272 complemented with *tonB* (pIJ159) (B) containing a cloned copy of *iha* (pIJ84, ▲), *fepA* (pIJ68, △), or the control vector (pACYC184, ◇) in minimal medium (M63 glucose) supplemented with 50 μM 2,2′-dipyridyl and 50 μM of enterobactin and its DHBS products.

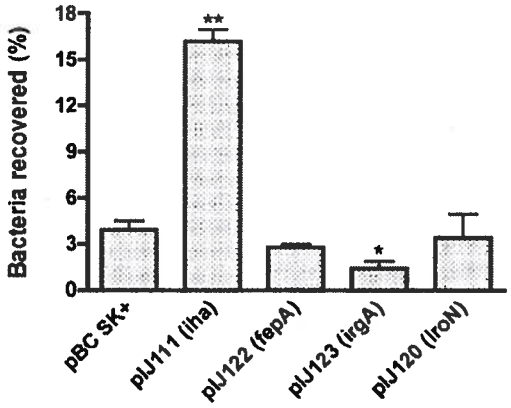

FIG. 4. Quantitative adherence of *E. coli* K-12 *fim* ORN172 containing *iha* (pIJ111), *fepA* (pIJ122), *irgA* (pIJ123), or *iroN* (pIJ120) cloned on high-copy vector pBC SK+ or the control vector on T24 bladder epithelial cells. Statistical differences compared to the vector control pBC SK+ were as follows: **, $P < 0.0002$; *, $P < 0.03$.

sion assays were performed on T24 human bladder epithelial cells using high-copy clones of *iha*, *fepA*, *iroN*, and *irgA*. Except for the *iha*-containing clone (pIJ111), no increase in adherence was conferred by the presence of any of the other siderophore receptors on high-copy plasmids (Fig. 4). Similar results were obtained using the 293 human kidney epithelial cell lines. To determine whether plasmid copy number had an effect on adherence to epithelial cells, *iha* and *fepA* (as a control) were cloned into the medium-copy vector pBR322. Quantitative adherence assays were performed, and similar adherence results were obtained using the mid-copy clones or the high-copy clones (data not shown). However, no difference in adherence to T24 or 293 cells was observed between (*iha*-positive) wild-type strain UCB34 and its Δ*iha*::*tetAR*(B) derivative strain QT686, with or without the addition of 2.5% mannose to the medium (data not shown), consistent with the known presence of additional mannose-resistant adhesins (e.g., P fimbriae) in strain UCB34.

As mentioned earlier, the *iha* promoter region contains a predicted Fur-binding site. The presence of Fur-binding sites on high-copy plasmids has the potential to titrate the Fur regulatory protein and hypothetically could result in the deregulated expression of many proteins in *E. coli* ORN172, which in turn could potentially be responsible for the increased adherence observed in this and previous studies (39, 60). To assess whether Fur exerts a regulatory effect on adhesion, *fur* null mutants of strains UCB34 and ORN172 were constructed and used in adherence assays. No differences in adherence to epithelial cells were observed compared to that of the parental strains (data not shown), providing evidence against this hypothesis.

***iha* expression is modulated by iron availability and Fur but not by contact with host cells.** The expression level of *iha* by CGA strain UCB34 under different culture conditions was determined using real-time RT-PCR experiments and was compared to the level of expression of *fepA*. The wild-type strain UCB34 and isogenic *fur* null mutant QT796 were grown in NB medium, iron-limited medium (NB supplemented with 75 μM 2,2′-dipyridyl), or iron-replete medium (NB supplemented with 30 μM $FeCl_3$). Results shown in Fig. 5 represent the increases (*n*-fold) in expression level compared to the expression level of the wild-type strain grown in NB (onefold increase). In strain UCB34, we observed a 12-fold increase in *iha* expression following growth in iron-depleted medium, compared to a 9-fold increase for *fepA*. In contrast, no expression for either *iha* or *fepA* was detectable in iron-replete medium. Additionally, no expression of *iha* by UCB34 was detected in LB medium (data not shown). In the *fur* mutant QT796, *iha* and *fepA* expression were increased 16- and 28-fold, respectively, in NB medium, and regulation by iron of both *iha* and *fepA* expression was abrogated, since expression could be detected under all culture conditions.

Since contact with host cells has been shown to induce expression of iron-regulated proteins by pathogenic *E. coli* (65), the influence of bacterial interaction with host cells on the expression level of *iha* was investigated by real-time RT-PCR. In a representative adhesion assay, the level of expression by UCB34 following a 2-h incubation in minimal essential medium was not any different when the incubation was done in the presence, versus the absence, of 293 cells (data not shown).

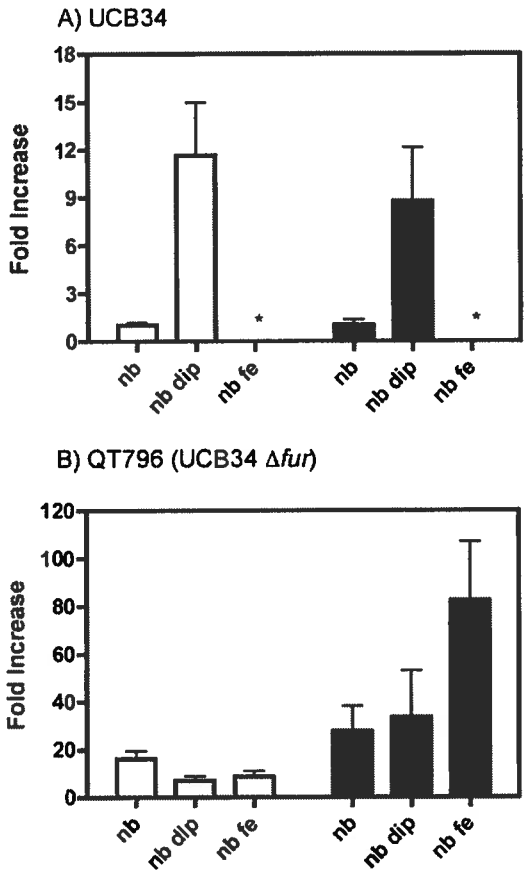

FIG. 5. Expression levels of *iha* (white bars) and *fepA* (black bars), as determined by real-time PCR under different culture conditions for wild-type strain UCB34 (A) and its *fur* derivative QT796 (B). Results are presented as increases (*n*-fold) in expression levels compared to that of the wild-type UCB34 strain grown in NB (onefold increase), NB supplemented with 75 μM dipyridyl (nb dip), and NB supplemented with 30 μM $FeCl_3$ (nb fe). *, No expression could be detected.

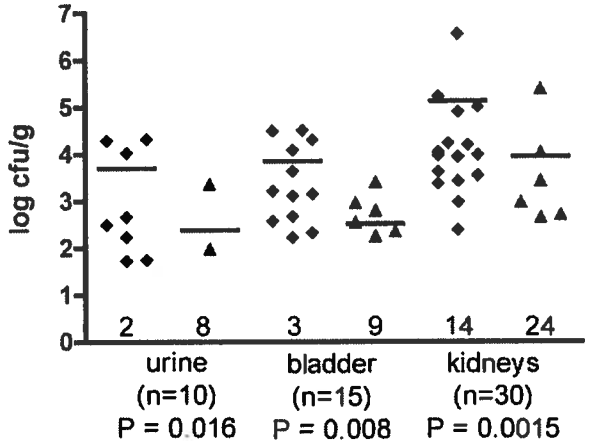

FIG. 6. Bacterial numbers (log CFU/g) present in the urine, bladder, and kidneys of mice coinfected with wild-type strain UCB34 (◆) and isogenic *iha* mutant QT686 (▲). Data points represent bacterial adjusted counts (normalized with the input ratio) from tissues and urine isolated from different mice. Horizontal bars represent the means. Numbers near the log 0 limit indicate samples in which no bacteria where detected. *n* indicates the number of tissue or urine samples harvested from the 15 mice (urine samples were available for only 10 mice). Statistical analysis was done using the Wilcoxon matched-pairs test. *P* values represent statistical significance between the wild type and the mutant in each sample.

Iha contributes to virulence of CGA strain UCB34 during UTI. To assess whether Iha contributes to virulence of the CGA strain in the mouse UTI model, dual-strain competition infections were done in female CBA/J mice using wild-type strain UCB34 and its isogenic *iha*::*tetAR*(B) derivative QT686. Fifteen mice were challenged via the urethra under nonrefluxing conditions. Figure 6 shows the bacterial numbers for the wild-type or mutant strain in bladders, kidneys, and urine. Wild-type strain UCB34 significantly outcompeted the *iha* mutant at each site assessed (Fig. 6). For many of the samples, only wild-type strain UCB34 was recovered, indicating a marked deficiency in persistence of the *iha* mutant in the host compared to that of the wild-type parent strain.

DISCUSSION

In the current report, we have studied Iha from strain UCB34, a representative of the recently emerged ExPEC clonal group designated CGA. Our results demonstrate that Iha functions as a catecholate siderophore receptor, based on growth promotion and uptake experiments using enterobactin and DHBS siderophore by-products. We also investigated the previously reported adhesin phenotype associated with Iha in comparison to other siderophore receptors. Further, coinfection experiments between an *iha* null mutant and its isogenic parent demonstrated that Iha contributes to colonization and virulence in the mouse urinary tract. Iha thus represents the first characterized virulence factor for a CGA ExPEC strain.

Iha shares high identity/similarity with putative and confirmed siderophore receptors of gram-negative bacteria, including IrgA from *Vibrio cholerae*. Iha also contains a putative TonB interaction box at the N-terminal region (60), and there is a putative Fur-binding regulatory site in the *iha* promoter region. Our results demonstrate the previously hypothesized but unconfirmed role of Iha as a siderophore receptor. We investigated this phenotype by determining growth in iron-limited defined minimal medium supplemented with enterobactin and DHBS derivatives (monomers, dimers, and trimers) and by performing uptake experiments using ^{55}Fe-siderophore complexes. Both sets of experiments demonstrated that Iha functions as a siderophore receptor for linear DHBS products and, to a lesser extent, for enterobactin in a catecholate siderophore receptor-negative *E. coli* K-12 strain (Fig. 1 and 2). However, in these tests, Iha was not as efficient as FepA, the native enterobactin siderophore receptor. Typically, siderophore-mediated iron uptake is TonB dependent. Since Iha possesses a predicted TonB box (60), enterobactin-mediated growth promotion observed in iron-limited medium should be dependent on TonB. Consistent with this, a cloned copy of *iha* did not restore growth of a catecholate siderophore receptor-negative *E. coli* K-12 *tonB* mutant in iron-limited medium, whereas reintroduction of a cloned copy of *tonB* in this strain, when complemented with either *iha* or *fepA*, restored growth (Fig. 3).

Although Iha functions as a catecholate siderophore recep-

tor, an *iha* mutant of UCB34 grew, as well as its isogenic wild-type parent, in iron-depleted medium (data not shown). This is most likely due to the redundancy of iron acquisition systems present in most ExPEC strains (41). UCB34 is known to possess the enterobactin, aerobactin, and yersiniabactin siderophore systems (Table 1), additional siderophore receptors, and possibly other iron transporters. By contrast, compared to wild-type CGA strain UCB34, the *iha* mutant demonstrated a significantly reduced capacity to take up iron from an enterobactin-DHBS siderophore mixture, suggesting a direct role in siderophore-mediated iron transport for Iha in the CGA strain. Potential advantages for siderophore receptor redundancy have been previously suggested and include the possibility that multiple acquisition systems may maximize iron uptake, thereby increasing the ability of a pathogenic strain to acquire iron during host infection (54, 56). In addition, some systems might be adapted to specific conditions in different host niches during infection or permit utilization of siderophores produced by other bacterial species within the microbial flora during colonization of host tissues (54, 56).

In addition to transporting specific siderophores, numerous siderophore receptors can also mediate transport of DHBS (34, 53). Interestingly, the ability to take up DHBS by siderophore receptors (FepA, IroN, and Cir) was shown to be required for full virulence of *Salmonella enterica* serovars in both murine and avian infection models (53). Therefore, DHBS products may be an important means of iron acquisition in vivo, and one role Iha may play in virulence, based on our results, could be the uptake of iron via DHBS products. There might also be some other as-yet-unidentified siderophore(s) produced by certain *E. coli* strains or other bacteria specific to Iha, and uptake of DHBS products or enterobactin by Iha may be only ancillary. For example, IroN is a urovirulence factor and is the specific siderophore receptor for salmochelins but can also mediate the uptake of enterobactin and DHBS (35, 53, 56).

To further investigate Iha as a potential iron-regulated siderophore receptor, we analyzed *iha* and *fepA* expression under different conditions of iron availability. As with *fepA*, *iha* expression increased when iron availability was reduced, whereas it was suppressed to below our detection limits when iron was replete in the medium. An analogous increase in expression of *fepA* in iron-limited medium has been previously reported (36, 48). However, in contrast to the responsiveness of *iha* expression to iron concentrations, *iha* expression was not increased in cell adherence assays and is therefore apparently independent of cell-cell contact. Additionally, in accordance with results obtained by Johnson et al. (39), who did not detect Iha from extracts of ExPEC strain CFT073 by Western blotting following growth in LB, no expression of *iha* by UCB34 was detected in LB medium. Since LB medium is iron rich, it is not surprising that growth in LB represses *iha* expression.

Fur, the "ferric uptake regulator," is an established regulator of genes involved in iron homeostasis (1, 24). As we identified a region upstream of the *iha* start codon that could be a Fur box for *iha*, we investigated the role of Fur on *iha* and *fepA* (as a control) expression by using quantitative RT-PCR. Previous studies have reported an increased expression level for *fepA* in an *E. coli fur* mutant compared to that in its parental strain by using microarrays and real-time RT-PCR (67), macroarrays (48), or protein quantification (36). Our results similarly demonstrate a role for *fur* in the regulation of *iha* and *fepA* expression. In the UCB34 *fur* mutant, *iha* and *fepA* expression were constitutive. However, under all growth conditions, the increased expression observed in the *fur* mutant was considerably higher for *fepA* than for *iha* (Fig. 6). Based on these results, Fur regulation of *fepA* may be more stringent than that of *iha*, and/or *iha* may be coregulated by other regulators in addition to Fur. In any case, it is clear that Iha is negatively regulated by iron and that inactivation of the *fur* gene derepresses *iha* expression under conditions of iron availability.

Despite the fact that Iha from two archetypal strains (39, 60) has been demonstrated to promote adherence, Iha exhibits no similarity to any characterized adhesins in the available sequence databases (January 2006). Siderophore receptors have not typically been described or investigated as potential adhesins. Based on the considerable identity of Iha with siderophore receptors, we investigated whether three other siderophore receptor-encoding genes (*fepA*, *iroN*, and *irgA*), when cloned in high-copy vectors, could also confer adherence of *E. coli* ORN172 to uroepithelial cells. Among these siderophore receptors, only *iha* conferred increased adherence (Fig. 4). These results confirmed those reported previously for Iha obtained from *E. coli* O157:H7 strain EDL933 and ExPEC strain CFT073 (39, 60) and showed that this phenotype is not simply an artifact broadly characteristic of high-copy siderophore receptor clones in this adhesion model. In addition, when *iha* from UCB34 was cloned on the medium-copy cloning vector pBR322, the increase in adherence to epithelial cells was similar to what was observed with a high-copy clone. Hence, our results suggest that Iha confers an adhesin function, which is lacking in other siderophore receptors, and is not dependent on high copy number.

The ability of CGA strain UCB34 to colonize the mouse urinary tract was significantly lower for a UCB34 *iha* null mutant than for the wild-type strain, as demonstrated by competitive infection experiments. This result confirmed the importance of *iha* in vivo. Additionally, Iha is the first virulence factor to be demonstrated as important for a representative of CGA, or for any phylogenetic group D strain, in the mouse UTI model. In conclusion, Iha may be a dual-function urovirulence factor for *E. coli* CGA strains and other pathogenic *E. coli*. Whether the siderophore receptor activity, the adhesin phenotype, or both are important for Iha's demonstrated enhancement of in vivo persistence within the urinary tract remains to be defined.

ACKNOWLEDGMENTS

We give kind thanks to A. R. Manges, E. E. Wyckoff, K. Hantke, P. E. Orndorff, and M. Cellier for the gift of strains or plasmids. We give special thanks to F. Lépine for the use of the mass spectrometer.

S.L. was funded by a Fonds de recherches en Santé du Québec (FRSQ) master's level scholarship. M.C. and M.S. were funded by Fondation Armand-Frappier scholarships. Funding for this project was provided by the Canadian Institutes of Health Research (CIHR) and the Canadian Foundation for Innovation (C.M.D.) and by the Office of Research and Development, Medical Research Service, Department of Veterans Affairs (J.R.J.).

REFERENCES

1. **Andrews, S. C., A. K. Robinson, and F. Rodriguez-Quinones.** 2003. Bacterial iron homeostasis. FEMS Microbiol. Rev. 27:215–237.

2. **Anonymous.** 1997. Applied Biosystems user bulletin 2. The Perkin-Elmer Corp., Norwalk, Conn.
3. **Bader, M. W., W. W. Navarre, W. Shiau, H. Nikaido, J. G. Frye, M. McClelland, F. C. Fang, and S. I. Miller.** 2003. Regulation of *Salmonella typhimurium* virulence gene expression by cationic antimicrobial peptides. Mol. Microbiol. **50:**219–230.
4. **Bauer, R. J., L. Zhang, B. Foxman, A. Siitonen, M. E. Jantunen, H. Saxen, and C. F. Marrs.** 2002. Molecular epidemiology of 3 putative virulence genes for *Escherichia coli* urinary tract infection—*usp*, *iha*, and $iroN_{E.\ coli}$. J. Infect. Dis. **185:**1521–1524.
5. **Baumler, A. J., T. L. Norris, T. Lasco, W. Voight, R. Reissbrodt, W. Rabsch, and F. Heffron.** 1998. IroN, a novel outer membrane siderophore receptor characteristic of *Salmonella enterica*. J. Bacteriol. **180:**1446–1453.
6. **Beall, B., and T. Hoenes.** 1997. An iron-regulated outer-membrane protein specific to *Bordetella bronchiseptica* and homologous to ferric siderophore receptors. Microbiology **143:**135–145.
7. **Berner, I., M. Greiner, J. Metzger, G. Jung, and G. Winkelmann.** 1991. Identification of enterobactin and linear dihydroxybenzoylserine compounds by HPLC and ion spray mass spectrometry (LC/MS and MS/MS). Biol. Met. **4:**113–118.
8. **Bingen-Bidois, M., O. Clermont, S. Bonacorsi, M. Terki, N. Brahimi, C. Loukil, D. Barraud, and E. Bingen.** 2002. Phylogenetic analysis and prevalence of urosepsis strains of *Escherichia coli* bearing pathogenicity island-like domains. Infect. Immun. **70:**3216–3226.
9. **Blattner, F. R., G. Plunkett III, C. A. Bloch, N. T. Perna, V. Burland, M. Riley, J. Collado-Vides, J. D. Glasner, C. K. Rode, G. F. Mayhew, J. Gregor, N. W. Davis, H. A. Kirkpatrick, M. A. Goeden, D. J. Rose, B. Mau, and Y. Shao.** 1997. The complete genome sequence of *Escherichia coli* K-12. Science **277:**1453–1474.
10. **Bolivar, F., R. L. Rodriguez, P. J. Greene, M. C. Betlach, H. L. Heyneker, and H. W. Boyer.** 1977. Construction and characterization of new cloning vehicles. II. A multipurpose cloning system. Gene **2:**95–113.
11. **Bower, J. M., D. S. Eto, and M. A. Mulvey.** 2005. Covert operations of uropathogenic *Escherichia coli* within the urinary tract. Traffic **6:**18–31.
12. **Braun, V., and M. Braun.** 2002. Iron transport and signaling in *Escherichia coli*. FEBS Lett. **529:**78–85.
13. **Chain, P. S., E. Carniel, F. W. Larimer, J. Lamerdin, P. O. Stoutland, W. M. Regala, A. M. Georgescu, L. M. Vergez, M. L. Land, V. L. Motin, R. R. Brubaker, J. Fowler, J. Hinnebusch, M. Marceau, C. Medigue, M. Simonet, V. Chenal-Francisque, B. Souza, D. Dacheux, J. M. Elliott, A. Derbise, L. J. Hauser, and E. Garcia.** 2004. Insights into the evolution of *Yersinia pestis* through whole-genome comparison with *Yersinia pseudotuberculosis*. Proc. Natl. Acad. Sci. USA **101:**13826–13831.
14. **Chang, A. C., and S. N. Cohen.** 1978. Construction and characterization of amplifiable multicopy DNA cloning vehicles derived from the P15A cryptic miniplasmid. J. Bacteriol. **134:**1141–1156.
15. **Daigle, F., J. Y. Hou, and J. E. Clark-Curtiss.** 2002. Microbial gene expression elucidated by selective capture of transcribed sequences (SCOTS). Methods Enzymol. **358:**108–122.
16. **Datsenko, K. A., and B. L. Wanner.** 2000. One-step inactivation of chromosomal genes in *Escherichia coli* K-12 using PCR products. Proc. Natl. Acad. Sci. USA **97:**6640–6645.
17. **Deng, W., V. Burland, G. Plunkett III, A. Boutin, G. F. Mayhew, P. Liss, N. T. Perna, D. J. Rose, B. Mau, S. Zhou, D. C. Schwartz, J. D. Fetherston, L. E. Lindler, R. R. Brubaker, G. V. Plano, S. C. Straley, K. A. McDonough, M. L. Nilles, J. S. Matson, F. R. Blattner, and R. D. Perry.** 2002. Genome sequence of *Yersinia pestis* KIM. J. Bacteriol. **184:**4601–4611.
18. **Dozois, C. M., F. Daigle, and R. Curtiss III.** 2003. Identification of pathogen-specific and conserved genes expressed *in vivo* by an avian pathogenic *Escherichia coli* strain. Proc. Natl. Acad. Sci. USA **100:**247–252.
19. **Dozois, C. M., M. Dho-Moulin, A. Bree, J. M. Fairbrother, C. Desautels, and R. Curtiss III.** 2000. Relationship between the Tsh autotransporter and pathogenicity of avian *Escherichia coli* and localization and analysis of the Tsh genetic region. Infect. Immun. **68:**4145–4154.
20. **Dubrac, S., and D. Touati.** 2000. Fur positive regulation of iron superoxide dismutase in *Escherichia coli*: functional analysis of the *sodB* promoter. J. Bacteriol. **182:**3802–3808.
21. **Eisenhauer, H. A., S. Shames, P. D. Pawelek, and J. W. Coulton.** 2005. Siderophore transport through *Escherichia coli* outer membrane receptor FhuA with disulfide-tethered cork and barrel domains. J. Biol. Chem. **280:**30574–30580.
22. **Elsingborst, E. A.** 1994. Measurement of invasion by gentamicin resistance. Methods Enzymol. **236:**405–420.
23. **Emody, L., M. Kerenyi, and G. Nagy.** 2003. Virulence factors of uropathogenic *Escherichia coli*. Int. J. Antimicrob. Agents **22**(Suppl. 2):29–33.
24. **Escolar, L., J. Perez-Martin, and V. de Lorenzo.** 1999. Opening the iron box: transcriptional metalloregulation by the Fur protein. J. Bacteriol. **181:**6223–6229.
25. **Finer, G., and D. Landau.** 2004. Pathogenesis of urinary tract infections with normal female anatomy. Lancet Infect. Dis. **4:**631–635.
26. **Foxman, B.** 2002. Epidemiology of urinary tract infections: incidence, morbidity, and economic costs. Am. J. Med. **113**(Suppl. 1A):5S–13S.
27. **France, A. M., K. M. Kugeler, A. Freeman, C. A. Zalewski, M. Blahna, L. Zhang, C. F. Marrs, and B. Foxman.** 2005. Clonal groups and the spread of resistance to trimethoprim-sulfamethoxazole in uropathogenic *Escherichia coli*. Clin. Infect. Dis. **40:**1101–1107.
28. **Gibson, F., and D. I. Magrath.** 1969. The isolation and characterization of a hydroxamic acid (aerobactin) formed by *Aerobacter aerogenes* 62-1. Biochim. Biophys. Acta **192:**175–184.
29. **Gibson, F., and J. Pittard.** 1968. Pathways of biosynthesis of aromatic amino acids and vitamins and their control in microorganisms. Bacteriol. Rev. **32:**465–492.
30. **Gordon, D. M., S. E. Stern, and P. J. Collignon.** 2005. Influence of the age and sex of human hosts on the distribution of *Escherichia coli* ECOR groups and virulence traits. Microbiology **151:**15–23.
31. **Guerry, P., J. Perez-Casal, R. Yao, A. McVeigh, and T. J. Trust.** 1997. A genetic locus involved in iron utilization unique to some *Campylobacter* strains. J. Bacteriol. **179:**3997–4002.
32. **Gupta, K., T. M. Hooton, and W. E. Stamm.** 2001. Increasing antimicrobial resistance and the management of uncomplicated community-acquired urinary tract infections. Ann. Intern. Med. **135:**41–50.
33. **Haag, H., K. Hantke, H. Drechsel, I. Stojiljkovic, G. Jung, and H. Zahner.** 1993. Purification of yersiniabactin: a siderophore and possible virulence factor of *Yersinia enterocolitica*. J. Gen. Microbiol. **139:**2159–2165.
34. **Hantke, K.** 1990. Dihydroxybenzoylserine—a siderophore for *E. coli*. FEMS Microbiol. Lett. **55:**5–8.
35. **Hantke, K., G. Nicholson, W. Rabsch, and G. Winkelmann.** 2003. Salmochelins, siderophores of *Salmonella enterica* and uropathogenic *Escherichia coli* strains, are recognized by the outer membrane receptor IroN. Proc. Natl. Acad. Sci. USA **100:**3677–3682.
36. **Higgs, P. I., R. A. Larsen, and K. Postle.** 2002. Quantification of known components of the *Escherichia coli* TonB energy transduction system: TonB, ExbB, ExbD and FepA. Mol. Microbiol. **44:**271–281.
37. **Johnson, J. R., T. Berggren, and J. C. Manivel.** 1992. Histopathologic-microbiologic correlates of invasiveness in a mouse model of ascending unobstructed urinary tract infection. J. Infect. Dis. **165:**299–305.
38. **Johnson, J. R., and J. J. Brown.** 1996. Defining inoculation conditions for the mouse model of ascending urinary tract infection that avoid immediate vesicoureteral reflux yet produce renal and bladder infection. J. Infect. Dis. **173:**746–749.
39. **Johnson, J. R., S. Jelacic, L. M. Schoening, C. Clabots, N. Shaikh, H. L. Mobley, and P. I. Tarr.** 2005. The IrgA homologue adhesin Iha is an *Escherichia coli* virulence factor in murine urinary tract infection. Infect. Immun. **73:**965–971.
40. **Johnson, J. R., A. R. Manges, T. T. O'Bryan, and L. W. Riley.** 2002. A disseminated multidrug-resistant clonal group of uropathogenic *Escherichia coli* in pyelonephritis. Lancet **359:**2249–2251.
41. **Johnson, J. R., A. C. Murray, M. A. Kuskowski, S. Schubert, M. F. Prere, B. Picard, R. Colodner, and R. Raz.** 2005. Distribution and characteristics of *Escherichia coli* clonal group A. Emerg. Infect. Dis. **11:**141–145.
42. **Johnson, J. R., T. T. O'Bryan, P. Delavari, M. Kuskowski, A. Stapleton, U. Carlino, and T. A. Russo.** 2001. Clonal relationships and extended virulence genotypes among *Escherichia coli* isolates from women with a first or recurrent episode of cystitis. J. Infect. Dis. **183:**1508–1517.
43. **Johnson, J. R., T. A. Russo, P. I. Tarr, U. Carlino, S. S. Bilge, J. C. Vary, Jr., and A. L. Stell.** 2000. Molecular epidemiological and phylogenetic associations of two novel putative virulence genes, *iha* and $iroN_{E.\ coli}$, among *Escherichia coli* isolates from patients with urosepsis. Infect. Immun. **68:**3040–3047.
44. **Kanamaru, S., H. Kurazono, S. Ishitoya, A. Terai, T. Habuchi, M. Nakano, O. Ogawa, and S. Yamamoto.** 2003. Distribution and genetic association of putative uropathogenic virulence factors *iroN*, *iha*, *kpsMT*, *ompT* and *usp* in *Escherichia coli* isolated from urinary tract infections in Japan. J. Urol. **170:**2490–2493.
45. **Lundrigan, M. D., and R. J. Kadner.** 1986. Nucleotide sequence of the gene for the ferrienterochelin receptor FepA in *Escherichia coli*. Homology among outer membrane receptors that interact with TonB. J. Biol. Chem. **261:**10797–10801.
46. **Manges, A. R., J. R. Johnson, B. Foxman, T. T. O'Bryan, K. E. Fullerton, and L. W. Riley.** 2001. Widespread distribution of urinary tract infections caused by a multidrug-resistant *Escherichia coli* clonal group. N. Engl. J. Med. **345:**1007–1013.
47. **Martinez, J. J., M. A. Mulvey, J. D. Schilling, J. S. Pinkner, and S. J. Hultgren.** 2000. Type 1 pilus-mediated bacterial invasion of bladder epithelial cells. EMBO J. **19:**2803–2812.
48. **McHugh, J. P., F. Rodriguez-Quinones, H. Abdul-Tehrani, D. A. Svistunenko, R. K. Poole, C. E. Cooper, and S. C. Andrews.** 2003. Global iron-dependent gene regulation in *Escherichia coli*. A new mechanism for iron homeostasis. J. Biol. Chem. **278:**29478–29486.
49. **Mey, A. R., E. E. Wyckoff, A. G. Oglesby, E. Rab, R. K. Taylor, and S. M. Payne.** 2002. Identification of the *Vibrio cholerae* enterobactin receptors VctA and IrgA: IrgA is not required for virulence. Infect. Immun. **70:**3419–3426.
50. **Mount, D. W.** 1977. A mutant of *Escherichia coli* showing constitutive ex-

pression of the lysogenic induction and error-prone DNA repair pathways. Proc. Natl. Acad. Sci. USA **74**:300–304.

51. **Parkhill, J., B. W. Wren, K. Mungall, J. M. Ketley, C. Churcher, D. Basham, T. Chillingworth, R. M. Davies, T. Feltwell, S. Holroyd, K. Jagels, A. V. Karlyshev, S. Moule, M. J. Pallen, C. W. Penn, M. A. Quail, M. A. Rajandream, K. M. Rutherford, A. H. van Vliet, S. Whitehead, and B. G. Barrell.** 2000. The genome sequence of the food-borne pathogen *Campylobacter jejuni* reveals hypervariable sequences. Nature **403**:665–668.
52. **Provence, D. L., and R. Curtiss III.** 1992. Role of *crl* in avian pathogenic *Escherichia coli*: a knockout mutation of *crl* does not affect hemagglutination activity, fibronectin binding, or curli production. Infect. Immun. **60**:4460–4467.
53. **Rabsch, W., U. Methner, W. Voigt, H. Tschape, R. Reissbrodt, and P. H. Williams.** 2003. Role of receptor proteins for enterobactin and 2,3-dihydroxybenzoylserine in virulence of *Salmonella enterica*. Infect. Immun. **71**: 6953–6961.
54. **Russo, T. A., U. B. Carlino, and J. R. Johnson.** 2001. Identification of a new iron-regulated virulence gene, *ireA*, in an extraintestinal pathogenic isolate of *Escherichia coli*. Infect. Immun. **69**:6209–6216.
55. **Russo, T. A., U. B. Carlino, A. Mong, and S. T. Jodush.** 1999. Identification of genes in an extraintestinal isolate of *Escherichia coli* with increased expression after exposure to human urine. Infect. Immun. **67**:5306–5314.
56. **Russo, T. A., C. D. McFadden, U. B. Carlino-MacDonald, J. M. Beanan, T. J. Barnard, and J. R. Johnson.** 2002. IroN functions as a siderophore receptor and is a urovirulence factor in an extraintestinal pathogenic isolate of *Escherichia coli*. Infect. Immun. **70**:7156–7160.
57. **Sabri, M., S. Léveillé, and C. M. Dozois.** A plasmid-encoded SitABCD homologue from an avian pathogenic *Escherichia coli* strain mediates transport of iron and manganese and resistance to hydrogen peroxide. Microbiology **152**:745–758.
58. **Schmittgen, T. D., B. A. Zakrajsek, A. G. Mills, V. Gorn, M. J. Singer, and M. W. Reed.** 2000. Quantitative reverse transcription-polymerase chain reaction to study mRNA decay: comparison of endpoint and real-time methods. Anal. Biochem. **285**:194–204.
59. **Song, Y., Z. Tong, J. Wang, L. Wang, Z. Guo, Y. Han, J. Zhang, D. Pei, D. Zhou, H. Qin, X. Pang, Y. Han, J. Zhai, M. Li, B. Cui, Z. Qi, L. Jin, R. Dai, F. Chen, S. Li, C. Ye, Z. Du, W. Lin, J. Wang, J. Yu, H. Yang, J. Wang, P. Huang, and R. Yang.** 2004. Complete genome sequence of *Yersinia pestis* strain 91001, an isolate avirulent to humans. DNA Res. **11**:179–197.
60. **Tarr, P. I., S. S. Bilge, J. C. Vary, Jr., S. Jelacic, R. L. Habeeb, T. R. Ward, M. R. Baylor, and T. E. Besser.** 2000. Iha: a novel *Escherichia coli* O157:H7 adherence-conferring molecule encoded on a recently acquired chromosomal island of conserved structure. Infect. Immun. **68**:1400–1407.
61. **Warren, J. W., E. Abrutyn, J. R. Hebel, J. R. Johnson, A. J. Schaeffer, and W. E. Stamm.** 1999. Guidelines for antimicrobial treatment of uncomplicated acute bacterial cystitis and acute pyelonephritis in women. Infectious Diseases Society of America (IDSA). Clin. Infect. Dis. **29**:745–758.
62. **Winkelmann, G., A. Cansier, W. Beck, and G. Jung.** 1994. HPLC separation of enterobactin and linear 2,3-dihydroxybenzoylserine derivatives: a study on mutants of *Escherichia coli* defective in regulation (*fur*), esterase (*fes*) and transport (*fepA*). Biometals **7**:149–154.
63. **Woodall, L. D., P. W. Russell, S. L. Harris, and P. E. Orndorff.** 1993. Rapid, synchronous, and stable induction of type 1 piliation in *Escherichia coli* by using a chromosomal *lacUV5* promoter. J. Bacteriol. **175**:2770–2778.
64. **Young, I. G., and F. Gibson.** 1979. Isolation of enterochelin from *Escherichia coli*. Methods Enzymol. **56**:394–398.
65. **Zhang, J. P., and S. Normark.** 1996. Induction of gene expression in *Escherichia coli* after pilus-mediated adherence. Science **273**:1234–1238.
66. **Zhang, L., B. Foxman, and C. Marrs.** 2002. Both urinary and rectal *Escherichia coli* isolates are dominated by strains of phylogenetic group B2. J. Clin. Microbiol. **40**:3951–3955.
67. **Zhang, Z., G. Gosset, R. Barabote, C. S. Gonzalez, W. A. Cuevas, and M. H. Saier, Jr.** 2005. Functional interactions between the carbon and iron utilization regulators, Crp and Fur, in *Escherichia coli*. J. Bacteriol. **187**:980–990.

Editor: A. D. O'Brien

Annexe II

Contribution of the SitABCD, MntH, and FeoB Metal Transporters to the Virulence of Avian Pathogenic *Escherichia coli* O78 Strain χ7122.

Mourad Sabri, **Mélissa Caza**, Julie Proulx, Maria H. Lymberopoulos, Annie Brée, Maryvonne Moulin-Schouleur, Roy Curtiss III and Charles M. Dozois **(2008)** ***Infection and Immunity*** **76: 601-11**

A) Contribution de l'étudiante

1- L'article publié dans Infection and Immunity, démontre l'importance du transporteur de fer ferreux et de manganèse SitABCD pour la virulence de la souche χ7122 dans un modèle d'infection septicémique aviaire en infections simples et mixtes. La contribution pour la virulence des autres transporteurs de fer ferreux et manganèse MntH et FeoB a également été évaluée, démontrant un rôle auxiliaire à MntH. De plus, il a été démontré que les transporteurs SitABCD et MntH contribuent à la résistance aux stress oxydatifs.

2- L'étude a été réalisée en utilisant des techniques de génétique bactérienne, un modèle d'infection aviaire et des tests de sensibilité aux stress oxydatifs.

3- L'étudiante a réalisé les infections simples dans le modèle aviaire du mutant Δ*sit* et aussi établi le modèle d'infections mixtes avec la souche sauvage et le mutant Δ*lacZYA*.

B) Résumé de l'article:

Les rôles des transporteurs de métal SitABCD, MntH et FeoB pour la virulence de la souche O78 d'*Escherichia coli* pathogène aviaire (APEC) χ7122 a été évalués dans le modèle d'infection aviaire en utilisant des mutants isogéniques. Lors d'une infection simple, la souche Δ*sit* a démontré une colonisation réduite des poumons, du foie et de la rate en comparaison à la souche χ7122. La complémentation de la souche Δ*sit* a rétablit la virulence. Dans le modèle d'infection mixte, la souche Δ*sit* a démontré une réduction moyenne de 50 fois, 126 fois et 25 fois de la colonisation des poumons, du foie et de la

rate, respectivement. La souche Δ*mntH*Δ*sit* fut encore plus atténuée, démontrant une réduction de la persistance dans le sang et de 1400 fois, 954 fois et 83 fois dans la colonisation des poumons, du foie et de la rate, respectivement. En infections mixtes, la souche Δ*feoB*Δ*sit* a démontré une réduction dans la persistance dans le sang, mais une augmentation de la colonisation du foie. Les souches Δ*mntH*, Δ*feoB* et Δ*feoB*Δ*mntH* sont demeuré aussi virulent que la souche sauvage dans les deux modèles d'infections. Les mutants ont aussi été testés pour leur sensibilité au stress oxydatif généré par des agents chimiques. Le mutant Δ*mntH*Δ*sit* fut le plus sensible des souches et fut significativement plus sensible que les autres souches au peroxyde d'hydrogène, à la plombagine et au paraquate. Les séquences de *sit* sont hautement associées avec les souches d'*E. coli* pathogène extra-intestinal humain et les souches APEC en comparaison avec les isolats commensales et de diarrhée d'*E. coli*. Les analyses comparatives génomiques ont aussi démontré que les séquences de *sit* sont retrouvées sur des plasmides de conjugaison ou associées avec aux éléments de phages, en plus d'être vraisemblablement acquis par des événements distincts parmi les souches pathogènes d'*E. coli* et de *Shigella* spp. En somme, les résultats démontrent que SitABCD contribue à la virulence et, avec MntH, augmente la résistance au stress oxydatif.

INFECTION AND IMMUNITY, Feb. 2008, p. 601–611 Vol. 76, No. 2
0019-9567/08/$08.00+0 doi:10.1128/IAI.00789-07

Contribution of the SitABCD, MntH, and FeoB Metal Transporters to the Virulence of Avian Pathogenic *Escherichia coli* O78 Strain χ7122[▽]

Mourad Sabri,[1] Mélissa Caza,[1] Julie Proulx,[1] Maria H. Lymberopoulos,[1] Annie Brée,[2] Maryvonne Moulin-Schouleur,[2] Roy Curtiss III,[3,4] and Charles M. Dozois[1]*

INRS-Institut Armand-Frappier, Laval, Québec, Canada[1]; INRA, Centre de Tours, Infectiologie Animale et Santé Publique UR1282, 37380 Nouzilly, France[2]; Center for Infectious Diseases, The Biodesign Institute, Arizona State University, Tempe, Arizona 85287[3]; and Department of Biology, Washington University, St. Louis, Missouri 63130[4]

Received 8 June 2007/Returned for modification 25 July 2007/Accepted 5 November 2007

The roles of SitABCD, MntH, and FeoB metal transporters in the virulence of avian pathogenic *Escherichia coli* (APEC) O78 strain χ7122 were assessed using isogenic mutants in chicken infection models. In a single-strain infection model, compared to χ7122, the Δ*sit* strain demonstrated reduced colonization of the lungs, liver, and spleen. Complementation of the Δ*sit* strain restored virulence. In a coinfection model, compared to the virulent APEC strain, the Δ*sit* strain demonstrated mean 50-fold, 126-fold, and 25-fold decreases in colonization of the lungs, liver, and spleen, respectively. A Δ*mntH* Δ*sit* strain was further attenuated, demonstrating reduced persistence in blood and mean 1,400-fold, 954-fold, and 83-fold reduced colonization in the lungs, liver, and spleen, respectively. In coinfections, the Δ*feoB* Δ*sit* strain demonstrated reduced persistence in blood but increased colonization of the liver. The Δ*mntH*, Δ*feoB*, and Δ*feoB* Δ*mntH* strains were as virulent as the wild type in either of the infection models. Strains were also tested for sensitivity to oxidative stress-generating agents. The Δ*mntH* Δ*sit* strain was the most sensitive strain and was significantly more sensitive than the other strains to hydrogen peroxide, plumbagin, and paraquat. *sit* sequences were highly associated with APEC and human extraintestinal pathogenic *E. coli* compared to commensal isolates and diarrheagenic *E. coli*. Comparative genomic analyses also demonstrated that *sit* sequences are carried on conjugative plasmids or associated with phage elements and were likely acquired by distinct genetic events among pathogenic *E. coli* and *Shigella* sp. strains. Overall, the results demonstrate that SitABCD contributes to virulence and, together with MntH, to increased resistance to oxidative stress.

The *Salmonella* iron transporter, SitABCD, was first identified in *Salmonella enterica* serovar Typhimurium as a homolog of the *Yersinia pestis* YfeABCD transporter (68) and is a member of the periplasmic binding protein-dependent ATP-binding-cassette (ABC) family of metal transporters (12). In *Y. pestis* and *S. enterica* serovar Typhimurium, inactivation of the genes encoding the Yfe and Sit transporters, respectively, resulted in decreased virulence in murine experimental infection models (3, 25). SitABCD homologs are also present in other pathogenic enterobacteria, including *Shigella* spp. (26, 55, 66), uropathogenic *Escherichia coli* (UPEC) (6, 11, 67), and avian pathogenic *E. coli* (APEC) (28, 50, 56, 59). The genes encoding the Sit system are located on either genomic islands or large plasmids, and some strains carry more than one copy of the *sit* system (27, 28, 56, 59).

Previously, SitABCD from APEC strain χ7122 was shown to transport iron and manganese, and in the absence of the endogenous manganese transporter MntH, SitABCD contributed to protection of APEC and *E. coli* K-12 against hydrogen peroxide (56). SitABCD from *S. enterica* serovar Typhimurium similarly mediated transport of manganese and iron and, in combination with MntH, contributed to resistance to hydrogen peroxide (4). Furthermore, the loss of Sit in combination with the loss of either MntH or the Feo ferrous iron transporter resulted in greater attenuation of *Salmonella* virulence in susceptible mice (4). A *Shigella flexneri* 2a *sit* mutant was less able to grow in iron-restricted medium (38, 55). However, loss of Sit had no appreciable effect on intracellular multiplication or cell-to-cell spread in epithelial cells or on virulence in the guinea pig keratoconjunctivitis model (38, 55). In contrast, the cumulative loss of Sit and iron transporters such as Feo or the aerobactin siderophore system resulted in a reduced capacity to form plaques on epithelial cells (55). In addition, the cumulative loss of Sit and MntH resulted in a reduced capacity of *Shigella flexneri* 2a to survive in macrophage cell lines (53).

Divalent ion transporters such as SitABCD, MntH, and Feo may contribute to the virulence of APEC and other bacterial pathogens by facilitating acquisition of iron and/or manganese. Both manganese and iron are essential cofactors for enzymes required for metabolic processes and protection against oxidative stress (1, 23, 33). Thus far, the role of the SitABCD transporter, alone or in combination with other divalent metal transporters, such as MntH and Feo, in the virulence of pathogenic *E. coli* has not been investigated. A *sitABCD* mutant derivative of APEC strain χ7122 (O78:K80:H9) caused lesions in chickens similar to those induced by the parental strain and was also as resistant to hydrogen peroxide as the wild-type parent, suggesting that other metal transporters were possibly compensating for the absence of the Sit system (56). However, a *sitB* signature-tagged transposon mutant of APEC strain

* Corresponding author. Mailing address: INRS-Institut Armand-Frappier, 531 boul. des Prairies, Laval, Québec, Canada H7V 1B7. Phone: (450) 687-5010, ext. 4221. Fax: (450) 686-5501. E-mail: charles.dozois@iaf.inrs.ca.

▽ Published ahead of print on 19 November 2007.

TABLE 1. Bacterial strains and plasmids used in this study

Strain or plasmid	Characteristic(s)[a]	Reference or source
E. coli K-12 strains		
BW25113	*rrnB3ΔlacZ4787 hsdR514 ΔaraBAD ΔrhaBAD568 rph-1*	2
DH5α	F⁻ λ⁻ ϕ80 Δ(*lacZYA-argF*) *endA1 recA1 hsdR17 deoR thi-1 supE44 gyrA96 relA1*	Invitrogen
JW3372	BW25113 Δ*feoB*::*kan* Km^r	2
JW3933	BW25113 Δ*oxyR*::*kan* Km^r	2
JW4023	BW25113 Δ*soxS*::*kan* Km^r	2
MGN-617	*thi thr leu tonA lacY glnV supE ΔasdA4 recA*::RP4 2-Tc::Mu ⌊λpir⌋ Km^r	16
APEC χ7122 and derivatives		
χ7122	Wild-type APEC O78:K80:H9; *gyrA* Nal^r	47
QT51	χ7122 Δ*lacZYA* Nal^r	40
QT205	χ7122 Δ*sitABCD*::*tetAR* Tc^r	56
QT770	QT205::pIJ93; *sitABCD* single-copy integrant	This study
QT877	χ7122 Δ*feoB*::*kan* Nal^r Km^r	This study
QT878	χ7122 Δ*mntH*::*kan* Nal^r Km^r	56
QT1239	QT205 Δ*mntH*::*kan* Tc^r Nal^r Km^r	56
QT1240	QT205 Δ*feoB*::*kan* Tc^r Nal^r Km^r	This study
QT1517	QT878 Δ*mntH*::FRT Nal^r	
QT1539	QT1517 Δ*feoB*::*kan* Nal^r Km^r	This study
Plasmids		
pACYC184	p15A replicon cloning vector; Cm^r Tc^r	9
pCP20	FLP helper plasmid; Ts replicon; Ap^r Cm^r	14
pGP704	ori*R6K mobRP4* Ap^r	45
pIJ28	8-kb HindIII fragment containing *sitABCD* from χ7122 cloned into pACYC184; Cm^r	56
pIJ93	*sitABCD* genes from pIJ28 cloned into pGP704	This study
pKD46	λ red recombinase plasmid; Ts replicon; Ap^r	14

[a] Ap, ampicillin; Cm, chloramphenicol; Km, kanamycin; Nal, naladixic acid; Tc, tetracycline; Ts, temperature sensitive.

IMT5155 (O2:K5), which contains two copies of the *sit* genes, was moderately attenuated compared to its wild-type parent in a coinfection competition model in chickens (37), suggesting a role for the Sit transporter in virulence. Herein we investigate the individual role of SitABCD in the virulence of APEC O78:K80 strain χ7122 in single-strain infection and competitive infection models in chickens. In addition, we determined the roles of the MntH and Feo transporters, alone or combined with SitABCD, in the virulence of APEC strain χ7122 in the chicken and in resistance to oxidative stress agents. The distribution of *sit* genes among pathogenic *E. coli* and *E. coli* reference strains was also assessed. Finally, the *sit* sequences available from genomic databases were compared and suggest that *sit* genes were likely inherited through distinct transfer events leading to integration within conjugative plasmids in APEC or on prophage-associated genomic islands among *E. coli* and *Shigella* sp. strains.

MATERIALS AND METHODS

Bacterial strains, plasmids, media, and growth conditions. Bacterial strains and plasmids used in this study are listed in Table 1. In addition, clinical and commensal fecal isolates from various sources were used to screen for the presence of *sit* sequences. The 72 members of the *Escherichia coli* reference (ECOR) collection represent a diverse population of *E. coli* strains that have been grouped phylogenetically by multilocus enzyme electrophoresis (22). The 297 APEC clinical isolates were described elsewhere (16). APEC strains were previously classified for virulence based on lethality for 1-day-old chicks following subcutaneous inoculation, where LC1 corresponds to the high-lethality class, LC2 corresponds to the low-lethality class, and LC3 corresponds to the nonlethal class (16). Human extraintestinal pathogenic *E. coli* (ExPEC) isolates included 32 strains from urosepsis and other extraintestinal infections from the United States obtained from J. R. Johnson (Veterans Administration Medical Center, Minneapolis, MN). Thirty-two *E. coli* fecal isolates from healthy poultry and 23 diarrheagenic *E. coli* isolates belonging to various pathotypes (12 enterotoxigenic *E. coli* [ETEC], 6 enteropathogenic *E. coli*, and 5 enterohemorrhagic *E. coli* strains) were kindly provided by J. M. Fairbrother (University of Montreal, Canada). Strains were grouped phylogenetically by either multilocus enzyme electrophoresis or a multiplex PCR method (13). Strains were maintained at −80°C in 25% glycerol following overnight culture in Luria-Bertani (LB) broth (10 g yeast extract, 5 g tryptone, and 10 g NaCl per liter). Strains and clones were routinely grown in LB broth or on LB agar plates (15 g agar per liter) at 37°C. *E. coli* strain DH5α was routinely used for plasmid cloning and recovery. Antibiotics were added, as required, at the following concentrations: kanamycin, 30 μg/ml; ampicillin, 100 to 200 μg/ml; chloramphenicol, 30 μg/ml; nalidixic acid, 15 μg/ml; and tetracycline, 10 μg/ml.

DNA and genetic manipulations. Standard methods were used for isolation of bacterial genomic DNA, DNA manipulation, and cloning (58). Restriction enzymes and DNA ligase used in this study were purchased from New England Biolabs, Invitrogen, or Amersham Pharmacia and used according to the suppliers' recommendations. Recombinant plasmids, PCR products, and restriction fragments were purified using plasmid miniprep, PCR cleanup, and gel extraction kits (Qiagen or Sigma) as recommended by the supplier. Transformation of *E. coli* strains was routinely done by using the calcium/manganese-based or electroshock method, as described previously (19).

Presence of *sit* sequences among *E. coli* strains. The presence of *sit* sequences among different *E. coli* strains was investigated by PCR amplification of segments of the *sitA* and *sitD* genes that span the length of the *sitABCD* system. The *sitA* primers (sitA-F [5′-CGCAGGGGGCACAACTGAT-3′] and sitA-R [5′ CCCT GTACCAGCGTACTGG-3′]) amplify a 663-bp segment of *sitA*, and the *sitD* primers (sitD-F [5′-CTGTGCGCTGCTGTCGGTC-3′] and sitD-R [5′-GCGTT GTGTCAGGAGTAC-3′]) amplify a 570-bp segment of *sitD*. The specificity of each of the primers and the predicted amplification products were verified by comparative genomic/bioinformatic analysis against the *sit* genes from the *E. coli* and *Shigella* genomes or other nucleotide entries in the available databases, including GenBank (http://www.ncbi.nlm.nih.gov/) and *coli*BASE, an online database for comparative genomics of *E. coli* and related enterobacteria (http://colibase.bham.ac.uk/) (10). Crude DNA extracts of strains were prepared by alkaline lysis (48). The reactions were carried out using *Taq* DNA polymerase (New England Biolabs). A 5-μl volume of each bacterial cell lysate was added to a PCR mixture with a final volume of 25 μl containing 6.25 pmol of each primer, 5 nmol of each deoxynucleoside triphosphate, and 0.5 U of *Taq* polymerase in 1× buffer. PCR conditions were as follows: 95°C for 1 min, followed by 30 cycles of

94°C for 30 s, 54°C for 30 s, and 72°C for 1 min and then an extension period of 72°C for 1 min. Specific amplification was confirmed using strains χ7122 and CFT073 as positive controls and *E. coli* K-12 MG1655, which lacks the *sit* genes, as a negative control.

Construction of mutant derivatives of APEC strain χ7122 and single-copy complementation of the Δ*sit* mutation. The Δ*sitABCD*::*tetAR* (QT205), Δ*mntH*::*kan* (QT878), and Δ*mntH* Δ*sitABCD* (QT1239) derivatives of strain χ7122 are described elsewhere (56). QT1517 was generated by FLP-mediated excision of the Δ*mntH*::*kan* allele from strain QT878 by using plasmid pCP20 (14). The Δ*feoB*::*kan* allele from *E. coli* K-12 strain JWK3372_1 (2) was used to introduce Δ*feoB* mutations into APEC strains. Briefly, the Δ*feoB*::*kan* allele was amplified from genomic DNA of strain JWK3372_1 by using primers MfeoB1 (5′-TCTGGTCTCATGTCGCTGTC-3′) and MfeoB2 (5′-GGTGGAACTCTG CTTTTTGC-3′) and was introduced into strains χ7122, QT205, and QT1517 by homologous recombination using the λ red recombinase method (14). Successful transfer of the Δ*feoB*::*kan* mutation was confirmed by PCR, using primers flanking the *feoB* region. The Δ*feoB*::*kan* derivatives of χ7122, QT205, and QT1517 were designated QT877, QT1240, and QT1539, respectively.

The Δ*sitABCD* mutant strain QT205 was complemented by single-copy integration of plasmid pIJ93. pIJ93 was constructed by subcloning the XbaI-SalI fragment of pIJ28, containing the *sitABCD* operon, into the same sites of suicide vector pGP704. pIJ93 was conjugated from strain MGN-617 (16) to strain QT205. A strain that was resistant to ampicillin and found to contain a full-length copy of the *sit* genes, as confirmed by PCR, was designated QT770.

Sensitivity of *E. coli* strains to reactive oxygen intermediate (ROI)-generating agents. Sensitivity to oxidative stress was determined by an agar overlay diffusion method on LB and M9-glucose plates (1.5% agar) as described by Boyer et al. (4), with some modifications. Overnight cultures grown in LB broth were adjusted to an optical density at 600 nm (OD_{600}) of 0.5. For tests on M9 medium, the overnight cultures were washed with M9-glucose prior to OD_{600} adjustment. One hundred microliters of each culture was suspended in molten top agar (0.5% agar) and poured over the agar plates. Filter paper disks (6-mm diameter; Becton Dickinson) were added to the surfaces of the solidified overlays, and 10 μl of hydrogen peroxide (30%), paraquat (200 mM for LB and 40 mM for M9), plumbagin (53 mM), phenazine methosulfate (PMS) (15 mM), or phenazine ethosulfate (PES) (15 mM) was spotted onto the disks. The plates were then incubated overnight at 37°C, and following growth, the diameters of inhibition zones were measured.

Experimental infection of chickens via the air sacs. Two different infection models, a comparative single-strain infection model and a competitive coinfection model, were used to investigate the importance of different metal transporters for the virulence of APEC. Chickens used in these studies were White Leghorn specific-pathogen-free chickens obtained from either Charles River Spafas (now Charles River Laboratories [Franklin, CT]) or the Canadian Food Inspection Agency (Ottawa, Canada). For the single-strain infection model, groups of 3-week-old White Leghorn chickens were inoculated in the right thoracic air sac with 0.1 ml (10^7 CFU) of a bacterial inoculum consisting of a diluted 24-h beef heart infusion broth culture of APEC strain χ7122 or an isogenic mutant derivative. For the coinfection experiments, strains were prepared as for the single-strain infections, and equal quantities (5×10^6 CFU) of each mutant strain and a virulent Δ*lacZYA* derivative of strain χ7122 (QT51) were used as the inoculum. Use of the Δ*lacZYA* derivative of strain χ7122 (QT51) in coinfections permitted a direct evaluation of the number of colonies of QT51 (Lac^- colonies) compared to the metal transporter mutant (Lac^+ colonies) on each plate. For the coinfection studies, blood samples were collected aseptically from each chicken 6, 24, and 48 h following bacterial inoculation and were plated directly or diluted and then plated on MacConkey-lactose agar plates (Difco) supplemented with nalidixic acid (40 μg/ml). All birds were euthanized at 48 h postinfection and then necropsied. For the single-strain infection experiments, gross mean lesion scores for the air sacs and combined lesion scores for the pericardium and liver were determined as described by Lamarche et al. (36). Organs were removed aseptically. The left lung, liver, and spleen of each animal were weighed, suspended in phosphate-buffered saline, and homogenized with an Omnimixer homogenizer. Dilutions of homogenates were plated onto MacConkey-lactose agar plates with appropriate antibiotics for bacterial quantification. Several randomly selected colonies per organ were verified by serotyping using O78-specific antiserum.

Bioinformatic analysis and comparison of *sit* sequences from different *E. coli* and *Shigella* strains. The sequences and locations of *sit* gene clusters within the genomes of various *E. coli* and *Shigella* strains were identified from the available databases, including GenBank (http://www.ncbi.nlm.nih.gov/) and *coli*BASE. Sequence analyses, multiple sequence alignment by CLUSTALW, and generation of a phylogenetic tree were done using the MEGA3 software package (35; http://www.megasoftware.net). The phylogenetic tree of the *sitABCD* gene clusters was constructed by using the neighbor-joining method (57) of pairwise comparison by maximum likelihood analysis using the Jukes-Cantor estimate (30) to calculate nucleotide substitution rates.

Statistical analyses. Statistical analyses were performed using the Prism 4.0b software package (GraphPad Software).

RESULTS

The *sit* genes are associated with prophage elements and conjugative plasmids. A previous report indicated that depending on the *E. coli* strain, *sitABCD* genes were located either on pColV-type plasmids or on the bacterial chromosome in ExPEC or APEC, and certain strains contained both genomic and plasmid-carried copies of the *sit* genes (56). Analysis of the genome and nucleotide sequence databases indicated that *sit* sequences are present in ExPEC-UPEC strains CFT073, 536, and UTI89, APEC strain O1, enteroaggregative *E. coli* (EAEC) O42 (Fig. 1), and all of the currently available *Shigella* genomes but are absent from *E. coli* K-12 strains and the genomes of other pathogenic *E. coli* strains. *sit* gene clusters are also present on the plasmids of APEC O1(pAPEC-O1-ColBM), APEC O2(pAPEC-O2-ColV), and APEC χ7122 (pAPEC-1) (Fig. 1), and genomic and plasmid-carried copies of *sit* sequences are present in APEC O2:K5 strain IMT5155 (GenBank accession no. AM072350 and AM072351).

The *sit* gene clusters are present at four distinct chromosomal locations in the *E. coli-Shigella* genomes (Fig. 1A). Among the sequenced ExPEC-UPEC strains and APEC O1, the *sitABCD* genes are all part of genomic regions containing prophage sequences that are inserted at the *icd-ycgX* intergenic region, which is the *attB* attachment site for certain lambdoid bacteriophages. These prophage element-containing regions have identical junction borders to those in the *E. coli* K-12 genome and vary in size from 55 kb (CFT073) (67) to 47.3 kb (APEC O1) (28). In *E. coli* K-12 MG1655, this region harbors the e14 element, a vestige of a lambdoid prophage, which encompasses 15.4 kb (43). In EAEC strain O42, *Shigella sonnei*, and *Shigella dysenteriae*, the *sit* genes are part of 48.4-kb, 25.6-kb, and 19.9-kb regions, respectively, comprised mainly of phage elements, and are inserted at the *ydaO* (b1344)-*ynaF* (b1376) region of *E. coli* K-12 MG1655 (10). This region is the attachment site for Rac prophage and related prophage elements in *E. coli* K-12 and O157:H7 strains (8). In *S. flexneri* 2a strain 301, *sit* genes are in the middle of a 42-kb genomic island, *Shigella* island 19 (SI-19), located in a region that has undergone rearrangements compared to *E. coli* MG1655. SI-19 contains genes that are homologous to phage sequences and insertion sequence elements and is flanked by sequences corresponding to *ycjI* and *yebU* in *E. coli* K-12 MG1655 (26). In *S. flexneri* 2a strain 2457T, *sit* genes are in the middle of a 37-kb genomic island that is adjacent to *aspS*. Despite differences in the locations of the *sit* genes within the genomes of *S. flexneri* 2a strains 301 and 2457T, the lambdoid prophage sequences immediately flanking the *sit* genes in these two genomes are similar. Sequences flanking the *sit* genes on plasmids are similar to each other but are distinct from those adjacent to the *sit* genes present on the genomic islands of any of the *E. coli* or *Shigella* strains.

Comparison of the nucleotide sequences encoding SitABCD from *E. coli* and *Shigella* strains in a neighbor-joining tree

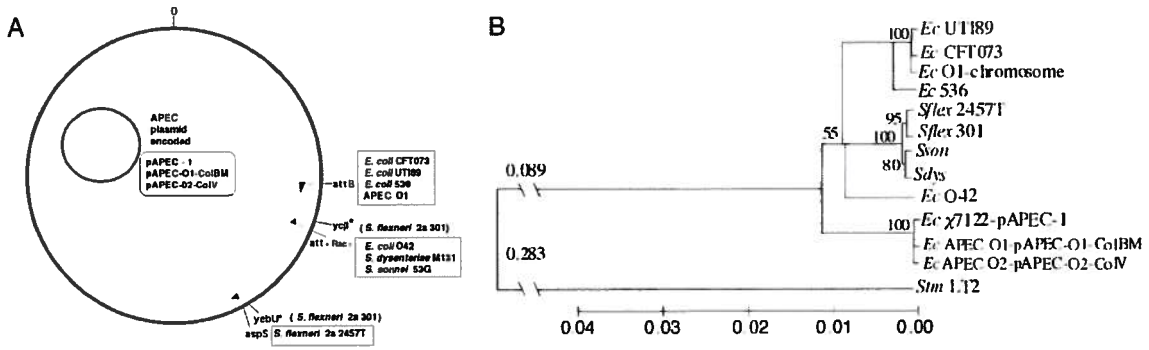

FIG. 1. (A) Map location of *sit* genes in *E. coli* and *Shigella* strains. The large circle represents the *E. coli* K-12 MG1655 genome as a comparative reference, with 0 indicating the start of the sequence. The insertion locations corresponding to *E. coli* K-12 are indicated on the outer perimeter. The inner black arrows represent the genomic islands and the orientation of the *sit* genes in different pathogenic strains. The outer gray arrows indicate corresponding e14 and Rac prophage elements located in the same regions in strain MG1655. The asterisks denote the *E. coli* K-12 corresponding genes flanking either side of SI-19, the genomic island encompassing the *sit* genes in *S. flexneri* 2a strain 301 (26). (B) Phylogenetic tree of the *sitABCD* genes from *E. coli* and *Shigella* spp., constructed using the neighbor-joining method with MEGA3 software (35). *Ec*, *Escherichia coli*; *Sflex*, *Shigella flexneri*; *Sson*, *Shigella sonnei* 53G; *Sdys*, *Shigella dysenteriae* M131. The full-length sequences spanning from the *sitA* start codon to the *sitD* stop codon were analyzed, and *sitABCD* genes from *Salmonella enterica* serovar Typhimurium LT2 were used as the outlier sequence. Distances were calculated using the Jukes and Cantor estimate, which assumes a uniform rate of nucleotide substitutions. Branch lengths are indicated on the scale or above branches that are off the scale. Bootstrap confidence levels are indicated adjacent to the nodes. *sit* sequence data were obtained from NCBI with GenBank accession numbers AY598030 (pAPEC-1 of *E. coli* χ7122) (56), AY545598 (*E. coli* APEC O2/pAPEC-O2-ColV) (29), DQ381420 (*E. coli* APEC O1/pAPEC-O1-ColBM) (27), NC_004431 (*E. coli* CFT073) (67), NC_008563 (*E. coli* APEC O1) (28), NC_007946 (*E. coli* UTI89) (11), NC_008253 (*E. coli* 536) (6), NC_004337 (*S. flexneri* 2a 301) (26), NC_004741 (*S. flexneri* 2a 2457T) (66), and NC_003197 (*S. enterica* LT2) (42) or from *coli*BASE (10; http://colibase.bham.ac.uk/) for *E. coli* O42, *Shigella dysenteriae* M131, and *Shigella sonnei* 53G. Data available from *coli*BASE were produced by the sequencing group at the Sanger Institute (http://www.sanger.ac.uk/Projects/Escherichia_Shigella/).

demonstrated that *sit* gene clusters form three main groups, comprised of the ExPEC-APEC genomic *sit* sequences, the *Shigella sit* sequences, and the plasmid-carried APEC *sit* sequences (Fig. 1B). The *E. coli* O42 *sit* sequence branched separately but was most closely related to *Shigella* sequences. Phylogenetic analyses of each of the *sit* genes generated the same distinct groupings (data not shown). Overall, the *sit* sequences demonstrated nucleotide variability at 156 sites, which corresponded to a variability of 4.5% of the *sit* gene cluster. Sequences within each of the three main cluster groups demonstrated low variability (from 0.4% to 0.6% overall) within their respective clusters. In contrast, between cluster groups, variability increased two- to sixfold (from 1.2% to 2.5%). Taken together, these differences in genomic locations and nucleotide sequence variability among the *sit* genes from different *E. coli* and *Shigella* strains support the likelihood that *sit* genes were acquired by these two closely related species via a number of distinct genetic events involving horizontal gene transfer mediated by phages, plasmids, or other mobile genetic elements.

Distribution of *sit* genes among ECOR collection and *E. coli* clinical and fecal commensal isolates. The presence and distinct localization of *sit* sequences among different *E. coli* and *Shigella* sp. strains prompted us to further investigate the distribution of *sit* sequences among a diverse population of strains, including ECOR collection, ExPEC, diarrheagenic *E. coli*, APEC, and avian fecal commensal *E. coli* strains. PCR analysis was performed using *sitA*- and *sitD*-specific primers which correspond to conserved regions in the *sitA* and *sitD* genes currently available from the sequence databases. For all strains tested, there was no discrepancy between results when using either the *sitA* or *sitD* primers. Among the 72 members of

TABLE 2. Distribution of *sit*-positive strains within phylogenetic groups among ECOR collection and *Escherichia coli* clinical isolates

Phylogenetic group	ECOR collection		Clinical isolate[c]			
			ExPEC		Diarrheagenic *E. coli*	
	Total no. of strains	No. (%) of *sit*-positive strains[a] (%)	No. of isolates	No. (%) of *sit*-positive isolates	No. of isolates	No. (%) of *sit*-positive isolates
A	25	5 (20)	6	6 (100)	12	1 (8.3)
B1	16	7 (43.8)	0	0	8	1 (12.5)
B2	15	15 (100)[b]	20	20 (100)	1	0
D	12	6 (50)	6	6 (100)	2	0
Other	4	1 (25)	NA	NA	NA	NA
Total	72	34 (47.2)	32	32 (100)[d]	23	2 (8.7)

[a] Positive PCR amplification using the *sitA* and *sitD* primer pairs.
[b] Among the ECOR collection strains, *sit* was significantly associated with group B2 compared to any other phylogenetic group ($P < 0.0001$).
[c] NA, not applicable.
[d] *sit* was significantly associated with ExPEC strains compared to diarrheagenic *E. coli* or the ECOR collection strains ($P < 0.0001$).

TABLE 3. Distribution of *sit* genes among APEC and avian commensal fecal isolates according to lethality class

Lethality class	APEC		Commensal fecal isolate	
	Total no. of isolates	No. (%) of *sit*-positive isolates[a]	Total no. of isolates	No. (%) of *sit*-positive isolates[a]
LC1[b]	221	218 (99)[c]	1	0 (0)
LC2	38	31 (82)	12	5 (42)
LC3	38	26 (68)	19	9 (47)
Total	297	275 (93)[d]	32	14 (44)

[a] Positive PCR amplification using the *sitA* and *sitD* primer pairs.
[b] Lethality classes were defined as follows: LC1, 50% lethal dose (LD_{50}) of $<10^8$ CFU; LC2, LD_{50} of $\geq 10^8$ CFU; LC3, not lethal at $\geq 10^8$ CFU (16).
[c] *sit* sequences were significantly associated with APEC isolates from LC1 compared to APEC isolates from either LC2 or LC3 ($P < 0.001$).
[d] *sit* sequences were significantly associated with APEC isolates compared to commensal fecal isolates ($P < 0.001$).

the ECOR collection, which have been arranged into four phylogenetic groups (A, B1, B2, and D) on the basis of multilocus enzyme electrophoresis (22), the presence of *sit* sequences was significantly associated with phylogenetic group B2 compared to the other groups ($P < 0.0001$) (Table 2). All B2 group strains from the ECOR collection were *sit* positive, whereas in the other phylogenetic groups 50% or fewer were *sit* positive. In addition, all 32 human ExPEC strains tested were *sit* positive, whereas only 2 of 23 diarrheagenic *E. coli* isolates contained *sit* sequences (Table 2). The presence of *sit* sequences was also investigated in APEC and avian fecal commensal isolates (Table 3). Among 297 APEC strains classified according to their lethality for 1-day-old chicks, *sit* sequences were more common in the highly virulent APEC (class 1 lethality) strains (99%) than in the less virulent strains (81% for class 2 and 68% for class 3) ($P < 0.001$). In addition, *sit* sequences were highly associated with APEC compared to avian fecal commensal isolates ($P < 0.001$). For APEC isolates, 275/297 (93%) isolates were *sit* positive, whereas only 14/32 (44%) avian fecal isolates were *sit* positive. Overall, the results demonstrate that *sit* sequences are highly prevalent in *E. coli* strains associated with extraintestinal infections compared to diarrheagenic *E. coli* and commensal fecal isolates.

SitABCD contributes to virulence of APEC during infection of chickens. Since *sit* sequences were highly associated with *E. coli* isolates from extraintestinal infections in poultry, we investigated the importance of *sit* genes for the virulence of APEC O78 strain χ7122 in chickens. We first compared the virulence potential of the Δ*sitABCD* mutant strain QT205 with that of its isogenic wild-type parent strain, χ7122, in a single-strain infection model. Compared to wild-type parent strain χ7122, strain QT205 (Δ*sitABCD*) was attenuated and demonstrated significantly reduced bacterial numbers in the lungs and livers of infected chickens (Fig. 2a and b). QT205 demonstrated a mean 1-log reduction in colonization of the spleens; however, the difference was not significant ($P = 0.0545$) (Fig. 2c). The *sit*-complemented derivative of QT205 (QT770) regained virulence to levels comparable to that of the wild-type parent strain, χ7122 (Fig. 2). Despite the decreased persistence of QT205 in chickens, this strain caused gross lesions of airsacculitis and pericarditis/perihepatitis that were similar to those caused by the wild-type parent (data not shown).

We also investigated the role of the Feo ferrous iron transporter and the MntH manganese transporter in the virulence of APEC strain χ7122. In single-strain infection experiments, in contrast to strain QT205 (Δ*sitABCD*), strains QT877 (Δ*feoB*) and QT878 (Δ*mntH*) persisted in all tissues at levels similar to that of wild-type APEC strain χ7122. Thus, in the presence of a functional SitABCD system, FeoB or MntH did not appear to be of major importance for the virulence of APEC χ7122 in chickens. In addition, in the single-strain infection model, mutant strains QT1239 (Δ*sitABCD* Δ*mntH*) and QT1240 (Δ*sitABCD* Δ*feoB*) were not any more attenuated than the Δ*sitABCD* single mutant QT205 (data not shown). The mutant derivatives lacking functional Sit, MntH, and/or Feo transporters demonstrated no appreciable difference in growth rate compared to the wild-type parent when cultured in either rich (Luria broth) or minimal (M9-glucose) medium (data not shown). Therefore, the reduced colonization of tissues by the *sit* and other attenuated mutants during infection of chickens was most likely due to a decreased capacity to survive in vivo, not a global reduction in fitness or growth.

Compared to single-strain infection models, competitive

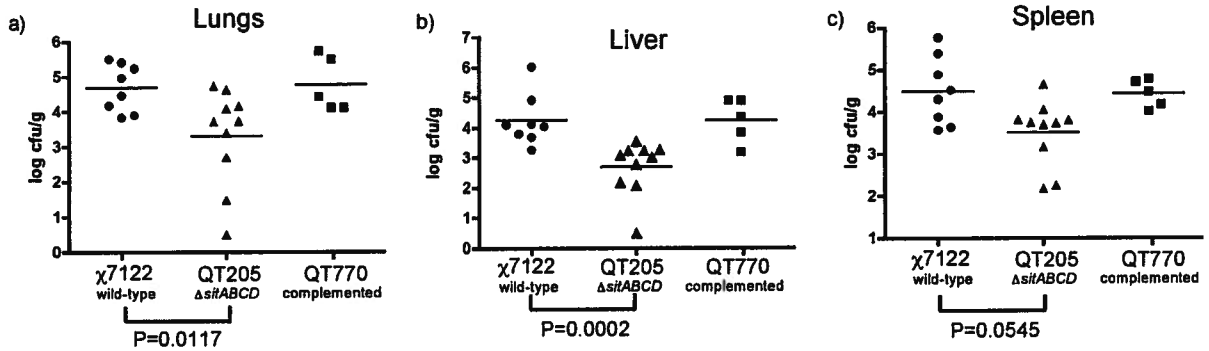

FIG. 2. Colonization of extraintestinal organs of chickens by APEC strain χ7122 and derivatives in the single-strain infection model. Data are presented as log CFU/gram of tissue. Each data point represents a tissue sample from an individual infected chicken at 48 h postinfection. Organs sampled were the lungs (a), liver (b), and spleen (c). Strains tested were wild-type APEC strain χ7122 (●), QT205 (Δ*sitABCD*) (▲), and QT770 (QT205::*sitABCD*) (■). *P* values for comparative differences in colonization by QT205 and the wild-type strain, as determined by the Mann-Whitney test, are indicated below the *x* axes.

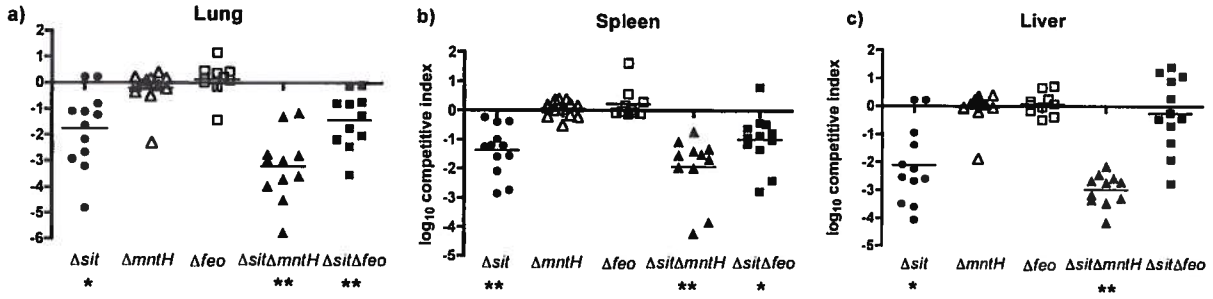

FIG. 3. Comparative colonization of chicken tissues by APEC χ7122 derivatives lacking the Sit, MntH, or Feo metal transporter and virulent χ7122 Δ*lac* derivative strain QT51. A competitive coinfection model was used in which QT51 and different metal transporter mutants were inoculated simultaneously. At 48 h postinfection, tissues were sampled, and results are presented as the $\log_{10}$ CI. The CI represents the relative numbers of the two test strains from the tissues sampled (the output ratio) compared to the initial numbers of the strains in the inoculum (input ratio). Negative CI values indicate a decreased capacity for the mutant to compete with the virulent test strain (QT51). Horizontal bars indicate the mean $\log_{10}$ CI values. Each data point represents a sample from an individual chicken. Ten to 12 chickens were used for each infection group. Organs sampled were the lungs (a), spleen (b), and liver (c). Strains tested were QT205 (Δ*sitABCD*) (●), QT878 (Δ*mntH*) (△), QT877 (Δ*feoB*) (□), QT1239 (Δ*sitABCD* Δ*mntH*) (▲), and QT1240 (Δ*sitABCD* Δ*feoB*) (■). Statistically significant decreases in CI values are indicated with asterisks (*, $P < 0.005$; **, $P < 0.001$), as determined by the Wilcoxon matched-pair test.

coinfection models using virulent strains and isogenic mutants can demonstrate more sensitivity to differences in colonization or virulence. Because single-strain infections in chickens did not show any attenuation for strains QT877 (Δ*feoB*) and QT878 (Δ*mntH*), and since no differences in attenuation between strain QT205 (Δ*sitABCD*) and the double mutants QT1239 (Δ*sitABCD* Δ*mntH*) and QT1240 (Δ*sitABCD* Δ*feoB*) were observed in single-strain infections, we tested these strains in a competitive coinfection model. For this model, we used APEC strain QT51, a Δ*lacZYA* derivative of strain χ7122, as the competitor strain. QT51 was shown to be as virulent as the wild-type parent strain χ7122 in both single-strain infection and coinfection experiments (data not shown). The use of a virulent Lac-negative wild-type derivative permitted us to directly compare the levels of the Lac-positive mutant derivative and the virulent Lac-negative competitor strain from the same biological samples by differential counts on MacConkey-lactose agar plates.

In coinfection experiments, strain QT205 (Δ*sitABCD*) was clearly attenuated and showed a significantly reduced competitive index (CI) compared to that of competitor strain QT51, with a mean 50-fold decrease in the lung (Fig. 3a) and a mean 126-fold decrease in the liver (Fig. 3b). These results were consistent with the results observed for the single-strain infection experiments. In addition, QT205 was also significantly reduced, by a mean of 25-fold, in the spleen (Fig. 3c). During the course of the infection, no significant differences between QT51 and QT205 were apparent in the blood at 6 h and 24 h postinfection (Fig. 4). However, QT205 was significantly reduced, by a mean of 3.6-fold, in the blood by 48 h postinfection. Unlike strain QT205, strains QT877 (Δ*feoB*) and QT878 (Δ*mntH*) were present at similar levels to those of strain QT51 in all tissues and blood (Fig. 3 and 4). These results were consistent with the lack of attenuation of these strains in the single-strain infection model.

In coinfections using the double mutants, strain QT1239 (Δ*sitABCD* Δ*mntH*) was the most attenuated strain (Fig. 3 and 4). QT1239 demonstrated a significantly reduced CI in the blood at all times, with mean decreases of 2.2-fold, 16.2-fold, and 10-fold compared to the competitor strain at 6 h, 24 h, and 48 h, respectively. QT1239 also demonstrated a mean 1,400-fold reduction in the lungs, 954-fold reduction in the liver, and 83-fold reduction in the spleen compared to strain QT51. In contrast, strain QT1240 (Δ*sitABCD* Δ*feoB*) demonstrated sig-

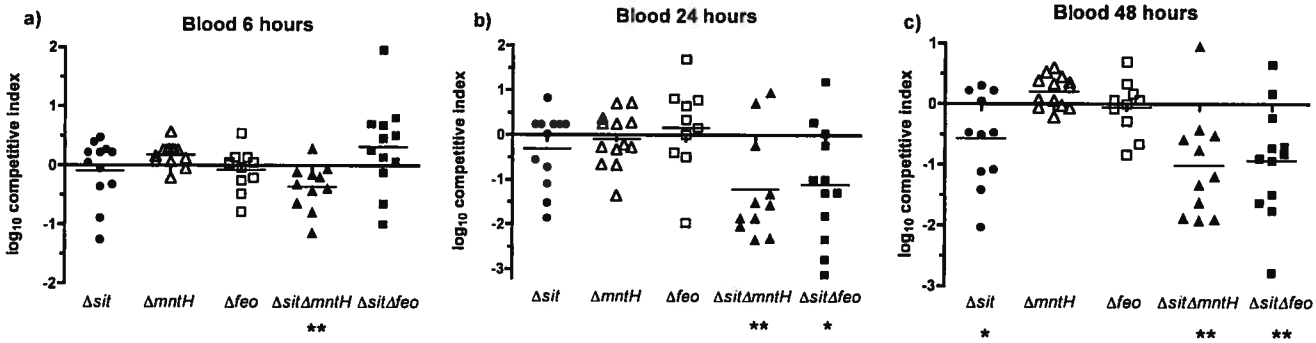

FIG. 4. Comparative persistence of APEC χ7122 derivatives lacking the Sit, MntH, or Feo metal transporter and virulent χ7122 Δ*lac* derivative strain QT51 in the blood of infected chickens. Experiments were conducted using a coinfection model as described in the legend to Fig. 3. Blood was sampled at 6 h (a), 24 h (b), and 48 h (c) postinfection. Strains tested were QT205 (Δ*sitABCD*) (●), QT878 (Δ*mntH*) (△), QT877 (Δ*feoB*) (□), QT1239 (Δ*sitABCD* Δ*mntH*) (▲), and QT1240 (Δ*sitABCD* Δ*feoB*) (■). Statistically significant decreases in CI values, as determined by the Wilcoxon matched-pair test, are indicated with asterisks (*, $P < 0.005$; **, $P < 0.001$).

nificant, 2.2-fold and 5.6-fold reductions in the blood at 24 h and 48 h, respectively. QT1240 was also reduced 26.8-fold in the lungs and 6.8-fold in the spleen but was not significantly reduced in the liver (Fig. 3). Strain QT1539 (Δ*feoB* Δ*mntH*) did not demonstrate any significant decrease compared to strain QT51 in either the blood or tissues (data not shown). Comparison of the mean CIs for strains QT205 (Δ*sitABCD*), QT1239 (Δ*sitABCD* Δ*mntH*), and QT1240 (Δ*sitABCD* Δ*feoB*) demonstrated no significant differences between the groups in the blood and spleen. In the lung, QT1239 (Δ*sitABCD* Δ*mntH*) was significantly more attenuated in the coinfection model than was QT205 (Δ*sitABCD*) ($P = 0.0178$). In contrast, QT205 (Δ*sitABCD*) was significantly more attenuated than QT1240 (Δ*sitABCD* Δ*feoB*) ($P = 0.0061$) in the liver. Taken together, these results demonstrate that, individually, the Sit system is most important for competitive survival and persistence compared to the Feo and MntH transporters. In addition, a cumulative loss of Sit and MntH transporters globally resulted in more marked attenuation than that with the loss of only the Sit transporter. In contrast, a cumulative loss of the Sit and Feo systems compared to the individual loss of Sit actually resulted in reduced persistence in the blood but increased colonization of the liver.

Sensitivity of *E. coli* strains to ROI-generating compounds. The sensitivities of APEC strain χ7122 and its mutant derivatives to ROI-generating compounds was assessed on both rich (LB) and minimal (M9-glucose) media (Fig. 5). On LB medium, only the Δ*mntH* Δ*sitABCD* (QT1239) strain was more sensitive than the wild-type parent strain to the ROI-generating compounds H_2O_2 ($P = 0.002$) and plumbagin ($P = 0.027$). On minimal medium, QT1239 was more sensitive to H_2O_2 ($P = 0.015$), plumbagin ($P = 0.004$), and paraquat ($P = 0.004$). On minimal medium, the Δ*mntH* mutant QT878 was more sensitive to H_2O_2 ($P = 0.012$) and paraquat ($P < 0.001$) than the APEC wild-type parent but was less sensitive to these products than the Δ*mntH* Δ*sitABCD* derivative. In addition, on minimal medium, the Δ*feoB* Δ*sitABCD* strain (QT1539) was also somewhat more sensitive to H_2O_2 ($P = 0.007$) than the wild-type parent. In contrast, the Δ*sitABCD* mutant QT205 did not demonstrate any increased sensitivity to ROI-generating products compared to the wild-type parent (data not shown).

APEC strain χ7122 was intrinsically more resistant to all of the ROI-generating compounds tested than the K-12 control strain following growth on either LB or minimal medium ($P < 0.05$) (Fig. 5). In addition, the APEC metal transporter mutants that were more sensitive to certain ROI-generating compounds were always resistant to PMS and PES. Compared to the other ROI-generating compounds, PMS and PES specifically generated a superoxide stress response, as the Δ*soxS* K-12 strain, but not the Δ*oxyR* derivative, demonstrated sensitivity to these compounds (Fig. 5). Taken together, these results demonstrate that the MntH and SitABCD divalent metal transporters synergistically contributed to increased resistance to ROIs that generate either a H_2O_2-specific or a mixed H_2O_2 and superoxide stress response. In contrast to the in vivo studies with chickens, in which the Sit transporter was the only system studied that individually contributed to virulence, in vitro only the MntH transporter was shown to individually contribute to resistance to oxidative stress.

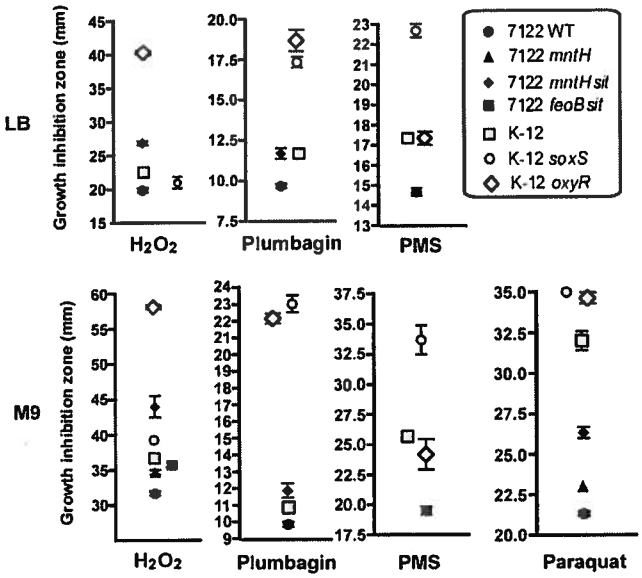

FIG. 5. Sensitivities of wild-type APEC strain χ7122 and isogenic metal transport mutants to ROI-generating compounds. Strains were grown on either LB agar or M9 agar, and tests were performed as described in Materials and Methods. ROI-generating compounds tested were 30% hydrogen peroxide (H_2O_2), 53 mM plumbagin, 15 mM PMS or PES, and 40 mM paraquat. Paraquat was ineffective against all strains grown on LB medium, even at higher concentrations (up to 200 mM). Sensitivity to PES was similar to sensitivity to PMS (not shown). The results represent the means of replicate experiments for a minimum of three samples. Vertical bars represent the standard errors of the means. Only wild-type (WT) strain χ7122 and its mutant derivatives that demonstrated a significant increase ($P < 0.05$) in sensitivity to ROI-generating products are indicated. APEC strains indicated in the legend are χ7122 (7122 WT; ●), QT878 (7122 *mntH*; ▲), QT1239 (7122 *mntH sit*; ◆), and QT1240 (7122 *feoB sit*; ■). *E. coli* K-12 strains BW25113 (K-12 ■), JW3933 (K-12 *oxyR*; ◆), and JW4023 (K-12 *soxS*; ●) were used as comparative controls. For all conditions tested, K-12 strain BW25113 was significantly more sensitive ($P < 0.05$) to ROI-generating compounds than was APEC strain χ7122.

DISCUSSION

In this report, we investigated the individual and combined roles of the SitABCD, MntH, and FeoB transporters in the virulence of APEC strain χ7122. These transport systems are mainly involved in the import of manganese and/or ferrous iron. MntH is a proton-dependent NRAMP-related transporter that is highly selective for manganese (33, 41), FeoB is a GTPase that functions in ferrous iron transport (20, 31), and SitABCD (YfeABCD in *Yersinia* spp.) is an ABC transporter that mediates uptake of manganese and iron (3, 33, 56).

Iron plays a number of vital functions in bacterial cells and is a cofactor of numerous enzymes (1). Importantly, iron plays a role in protection against oxidative stress, as it is a component of the SodB superoxide dismutase (SOD) and catalase enzymes, which eliminate superoxide (O_2^-) and H_2O_2, respectively. However, excess iron can also contribute to oxidative damage through the generation of free radicals (1). Due to the limited availability of iron in the host, pathogenic bacteria have acquired numerous iron transport systems, some of which are major virulence factors (5). Bacteria obtain ferric iron from the host via either siderophore systems, low-molecular-weight

chelators that solubilize iron, or host iron transport protein receptors, whereas ferrous iron is transported by FeoB and SitABCD-like systems (5). Manganese is also a cofactor for a number of bacterial enzymes, contributes to protection against oxidative stress (33), and can contribute directly to the detoxification of ROIs (23). In *E. coli* and other enterobacteria, two main systems, MntH and SitABCD, have been identified as being involved in manganese transport (33, 41, 56). Since iron and manganese are critical for bacterial tolerance to oxidative stress as well as other metabolic functions, SitABCD, MntH, and FeoB could potentially promote bacterial survival during infection by facilitating the transport of these trace metals and by countering oxidative stress during infection of the host.

FeoB and MntH orthologs are widespread among a diverse population of bacteria (20, 49), and these systems are conserved among *E. coli* strains, as they are present in all the currently sequenced *E. coli* and *Shigella* genomes. Unlike *feoB* and *mntH*, *sit* genes are present in only a subset of *E. coli* strains. *sit* genes were predominant among ExPEC and APEC isolates and *E. coli* strains belonging to phylogenetic group B2 but were absent from *E. coli* K-12 and most diarrheagenic *E. coli* strains, except for enteroaggregative *E. coli* strain O42 (Fig. 1A; Tables 2 and 3). Among avian *E. coli* strains, we determined that *sit* genes were highly associated with the virulence of APEC for 1-day-old chicks (Table 3). This is the first report describing an association of *sit* genes with the virulence of APEC. In addition, *sit* genes were significantly associated with APEC (93%) compared to avian fecal commensal isolates (44%) (Table 3). Similarly, Rodriguez-Seik et al. (51) detected *sit* in 86.4% of APEC strains, compared to 42.7% of fecal commensal isolates from poultry. Overall, *sit* sequences are clearly prevalent among ExPEC and APEC strains compared to intestinal commensal *E. coli* strains.

In some *E. coli* strains, two or more copies of the *sit* genes are present, with one copy being carried on a plasmid and another copy being chromosomally carried (17, 27–29). Recently, Ewers et al. (17) also detected the specific presence of episomal and chromosomal copies of *sit* by PCR using specific primers. They detected 31.6% prevalence of *sit* among APEC strains by using chromosome-specific primers and 73.2% prevalence of *sit* among APEC strains by using episome-specific primers. These results suggest that APEC strains more commonly contain a plasmid-carried copy of *sit* than chromosomally carried *sit* genes. Chromosomal copies of *sit* genes are associated with different phage elements (Fig. 1A). Hence, in certain strains, *sitABCD* represents another virulence factor that may have been acquired via bacteriophages, which are common contributors to bacterial diversification and adaptability (8, 46). It is tempting to speculate that recombination or integration events within a single strain may have led to the duplication of *sit* genes. However, comparative sequence analysis demonstrates higher identity among *sit* sequences located in genomic islands from different strains than between genomic island- and plasmid-carried *sit* sequences from the same strain (Fig. 1B). These findings favor the likelihood that *sit* genes may have been acquired independently from different sources by distinct events resulting in the incorporation of these genes into either plasmids or prophage-associated genomic islands in the genomes of *Shigella* and ExPEC.

The increased association of *sit* genes with ExPEC and APEC compared to other *E. coli* strains suggested a possible role for this transporter in virulence during extraintestinal infection. In UPEC strain CFT073, *sit* genes were upregulated in the urines of mice during urinary tract infection or in vitro following growth in human urine (63). Also, in *Shigella flexneri* 2a, the expression of *sit* genes was upregulated during infection of cells (39, 54). This further suggests that SitABCD may contribute to metal transport in vivo and to virulence during extraintestinal infections. In both the single-strain infection and competitive infection models, the APEC Δ*sitABCD* mutant was clearly attenuated and less able to colonize the tissues and persist in the blood of infected chickens (Fig. 2 to 4). In contrast, the single-strain infection and coinfection results demonstrated that in the presence of a functional SitABCD transporter, the inactivation of FeoB or MntH did not reduce the virulence of APEC strain χ7122. In addition, the combined loss of *feoB* and *mntH* did not reduce virulence. Hence, in contrast to the MntH and FeoB transporters, the Sit transporter contributed significantly to the survival of APEC in extraintestinal tissues. These results indicate that the divalention transporter SitABCD imparts a selective advantage compared to the MntH or FeoB transporter in vivo. The infection model used for these studies was the air sac inoculation model (15, 16), which has been shown to result in a more uniform rate of infection of extraintestinal tissues and blood than that obtained with the more natural aerosol route of infection (18, 64). However, by using the air sac route in the single-strain infection model, despite the significantly decreased survival of the Δ*sitABCD* mutant in chickens, this strain caused gross lesions of airsacculitis and pericarditis/perihepatitis that were similar to those caused by the wild-type parent. This is likely because the attenuated strains remained in the tissues at levels of 3 log or above at 48 h postinfection in most birds. Such bacterial levels are likely to be sufficient to still elicit a strong inflammatory response and the generation of gross lesions. It is possible that the use of the aerosol route in single-strain infection experiments could potentially demonstrate differences in pathology of colibacillosis between strains that were not observed via the air sac route, as the aerosol route requires APEC to initially colonize and proliferate in the upper respiratory tract and then subsequently invade deeper tissues.

The use of the competitive infection model provided increased sensitivity compared to that of the single-strain infections. This was most evident in analyses of mutants that had lost both SitABCD and MntH divalent manganese transport functions or SitABCD and FeoB divalent iron transport functions (Fig. 3 and 4). No significant difference at any site was observed in the single-strain infections by comparing these double mutants to the mutants which lacked the Sit transporter alone. This is likely due to the combination of competitive pressure between strains, in addition to pressures due to immune defenses and nutritional limitations within the host, in the competitive infection model (52, 65).

The contribution of Sit to the virulence of APEC may be due in large part to its function as an efficient manganese transporter (56) and to the importance of manganese for coping with oxidative stress. Cellular accumulation of manganese contributes to protection against oxidative stress by direct catalytic scavenging of ROIs and can also lead to increased activity of bacterial manganese-dependent SOD (MnSOD) (23). In *E.*

coli, MnSOD, encoded by *sodA*, is an inducible SOD that responds to increases in oxidative stress, and MnSOD more effectively protected *E. coli* against paraquat and H_2O_2 than did FeSOD, encoded by *sodB* (7). An efficient capacity to accumulate Mn by APEC via the Sit and MntH transporters is therefore likely to contribute to survival in host extraintestinal sites. The infection results demonstrated that loss of MntH alone had no discernible effect on virulence in the chicken, whereas loss of Sit alone did reduce virulence. Conversely, MntH alone contributed to protection of APEC against ROIs, whereas Sit alone had no significant contribution to resistance to oxidative stress in vitro (Fig. 5). This may be explained by differences in environmental conditions, which may affect the activity of each of these transport systems. MntH transports metals via a proton-dependent gradient and, as such, functions best under acidic conditions (32). In contrast, Sit-mediated transport is most efficient under alkaline conditions (32, 56). The pH in chicken blood and tissues is maintained at approximately 7.4, a pH at which Sit efficiently mediates Mn transport (4, 56). It is also possible that the ATPase-mediated Sit ABC transporter may be more effective at tolerating stresses within the host that could impede the proton gradient required for proper functioning of MntH-mediated transport. Although Sit alone appeared to be more important than MntH in vivo, it is clear that the combined loss of the Sit and MntH transporters resulted in the greatest attenuation, particularly in the lung, and in greater sensitivity to a number of ROI-generating compounds. Taken together, these results support a synergistic role for Sit and MntH to transport manganese and contribute to a greater overall resistance to oxidative stress and persistence during infection.

Loss of Sit and MntH rendered the APEC strain more susceptible to a number of ROI-generating compounds, particularly on minimal medium (Fig. 5). Manganese transporters in a number of bacteria have been shown to contribute to resistance to H_2O_2 and superoxide (23). As observed for *Salmonella enterica* serovar Typhimurium and *Shigella flexneri* 2a *mntH sit* mutants (4, 53), the APEC Δ*mntH* Δ*sitABCD* mutant was more sensitive to H_2O_2 (Fig. 5) (56). In addition, the APEC Δ*mntH* Δ*sitABCD* mutant was also more sensitive to certain redox cycling agents, including plumbagin and paraquat. These compounds generate superoxide radicals, but superoxide can be converted readily into H_2O_2 by SODs within bacterial cells. The use of Δ*oxyR* and Δ*soxS* K-12 control strains, which were both more sensitive to plumbagin and paraquat, also suggested that subsequent generation of H_2O_2 occurred following exposure to these compounds. In contrast, neither APEC Δ*mntH* Δ*sitABCD* nor the Δ*oxyR* control was more sensitive to phenazines (PMS and PES) than the relevant parent strain, although these compounds more effectively killed the Δ*soxS* control. Differences in sensitivity to redox cycling agents may therefore be due to their mechanisms of action for generation of oxidative stress or possibly other toxic effects. In *E. coli*, the response to oxidative stress generated by PMS differs considerably from that generated by paraquat or plumbagin, with PMS generating a high level of catalase activity and little increase in SOD activity, whereas paraquat and plumbagin induce increases in both SOD and catalase activities (21, 60).

Although the Sit transporter from APEC strain χ7122 was shown to mediate uptake of iron in an iron transport-deficient *E. coli* K-12 mutant (56), it is unlikely that iron transport by SitABCD is a key feature of APEC virulence. Strain χ7122 uses three confirmed siderophore systems (aerobactin, salmochelins, and enterobactin) in addition to the Feo and SitABCD transporters. Elimination of the aerobactin and salmochelin siderophore systems resulted in a nearly complete loss of persistence of APEC strain χ7122 in chickens (15), suggesting that the remaining iron transport systems (FeoB, SitABCD, and enterobactin) were unable to meet the iron transport requirements for survival of APEC during extraintestinal infection. This is not surprising, since FeoB and SitABCD function mainly as ferrous iron transporters (20, 56), and iron present in extraintestinal tissues is predominantly ferric iron associated with host ferro-proteins. Furthermore, although enterobactin is a highly efficient siderophore in vitro, it competes poorly as a siderophore in host tissues (1, 5). The finding that the cumulative loss of the Sit and Feo ferrous iron transporters did not result in greater attenuation than that of the Δ*sitABCD* mutant is in further support of a limited requirement of these systems for iron acquisition in extraintestinal tissues (Fig. 3). However, the combined loss of Sit and Feo resulted in a decreased capacity to persist in the blood (Fig. 4). It is possible that in the blood, where iron availability is minimal, the ferrous transport functions of Feo and Sit in combination with efficient ferric siderophore systems could provide a modest competitive edge. Furthermore, the combined loss of Feo and Sit also increased the sensitivity to hydrogen peroxide (Fig. 5), suggesting the cumulative importance of these two transporters under certain conditions. In contrast, combined loss of Sit and Feo actually resulted in a significant regain in colonization of the liver compared to that of the Δ*sitABCD* mutant in the competitive coinfection model (Fig. 3c). The liver functions in iron storage and recycling. During infection, increased cell death and tissue necrosis in the liver may lead to localized tissue anoxia and increased availability of ferrous iron at lesion sites. Under anaerobic conditions and with increased availability of ferrous iron, the Feo transporter may therefore be deleterious. In support of this, compared to its wild-type parent, an *E. coli* K-12 *feo* mutant grown anaerobically was more resistant to H_2O_2-mediated killing than its isogenic parent strain (34).

In APEC, the *sit* genes are commonly located on large conjugative (ColV or ColBM) plasmids (17, 27, 29, 56, 59). The roles of such plasmids in various APEC or pathogenic *E. coli* strains have been established in a number of reports (16, 18, 24, 61, 62, 64), although specific plasmid-carried genes contributing to APEC virulence are less well characterized. The Sit transporter, along with the aerobactin and salmochelin siderophores (15) and Tsh (16), represents another plasmid-encoded virulence factor of APEC strain χ7122. Compared with the divalent manganese or iron transporter MntH or FeoB, the importance of SitABCD iron and manganese transport for virulence of APEC is preponderant. Hence, in addition to providing an advantage for intracellular survival for *Salmonella enterica* and *Shigella flexneri* 2a, in APEC Sit appears to provide an adaptive advantage during extraintestinal survival. The reduction in virulence together with the increased sensitivity to ROI-generating compounds observed for some of the APEC metal transport mutants suggests that reduced survival during infection could possibly be due to increased killing by phago-

cytes or the products they may liberate into the extracellular environment. Although APEC strain χ7122 is refractory to internalization by avian phagocytes, APEC strains belonging to other serogroups, such as O2 or O1, are more readily internalized and can survive within phagocytes (44). In future studies, it will be interesting to determine if Sit contributes to increased survival of certain APEC strains within host cells and its potential role in the virulence of ExPEC in human extraintestinal infections.

ACKNOWLEDGMENTS

We acknowledge Geneviève Garriss for construction of strain QT770.

Funding for research was provided by the Natural Sciences and Engineering Research Council (NSERC), Canada, the Canadian Foundation for Innovation (CFI), and a Canada Research Chair (CRC) to C.M.D. and by USDA grant 00-35204-9224 to R.C. and C.M.D. M.S., M.C., and M.H.L. were the recipients of Fondation Armand-Frappier scholarships. J.P. was funded by a scholarship from Fonds de la Recherche en Santé Québec (FRSQ).

REFERENCES

1. **Andrews, S. C., A. K. Robinson, and F. Rodriguez-Quinones.** 2003. Bacterial iron homeostasis. FEMS Microbiol. Rev. **27**:215–237.
2. **Baba, T., T. Ara, M. Hasegawa, Y. Takai, Y. Okumura, M. Baba, K. A. Datsenko, M. Tomita, B. L. Wanner, and H. Mori.** 2006. Construction of *Escherichia coli* K-12 in-frame, single-gene knockout mutants: the Keio collection. Mol. Syst. Biol. **2**:2006.0008.
3. **Bearden, S. W., and R. D. Perry.** 1999. The Yfe system of *Yersinia pestis* transports iron and manganese and is required for full virulence of plague. Mol. Microbiol. **32**:403–414.
4. **Boyer, E., I. Bergevin, D. Malo, P. Gros, and M. F. Cellier.** 2002. Acquisition of Mn(II) in addition to Fe(II) is required for full virulence of *Salmonella enterica* serovar Typhimurium. Infect. Immun. **70**:6032–6042.
5. **Braun, V.** 2005. Bacterial iron transport related to virulence. Contrib. Microbiol. **12**:210–233.
6. **Brzuszkiewicz, E., H. Bruggemann, H. Liesegang, M. Emmerth, T. Olschlager, G. Nagy, K. Albermann, C. Wagner, C. Buchrieser, L. Emody, G. Gottschalk, J. Hacker, and U. Dobrindt.** 2006. How to become a uropathogen: comparative genomic analysis of extraintestinal pathogenic *Escherichia coli* strains. Proc. Natl. Acad. Sci. USA **103**:12879–12884.
7. **Carlioz, A., and D. Touati.** 1986. Isolation of superoxide dismutase mutants in *Escherichia coli*: is superoxide dismutase necessary for aerobic life? EMBO J. **5**:623–630.
8. **Casjens, S.** 2003. Prophages and bacterial genomics: what have we learned so far? Mol. Microbiol. **49**:277–300.
9. **Chang, A. C., and S. N. Cohen.** 1978. Construction and characterization of amplifiable multicopy DNA cloning vehicles derived from the P15A cryptic miniplasmid. J. Bacteriol. **134**:1141–1156.
10. **Chaudhuri, R. R., A. M. Khan, and M. J. Pallen.** 2004. coliBASE: an online database for *Escherichia coli*, *Shigella* and *Salmonella* comparative genomics. Nucleic Acids Res. **32**:D296–D299.
11. **Chen, S. L., C. S. Hung, J. Xu, C. S. Reigstad, V. Magrini, A. Saho, D. Blasiar, T. Bieri, R. R. Meyer, P. Ozersky, J. R. Armstrong, R. S. Fulton, J. P. Latreille, J. Spieth, T. M. Hooton, E. R. Mardis, S. J. Hultgren, and J. I. Gordon.** 2006. Identification of genes subject to positive selection in uropathogenic strains of *Escherichia coli*: a comparative genomics approach. Proc. Natl. Acad. Sci. USA **103**:5977–5982.
12. **Claverys, J. P.** 2001. A new family of high-affinity ABC manganese and zinc permeases. Res. Microbiol. **152**:231–243.
13. **Clermont, O., S. Bonacorsi, and E. Bingen.** 2000. Rapid and simple determination of the *Escherichia coli* phylogenetic group. Appl. Environ. Microbiol. **66**:4555–4558.
14. **Datsenko, K. A., and B. L. Wanner.** 2000. One-step inactivation of chromosomal genes in *Escherichia coli* K-12 using PCR products. Proc. Natl. Acad. Sci. USA **97**:6640–6645.
15. **Dozois, C. M., F. Daigle, and R. Curtiss III.** 2003. Identification of pathogen-specific and conserved genes expressed in vivo by an avian pathogenic *Escherichia coli* strain. Proc. Natl. Acad. Sci. USA **100**:247–252.
16. **Dozois, C. M., M. Dho-Moulin, A. Brée, J. M. Fairbrother, C. Desautels, and R. Curtiss III.** 2000. Relationship between the Tsh autotransporter and pathogenicity of avian *Escherichia coli* and localization and analysis of the Tsh genetic region. Infect. Immun. **68**:4145–4154.
17. **Ewers, C., G. Li, H. Wilking, S. Kiessling, K. Alt, E. M. Antao, C. Laturnus, I. Diehl, S. Glodde, T. Homeier, U. Bohnke, H. Steinruck, H. C. Philipp, and L. H. Wieler.** 2007. Avian pathogenic, uropathogenic, and newborn meningitis-causing *Escherichia coli*: how closely related are they? Int. J. Med. Microbiol. **297**:163–176.
18. **Ginns, C. A., M. L. Benham, L. M. Adams, K. G. Whithear, K. A. Bettelheim, B. S. Crabb, and G. F. Browning.** 2000. Colonization of the respiratory tract by a virulent strain of avian *Escherichia coli* requires carriage of a conjugative plasmid. Infect. Immun. **68**:1535–1541.
19. **Hanahan, D., J. Jessee, and F. R. Bloom.** 1995. Techniques for transformation of *E. coli*, p. 1–35. *In* D. M. Glover and B. D. Hames (ed.), DNA cloning I: core techniques, 2nd ed. Oxford University Press, New York, NY.
20. **Hantke, K.** 2003. Is the bacterial ferrous iron transporter FeoB a living fossil? Trends Microbiol. **11**:192–195.
21. **Hassan, H. M., and I. Fridovich.** 1979. Intracellular production of superoxide radical and of hydrogen peroxide by redox active compounds. Arch. Biochem. Biophys. **196**:385–395.
22. **Herzer, P. J., S. Inouye, M. Inouye, and T. S. Whittam.** 1990. Phylogenetic distribution of branched RNA-linked multicopy single-stranded DNA among natural isolates of *Escherichia coli*. J. Bacteriol. **172**:6175–6181.
23. **Horsburgh, M. J., S. J. Wharton, M. Karavolos, and S. J. Foster.** 2002. Manganese: elemental defence for a life with oxygen. Trends Microbiol. **10**:496–501.
24. **Ike, K., K. Kawahara, H. Danbara, and K. Kume.** 1992. Serum resistance and aerobactin iron uptake in avian *Escherichia coli* mediated by conjugative 100-megadalton plasmid. J. Vet. Med. Sci. **54**:1091–1098.
25. **Janakiraman, A., and J. M. Slauch.** 2000. The putative iron transport system SitABCD encoded on SPI1 is required for full virulence of *Salmonella typhimurium*. Mol. Microbiol. **35**:1146–1155.
26. **Jin, Q., Z. Yuan, J. Xu, Y. Wang, Y. Shen, W. Lu, J. Wang, H. Liu, J. Yang, F. Yang, X. Zhang, J. Zhang, G. Yang, H. Wu, D. Qu, J. Dong, L. Sun, Y. Xue, A. Zhao, Y. Gao, J. Zhu, B. Kan, K. Ding, S. Chen, H. Cheng, Z. Yao, B. He, R. Chen, D. Ma, B. Qiang, Y. Wen, Y. Hou, and J. Yu.** 2002. Genome sequence of *Shigella flexneri* 2a: insights into pathogenicity through comparison with genomes of *Escherichia coli* K12 and O157. Nucleic Acids Res. **30**:4432–4441.
27. **Johnson, T. J., S. J. Johnson, and L. K. Nolan.** 2006. Complete DNA sequence of a ColBM plasmid from avian pathogenic *Escherichia coli* suggests that it evolved from closely related ColV virulence plasmids. J. Bacteriol. **188**:5975–5983.
28. **Johnson, T. J., S. Kariyawasam, Y. Wannemuehler, P. Mangiamele, S. J. Johnson, C. Doetkott, J. A. Skyberg, A. M. Lynne, J. R. Johnson, and L. K. Nolan.** 2007. The genome sequence of avian pathogenic *Escherichia coli* strain O1:K1:H7 shares strong similarities with human extraintestinal pathogenic *E. coli* genomes. J. Bacteriol. **189**:3228–3236.
29. **Johnson, T. J., K. E. Siek, S. J. Johnson, and L. K. Nolan.** 2006. DNA sequence of a ColV plasmid and prevalence of selected plasmid-encoded virulence genes among avian *Escherichia coli* strains. J. Bacteriol. **188**:745–758.
30. **Jukes, T. H., and C. R. Cantor.** 1969. Evolution of protein molecules, p. 21–132. *In* H. N. Munro (ed.), Mammalian protein metabolism. Academic Press, New York, NY.
31. **Kammler, M., C. Schon, and K. Hantke.** 1993. Characterization of the ferrous iron uptake system of *Escherichia coli*. J. Bacteriol. **175**:6212–6219.
32. **Kehres, D. G., A. Janakiraman, J. M. Slauch, and M. E. Maguire.** 2002. SitABCD is the alkaline Mn^{2+} transporter of *Salmonella enterica* serovar Typhimurium. J. Bacteriol. **184**:3159–3166.
33. **Kehres, D. G., and M. E. Maguire.** 2003. Emerging themes in manganese transport, biochemistry and pathogenesis in bacteria. FEMS Microbiol. Rev. **27**:263–290.
34. **Keyer, K., A. S. Gort, and J. A. Imlay.** 1995. Superoxide and the production of oxidative DNA damage. J. Bacteriol. **177**:6782–6790.
35. **Kumar, S., K. Tamura, and M. Nei.** 2004. MEGA3: Integrated software for molecular evolutionary genetics analysis and sequence alignment. Brief. Bioinform. **5**:150–163.
36. **Lamarche, M. G., C. M. Dozois, F. Daigle, M. Caza, R. Curtiss III, J. D. Dubreuil, and J. Harel.** 2005. Inactivation of the *pst* system reduces the virulence of an avian pathogenic *Escherichia coli* O78 strain. Infect. Immun. **73**:4138–4145.
37. **Li, G., C. Laturnus, C. Ewers, and L. H. Wieler.** 2005. Identification of genes required for avian *Escherichia coli* septicemia by signature-tagged mutagenesis. Infect. Immun. **73**:2818–2827.
38. **Liu, M., H. Liu, L. Sun, J. Dong, Y. Xue, S. Chen, and Q. Jin.** 2005. Construction, detection and microarray analysis on the *Shigella flexneri* 2a *sitC* mutant. Sci. China C **48**:228–240.
39. **Lucchini, S., H. Liu, Q. Jin, J. C. Hinton, and J. Yu.** 2005. Transcriptional adaptation of *Shigella flexneri* during infection of macrophages and epithelial cells: insights into the strategies of a cytosolic bacterial pathogen. Infect. Immun. **73**:88–102.
40. **Lymberopoulos, M. H., S. Houle, F. Daigle, S. Léveillé, A. Brée, M. Moulin-Schouleur, J. R. Johnson, and C. M. Dozois.** 2006. Characterization of Stg fimbriae from an avian pathogenic *Escherichia coli* O78:K80 strain and assessment of their contribution to colonization of the chicken respiratory tract. J. Bacteriol. **188**:6449–6459.
41. **Makui, H., E. Roig, S. T. Cole, J. D. Helmann, P. Gros, and M. F. Cellier.**

2000. Identification of the *Escherichia coli* K-12 Nramp orthologue (MntH) as a selective divalent metal ion transporter. Mol. Microbiol. **35:**1065–1078.
42. **McClelland, M., K. E. Sanderson, J. Spieth, S. W. Clifton, P. Latreille, L. Courtney, S. Porwollik, J. Ali, M. Dante, F. Du, S. Hou, D. Layman, S. Leonard, C. Nguyen, K. Scott, A. Holmes, N. Grewal, E. Mulvaney, E. Ryan, H. Sun, L. Florea, W. Miller, T. Stoneking, M. Nhan, R. Waterston, and R. K. Wilson.** 2001. Complete genome sequence of *Salmonella enterica* serovar Typhimurium LT2. Nature **413:**852–856.
43. **Mehta, P., S. Casjens, and S. Krishnaswamy.** 2004. Analysis of the lambdoid prophage element e14 in the *E. coli* K-12 genome. BMC Microbiol. **4:**4.
44. **Mellata, M., M. Dho-Moulin, C. M. Dozois, R. Curtiss III, B. Lehoux, and J. M. Fairbrother.** 2003. Role of avian pathogenic *Escherichia coli* virulence factors in bacterial interaction with chicken heterophils and macrophages. Infect. Immun. **71:**494–503.
45. **Miller, V. L., R. K. Taylor, and J. J. Mekalanos.** 1987. Cholera toxin transcriptional activator toxR is a transmembrane DNA binding protein. Cell **48:**271–279.
46. **Ohnishi, M., K. Kurokawa, and T. Hayashi.** 2001. Diversification of *Escherichia coli* genomes: are bacteriophages the major contributors? Trends Microbiol. **9:**481–485.
47. **Provence, D. L., and R. Curtiss III.** 1992. Role of *crl* in avian pathogenic *Escherichia coli*: a knockout mutation of *crl* does not affect hemagglutination activity, fibronectin binding, or Curli production. Infect. Immun. **60:**4460–4467.
48. **Restieri, C., G. Garriss, M. C. Locas, and C. M. Dozois.** 2007. Autotransporter-encoding sequences are phylogenetically distributed among *Escherichia coli* clinical isolates and reference strains. Appl. Environ. Microbiol. **73:**1553–1562.
49. **Richer, E., P. Courville, I. Bergevin, and M. F. Cellier.** 2003. Horizontal gene transfer of "prototype" Nramp in bacteria. J. Mol. Evol. **57:**363–376.
50. **Rodriguez-Siek, K. E., C. W. Giddings, C. Doetkott, T. J. Johnson, M. K. Fakhr, and L. K. Nolan.** 2005. Comparison of *Escherichia coli* isolates implicated in human urinary tract infection and avian colibacillosis. Microbiology **151:**2097–2110.
51. **Rodriguez-Siek, K. E., C. W. Giddings, C. Doetkott, T. J. Johnson, and L. K. Nolan.** 2005. Characterizing the APEC pathotype. Vet. Res. **36:**241–256.
52. **Roos, V., G. C. Ulett, M. A. Schembri, and P. Klemm.** 2006. The asymptomatic bacteriuria *Escherichia coli* strain 83972 outcompetes uropathogenic *E. coli* strains in human urine. Infect. Immun. **74:**615–624.
53. **Runyen-Janecky, L., E. Dazenski, S. Hawkins, and L. Warner.** 2006. Role and regulation of the *Shigella flexneri* Sit and MntH systems. Infect. Immun. **74:**4666–4672.
54. **Runyen-Janecky, L. J., and S. M. Payne.** 2002. Identification of chromosomal *Shigella flexneri* genes induced by the eukaryotic intracellular environment. Infect. Immun. **70:**4379–4388.
55. **Runyen-Janecky, L. J., S. A. Reeves, E. G. Gonzales, and S. M. Payne.** 2003. Contribution of the *Shigella flexneri* Sit, Iuc, and Feo iron acquisition systems to iron acquisition in vitro and in cultured cells. Infect. Immun. **71:**1919–1928.
56. **Sahri, M., S. Léveillé, and C. M. Dozois.** 2006. A SitABCD homologue from an avian pathogenic *Escherichia coli* strain mediates transport of iron and manganese and resistance to hydrogen peroxide. Microbiology **152:**745–758.
57. **Saitou, N., and M. Nei.** 1987. The neighbor-joining method: a new method for reconstructing phylogenetic trees. Mol. Biol. Evol. **4:**406–425.
58. **Sambrook, J., and D. W. Russell.** 2001. Molecular cloning: a laboratory manual, 3rd ed. Cold Spring Harbor Laboratory Press, Cold Spring Harbor, NY.
59. **Schouler, C., F. Koffmann, C. Amory, S. Leroy-Setrin, and M. Moulin-Schouleur.** 2004. Genomic subtraction for the identification of putative new virulence factors of an avian pathogenic *Escherichia coli* strain of O2 serogroup. Microbiology **150:**2973–2984.
60. **Schwartz, C. E., J. Krall, L. Norton, K. McKay, D. Kay, and R. E. Lynch.** 1983. Catalase and superoxide dismutase in *Escherichia coli*. J. Biol. Chem. **258:**6277–6281.
61. **Skyberg, J. A., T. J. Johnson, J. R. Johnson, C. Clabots, C. M. Logue, and L. K. Nolan.** 2006. Acquisition of avian pathogenic *Escherichia coli* plasmids by a commensal *E. coli* isolate enhances its abilities to kill chicken embryos, grow in human urine, and colonize the murine kidney. Infect. Immun. **74:**6287–6292.
62. **Smith, H. W.** 1974. A search for transmissible pathogenic characters in invasive strains of *Escherichia coli*: the discovery of a plasmid-controlled toxin and a plasmid-controlled lethal character closely associated, or identical, with colicine V. J. Gen. Microbiol. **83:**95–111.
63. **Snyder, J. A., B. J. Haugen, E. L. Buckles, C. V. Lockatell, D. E. Johnson, M. S. Donnenberg, R. A. Welch, and H. L. Mobley.** 2004. Transcriptome of uropathogenic *Escherichia coli* during urinary tract infection. Infect. Immun. **72:**6373–6381.
64. **Tivendale, K. A., J. L. Allen, C. A. Ginns, B. S. Crabb, and G. F. Browning.** 2004. Association of *iss* and *iucA*, but not *tsh*, with plasmid-mediated virulence of avian pathogenic *Escherichia coli*. Infect. Immun. **72:**6554–6560.
65. **Torres, A. G., P. Redford, R. A. Welch, and S. M. Payne.** 2001. TonB-dependent systems of uropathogenic *Escherichia coli*: aerobactin and heme transport and TonB are required for virulence in the mouse. Infect. Immun. **69:**6179–6185.
66. **Wei, J., M. B. Goldberg, V. Burland, M. M. Venkatesan, W. Deng, G. Fournier, G. F. Mayhew, G. Plunkett III, D. J. Rose, A. Darling, B. Mau, N. T. Perna, S. M. Payne, L. J. Runyen-Janecky, S. Zhou, D. C. Schwartz, and F. R. Blattner.** 2003. Complete genome sequence and comparative genomics of *Shigella flexneri* serotype 2a strain 2457T. Infect. Immun. **71:**2775–2786.
67. **Welch, R. A., V. Burland, G. Plunkett III, P. Redford, P. Roesch, D. Rasko, E. L. Buckles, S. R. Liou, A. Boutin, J. Hackett, D. Stroud, G. F. Mayhew, D. J. Rose, S. Zhou, D. C. Schwartz, N. T. Perna, H. L. Mobley, M. S. Donnenberg, and F. R. Blattner.** 2002. Extensive mosaic structure revealed by the complete genome sequence of uropathogenic *Escherichia coli*. Proc. Natl. Acad. Sci. USA **99:**17020–17024.
68. **Zhou, D., W. D. Hardt, and J. E. Galan.** 1999. *Salmonella typhimurium* encodes a putative iron transport system within the centisome 63 pathogenicity island. Infect. Immun. **67:**1974–1981.

Editor: J. B. Bliska

Annexe III

A small RNA promotes siderophore production through transcriptional and metabolic remodelling

Hubert Salvail, Pascale Lanthier-Bourbonnais, Jason Michael Sobota, **Mélissa Caza,** Julie-Anna M. Benjamin, Martha Eugènia Sequeira Mendieta, François Lépine, Charles M. Dozois, James Imlay, and Eric Massé

A) Contribution de l'étudiante

1- L'article publié dans PNAS, démontre un nouveau mécanisme de régulation de l'entérobactine de façon directe et indirecte exercés par le petit ARN non-codant RyhB. D'abord, RyhB est nécessaire pour l'expression des gènes de synthèse (*entCBA*) et transport (*fepA*) de l'entérobactine. Ensuite, RyhB régule la traduction de la sérine acétyltransférase CysE en s'appariant et initiant la dégradation aux ARNm de *cysE*, réprimant ainsi la biosynthèse de la cystéine.

2- L'étude a été réalisée en utilisant des techniques de génétique bactérienne et de biologie moléculaire, ainsi que de la chromatographie liquide couplée au spectromètre de masse (LC-MS/MS).

3- L'étudiante a réalisé la quantification de l'entérobactine et des molécules dégradées sécrétés par la souche *E. coli* et des différents mutants par LC-MS/MS.

B) Résumé de l'article:

Les sidérophores sont des facteurs essentiels pour l'acquisition du fer (Fe) chez les bactéries pendant la colonisation et l'infection des hôtes eucaryotes, puisque les protéines de liaison au fer, telles que la lactoferrine et la transferrine, restreignent l'accès au fer. La synthèse des sidérophores par *Escherichia coli* est considérée d'être complètement régulée au niveau transcriptionnel par le répresseur répondant au fer Fur. Dans cette étude, nous avons caractérisé deux voies différentes qui induisent la production du sidérophore entérobactine par le biais de

l'action du petit ARN RyhB. Tout d'abord, RyhB est requis pour l'expression normale d'un important polycistron de la biosynthèse de l'entérobactine, *entCEBAH*. Deuxièmement, RyhB réprime directement la traduction de *cysE*, qui encode pour une sérine acétyltransférase qui utilise la sérine comme un substrat pour la biosynthèse de la cystéine. La réduction de l'activité de CysE par RyhB permet à la sérine d'être utilisé pour la biosynthèse de l'entérobactine par la voie de synthèse de peptide indépendant aux ribosomes (NRPS). Ainsi, RyhB joue un rôle essentiel pour la production de sidérophore et peut moduler la virulence bactérienne par l'optimisation de la production de sidérophore.

A small RNA promotes siderophore production through transcriptional and metabolic remodeling

Hubert Salvail[a], Pascale Lanthier-Bourbonnais[a], Jason Michael Sobota[b], Mélissa Caza[c], Julie-Anna M. Benjamin[a], Martha Eugènia Sequeira Mendieta[a], François Lépine[c], Charles M. Dozois[c], James Imlay[b], and Eric Massé[a,1]

[a]Department of Biochemistry, University of Sherbrooke, Sherbrooke, Quebec, QC, Canada J1H 5N4; [b]Department of Microbiology, University of Illinois at Urbana-Champaign, Urbana, IL 61801; and [c]Institut National de la Recherche Scientifique-Institut Armand-Frappier, Quebec, QC, Canada H7V 1B7

Edited* by Susan Gottesman, National Cancer Institute, Bethesda, MD, and approved July 20, 2010 (received for review June 3, 2010)

Siderophores are essential factors for iron (Fe) acquisition in bacteria during colonization and infection of eukaryotic hosts, which restrain iron access through iron-binding protein, such as lactoferrin and transferrin. The synthesis of siderophores by *Escherichia coli* is considered to be fully regulated at the transcriptional level by the Fe-responsive transcriptional repressor Fur. Here we characterized two different pathways that promote the production of the siderophore enterobactin via the action of the small RNA RyhB. First, RyhB is required for normal expression of an important enterobactin biosynthesis polycistron, entCEBAH. Second, RyhB directly represses the translation of cysE, which encodes a serine acetyltransferase that uses serine as a substrate for cysteine biosynthesis. Reduction of CysE activity by RyhB allows serine to be used as building blocks for enterobactin synthesis through the nonribosomal peptide synthesis pathway. Thus, RyhB plays an essential role in siderophore production and may modulate bacterial virulence through optimization of siderophore production.

enterobactin | iron | RyhB | sRNA

In a mammalian host at neutral pH, iron (Fe) is mostly inaccessible to bacteria, because it is either insoluble in its ferric (Fe^{3+}) form or is bound to host proteins such as serum transferrin, which comprise the first line of host defense against bacterial pathogens (1–3). Thus, to scavenge extracellular Fe^{3+}, many bacteria have developed uptake strategies using high-affinity molecules known as siderophores (4–6). Because they are often critical to survival within the host, many siderophores synthesized by pathogenic bacteria are virulence factors (7, 8).

The archetypal siderophore, called enterobactin, is produced by *Escherichia coli*, *Salmonella enterica*, *Shigella dysenteriae*, and *Klebsiella pneumoniae* species (5). Synthesis of enterobactin (see Fig. S1 for synthesis pathway) depends on 2,3-dihydroxybenzoic acid (DHB) and serine, which are assembled together by the nonribosomal peptide synthesis machinery (9). To synthesize DHB, the primary metabolite shikimate is first converted into chorismate (by AroK, AroA, and AroC), which is then converted into DHB through the action of EntC, EntB, and EntA (10). The final assembly of DHB and serine into enterobactin depends on the action of EntD, EntB, EntE, and EntF (11). Once enterobactin has been synthesized, it is transported through the inner membrane by EntS (12) and the outer membrane by TolC (13). Outside the cell, enterobactin will bind to ferric Fe (Fe^{3+}) with an extremely high affinity (14). Then, Fe-loaded enterobactin complexes are imported into the cell through the outer membrane receptor FepA protein and the TonB energy transducer system found in the cell envelope (15, 16).

When bacterial intracellular Fe levels become sufficiently high, transcription of Fe uptake genes is repressed by the Fur (*F*erric *u*ptake *r*egulator) protein (17–19). Fe-complexed Fur binds to the promoters of a number of genes involved in Fe uptake to repress transcription initiation (20). In contrast, at low Fe concentrations, Fur becomes inactive, which relieves the repression of genes involved in the biosynthesis, export, and import of siderophores.

Although the Fe^{3+}-siderophore import mechanisms are well defined, molecular mechanisms governing siderophore biosynthesis and export are much less characterized (reviewed in refs. 5, 21). The biosynthesis of catecholate siderophores in *E. coli* as well as other medically important bacterial species depends on chorismate, a metabolite produced as part of the shikimate pathway (22). The shikimate pathway is also responsible for synthesis of aromatic amino acids and folic acid, as well as ubiquinone (22). In bacteria, shikimate can either be synthesized de novo or imported from the extracellular environment through the inner membrane-bound permease ShiA (23). We recently reported that the activation of ShiA translation depends on the 90-nucleotide small regulatory RNA (sRNA) RyhB (24). RyhB sRNA is specifically expressed under low Fe conditions through Fur to help the cell adapt to depleted Fe conditions (24–27). As RyhB represses about 20 transcripts encoding abundant Fe-using proteins, an increase in free intracellular Fe level, namely Fe sparing, is observed (27, 28). Remarkably, RyhB also partially regulates *fur* translation (29). However, no physiological consequence of this regulation has ever been reported.

Here, we describe the essential role of RyhB sRNA in the normal production of the siderophore enterobactin through posttranscriptional mechanisms. RyhB expression allows normal levels of *entCEBAH*, which is a critical transcript encoding for part of the siderophore synthesis machinery. In Δ*ryhB* cells, the operon is reduced by a 3-fold factor, which correlates with reduced enterobactin production. In addition, we observed that the gene *cysE*, encoding the enzyme serine acetyltransferase that uses serine in the first step of the pathway necessary to synthesize cysteine, must be repressed through RyhB action to allow siderophore production. Inactivation of *cysE* in a Δ*ryhB* background permits recovery of the siderophore production to WT level. The *cysE* mRNA is the first RyhB target that is not encoding an Fe-using protein. With this work, we demonstrate two essential posttranscriptional mechanisms that were unsuspected in the mechanism of siderophore synthesis.

Results

The sRNA RyhB Is Essential for Siderophore Production in Fe-Limited Conditions. The production of siderophores from *E. coli* K-12 was monitored for WT and Δ*ryhB* cells growing in minimal M63 medium with or without addition of 1 μM $FeSO_4$. In absence of Fe, the WT strain produces a considerable amount of siderophores (Fig. 1*A*, lane 2), which migrates to the same level as

Author contributions: H.S., J.M.S., M.C., M.E.S.M., C.M.D., J.I., and E.M. designed research; H.S., P.L.-B., J.M.S., M.C., J.-A.M.B., M.E.S.M., F.L., C.M.D., and J.I. performed research; H.S., P.L.-B., J.M.S., M.C., J.-A.M.B., M.E.S.M., F.L., C.M.D., and J.I. contributed new reagents/analytic tools; H.S., P.L.-B., J.M.S., M.C., J.-A.M.B., M.E.S.M., F.L., C.M.D., J.I., and E.M. analyzed data; and H.S., C.M.D., J.I., and E.M. wrote the paper.

The authors declare no conflict of interest.

*This Direct Submission article had a prearranged editor.

[1]To whom correspondence should be addressed. E-mail: eric.masse@usherbrooke.ca.

This article contains supporting information online at www.pnas.org/lookup/suppl/doi:10.1073/pnas.1007805107/-/DCSupplemental.

the purified enterobactin control (lane 1). In contrast, we observed a dramatic decrease in siderophore production in the Δ*ryhB* mutant even in the absence of Fe (Fig. 1*A*, lane 4). This is unexpected because, to our knowledge, almost every gene involved in siderophore biosynthesis and export is known to be regulated at the promoter level by Fur (30). These data indicate that even in low Fe conditions, when Fur is inactive, RyhB has a critical role in biosynthesis and/or secretion of siderophores.

Because the expression of siderophore genes is strongly linked to the Fur regulon, we examined the effect of a Δ*fur* mutation in a Δ*ryhB* mutant. Our results indicate that inactivation of *fur* in a Δ*ryhB* background restores the production of siderophores to a level similar to that of the WT (Fig. 1*A*, compare lanes 2 and 8). Nevertheless, the double Δ*fur* Δ*ryhB* mutant produces significantly fewer siderophores than the Δ*fur* mutant (Fig. 1*A*, compare lanes 6 and 8). This suggests that even in the absence of *fur*, when siderophore biosynthesis genes are fully derepressed, RyhB expression still enhances the production of enterobactin. These results demonstrate a specific role for RyhB in the production of siderophores. Notably in the conditions we used, the growth curves for all cells were comparable with or without Fe supplementation as determined on a bioscreen (Fig. S2).

To investigate the role of RyhB in enterobactin production, we quantified the levels of enterobactin siderophores produced from cells growing in increasing amounts of Fe. To do this, we measured siderophores directly from culture supernatants using liquid chromatography coupled with mass spectrometry (LC–MS). The amounts of siderophores produced during growth without Fe (Fig. 1*B*) are consistent with the data observed by TLC (Fig. 1*A* lanes 2, 4, 6, and 8). When Fe was added at 1 μM in the culture, the WT strain shows reduced siderophore production (Fig. 1*B*), which is consistent with the conventional idea that more Fe enables Fur to shut down *ent* genes. As expected, when RyhB is expressed from a plasmid vector in Δ*ryhB* cells, the production of siderophores becomes similar to that of WT cells (Fig. 1*C*, pRS-c25).

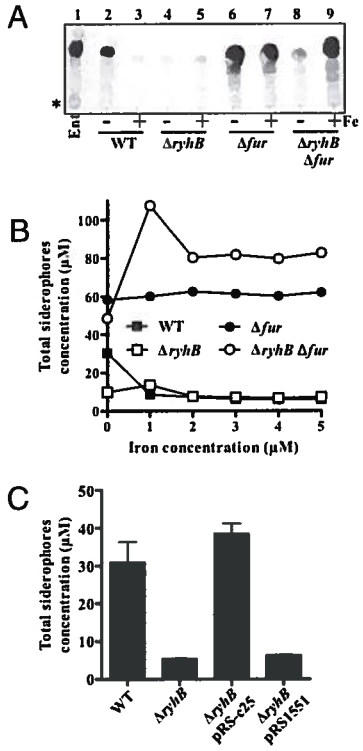

Fig. 1. The sRNA RyhB is essential for siderophore production in Fe-limited conditions. (*A*) Siderophore production as detected by TLC performed on *E. coli* WT, Δ*ryhB*, Δ*fur*, and Δ*ryhB* Δ*fur* strains growing in M63 minimal medium in the absence or presence of 1 μM of $FeSO_4$. The asterisk represents the loading spot on the TLC. (*B*) Determination of siderophore production by LC–MS on strains grown in the presence of increasing amounts of $FeSO_4$ (from 0 to 5 μM). Siderophore concentration at 0 μM Fe: WT (30.4 μM), Δ*ryhB* (9.8 μM), Δ*fur* (58.2 μM), and Δ*fur* Δ*ryhB* (48.5 μM). (*C*) Determination by LC–MS of siderophores produced in WT, Δ*ryhB*, and Δ*ryhB* overproducing RyhB (pRS–c25) or not (empty vector pRS1551).

RyhB Is Essential for Intracellular Fe Homeostasis and Fe Sparing Under Low Fe Conditions. The reduction of siderophores observed in a Δ*ryhB* mutant raises the possibility that, without RyhB, the free intracellular Fe becomes sufficiently elevated to activate the Fur repressor. Thus, we monitored the intracellular concentration of free Fe by using electron-paramagnetic resonance (EPR) on various cells (31). Our results demonstrate that, when Δ*ryhB* cells grow in M63 medium without Fe, they have about 3-fold less free intracellular Fe than WT cells (Fig. 2, compare WT and Δ*ryhB*, without Fe). Therefore, we cannot conclude that siderophore production decreases in the Δ*ryhB* mutant because of increased free Fe and Fur activation. However, this confirms that RyhB increases free intracellular Fe levels in the WT background growing under Fe starvation (Fig. 2, compare columns 1 and 3), demonstrating the Fe-sparing activity of RyhB.

In addition, although the Δ*fur* cells (column 5) have about 4-fold more free intracellular Fe than WT cells (column 1), the double Δ*fur* Δ*ryhB* cells (column 7) have as little free Fe as the Δ*ryhB* cells (column 3) when grown without Fe. This demonstrates the strong effect of RyhB on the levels of free intracellular Fe. However, when 1 μM Fe was added to the culture, both the Δ*ryhB* and the Δ*fur* Δ*ryhB* cells (columns 4 and 8) demonstrated a dramatic increase in free intracellular Fe. In contrast, the WT cells do not show any significant variation whether Fe is present or not (columns 1 and 2), demonstrating the robust mechanism for maintaining intracellular Fe homeostasis when both Fur and RyhB are functional.

RyhB Is Required for Normal Expression of Siderophore Synthesis Genes in Fe-Restricted Medium. As shown in Fig. 2, the free intracellular Fe is dramatically decreased in a Δ*ryhB* mutant as compared with WT under low Fe growth conditions. This low Fe availability leads one to expect that, in the Δ*ryhB* mutant, the Fur repressor must be inactive and Fur-regulated genes are fully derepressed. This was tested by monitoring the mRNA level of several genes involved in siderophore synthesis (*entC*, *entB*, and *entA*), secretion (*entS* and *tolC*), uptake (*fepA*), and transcriptional regulation (*fur*). In fact, the results in Fig. 3*A* clearly indicate that not only *entC*, *entB*, and *entA* genes are not

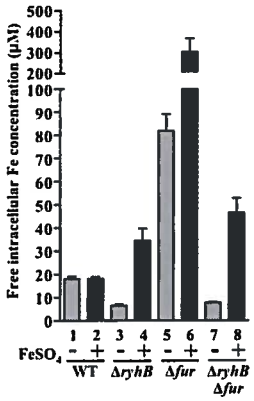

Fig. 2. RyhB is essential for intracellular Fe homeostasis and Fe-sparing under low Fe conditions as determined by EPR. Cells were grown in the absence or presence of 1 μM of $FeSO_4$ until an OD_{600} of 0.9, at which point they were assayed for free intracellular Fe (see *Materials and Methods* for details).

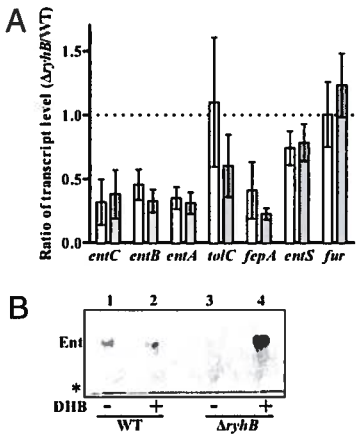

Fig. 3. RyhB is required for normal expression of siderophore synthesis genes in Fe-restricted medium. (*A*) Quantitative RT-PCR (qRT-PCR) showing the ratio of transcript level (Δ*ryhB*/WT) for several mRNAs involved in enterobactin synthesis (*entCEBAH*), enterobactin secretion (*tolC* and *entS*), enterobactin uptake (*fepA*), and transcriptional regulation (*fur*). The transcript levels were determined at OD_{600} of 0.9 (white bars) and 1.2 (gray bars). (*B*) The addition of DHB to the culture medium restores siderophore production specifically in Δ*ryhB* cells. Siderophore production as detected by TLC performed on *E. coli* WT and Δ*ryhB* strains growing in M63 minimal medium in the absence or presence of 5 μM of DHB. The asterisk represents the loading spot on the TLC.

derepressed but they are significantly reduced in the Δ*ryhB* background as compared with WT at OD_{600} of 0.9 and 1.2 (ratio Δ*ryhB*/WT <1). In contrast, both *entS* and *tolC* mRNAs remained equally expressed whether RyhB is present or not (ratio Δ*ryhB*/WT ~1). Although *entC*, *entB*, *entA*, *fepA*, *entS*, and *fur* are Fur-regulated genes, *tolC* expression is independent from Fur. Because *entS* and *fur* are not affected in these conditions, we cannot conclude that all Fur-regulated genes are repressed in Δ*ryhB* cells. Thus, even if intracellular Fe is low enough to inactivate Fur repression, we nevertheless observe significant repression of many Fur-regulated genes in Δ*ryhB* cells.

The previous results in Figs. 2 and 3*A* demonstrate that even though intracellular free Fe is low in a Δ*ryhB* mutant, it is not sufficient to induce Fur-regulated genes. This suggests that Fur is still active under low Fe in a Δ*ryhB* mutant. Indeed, RyhB was previously shown to partially repress *fur* translation (29). Thus, when growing under Fe starvation we expect Fur protein level to be higher in Δ*ryhB* cells as compared with WT cells. However, as shown in Fig. S3, a Western blot performed from cells expressing RyhB (WT) or not (Δ*ryhB*) indicates that the Fur protein levels are similar in Δ*ryhB* background as compared with WT. This demonstrates that RyhB does not affect *fur* translation in WT cells growing under Fe starvation. These data suggest that increased Fe, through the Fe-sparing action of RyhB, plays a key role in activating the expression of enterobactin synthesis genes. We tested this hypothesis by monitoring the effect of Fe on the levels of a number of transcripts in Δ*ryhB* Δ*fur* cells, which should not have any Fe-dependent effectors. As shown in Fig. S4, the mRNA levels of genes related to enterobactin, namely *entCEBAH*, *entS*, and *fepA* are significantly higher in Δ*ryhB* Δ*fur* cells in the presence of 1 μM $FeSO_4$. Thus, when growing under Fe starvation, RyhB-expressing cells will have increased intracellular Fe (Fig. 2, compare columns 1 and 3), which may contribute to the transcriptional activity or transcript stability of genes involved in synthesis of enterobactin.

The *entCEBAH* polycistron is required for the synthesis of DHB, which is one of the building blocks for enterobactin synthesis (Fig. S1). If *entCEBAH* expression is reduced in a Δ*ryhB* mutant, then DHB may not be sufficiently synthesized to allow siderophore production. To investigate this, we supplemented DHB in our Δ*ryhB* culture and monitored siderophore synthesis. As shown in Fig. 3*B*, the addition of 5 μM DHB to WT and Δ*ryhB* cells increases dramatically the production of siderophores specifically in Δ*ryhB* cells. This demonstrates that DHB is limiting in Δ*ryhB* cells, most likely due to reduced expression of siderophore synthesis genes (*entCEBAH*), as shown in Fig. 3*A*.

RyhB sRNA Pairs in Vitro with *cysE* mRNA to Reduce Translation Initiation. Although an explanation for the low *entCEBAH* expression in Δ*ryhB* cells remains elusive, another role for RyhB in regulation of siderophore synthesis was observed. In addition to DHB, the synthesis of enterobactin depends on the availability of the amino acid serine as a substrate. Serine is added to DHB through the nonribosomal peptide synthesis (9) in the final steps of the synthesis pathway to form enterobactin (Fig. S1). By using the bioinformatic tool TargetRNA (32), we observed that the gene *cysE*, encoding serine acetyltransferase, is a potential mRNA target of RyhB (see pairing in Fig. 4*A*). Serine acetyltransferase converts serine to *O*-acetyl-L-serine as the first step in the synthesis of cysteine. Because serine acetyltransferase (CysE) activity could limit the availability of serine for enterobactin synthesis, we reasoned that, under low Fe conditions, RyhB might reduce *cysE* expression to retain sufficient serine for enterobactin assembly. To address this, we used in vitro RNase T1 (cleaves unpaired guanines) and TA (cleaves unpaired adenines) and lead acetate (PbAc, cleaves any unpaired residues) assays for RyhB pairing with *cysE* mRNA. As demonstrated in Fig. 4*B*, RyhB clearly pairs at the ribosome-binding site of *cysE* mRNA. This result suggests that RyhB pairing with *cysE* mRNA inhibits translation initiation. We tested this hypothesis by using in vitro toeprint assays. As shown in Fig. 4*C*, the presence of RyhB (lane 11) clearly blocks the binding of the 30S ribosome subunit on the *cysE* mRNA as compared with *cysE* without RyhB (lane 7). These results strongly suggest that RyhB specifically binds to *cysE* mRNA to reduce translation initiation.

RyhB Directly Reduces CysE Expression in Vivo. We then monitored the *cysE* translation activity by using a protein fusion with the *lacZ* reporter gene in vivo. As shown in Fig. 5*A*, the expression of the *cysE'–'lacZ* translational fusion is significantly reduced in the WT background as compared with Δ*ryhB* cells. This demonstrates that RyhB efficiently reduces CysE protein level, and most likely serine acetyltransferase activity. To confirm pairing in vivo, we expressed either RyhB or the mutated RyhB6 construct from an arabinose-inducible vector and monitored the effect on WT *cysE'–'lacZ* and mutated *cysE6'–'lacZ* fusions (described in Fig. S5). As shown in Fig. 5*B*, the expression of the RyhB6 affects only the complementary *cysE6'–'lacZ* construct without affecting the WT *cysE'–'lacZ* fusion. This demonstrates that RyhB directly represses *cysE* translation in vivo.

Finally, we monitored by quantitative real-time PCR the *cysE* mRNA level after a 10-min pulse expression of RyhB. This pulse expression limits the possible indirect effect of expressing a sRNA. As shown in Fig. 5*C*, the mRNA level of *cysE* is significantly lower in the presence of the sRNA (pBAD–*ryhB*) as compared with a strain without RyhB (pNM12) or a control nontarget mRNA such as *icd* (25).

Reduced CysE Levels in Δ*ryhB* Cells Favor Siderophore Production. The previous results indicated that RyhB reduces *cysE* mRNA and protein levels. This suggests that a high level of CysE is incompatible with siderophore synthesis. To address this, we monitored the siderophore production from a strain carrying the *cysE* gene and endogenous promoter on a multicopy pBR322-derivative plasmid to overproduce CysE. As shown in Fig. 6*A*, the level of siderophore production is significantly less (30%) in the strain

MICROBIOLOGY

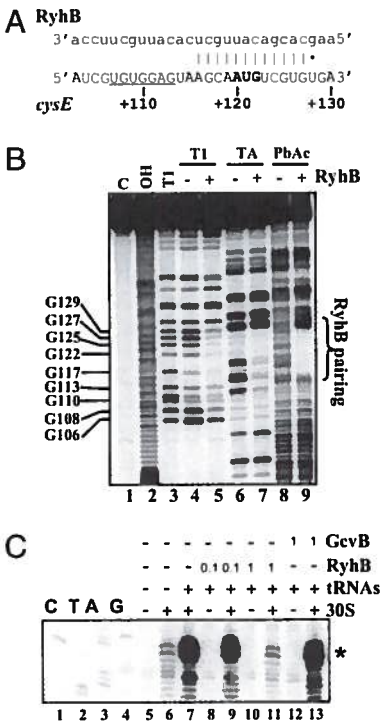

Fig. 4. RyhB sRNA pairs with *cysE* mRNA to reduce translation initiation. (*A*) Potential pairing between the sRNA RyhB and *cysE* mRNA. The ribosome-binding site of *cysE* is underlined and the first AUG codon is in bold. (*B*) In vitro pairing between the sRNA RyhB and 5'-end radiolabeled *cysE* mRNA as determined by RNase TI, RNase TA, and PbAc probing. Lane C is the control 5'-end radiolabeled *cysE* mRNA alone, lane OH is treated with NaOH, and TI is treated with RNase TI in denaturing conditions. The 5'-end radiolabeled *cysE* mRNA was incubated either with RNase TI (lanes 4, without RyhB and 5, with RyhB), RNase TA (lanes 6, without RyhB and 7, with RyhB), or PbAc (lanes 8, without RyhB and 9, with RyhB). The observed pairing between *cysE* and RyhB correlates with the potential pairing as shown in *A*. (*C*) Toeprint assay indicating that RyhB prevents *cysE* translation initiation by blocking the binding of ribosomal 30S subunit on the *cysE* mRNA. The GcvB sRNA was used as a negative control.

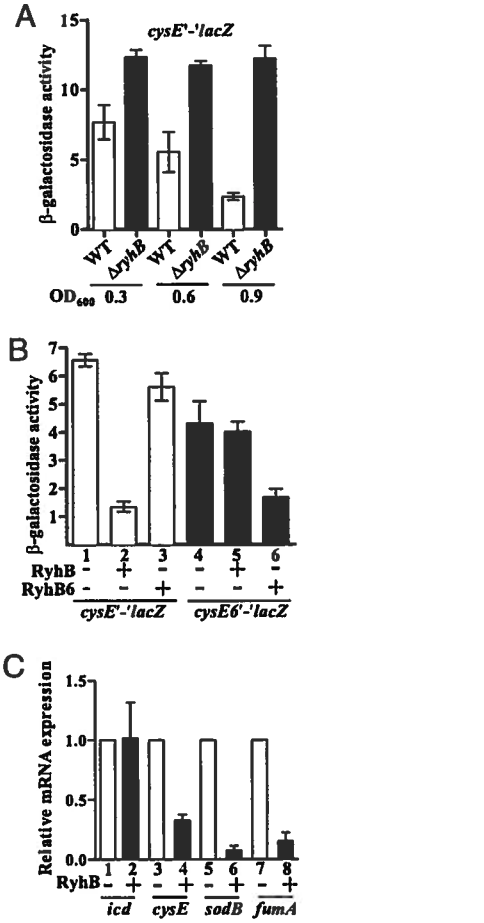

Fig. 5. RyhB directly reduces CysE expression in vivo. (*A*) β-Galactosidase assays of the translational *cysE'–'lacZ* reporter fusion in WT and Δ*ryhB* cells grown in minimal M63 medium without Fe at different OD_{600} (0.3, 0.6, and 0.9). (*B*) The effect of arabinose-induced WT RyhB and mutated RyhB6 on the translational WT *cysE'–'lacZ* and mutated *cysE6'–'lacZ* reporter fusions. See Fig. S5 for details. (*C*) The effect of arabinose-induced RyhB from pBAD-*ryhB* (as compared with the empty vector pNM12) on *cysE* mRNA, previously characterized target mRNAs (*sodB* and *fumA*), and a negative control mRNA (*icd*) as determined by qRT-PCR.

carrying the multicopy *cysE* (pFRΔ–*cysE*) gene as compared with the empty control vector (pFRΔ). We do not expect a full repression of siderophore production because the *ryhB* gene is present in this background. These data suggest that overexpression of CysE reduces the cell's ability to produce siderophores.

If *cysE* expression is too high in the Δ*ryhB* cells, then mutating the *cysE* gene should restore conditions in which siderophores are readily produced. Thus, we monitored siderophore production by a Δ*ryhB* Δ*cysE* double mutant. As expected, the production of siderophore by a Δ*ryhB* Δ*cysE* mutant is restored to normal WT levels (Fig. 6*B*). This shows the importance of keeping the expression of both RyhB and *cysE* in balance for normal siderophore production. Because both Δ*cysE* and Δ*ryhB* Δ*cysE* cells must be supplemented with cysteine to grow, we monitored the effect of the addition of cysteine (125 μM) on the production of siderophores from WT and Δ*ryhB* cells. As shown in Fig. S6, there is no significant effect of the addition of cysteine on the production of the siderophore enterobactin and derivatives.

Discussion

For more than 30 y, the transcriptional regulator Fur has been considered as the sole effector in the synthesis of siderophores (17). We show that posttranscriptional regulation through RyhB sRNA is equally important. RyhB takes part in two distinct pathways, both of which essential for siderophore production. One of these mechanisms relies on RyhB repression of the serine acetyltransferase CysE (see model in Fig. S7), which represents the first RyhB-repressed target mRNA that does not encode for an Fe-using protein. Repression of CysE potentially remodels the amino acids metabolism to increase the serine flux into the siderophore synthesis pathway to the detriment of the cysteine pathway (Figs. S1 and S7). Indeed, when serine is added to the medium, it partially suppresses the Δ*ryhB* phenotype and stimulates siderophore production (Fig. S6). Moreover, addition of high levels of cysteine in the medium also increases the siderophore production, probably by negative feedback (33), which results in reduction of CysE enzyme activity (Fig. S6).

The down-regulation of *cysE* transcript by RyhB is clearly not as strong as other target mRNAs (compare *cysE* mRNA levels with *sodB* or *fumA* in Fig. 5*C*). Also, although it is repressed by RyhB, the translational *cysE'–'lacZ* fusion in WT cells is still significantly active as compared with the Δ*ryhB* cells in midlog growth phase (Fig. 5*A*, OD_{600} of 0.3 and 0.6). This suggests that partial *cysE* repression by RyhB is preferred over classical full repression as observed with *sodB* and *fumA* target mRNAs (Fig. 5*C*). Because the CysE enzyme is essential for cysteine synthesis in minimal medium, we do not expect full repression of *cysE* by

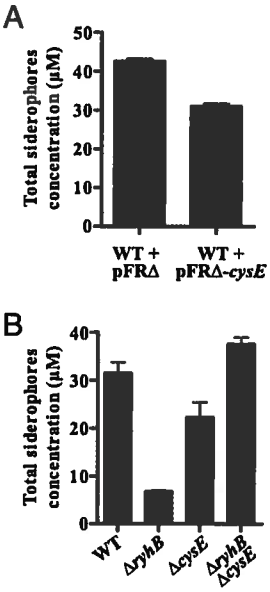

Fig. 6. RyhB reduces CysE levels to favor siderophore production. (*A*) Total siderophore production as measured by LC–MS in strains overproducing the CysE enzyme (pFRΔ–*cysE*) or not (empty vector pFRΔ). (*B*) Total siderophore production as measured by LC–MS in WT, Δ*ryhB*, Δ*cysE*, and Δ*ryhB* Δ*cysE* strains (see *Materials and Methods* for description).

RyhB. Additionally, because CysE does not encode an Fe-using protein, the RyhB-induced repression may not benefit from rapid full repression (<3–5 min) as observed with other target mRNAs encoding Fe-using proteins such as *sodB* and *fumA* (26). This type of repression prioritization of specific target mRNAs over other targets of the same sRNA reflects the powerful genetic modulation achieved by a sRNA.

An unexpected function of RyhB was suggested by our results in Fig. 3, which indicate that RyhB contributes to normal expression of transcripts involved in siderophores synthesis (*entCEBAH*) and uptake (*fepA*). This suggests a second mechanism in which RyhB contributes to siderophore production. Although the precise mechanism is unclear, our data indicate that RyhB-induced intracellular Fe level, namely Fe sparing, is central to this. Because many transcripts are affected independently from their cellular functions, this suggests a general effect of low intracellular Fe on gene expression. To analyze this further, we tested the effect of Fe alone on the double Δ*fur* Δ*ryhB* mutant, which should not have any Fe-dependent effector on mRNA expression or stability. As shown in Fig. S4, the presence of Fe greatly induces the expression of a number of genes, many of which involved in synthesis (*entB* and *entC*), secretion (*entS*), or uptake (*fepA*) of enterobactin. This result corroborates our siderophore analysis. Although the double Δ*fur* Δ*ryhB* mutant growing without Fe produces a fair amount of siderophore (Fig. 1*A*, lane 8, and *B*), the addition of Fe stimulates by a 2-fold factor the production of siderophore (Fig. 1*A*, lane 9, and *B*). These results indicate the essential role of RyhB in increasing intracellular Fe level to improve cellular function.

Indeed, the low intracellular Fe in Δ*ryhB* cells may reduce the activity of Fe-dependent enzymes involved in the shikimate–chorismate pathway (Fig. S1). However, we demonstrate that the activity of Fe-dependent aldolases (34), encoded by *aroFGH*, are not affected in our experimental growth conditions without Fe (Fig. S8) and remain fully active whether RyhB is present (WT) or not (Δ*ryhB*). It is therefore unlikely that the aldolases are involved in reduced expression of siderophores. Furthermore, despite the reduced intracellular Fe in Δ*ryhB* cells (Fig. 2, compare WT and Δ*ryhB* without Fe), this shows that not all Fe-dependent enzymes will be affected.

Remarkably, both Fur and RyhB regulate the siderophore production at different levels. Thus, one can question which gene is epistasic to the other in this system. Simply put, the *ryhB* gene expression depends on Fur, which depends on the Fe level in the medium. Our results, however, suggest that more factors than Fur and RyhB regulate the system. As shown in Fig. 1*A*, even in the absence of Fur and RyhB (Δ*ryhB* Δ*fur* background), Fe alone is sufficient to affect the system (lanes 8 and 9). These results add to the interpretation that siderophore production depends on more than just transcription activation in the absence of Fe. Three factors must be taken into account: (*i*) Fur inactivation, (*ii*) RyhB expression, and (*iii*) sufficient free intracellular Fe level (Fe sparing).

The measurements of free intracellular Fe by EPR (Fig. 2) demonstrate that both Fur and RyhB are needed to maintain a robust Fe homeostasis despite significant environmental Fe variation. The most significant results of this experiment are that Δ*ryhB* cells have 60% reduced free Fe [Fig. 2, lane 3 (6 μM) vs. lane 1 (18 μM)] as compared with WT. This is a unique demonstration that endogenous RyhB effectively generates free Fe in WT cells grown under Fe starvation. However, it is not clear why intracellular Fe becomes so high as compared with WT when Fe is available [Fig. 2, lane 4 (Δ*ryhB* + Fe) compared with lane 2 (WT + Fe)]. In addition, these results show that an important part of the free Fe levels in a Δ*fur* mutant depends on the action of RyhB [Fig. 2, compare lane 6 (Δ*fur* + Fe) with lane 8 (Δ*fur* Δ*ryhB* + Fe)]. Remarkably, as shown in Fig. S3 we did not reproduced previously published data suggesting that RyhB partly represses *fur* translation (29). We explain this by different experimental procedures used in our analysis (Fe-deprived medium) as compared with the previous analysis (addition of the Fe chelator 2,2′-dipyridyl in the medium).

This paper demonstrates that a single sRNA can act as a global regulator by adjusting simultaneously the cellular gene network and metabolism. Our study shows a unique role for RyhB extending beyond regulation of Fe-storage proteins and now includes modulation of metabolic pathways such as serine catabolism through down-regulation of *cysE* and modification of transcription of genes involved in enterobactin production (*entCEBAH*). By adjusting both gene expression and metabolic activity, the sRNA enables the cell to optimize to severe environmental changes. With these results in view, we should expect additional sRNAs conducting similar subtle metabolic adjustments that drive crucial cellular functions.

Materials and Methods

Analysis of Enterobactin Production by TLC. Enterobactin was extracted and visualized according to a previous report (12). Cells were grown in M63, 0.2% glucose, from a 10-fold or 100-fold dilution of an overnight culture in the same media. Depending on the experiment, 33 μM of DHB or 1 μM of $FeSO_4$ were added to the media. At an OD_{600} of 0.9, 4 mL of culture was pelleted. The supernatant was acidified with 25 μL of 10N HCl and extracted twice with a total of 4 mL of ethyl acetate. Aqueous phases were combined and dried in 874-μL aliquots in a SpeedVac Concentrator (Savant Instruments, SVC100). Extract residues were resuspended in 40 μL of methanol and 10 μL was spotted onto 250-μM layer-flexible (20 × 20 cm) PE SIL G/UV254 plates (Whatman). For some experiments, 25 μL of enterobactin (EMC Microcollections) was spotted as a control onto the plates. Plates were developed with benzene:glacial acetic acid:water (125:72:3 vol/vol/vol) in a closed chamber. Plates were then removed from the chamber and allowed to dry, then immersed briefly in 0.1% $FeCl_3$ to visualize Fe-binding compounds.

EPR Analysis of Whole Cells. Cells were grown overnight at 37 °C in M63 glucose medium, diluted 1:10 into 250 mL of freshly prepared M63 0.2% glucose ±1 μM of $FeSO_4$ and then grown at 37 °C in 1-L baffled flasks with vigorous shaking to an OD_{600} of 0.9. Cells were then harvested and prepared for EPR analysis as described in previous studies (28, 35), with the exception that M63 medium with 0.2% glucose was used in place of LB during the incubation of cells with DTPA and desferrioxamine.

Enzymatic and Chemical Probing of RyhB Interaction with *cysE* mRNA. Enzymatic and chemical probing experiments were performed as described earlier (36). Briefly, 50 pmol of *cysE* mRNA (transcribed from a PCR product—oligos EM1056–EM1153) was labeled using T4 polynucleotide kinase (New England Biolabs). Then, 0.1 μM of 5'-end radiolabeled *cysE* was incubated 15 min at 37 °C in the absence or in the presence of 1.6 μM RyhB RNA (transcribed from a PCR product—oligos EMBB–EMB9). Then, RNase T1 (0.05 U) (Ambion), or RNase TA (0.025 U) (Jena Bioscience), or PbAc (10 mM) (Sigma-Aldrich) were added to the reaction and the incubation continued for 2 min. Reactions were stopped by adding 10 μL of loading buffer II (Ambion). Samples were then separated on a 6% polyacrylamide/7 M urea gel.

ACKNOWLEDGMENTS. We thank Susan Gottesman for comments on the manuscript, Peter D. Pawelek for strains and discussions over the course of this work, Simon Labbé for constructive comments, Mike Vasil (University of Colorado Denver, Aurora, CO) for Fur antiserum, and Michael Maurizi (National Institutes of Health, Bethesda) for the elongation factor-thermo unstable (EF-Tu) antiserum. This work was funded by an operating grant to E. M. from the Natural Science and Engineering Research of Canada and to C. M.D. from Natural Science and Engineering Research of Canada and the Canada Research Chairs program. E.M. is a Canadian Institutes for Health Research New Investigator scholar. H.S. holds PhD fellowships from the Fonds Québécois de la Recherche sur la Nature et les Technologiques and Natural Science and Engineering Research of Canada. J.-A.M.B. holds a Natural Science and Engineering Research of Canada MSc fellowship.

1. Barasch J, Mori K (2004) Cell biology: Iron thievery. *Nature* 432:811–813.
2. Schaible UE, Kaufmann SH (2004) Iron and microbial infection. *Nat Rev Microbiol* 2: 946–953.
3. Braun V (2005) *Concepts in Bacterial Virulence*, eds Russell W, Herwald H (Karger, Basel, Switzerland), pp 210–233.
4. Wandersman C, Delepelaire P (2004) Bacterial iron sources: From siderophores to hemophores. *Annu Rev Microbiol* 58:611–647.
5. Raymond KN, Dertz EA, Kim SS (2003) Enterobactin: An archetype for microbial iron transport. *Proc Natl Acad Sci USA* 100:3584–3588.
6. Crosa JH, Walsh CT (2002) Genetics and assembly line enzymology of siderophore biosynthesis in bacteria. *Microbiol Mol Biol Rev* 66:223–249.
7. Fischbach MA, Lin H, Liu DR, Walsh CT (2006) How pathogenic bacteria evade mammalian sabotage in the battle for iron. *Nat Chem Biol* 2:132–138.
8. Valdebenito M, Crumbliss AL, Winkelmann G, Hantke K (2006) Environmental factors influence the production of enterobactin, salmochelin, aerobactin, and yersiniabactin in Escherichia coli strain Nissle 1917. *Int J Med Microbiol* 296:513–520.
9. Gehring AM, Mori I, Walsh CT (1998) Reconstitution and characterization of the Escherichia coli enterobactin synthetase from EntB, EntE, and EntF. *Biochemistry* 37: 2648–2659.
10. Rusnak F, Liu J, Quinn N, Berchtold GA, Walsh CT (1990) Subcloning of the enterobactin biosynthetic gene entB: Expression, purification, characterization, and substrate specificity of isochorismatase. *Biochemistry* 29:1425–1435.
11. Lambalot RH, et al. (1996) A new enzyme superfamily: The phosphopantetheinyl transferases. *Chem Biol* 3:923–936.
12. Furrer JL, Sanders DN, Hook-Barnard IG, McIntosh MA (2002) Export of the siderophore enterobactin in Escherichia coli: Involvement of a 43 kDa membrane exporter. *Mol Microbiol* 44:1225–1234.
13. Bleuel C, et al. (2005) TolC is involved in enterobactin efflux across the outer membrane of Escherichia coli. *J Bacteriol* 187:6701–6707.
14. Carrano CJ, Raymond KN (1979) Ferric ion sequestering agents. 2. Kinetics and mechanism of iron removal from transferrin by enterobactin and synthetic tricatechols. *J Am Chem Soc* 101:5401–5403.
15. Wiener MC (2005) TonB-dependent outer membrane transport: Going for Baroque? *Curr Opin Struct Biol* 15:394–400.
16. Pawelek PD, et al. (2006) Structure of TonB in complex with FhuA, E. coli outer membrane receptor. *Science* 312:1399–1402.
17. Ernst JF, Bennett RL, Rothfield LI (1978) Constitutive expression of the iron-enterochelin and ferrichrome uptake systems in a mutant strain of Salmonella typhimurium. *J Bacteriol* 135:928–934.
18. Hantke K (1981) Regulation of ferric iron transport in Escherichia coli K12: Isolation of a constitutive mutant. *Mol Gen Genet* 182:288–292.
19. Lee JW, Helmann JD (2007) Functional specialization within the Fur family of metalloregulators. *Biometals* 20:485–499.
20. Hantke K (1997) Ferrous iron uptake by a magnesium transport system is toxic for Escherichia coli and Salmonella typhimurium. *J Bacteriol* 179:6201–6204.
21. Grass G (2006) Iron transport in Escherichia coli: All has not been said and done. *Biometals* 19:159–172.
22. Herrmann KM, Weaver LM (1999) The shikimate pathway. *Annu Rev Plant Physiol Plant Mol Biol* 50:473–503.
23. Whipp MJ, Camakaris H, Pittard AJ (1998) Cloning and analysis of the shiA gene, which encodes the shikimate transport system of escherichia coli K-12. *Gene* 209: 185–192.
24. Prévost K, et al. (2007) The small RNA RyhB activates the translation of *shiA* mRNA encoding a permease of shikimate, a compound involved in siderophore synthesis. *Mol Microbiol* 64:1260–1273.
25. Massé E, Gottesman S (2002) A small RNA regulates the expression of genes involved in iron metabolism in Escherichia coli. *Proc Natl Acad Sci USA* 99:4620–4625.
26. Massé E, Escorcia FE, Gottesman S (2003) Coupled degradation of a small regulatory RNA and its mRNA targets in Escherichia coli. *Genes Dev* 17:2374–2383.
27. Massé E, Vanderpool CK, Gottesman S (2005) Effect of RyhB small RNA on global iron use in Escherichia coli. *J Bacteriol* 187:6962–6971.
28. Jacques JF, et al. (2006) RyhB small RNA modulates the free intracellular iron pool and is essential for normal growth during iron limitation in Escherichia coli. *Mol Microbiol* 62:1181–1190.
29. Vecerek B, Moll I, Bläsi U (2007) Control of Fur synthesis by the non-coding RNA RyhB and iron-responsive decoding. *EMBO J* 26:965–975.
30. Andrews SC, Robinson AK, Rodríguez-Quiñones F (2003) Bacterial iron homeostasis. *FEMS Microbiol Rev* 27:215–237.
31. Keyer K, Imlay JA (1996) Superoxide accelerates DNA damage by elevating free-iron levels. *Proc Natl Acad Sci USA* 93:13635–13640.
32. Tjaden B, et al. (2006) Target prediction for small, noncoding RNAs in bacteria. *Nucleic Acids Res* 34:2791–2802.
33. Kredich NM (1983) *Amino Acids: Biosynthesis and Genetic Regulation*, eds Herrmann KM, Sommerville RL (Addison-Wesley Publishing Company, London), pp 115–117.
34. Stephens CM, Bauerle R (1991) Analysis of the metal requirement of 3-deoxy-D-arabino-heptulosonate-7-phosphate synthase from Escherichia coli. *J Biol Chem* 266: 20810–20817.
35. Woodmansee AN, Imlay JA (2002) Quantitation of intracellular free iron by electron paramagnetic resonance spectroscopy. *Methods Enzymol* 349:3–9.
36. Desnoyers G, Morissette A, Prévost K, Massé E (2009) Small RNA-induced differential degradation of the polycistronic mRNA iscRSUA. *EMBO J* 28:1551–1561.

Annexe IV

***Klebsiella pneumoniae* Yersiniabactin predisposes to respiratory tract infection and allows evasion of Lipocalin 2**

Michael A. Bachman, Jennifer E. Oyler, Samuel Burns, **Mélissa Caza**, François Lépine, Charles Dozois, and Jeffrey N. Weiser

A) Contribution de l'étudiante

1- Le manuscrit en préparation présente une étude sur l'importance du sidérophore yersiniabactine chez les souches de *Klebsiella pneumoniae*. Une corrélation avec les souches causant des pneumonies, ainsi que les souches résistantes aux béta-lactames à large spectre et la production de yersiniabactine a été mise en évidence. De plus, il a été démontré que la yersniabactine est suffisante pour permettre une acquisition du fer par la bactérie en présence du lipocalin2.

2- L'étude a été réalisée en utilisant de la chromatographie liquide couplée au spectromètre de masse (LC-MS/MS).

3- L'étudiante a réalisé la quantification des sidérophores catécholates, de l'aérobactine et de la yersiniabactine par les isolats cliniques de *Klebsiella pneumoniae* par LC-MS/MS.

B) Résumé de l'article:

Introduction : *Klebsiella pneumoniae* est un pathogène d'intérêt grandissant à cause de la résistance aux antibiotiques dûe à l'utilisation des beta-lactames à spectre large et aux carbapenemases de *K. pneumoniae* (KPC). *K. pneumoniae* doit acquérir le fer pour se multiplier et pour ce, il utilize des sidérophores, tel que l'entérobactine (Ent). La proteine de l'immunité innée Lipocalin 2 (Lcn2) lie spécifiquement Ent et ainsi empêche l'acquisition du fer par la bactérie. Afin de causer une infection, *K. pneumoniae* encode d'autres systèmes de sidérophores

qui évite la sequestration par Lcn2. **Méthodes :** Des isolats cliniques de *K. pneumoniae* produisant des sidérophores (n=131) isolés du sang, tractus respiratoire, urinaire et fécale, et des mutants définis de synthèse de sidérophore ont été caractérisées génotypiquement et avec des analyses en chromatographie liquide couplée à la spectrométrie de masse (LC-MS/MS). Des essais de croissance dans des milieux *ex vivo* et des infections dans le modèle murin de pneumonie ont été réalisées. **Résultats :** Tous les isolats cliniques produisent l'entérobactine, 2 % produient de l'entérobactine glucosylé (Gly-Ent) et 17 % produisent la yersiniabactine (Ybt). Gly-ent permert l'évasion du Lcn2 dans le sérum humain; et les sidérophores ne sont pas requis pour la croissance dans l'urine humaine. Ybt est significativement représenté parmis les isolats du tractus respiratoire (p=0.0059) et les isolats résistants aux beta-lactames à large spectre (p=0.0024), incluant la souche épidémique KPC ST258. Ybt est également suffisant pour permettre l'évation au Lcn2 et causer une infection. **Conclusions :** Ybt est un facteur de virulence prévalent parmis les souches résistantes aux beta-lactame à large spectre et productrice de KPC. En plus, Ybt augmente l'habileté aux souches *K. pneumoniae* à causer une infection du tractus respiratoire.

Klebsiella pneumoniae Yersiniabactin predisposes to respiratory tract infection and allows evasion of Lipocalin 2

Michael A. Bachman[1#], Jennifer E. Oyler[2], Samuel Burns[2], Mélissa Caza[3], François Lépine[3], Charles Dozois[3], and Jeffrey N. Weiser[2,4]

Departments of Pathology[1], Microbiology[2], and Pediatrics[4], University of Pennsylvania School of Medicine, Philadelphia, Pennsylvania 19104

INRS-Institut Armand-Frappier[3], Laval, Québec, Canada

Corresponding Author

Running Title: *K. pneumoniae* Yersiniabactin evades Lcn2

Abstract Word Count: 194

Text Word Count: 3310

Abstract:

Background: *Klebsiella pneumoniae* is a pathogen of increasing concern because of antibiotic-resistance due to extended-spectrum beta-lactamases (ESBL) and *K. pneumoniae* carbapenemases (KPC). *K. pneumoniae* must acquire iron to replicate, and utilizes iron scavenging siderophores such as enterobactin (Ent). The innate immune protein Lipocalin 2 (Lcn2) is able to specifically bind Ent and disrupt iron acquisition. Therefore to cause disease, *K. pneumoniae* is predicted to encode additional siderophores that evade Lcn2. **Methods:** Siderophore production by *K. pneumoniae* clinical isolates (n=131) from respiratory, urine, blood and stool and by defined siderophore mutants was characterized by genotyping, liquid chromatography/ mass spectrometry, ex vivo growth assays and a murine pneumonia model. **Results:** All clinical isolates encoded Ent, 2% encoded Glycosylated Ent (Gly-Ent), and 17% encoded Yersiniabactin (Ybt). Gly-Ent allowed evasion of Lcn2 in human serum; siderophores were dispensable for growth in human urine. Ybt was significantly over-represented among respiratory tract isolates (p=0.0059) and beta-lactam resistant isolates (p=0.0024), including the epidemic KPC strain ST258, and was sufficient to evade Lcn2 and cause pneumonia. **Conclusions:** Ybt is a virulence factor prevalent among ESBL and KPC-producing *K. pneumoniae* and enhances the ability of *K. pneumoniae* to cause respiratory tract infections.

Key words: Lipocalin 2, NGAL, *Klebsiella pneumoniae*, yersiniabactin, enterobactin, *iroA*, pneumonia, KPC, carbapenemase

Introduction

Klebsiella pneumoniae colonizes >75% of hospitalized patients and causes an estimated 8% of all nosocomial infections in the United States [1]. A non-motile, encapsulated member of the Enterobacteriaceae family of gram-negative bacteria, *K. pneumoniae* is a common cause of urinary tract infections and septicemia and the third most common bacterial cause of hospital-acquired pneumonia [2].

Antimicrobial resistance among *K. pneumoniae* is rapidly increasing, by >1% per year, to fluoroquinolones, late-generation cephalosporins, and carbapenems [2]. Carbapenems has been the treatment of last resort against *K.* pneumoniae with extended-spectrum beta-lactometers (ESBLs), plasmid encoded enzymes that inactivate penicillins and cephalosporins [1]. However, strains encoding *Klebsiella pneumoniae* Carbapenemases (KPCs) have spread throughout United States and other regions worldwide [3] and are associated with nearly complete antibiotic resistance, a 25-60% treatment failure rate, and to fatal infections [3]. One clone, multi-locus sequence type 258 (ST258), accounts for over 70% of the KPC isolates that have been collected by the Centers for Disease Control [4].

The spread of antimicrobial resistance makes innate immunity to *K. pneumoniae* paramount. To acquire iron for DNA replication, amino acid synthesis, and electron transport [5], *K. pneumoniae* secretes the iron-scavenging molecule Enterobactin (Ent) that has higher affinity than either human lactoferrin or transferrin for iron [6]. To counteract Ent, neutrophils [7] and mucosal surfaces[8] [9] produce Lipocalin 2 (Lcn2, or neutrophil gelatinase-associated lipocalin (NGAL), siderocalin, 24p3, uterocalin). Lcn2, with an eight-stranded β-barrel structure enclosing a cup-shaped ligand site [10], binds

Ent to compete with the bacterial Ent receptor [11]. Lcn2 also stimulates an acute inflammatory response when bound to aferric Ent, inducing expression of the chemokine IL-8 from cultured respiratory cells [12] and promoting neutrophil influx in response to *K. pneumoniae* nasal colonization [13].

To evade Lcn2, some isolates of *K. pneumoniae* produce siderophores to which it cannot bind. Glycosylated Ent (Gly-Ent), encoded by the *iroA* locus is not bound to Lcn2 due to steric hindrance [14] [15]. Alternative siderophores, such as yersiniabactin (Ybt) or aerobactin (Aer), are structurally distinct from Ent [16, 17]. During nasal colonization, either Gly-Ent or Ybt are sufficient to evade Lcn2 and support bacterial growth [13]. In a pneumonia model, Ybt is required for maximal *K. pneumoniae* growth and lethality, although its interaction with Lcn2 has not been determined [16].

K. pneumoniae colonizes the colon, where Lcn2 is not normally expressed [18], but can cause disease in sites where Lcn2 is prevalent. In a human sepsis model, Lcn2 levels correlate with the degranulation of circulating neutrophils [19]. In the respiratory tract, Lcn2 is basally expressed [8, 9] and induced in response to *K. pneumoniae* infection [20]. In the urinary tract, Lcn2 is basally produced in the renal tubules and induced by kidney injury [21]. To determine whether Lcn2-resistant siderophores are required to cause disease, *K. pneumoniae* isolates from blood, the respiratory tract, urine, and stool were collected and characterized for siderophore genotype and phenotype, and their ability to evade Lcn2 in ex vivo and in vivo models of infection.

Materials and Methods

Bacterial strains and media

KPPR1, a rifampin-resistant derivative of *K. pneumoniae* subspecies *pneumoniae* (ATCC 43816), was used as the wild-type strain in these studies. Construction of isogenic single (*entB, ybtS, iroA*) and double (*entB ybtS, iroA ybtS*) siderophore mutants used herein has been previously described [13, 16]. *K. pneumoniae* isolates were prospectively collected without patient identifiers at the Hospital of the University of Pennsylvania (HUP) clinical microbiology laboratory. Respiratory, urine and blood isolates were identified and tested for anti-microbial susceptibility using the Vitek-2 system (Biomerieux, Durham, NC). Stool isolates were identified by conventional microbiological and biochemical methods [22]. For comparison of siderophore prevalence among β-lactamase-positive isolates, a curated collection of antibiotic resistant *K. pneumoniae* isolates from 2007 was examined (a gift from Paul Edelstein). All strains were cultivated overnight in Luria-Bertani (LB) media either at 30°C on agar or at 37° shaking in broth. For liquid chromatography coupled to mass spectrometry analyses, strains were cultivated in M63-glycerol media at 37 °C for 17 h (Caza et al., 2008). KPPR1 and derived mutants were grown with rifampin (30 mg/ml); kanamycin (50 mg/ml) was added for *iroA* and *iroA ybtS* mutants.

Genotyping of clinical isolates

To detect the presence of siderophore loci among hospital clinical isolates, genotyping was performed by PCR using primers targeting conserved gene sequences as follows: *entB* (forward 5'- TGAAGACGATACCGTGCTGGTGGA, reverse 5'-

GTCGGCGACAAAGAACGGTTTGAT), *entE* (forward 5'-GCTGGTGGTTGAACAAAGC, reverse 5'-CAATGTCGCCGAGTTTTACA) [16], *ybtS* (forward 5'- CAAAAATGGGCGGTGGATTC, reverse 5'-CCTGACGGAACATAAACGAGCG), *iroN* (forward 5'-GCATTGGTATTCCAGTTCAGACG, reverse 5'- GAAAGGCAACGGTTGTCCAAA) and *iucA* (forward 5'- GTACATCCGTGGCAGTGGCAG, reverse 5'-CAAGCGCGGCATAGCCTTCAT). Cycling parameters for *entB, ybtS,* and *iroN* were 94°C for 2 min, 25 cycles of 94°C for 15 seconds, 59°C for 15 seconds, and 72°C for 15 seconds, and one cycle of 72°C for 2 minutes. Cycling conditions for *entE* and *iucA* included an annealing temperature step-down of 1°C per cycle for the first seven cycles as follows: 94°C for 2 min, 30 cycles of 94°C for 15 seconds, 63°C-56°C (*entE*) or 69.6°C-62.6°C (*iucA*) for 15 seconds, and 72°C for 15 seconds, and one cycle of 72°C for 2 minutes. *E. coli* CFT073 was used as a positive control for *iucA*; KPPR1 was used for all other reactions.

Liquid Chromatography/Mass Spectrometry of Siderophores

Strains were grown in M63-glycerol (0.6%) without addition of iron at 37 °C for 17h. Each strain was cultured in triplicate. Multiple reaction monitoring (MRM) analyses were performed using a Waters 2795 Alliance HT HPLC coupled to a Micromass Quattro Premier XE mass spectrometer (Micromass MS Technologies). Samples were injected onto a Zorbax Eclipse XDB-C8 4.6- by 150-mm column at a flow rate of 400 µl/min and a linear gradient of water-acetonitrile with 1% acetic acid. Aliquots of 1 mL of supernatant were prepared and 0.12 ng/mL of 5,6,7,8-tetradeutero-3,4-dihydroxy-2-

heptylquinoline was added as an internal control. The specific transition ions monitored from psudomolecular ions to daughter of salmochelins, enterobactins and aerobactin are described elsewhere (Caza et al., 2008). The transition ion for yersiniabactin was 482>295 *m/z*. Relative quantification of siderophores was performed by integration of the pseudomolecular and the proper fragments ions.

Multi-locus sequence typing

Multi-locus sequence typing was performed to determine the diversity of a selection of clinical isolates. Genomic DNA was isolated from bacteria using a Qiagen DNeasy Blood and Tissue kit (Qiagen, Valencia, CA). Seven essential genes (*rpoB, gapA, mdh, pgi, phoE, inf, and tonB)* were amplified by PCR, using conditions and primers designated by the Pasteur Institute *Klebsiella pneumoniae* MLST database (http://www.pasteur.fr/recherche/genopole/PF8/mlst/Kpneumoniae.html), with 50 ng of genomic DNA as template. PCR products were purified using a QIAquick PCR purification kit (Qiagen, Valencia, CA). Sequencing was performed at the Nucleic Acid and Protein Research Core within the Children's Hospital of Philadelphia (Philadelphia, PA). Each primer set included an identical 5' sequence such that universal sequencing primers were used. Sequence alignment was performed using MacVector editing software and the resulting contig was queried against the Pasteur Institute MLST database to determine the designated allele. To identify the sequence type, allelic profiles were generated for each clinical isolate and compared to the MLST database.

Preparation of recombinant human lipocalin-2

157 Recombinant human lipocalin 2 expressed in *E. coli* strain BL-21 as a glutathione *S*-
158 transferase fusion protein (a gift from J. Cowland) was purified and cleaved with human
159 thrombin as previously described [13, 23, 24]. Purified Lcn2 was quantified using the
160 Micro BCA Protein Assay Kit (Pierce, Rockford, IL). Siderophore-binding activity was
161 confirmed by incubation with Fe-Ent followed by measurement of absorbance at 340 nm.
162
163 **Serum growth assay**
164 RPMI with 10% (v/v) heat inactivated human serum from two healthy volunteers and
165 with or without 1.6mM rLcn2 was inoculated with 1×10^3 cfu/ml of an overnight culture
166 of *K. pneumoniae* and incubated overnight in a final volume of 100 μL in 96-well plates
167 at 37°C with 5% CO_2 [25]. To determine bacterial density, samples were serially diluted
168 and plated on LB agar.
169
170 **Urine Growth Assay**
171 Urine was obtained from three healthy male volunteers, pooled, and passed through a
172 0.22 μm sterile filter (Millipore, Billerca, MA). Urine with or without 1.6mM rLcn2 was
173 inoculated with 1×10^3 cfu/ml of an overnight culture of *K. pneumoniae* and incubated
174 overnight in a final volume of 100 μL in 96-well plates at 37°C with 5% CO_2. To
175 determine bacterial density, samples were serially diluted and plated on LB agar.
176
177 **Murine pneumonia model**
178 All animal work was approved by the University of Pennsylvania Institutional Animal
179 Care and Use Committee (**Assurance #**). Six to eight week old C57BL/6 mice (Jackson

Labs, Jackson, ME) or isogenic *Lcn2*$^{-/-}$ mice were anesthetized with isoflurane and inoculated in the pharynx with 1 x 10^4 cfu of *K. pneumoniae*. LB broth grown cultures were centrifuged, resuspended and diluted in phosphate buffered saline (PBS) and 50 µL PBS of the suspension was administered. To determine bacterial density, mice were sacrificed by CO_2 asphyxiation and lungs were removed, homogenized in 400 µL PBS, and plated on LB agar with appropriate antibiotics.

Results

Clinical isolates of *K. pneumoniae* encoding Yersiniabactin are more prevalent in respiratory samples than other sites

In total, 131 clinical isolates (33 respiratory, 49 urine, 14 blood, 36 stool) were screened for siderophore gene loci by PCR. As expected, all strains contained Ent synthesis genes (Table 1). Twenty-two strains (17%) contained Ybt synthesis genes, and three strains (2%) encoded Aer and Gly-Ent (or salmochelins) genes. Ybt was significantly more prevalent in the respiratory tract than in other sites (33% vs 11% respectively, p=0.0059).

To confirm that detection of siderophore genes correlated with siderophore production, a subset of clinical isolates was tested for siderophore production by liquid chromatography/mass spectrometry (Table 2). As controls, a wild-type strain and five defined mutants in siderophore synthesis genes were assayed. These strains (KP4, 5, 6, 7, 20, and 25) had patterns of detectable siderophores that exactly matched their genotype. 12 of 12 clinical isolates had a siderophore complement that matched their phenotype. Together, this data indicates that the majority (106, 81%) of *K. pneumoniae*

clinical isolates produce only enterobactin. However in the respiratory tract, production of yersiniabactin is significantly more prevalent.

The yersiniabactin locus is often co-incident with B-lactam resistance

The spread of these antibiotic resistant strains, particularly KPC ST258, could be aided by additional fitness advantages. To determine whether carriage of the Ybt locus is associated with antibiotic resistance, available antimicrobial susceptibility data compared to Ybt prevalence (Table 3). Based on phenotype, 21 of 93 strains analyzed had enhanced B-lactam resistance attributable to a KPC (11), ESBL (6) or an unclassifiable mechanism (4). Of these strains, 43% encoded yersiniabactin compared to only 11% on non-resistant strains ($p=0.0024$, RR 3.35, CI 1.69-6.66). Strikingly, 64% of KPC-encoding strains also encoded yersiniabactin.

Because of the co-incidence of Ybt among KPC strains, it is possible that the high prevalence of Ybt in our collection is due to over-representation of a single strain. To test this hypothesis, we performed multi-locus sequence typing (MLST) on the 11 respiratory isolates encoding Ybt (Table 4). Eight of these strains were ST258, two strains were ST353 and one was ST234. However, when combined with the observed resistance patterns, there was significant heterogeneity such that 5 unique patterns were observed. Among ST258 three resistance patterns were observed: KPC, ESBL and levofloxacin/tobramycin resistance. These data indicate that although ST258 was common, there was both intra- and inter-strain variability among Ybt-encoding respiratory isolates.

If Ybt improves fitness in the lung independently from antibiotic resistance, then it should be more prevalent in B-lactam resistant isolates from the respiratory tract compared to resistant isolates from other sites. To test this hypothesis, a separate collection containing only B-lactam resistant isolates was genotyped for siderophores. Ybt was significantly more prevalent among respiratory isolates (13/16) compared to other sites of infection (6/16, p=0.0290, RR 2.97, CI 1.05-8.4). This data suggests that Ybt is often encoded by B-lactam producing strains, but among resistant strains Ybt is still more prevalent in the respiratory tract.

Glycosylated Enterobactin, but not Yersiniabactin, promotes growth in human serum

To determine which siderophores could evade Lcn2 in the bloodstream, bacterial growth was measured in human serum with or without recombinant human Lcn2 (Figure 1). As controls, isogenic siderophore were used. The wild-type strain (KP4) showed robust growth with or without added Lcn2. Siderophore-negative mutant KP7 had a >3 log growth defect in either condition. Ent+ KP20 and Ent+ Ybt+ KP25 were severely inhibited by Lcn2. Conversely, Gly-Ent+ KP6 was resistant to Lcn2. In this strain background, Gly-Ent is both necessary and sufficient to evade Lcn2 in serum.

For the clinical isolates, a sub-set was selected to represent each site of isolation and to include strains with LC/MS data. Two clinical isolates encoding Gly-Ent (KP78, 237) were Lcn2 resistant. KP102, which encodes Ybt and Aer, but only trace amounts of Gly-Ent, was also Lcn2 resistant. In contrast, five of seven strains that encoded only Ent were significantly inhibited by Lcn2. One exception, KP225, showed a non-significant

trend towards Lcn2-dependent inhibition. The other, KP238, was defective in serum growth compared to KP7 that completely lacks siderophores. Yersinibactin-positive strains displayed two phenotypes: Three strains (KP29, 48, 57) were defective for serum growth, and four strains were significantly inhibited by Lcn2. Together, this data suggests that Gly-Ent and perhaps Aer, but not Ybt, are able to evade Lcn2 in serum.

Ex vivo growth in human urine does not require siderophores

To determine whether production of alternative siderophores allows *K. pneumoniae* to evade Lcn2 in urine, bacterial growth was measured in pooled human samples with or without added recombinant hLcn2 (Figure 2). All control strains, including the siderophore-negative mutant KP7, showed robust growth in urine. Curiously, Lcn2 had a small but statistically significant inhibitory effect on KP7. This defect may be attributable to bacterial utilization of endogenous catecholate compounds [26, 27] that transport iron, ligands that Lcn2 also binds. The majority of clinical isolates tested had maximal growth regardless of Lcn2. Ybt-positive strain KP48 showed a significant defect in urine growth and was further inhibited by Lcn2. This strain may lack a common iron-acquisition mechanism. Together, these data indicate that most *K. pneumoniae* isolates efficiently obtain iron in urine without siderophores and are not inhibited by Lcn2.

Yersiniabactin is sufficient to evade Lcn2 and cause pneumonia

Because of the high prevalence of Ybt+ Ent+ clinical isolates in the respiratory tract and their inability to grow in serum, we asked whether Ybt evades Lcn2 by acquiring iron

from a respiratory tract source. Attempts to grow *K. pneumoniae* in human bronchoalveolar fluid were unsuccessful: samples either had antimicrobial activity that could not be inactivated or allowed siderophore-independent growth (data not shown). Instead, a model of murine pneumonia by *K. pneumoniae* was employed. To control for effects of capsular serotype on *in vivo* fitness, isogenic mutants were used. At day 3 post-infection, the siderophore-negative mutant KP7 had replicated poorly, with a median cfu of 4×10^4 (Figure 3A). The Ent+ mutant KP20 also replicated poorly. The Ybt+ Ent+ mutant KP25 had significantly improved growth in the lung compared to both KP20 and KP7.

To determine if Ybt is sufficient to evade Lcn2, mutants encoding either Ybt, Ent, or both were used to infect wild-type (WT) and *Lcn2*$^{-/-}$ mice. The Ent+ mutant KP20 was severely inhibited for growth in WT mice (Figure 4B). This growth inhibition was Lcn2-depedent, since KP20 replicated ~10,000x more in *Lcn2*$^{-/-}$ mice. Ybt was sufficient to evade Lcn2 for replication; the Ybt+ mutant KP5 grew robustly in both WT and *Lcn2*$^{-/-}$ mice. Ybt+ Ent+ KP25 grew robustly in WT mice, but in *Lcn2*$^{-/-}$ mice it replicated even further. Therefore, Ybt is sufficient to evade iron sequestration by Lcn2, although Lcn2 retains some protective effect.

Discussion:

The clinical isolates of *K. pneumoniae* characterized in this study can be roughly categorized into three groups based on siderophore production: Ent+ (81%), Ybt+ Ent+ (17%), and Ent+ Aer+ Gly-Ent+/- Ybt+/- (2%). Therefore, the majority of *K. pneumoniae* isolates are predicted to be sensitive to Lcn2. In contrast, diverse isolates of

294 *Salmonella enterica* all encode the Lcn2-resistant siderophore Gly-Ent (*iroA*) [28]. This
295 is consistent with the low frequency of *K. pneumoniae* as a cause of community-acquired
296 pneumonia and its high frequency as a cause of nosocomial infections [2]. Diseases
297 affecting myelopoiesis, renal tubule function and mucosal integrity would be predicted to
298 disrupt Lcn2 function. Furthermore, community-acquired pneumonia from *Klebsiella* is
299 strongly associated with alcoholism [33], where a shift to gram-negative colonization of
300 the respiratory tract and aspiration may predispose to pneumonia [34]. Community-
301 acquired pyogenic liver abscesses reported in Southeast Asia [33] are caused by strains
302 encoding multiple Lcn2-resistant siderophores including Gly-Ent and Ybt [15].
303 Together, these patterns of infection suggest that Lcn2 is a barrier to infection by *K.*
304 *pneumoniae*, and disease occurs either in conditions of Lcn2 deficiency or from isolates
305 producing Lcn2-resistant siderophores. A large correlation study of Lcn2 levels and
306 siderophore genotype in *K. pneumoniae* infections could test this hypothesis. For
307 pathogenesis studies, the widely used Gly-Ent+ Ybt+ Ent+ *K. pneumoniae* ATCC 43816
308 [20, 29-32] (its derivative KPPR1 was used herein) has siderophores similar to
309 community-acquired tissue invasive strains whereas Ent+ and Ent+ Ybt+ positive *K.*
310 *pneumoniae* may more accurately model nosocomial infections.

311 Our survey of clinical isolates and ex vivo growth assays indicate that Lcn2-
312 resistant siderophore carriage does not correlate with the ability to cause urinary tract
313 infections. This is in contrast to uropathogenic *E. coli*, in which Ybt and Gly-Ent were
314 present in over half of clinical isolates examined [35]. However, similarly to *E. coli* [35,
315 36], *K. pneumoniae* expression of Lcn2–resistant siderophores such as Ybt is induced
316 during urine growth (data not shown), suggesting that iron is limited. In *K. pneumoniae*,

317 siderophore-independent iron acquisition systems not tested here have been associated
318 with enhanced virulence [37]. Alternatively, siderophores may be required *in vivo*, again
319 limiting *K. pneumoniae* infection to either impaired patients or strains expressing Lcn2 –
320 resistant siderophores.

321 Despite the requirement for Gly-Ent to evade Lcn2 for growth in serum, no
322 isolates encoding this siderophore were found in the blood. This indicates that iron
323 acquisition from serum is not required for *K. pneumoniae* bacteremia. Perhaps this is not
324 surprising considering it is a rare cause of endovascular disease such as endocarditis [38].
325 Instead, *K. pneumoniae* bacteremia is likely caused by seeding from respiratory, urinary
326 or gastrointestinal tracts [39], and serum growth data indicates the bacteria can replicate
327 numerous times in serum without siderophores (Figure 1, KP7) before iron becomes
328 limiting.

329 The high prevalence of Ybt+ isolates in the respiratory tract compared to blood,
330 urine, and stool is consistent with the high expression of Lcn2 by the respiratory mucosa.
331 The trachea and lung have the highest levels of mRNA expression among 50 human
332 tissue types examined [8]. In our murine pneumonia model, Lcn2 prevented pneumonia
333 from Ent+ *K. pneumoniae* but Ybt was sufficient to evade Lcn2 and replicate to high
334 numbers. This explains why Ybt is a virulence factor in *K. pneumoniae*: it significantly
335 increases the ability to cause respiratory tract infection despite Lcn2. Intriguingly, Lcn2
336 retained partial activity against Ent+ Ybt+ *Klebsiella*, the genotype seen in clinical
337 isolates. Whether this is attributable to Lcn2-dependent inflammation is under
338 investigation.

339 The carriage of Ybt by epidemic KPC strain ST258 may be contributing to its
340 fitness and rapid spread. In fact, our MLST analysis of Ybt+ respiratory isolates
341 demonstrates that not all ST258 isolates are resistant to Carbapenems, and one isolate
342 (KP246) had no enhanced β-lactamase resistance. Larger analysis of KPC-harboring
343 ST258 strains also demonstrated significant diversity of the KPC plasmid and even
344 carriage of different KPC genes (bla_{KPC-2} or bla_{KPC-3}) [4]. Furthermore, the *tonB* gene
345 that partially defines MLST types is a proven *K. pneumoniae* virulence factor required for
346 energy transduction by Ent and Ybt siderophore uptake systems [15, 40]. Therefore, Ybt
347 carriage in ST258 is separable from KPC carriage. By allowing access to the respiratory
348 tract, carriage of Ybt likely enhances the ability of ST258 to colonize, infect and spread
349 among hospitalized patients independent of antibiotic resistance.
350 In summary, the results of this study indicate that *K. pneumoniae* encoding the
351 Ybt siderophore are prevalent in the respiratory tract, are often resistant to β-lactam
352 antibiotics, and are able to evade the innate immune protein Lcn2 to cause pneumonia.
353 The predilection of Ybt+ *K. pneumoniae* for the respiratory tract is further supported by
354 the fact that Ybt cannot evade Lcn2 in serum and was dispensable in urine. Isolates
355 without Lcn2-resistant siderophores were common, indicating that evasion of Lcn2 was
356 not an absolute requirement for infection. However, the fact that the majority of *K.*
357 *pneumoniae* infections are nosocomial suggests a lapse in normal barriers to infection.
358 The fact that the ability to evade Lcn2 is co-incident with enhanced β-lactamases
359 suggests that the antibiotic-resistant strains may spread due to enhanced iron acquisition.
360

Footnotes:

Potential conflicts of interest:

M.A.B., no conflict; J.E.O., no conflict; S.B., no conflict; M.C., no conflict; F.L., no conflict; C.D. no conflict; J.N.W., no conflict.

This work was supported by NIH grants K08GM085612 (MAB) and **Jeff's Grants Here** (JNW), and **Charles Dozois Funding here** (CD).

Portions of this manuscript were presented at the 45th Annual Meeting of the Academy of Clinical and Laboratory Physicians and Scientists, June 3rd-5th, 2010, Nashville, TN.

Address to which correspondence should be addressed:
Michael Bachman M.D., Ph.D.
401A Johnson Pavilion
3610 Hamilton Walk
Philadelphia, PA 19104
Phone: 215-573-3510
Fax 215-573-4856
michael.bachman@uphs.upenn.edu

382
383

384 **Figure Legends**

385 **Figure 1. Glycosylated Enterobactin, but not Yersiniabactin, promotes growth in**
386 **human serum.** Overnight growth in 10% heat-inactivated human serum with or without
387 1.6 uM recombinant human Lcn2 was determined for the *K. pneumoniae* (KP) strains
388 indicated (A). Mean ± SEM for at least three independent experiments is shown as $\log_{10}$
389 CFU/ml. Siderophores produced by each strain are indicated by a plus (+). For clinical
390 isolates, the site of infection is noted as R (respiratory), B (blood), U (urine), or S (stool).
391 * - Growth inhibited by hLcn2 as measured by unpaired t-test (* $p<0.05$; ** $p<0.01$; ***
392 $p<0.001$). # - Growth stimulated by hLcn2 as measured by unpaired t-test ($p<0.05$). & -
393 Growth inhibited in serum alone compared to KP7 by one-way ANOVA (& $p<0.05$; &&
394 $p<0.01$; &&& $p<0.001$).

395

396 **Figure 2. Siderophores are not required for growth in human urine.** Overnight
397 growth in pooled human urine with or without 1.6 uM recombinant human Lcn2 was
398 determined for the *K. pneumoniae* (KP) strains indicated. Mean ± SEM for at least three
399 independent experiments is shown as $\log_{10}$ CFU/ml. Siderophores produced by each
400 strain are indicated by a plus (+). For clinical isolates, the site of infection is noted as R
401 (respiratory), B (blood), U (urine), or S (stool). * - Growth inhibited by hLcn2 as
402 measured by unpaired t-test (* $p<0.05$; ** $p<0.01$; *** $p<0.001$). &&& - Growth
403 inhibited in urine compared to KP4 by one-way ANOVA ($p<0.001$). ## - Growth
404 stimulated by hLcn2 as measured by unpaired t-test ($p<0.01$).

405

406 **Figure 3. Yersiniabactin promotes growth in the lung and dissemination to the**
407 **spleen.** Lung bacterial burden (log_{10} cfu) at day 3 after retropharyngeal inoculation of 1
408 x 10^4 cfu of the *K. pneumoniae* mutants indicated was determined in C57BL/6 mice (A,
409 n≥10 mice per group). Box and whiskers graph shows the median and interquartile
410 ranges. Siderophores encoded by each mutant are indicated by a plus (+). * $p<0.05$, **
411 $p<0.01$ as determined by one-way ANOVA with Tukey's post test. Lung bacterial
412 burden at day 3 after inoculation of the *K. pneumoniae* mutants indicated was compared
413 between C57BL/6 (WT) or isogenic *Lcn2*$^{-/-}$ mice (B, ≥ 5 mice per group). * $p < 0.05$, ***
414 $p<0.0001$ as determined by the Mann-Whitney test.
415

Table 1: Comparison of Siderophore Prevalence by Site of Culture

	Number (%) of positive isolates by PCR[#]								
Siderophore System (PCR Target)	**All Sites (131)**	**Resp. (33)**	**Non-respiratory (49)**	**Urine (14)**	**Blood (36)**	**Stool (99)**	**Comb. p* (95% C.I.)**		**Relative Risk**
Ybt (*ybtS*)	**22(17)**	**11(33)**	**4(8)**	**1(7)**	**6(17)**	**11(11)**	**0.0059**	**2.5**	**(1.43 to 4.38)**
Aer (*iucA*)	3(2)	1(3)	0(0)	0(0)	2(6)	2(2)	1.0	1.3	(0.26 to 6.85)
Gly-Ent (*iroN*)	3(2)	1(3)	0(0)	0(0)	2(6)	2(2)	1.0	1.3	(0.26 to 6.85)
Ent (*entB/entE*)	131(100)	33(100)	49(100)	14(100)	36(100)	99(100)	ND	ND	

* Calculated using Fisher's exact test to compare respiratory and combined non-respiratory prevalence.

Prospectively collected in the HUP Microbiology laboratory 2009-2010

Table 2: Relative distribution of siderophores detected in culture supernatants of strains grown in M63-glycerol.

	Siderophore (Genotype and % of Total Detected by LC/MS)					
Strain			**Enterobactin**	**Salmochelins**	**Yersiniabactin**	**Aerobactin**
Isogenic Mutants						
KP4		WT (KPPR1)	**+ 39.3 ± 3.6**	**+ 40.8 ± 3.8**	**+ 20.0 ± 7.3**	- 0
KP5		*entB*	- 0	- 0	+ 100	- 0
KP6		*ybtS*	**+ 49.9 ± 0.4**	**+ 50.1 ± 0.4**	- 0	- 0
KP7		*entB ybtS*	- 0	- 0	- 0	- 0
KP20	*iroA ybtS*		**+ 100**	- 0	- 0	- 0
KP25	*iroA*		**+ 85.5 ± 4.3**	- 0	**+ 14.5 ± 4.3**	- 0
Clinical Isolates						
KP30	respiratory		**+ 100**	- 0	- 0.0 ± 0.0	- 0
KP33	urine		**+ 58.8 ± 5.3**	- 0	**+ 41.2 ± 5.3**	- 0
KP34	urine		**+ 74.4 ± 4.5**	**- 0.2 ± 0.02**	**+ 25.4 ± 4.5**	- 0
KP35	urine		**+ 100**	- 0	- 0	- 0
KP36	urine		**+ 100**	- 0	- 0	- 0
KP56	respiratory		**+ 100**	- 0	+ 0	- 0
KP57	respiratory		**+ 92.4 ± 2.3**	- 0	**+ 7.6 ± 2.3**	- 0
KP58	respiratory		**+ 100**	- 0	- 0	- 0
KP76	stool		**+ 100**	- 0	- 0	- 0
KP77	stool		**+ 100**	- 0	- 0	- 0
KP78	stool		**+ 26.4 ± 1.4**	**+ 9.6 ± 0.4**	**+ 1.9 ± 0.2**	**+ 62.1 ± 1.3**
KP102	stool		**+ 1.0 ± 0.2**	**+ 0.2 ± 0.02**	**+ 12.5 ± 3.4**	**+ 86.3 ± 3.6**

Table 3: Comparison of Yersiniabactin Prevalence among invasive isolates based on B-lactam resistance pattern

	Number (%) of positive isolates by PCR[#]						
	Total	**Prevalence by Antibiotic Resistance Pattern**					
		Enhanced B-lactam Resistance				**Classical**	**p***
	Relative Risk						
		KPC	ESBL	Other	Combined		(95% C.I.)
Siderophore	(93)	(11)	(6)	(4)	(21)	(72)	
Ybt (*ybtS*)	17 (18)	7 (64)	2 (33)	0 (0)	9 (43)	8 (11)	0.0024 3.35 (1.69-6.66)

Collected in the HUP Microbiology laboratory in 2007.

* Calculated using Fisher's exact test to compare resistant and non-resistant prevalence.

Table 4: Multi-locus Sequence Typing (MLST) of Yersiniabactin-Positive Respiratory Isolates

Strain (KP#)	Phenotype tonB Pattern	gapA	pgi	Allele infB	mdh	phoE	rpoB	Seq. Type	Resistance Pattern	Genotype/
156	79	3	1	3	1	1	1	258	KPC	1
223	79	3	1	3	1	1	1	258	KPC	1
228	79	3	1	3	1	1	1	258	KPC	1
248	79	3	1	3	1	1	1	258	KPC	1
250	79	3	1	3	1	1	1	258	KPC	1
216	79	3	1	3	1	1	1	258	ESBL	2
235	79	3	1	3	1	1	1	258	ESBL	2
246	79	3	1	3	1	1	1	258	Levo/Tobra	3
217	16	3	1	9	47	13	1	353	None	4
151	16	3	1	9	47	13	1	353	None	4
152	24	2	1	1	2	7	1	234	None	5

494 **Figure 1.**

495

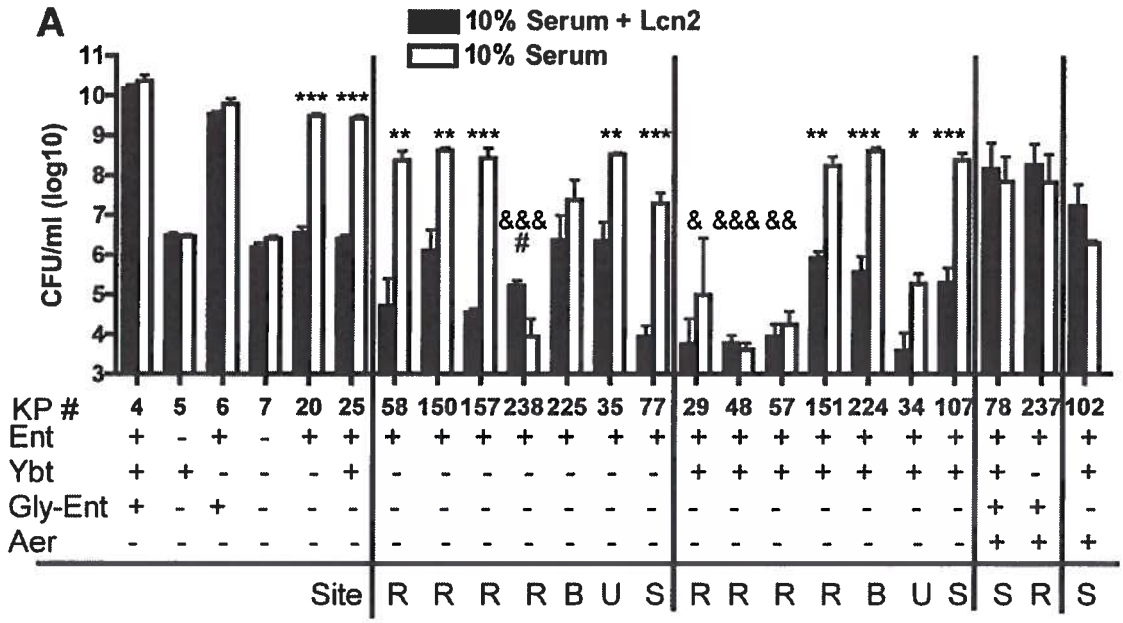

496

497

498 Figure 2.

499

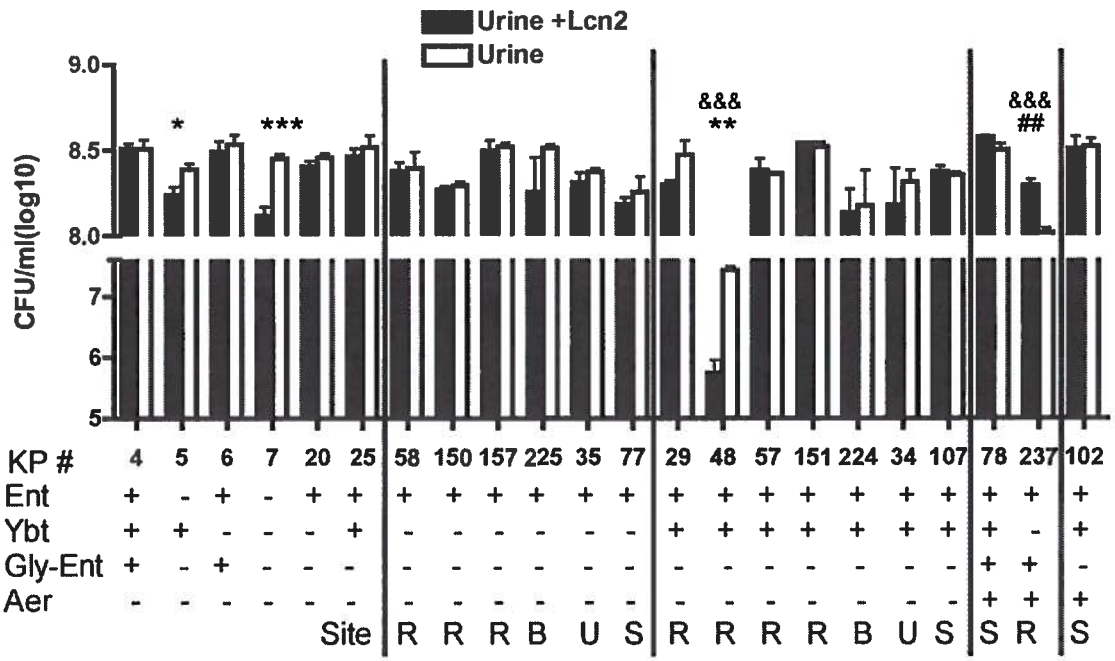

500

501

502 Figure 3.

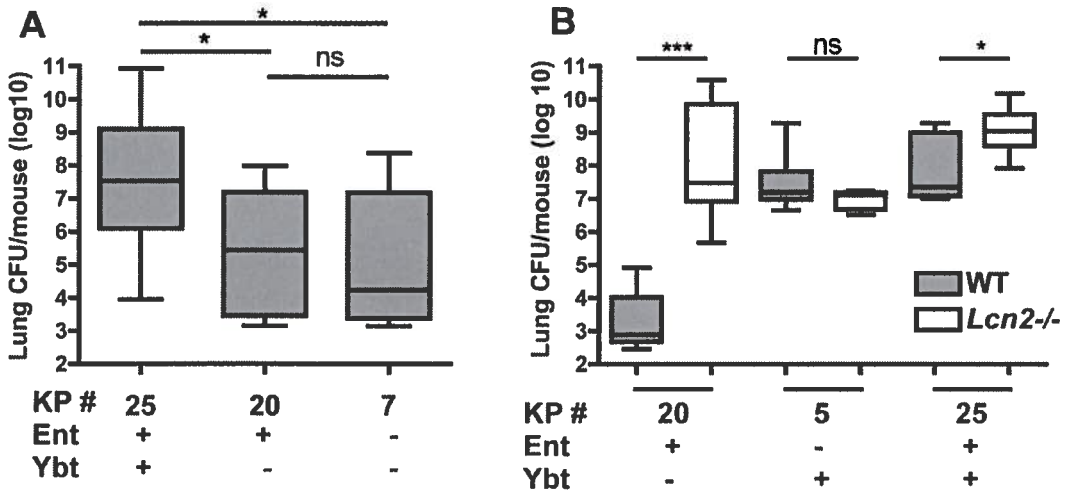

503

504

505 **References:**

506 1. Podschun R, Ullmann U. Klebsiella spp. as nosocomial pathogens: epidemiology,
507 taxonomy, typing methods, and pathogenicity factors. Clinical microbiology reviews
508 **1998**; 11:589-603.
509 2. Jones RN. Microbial etiologies of hospital-acquired bacterial pneumonia and
510 ventilator-associated bacterial pneumonia. Clin Infect Dis **2010**; 51 Suppl 1:S81-7.
511 3. Hirsch EB, Tam VH. Detection and treatment options for *Klebsiella pneumoniae*
512 carbapenemases (KPCs): an emerging cause of multidrug-resistant infection. J
513 Antimicrob Chemother **2010**; 65:1119-25.
514 4. Kitchel B, Rasheed JK, Patel JB, et al. Molecular epidemiology of KPC-producing
515 *Klebsiella pneumoniae* isolates in the United States: clonal expansion of multilocus
516 sequence type 258. Antimicrobial agents and chemotherapy **2009**; 53:3365-70.
517 5. Earhart CF. Uptake and Metabolism of Iron and Molybdenum. In: Neidhart F, ed. *E*
518 *coli* and *Salmonella*: ASM Press, **1996**.
519 6. Wooldridge KG, Williams PH. Iron uptake mechanisms of pathogenic bacteria. FEMS
520 microbiology reviews **1993**; 12:325-48.
521 7. Kjeldsen L, Johnsen AH, Sengelov H, Borregaard N. Isolation and primary structure of
522 NGAL, a novel protein associated with human neutrophil gelatinase. The Journal of
523 biological chemistry **1993**; 268:10425-32.
524 8. Cowland JB, Borregaard N. Molecular characterization and pattern of tissue expression
525 of the gene for neutrophil gelatinase-associated lipocalin from humans. Genomics **1997**;
526 45:17-23.
527 9. Nelson AL, Barasch JM, Bunte RM, Weiser JN. Bacterial colonization of nasal
528 mucosa induces expression of siderocalin, an iron-sequestering component of innate
529 immunity. Cellular microbiology **2005**; 7:1404-17.
530 10. Clifton MC, Corrent C, Strong RK. Siderocalins: siderophore-binding proteins of the
531 innate immune system. Biometals **2009**; 22:557-64.
532 11. Goetz DH, Holmes MA, Borregaard N, Bluhm ME, Raymond KN, Strong RK. The
533 neutrophil lipocalin NGAL is a bacteriostatic agent that interferes with siderophore-
534 mediated iron acquisition. Molecular cell **2002**; 10:1033-43.
535 12. Nelson AL, Ratner AJ, Barasch J, Weiser JN. Interleukin-8 secretion in response to
536 aferric enterobactin is potentiated by siderocalin. Infection and immunity **2007**; 75:3160-
537 8.
538 13. Bachman MA, Miller VL, Weiser JN. Mucosal lipocalin 2 has pro-inflammatory and
539 iron-sequestering effects in response to bacterial enterobactin. PLoS Pathog **2009**;
540 5:e1000622.
541 14. Fischbach MA, Lin H, Zhou L, et al. The pathogen-associated iroA gene cluster
542 mediates bacterial evasion of lipocalin 2. Proceedings of the National Academy of
543 Sciences of the United States of America **2006**; 103:16502-7.
544 15. Hsieh PF, Lin TL, Lee CZ, Tsai SF, Wang JT. Serum-induced iron-acquisition
545 systems and TonB contribute to virulence in *Klebsiella pneumoniae* causing primary
546 pyogenic liver abscess. The Journal of infectious diseases **2008**; 197:1717-27.
547 16. Lawlor MS, O'Connor C, Miller VL. Yersiniabactin is a virulence factor for
548 *Klebsiella pneumoniae* during pulmonary infection. Infection and immunity **2007**;
549 75:1463-72.

17. Koczura R, Kaznowski A. Occurrence of the *Yersinia* high-pathogenicity island and iron uptake systems in clinical isolates of *Klebsiella pneumoniae*. Microbial pathogenesis **2003**; 35:197-202.
18. Friedl A, Stoesz SP, Buckley P, Gould MN. Neutrophil gelatinase-associated lipocalin in normal and neoplastic human tissues. Cell type-specific pattern of expression. The Histochemical journal **1999**; 31:433-41.
19. Klausen P, Niemann CU, Cowland JB, Krabbe K, Borregaard N. On mouse and man: neutrophil gelatinase associated lipocalin is not involved in apoptosis or acute response. Eur J Haematol **2005**; 75:332-40.
20. Chan YR, Liu JS, Pociask DA, et al. Lipocalin 2 is required for pulmonary host defense against *Klebsiella* infection. J Immunol **2009**; 182:4947-56.
21. Mori K, Lee HT, Rapoport D, et al. Endocytic delivery of lipocalin-siderophore-iron complex rescues the kidney from ischemia-reperfusion injury. The Journal of clinical investigation **2005**; 115:610-21.
22. Winn WC, Allen SD, Janda WM, et al. The Enterobacteriaceae. Koneman's Color Atlas and Textbook of Diagnostic Microbiology. 6th ed. Baltimore: Lippincott Williams and Wilkins, **2006**:259-264.
23. Yang J, Goetz D, Li JY, et al. An iron delivery pathway mediated by a lipocalin. Molecular cell **2002**; 10:1045-56.
24. Bundgaard JR, Sengelov H, Borregaard N, Kjeldsen L. Molecular cloning and expression of a cDNA encoding NGAL: a lipocalin expressed in human neutrophils. Biochem Biophys Res Commun **1994**; 202:1468-75.
25. Flo TH, Smith KD, Sato S, et al. Lipocalin 2 mediates an innate immune response to bacterial infection by sequestrating iron. Nature **2004**; 432:917-21.
26. Bao G, Clifton M, Hoette TM, et al. Iron traffics in circulation bound to a siderocalin (Ngal)-catechol complex. Nature chemical biology **2010**; 6:602-9.
27. Miethke M, Skerra A. Neutrophil gelatinase-associated lipocalin expresses antimicrobial activity by interfering with L-norepinephrine-mediated bacterial iron acquisition. Antimicrobial agents and chemotherapy **2010**; 54:1580-9.
28. Baumler AJ, Heffron F, Reissbrodt R. Rapid detection of *Salmonella enterica* with primers specific for iroB. J Clin Microbiol **1997**; 35:1224-30.
29. Aujla SJ, Chan YR, Zheng M, et al. IL-22 mediates mucosal host defense against Gram-negative bacterial pneumonia. Nature medicine **2008**; 14:275-81.
30. Jeyaseelan S, Young SK, Yamamoto M, et al. Toll/IL-1R domain-containing adaptor protein (TIRAP) is a critical mediator of antibacterial defense in the lung against *Klebsiella pneumoniae* but not *Pseudomonas aeruginosa*. J Immunol **2006**; 177:538-47.
31. Cogen AL, Moore TA. Beta2-microglobulin-dependent bacterial clearance and survival during murine *Klebsiella pneumoniae* bacteremia. Infection and immunity **2009**; 77:360-6.
32. Bhan U, Lukacs NW, Osterholzer JJ, et al. TLR9 is required for protective innate immunity in Gram-negative bacterial pneumonia: role of dendritic cells. J Immunol **2007**; 179:3937-46.
33. Ko WC, Paterson DL, Sagnimeni AJ, et al. Community-acquired *Klebsiella pneumoniae* bacteremia: global differences in clinical patterns. Emerg Infect Dis **2002**; 8:160-6.

34. Carpenter JL. Klebsiella pulmonary infections: occurrence at one medical center and review. Rev Infect Dis **1990**; 12:672-82.
35. Henderson JP, Crowley JR, Pinkner JS, et al. Quantitative metabolomics reveals an epigenetic blueprint for iron acquisition in uropathogenic *Escherichia coli*. PLoS Pathog **2009**; 5:e1000305.
36. Alteri CJ, Mobley HL. Quantitative profile of the uropathogenic *Escherichia coli* outer membrane proteome during growth in human urine. Infection and immunity **2007**; 75:2679-88.
37. Ma LC, Fang CT, Lee CZ, Shun CT, Wang JT. Genomic heterogeneity in *Klebsiella pneumoniae* strains is associated with primary pyogenic liver abscess and metastatic infection. The Journal of infectious diseases **2005**; 192:117-28.
38. Anderson MJ, Janoff EN. *Klebsiella* endocarditis: report of two cases and review. Clin Infect Dis **1998**; 26:468-74.
39. Garcia de la Torre M, Romero-Vivas J, Martinez-Beltran J, Guerrero A, Meseguer M, Bouza E. *Klebsiella* bacteremia: an analysis of 100 episodes. Rev Infect Dis **1985**; 7:143-50.
40. Moeck GS, Coulton JW. TonB-dependent iron acquisition: mechanisms of siderophore-mediated active transport. Molecular microbiology **1998**; 28:675-81.